TTI: 0-6956

Texas A&M Transportation Institute

Synthesis of Load-Deflection Characteristics of Laterally Loaded Large Diameter Drilled Shafts: Technical Report

Technical Report 0-6956-R1

Cooperative Research Program

TEXAS A&M TRANSPORTATION INSTITUTE
COLLEGE STATION, TEXAS

in cooperation with the
Federal Highway Administration and the
Texas Department of Transportation
http://tti.tamu.edu/documents/0-6956-R1.pdf

Technical Report Documentation Page

1. Report No.	2. Government Accession No.	3. Recipient's Catalog No.
FHWA/TX-18/0-6956-R1		

4. Title and Subtitle	5. Report Date
SYNTHESIS OF LOAD-DEFLECTION CHARACTERISTICS OF LATERALLY LOADED LARGE DIAMETER DRILLED SHAFTS: TECHNICAL REPORT	Published: November 2018
	6. Performing Organization Code

7. Author(s)	8. Performing Organization Report No.
Jean-Louis Briaud and Yen-Chih Wang	Report 0-6956-R1

9. Performing Organization Name and Address	10. Work Unit No. (TRAIS)
Texas A&M Transportation Institute The Texas A&M University System College Station, Texas 77843-3135	11. Contract or Grant No. Project 0-6956

12. Sponsoring Agency Name and Address	13. Type of Report and Period Covered
Texas Department of Transportation Research and Technology Implementation Office 125 E. 11th Street Austin, Texas 78701-2483	Technical Report: September 2017–August 2018
	14. Sponsoring Agency Code

15. Supplementary Notes

Project performed in cooperation with the Texas Department of Transportation and the Federal Highway Administration.

Project Title: Synthesis of Load-Deflection Characteristics of Laterally Loaded Large Diameter Drilled Shafts

URL: http://tti.tamu.edu/documents/0-6956-R1.pdf

16. Abstract:

This project evaluated how well current P-y curves predict the behavior of large diameter piles subjected to monotonic lateral loading. Current P-y curves were developed about 60 years ago based on lateral load tests on piles, which were about 2 ft in diameter, while today's pile diameters can reach 12 ft. This significant difference in scale brings into question the application of these early P-y curves to today's large diameter piles (≥5 ft). A database of 35 piles with diameters larger than 5 ft (up to 9.8 ft) and 54 piles with diameters less than 5 ft both in sand and in clay was assembled. Predictions of load and displacement are carried out using P-y curves and LPILE. These predictions are compared to the measured loads and displacements. In sand, the ratio of predicted load over measured load L_{pred}/L_{meas} averages 0.9 for all piles and increases with diameter from 0.7 for smaller diameter piles to 1.1 for larger diameter piles. Overall, L_{pred}/L_{meas} is between 0.4 and 1.4 most of the time. In clay, L_{pred}/L_{meas} averages 0.9 for all piles and decreases with diameter from 1.3 for smaller diameter piles to 0.7 for larger diameter piles. Overall, L_{pred}/L_{meas} is between 0.4 and 1.6 most of the time. In sand, the ratio of predicted deflection over measured deflection y_{pred}/y_{meas} averages 1.9 for all piles and decreases with diameter from 2.25 for smaller diameter piles to about 1 for larger diameter piles. Overall, the ratio y_{pred}/y_{meas} is between 0.5 and 5 most of the time. In clay, y_{pred}/y_{meas} averages about 1.4 for all piles and increases with diameter from 0.9 for smaller diameter piles to 3 for larger diameter piles. Overall, y_{pred}/y_{meas} is between 0.2 and 5 most of the time with some values reaching 8 for larger diameter piles.

17. Key Words	18. Distribution Statement
Horizontal Load, Lateral Load, Large Diameter, Pile Load Tests, Database, P-y Curves, Predicted, Measured, Load, Displacement, LPILE, Sand, Clay	No restrictions. This document is available to the public through NTIS: National Technical Information Service Alexandria, Virginia http://www.ntis.gov

19. Security Classif. (of this report)	20. Security Classif. (of this page)	21. No. of Pages	22. Price
Unclassified	Unclassified	242	

Form DOT F 1700.7 (8-72) Reproduction of completed page authorized

SYNTHESIS OF LOAD-DEFLECTION CHARACTERISTICS OF LATERALLY LOADED LARGE DIAMETER DRILLED SHAFTS: TECHNICAL REPORT

by

Jean-Louis Briaud
Distinguished Professor
Zachry Department of Civil Engineering

and

Yen-Chih Wang
Research Assistant
Zachry Department of Civil Engineering

Report 0-6956-R1
Project 0-6956
Project Title: Synthesis of Load-Deflection Characteristics of Laterally Loaded Large Diameter Drilled Shafts

Performed in cooperation with the
Texas Department of Transportation
and the
Federal Highway Administration

Published: November 2018

TEXAS A&M TRANSPORTATION INSTITUTE
College Station, Texas 77843-3135

DISCLAIMER

This research was performed in cooperation with the Texas Department of Transportation (TxDOT) and the Federal Highway Administration (FHWA). The contents of this report reflect the views of the authors, who are responsible for the facts and the accuracy of the data presented herein. The contents do not necessarily reflect the official view or policies of the FHWA or TxDOT. This report does not constitute a standard, specification, or regulation.

This report is not intended for construction, bidding, or permit purposes. The engineer (researcher) in charge of the project was Dr. Jean-Louis Briaud, P.E. # Texas 48690.

ACKNOWLEDGMENTS

This project was conducted in cooperation with TxDOT and FHWA. At TxDOT, the authors thank the project director Chris Glancy, and the members of the project monitoring committee: John Delphia, David Fish, Justin Thomey, and Marie Fisk. Many people contributed lateral load test results to make the database possible. They are John Hayes, Southeast Regional Sales Manager at Equipment Corporation of America, Mohamed Ashour, Associate Professor at Alabama A&M University, Billy Camp, Technical Principal/Vice President at S&ME, Inc., Raymond Castelli, Technical Director, Geotechnical Engineering, at WSP, Jon Sinnreich, Engineer at Zeta Geotechnics LLC, John Turner, Senior Principal at Dan Brown & Associates, Ikuo Towhata, Director at Tohata Architects & Engineers (Professor Emeritus, University of Tokyo), James Long, Emeritus Professor at University of Illinois Department of Civil Engineering, and Dan Brown, President/Senior Principal Engineer at Dan Brown & Associates. Also, Kathryn Jennings and Rachel Holzhauser were undergraduate students helping many figures.

TABLE OF CONTENTS

Page

LIST OF FIGURES

Page

LIST OF TABLES

Page

EXECUTIVE SUMMARY

This project evaluated how well current P-y curves predict the behavior of large diameter piles subjected to monotonic lateral loading. Current P-y curves were developed starting about 60 years ago based on lateral load tests on piles, which were about 2 ft in diameter, while today's pile diameters can reach 12 ft. This significant difference in scale brings into question the application of these early P-y curves to today's large diameter piles. In this report, the boundary between small diameter and large diameter is set arbitrarily at 5 ft.

After a brief review of the classic P-y curve work of Matlock and Reese, a database of piles subjected to monotonic lateral loading was accumulated. The total number of load tests collected and organized in a spreadsheet was 89 with the distribution as shown in the table below. The data came primarily from the United States but also from seven other countries.

Category		Pile Diameter B<5 ft	Pile Diameter B≥5 ft
Pile diameter range (ft)		1–5	5–9.8
Pile length range (ft)		5–120	7.5–220
Number of case		54	35
Soil type	Sand	33	23
	Clay	21	12

Each load test case included the pile dimensions and material properties, the soil properties, and the lateral load versus lateral deflection curve. For each load test case, the work consisted of predicting the load-deflection curve using the program LPILE with the associated input parameters and comparing it to the measured curve.

Evaluation of the predictions took place along two main comparisons: comparison between the predicted load Lpred and the measured load Lmeas at given deflections of 0.25, 0.5, 1, and 2 inches and comparison between the predicted deflection ypred and measured defection ymeas at lateral loads H corresponding to set percentages of the ultimate load Hou equal to 10%, 25%, 33%, and 50%. The ultimate lateral load was defined as the load corresponding to a horizontal deflection equal to 10% of the pile diameter. This deflection was not always reached in the load tests; in those cases a hyperbolic extrapolation was used (33% of all cases).

The ratio L_{pred}/L_{meas} was plotted against the pile diameter to evaluate the predictions in general and the influence of the diameter in particular. The following summarizes the findings:

- In sand, L_{pred}/L_{meas} averages about 0.9 for all piles and increases with diameter from about 0.7 for smaller diameter piles to about 1.1 for larger diameter piles. Overall, L_{pred}/L_{meas} can be expected to be between 0.4 and 1.4 most of the time.
- In clay, L_{pred}/L_{meas} averages about 0.9 for all piles and decreases with diameter from about 1.3 for smaller diameter piles to about 0.7 for larger diameter piles. Overall, L_{pred}/L_{meas} can be expected to be between 0.4 and 1.6 most of the time.

The ratio y_{pred}/y_{meas} was plotted against the pile diameter to evaluate the predictions in general and the influence of the diameter in particular. Overall more scatter was observed in the prediction of deflections at lateral loads H corresponding to set percentages of the ultimate load Hou than in the prediction of loads at given deflection values. The following is a summary of the findings:

- In sand, y_{pred}/y_{meas} averages about 1.9 for all piles and decreases with diameter from about 2.25 for smaller diameter piles to about 1 for larger diameter piles. Overall, the ratio y_{pred}/y_{meas} can be expected to be between 0.5 and 5 most of the time.
- In clay, y_{pred}/y_{meas} averages about 1.4 for all piles and increases with diameter from about 0.9 for smaller diameter piles to about 3 for larger diameter piles. Overall, the ratio y_{pred}/y_{meas} can be expected to be between 0.2 and 5 most of the time with some values reaching 8 for larger diameter piles.

The fact that, in sand, the predicted deflection decreases as the pile diameter increases is attributed to the use of a flawed parameter: the modulus of subgrade reaction k. The reason is that while k increases with the soil stiffness, it also decreases with the pile diameter. Therefore, recommending set values of k for all pile diameters leads to underpredicting deflections for large diameter piles. Indeed, in this case the k value will be too large. A better approach would be to use the soil modulus, which is solely dependent on the soil and independent of the pile diameter.

The fact that, in clay, the predicted deflection increases significantly as the pile diameter increases is attributed to the following fact: The depth Z_c at which the soil resistance to lateral loading switched from the shallow depth equation to the larger depth equation increases with the pile diameter. As such, the P-y curves near the surface are softer for larger diameter piles and the predicted deflections are accordingly larger. An improved way to obtain Z_c for large diameter piles is needed.

CHAPTER 1 INTRODUCTION

Piles with diameters up to 12 ft are increasingly used for bridges and other structures. When they are subjected to lateral loading, the most common design approach is the P-y curves approach developed by Matlock (1970) and Reese et al. (1974). This approach was developed and calibrated for piles that would now be considered small diameter piles (1 ft to 2 ft in diameter). The significant difference between the diameter of the piles that were used to calibrate the design approach and the diameter of the piles currently used brings to question the validity of the P-y curves for large diameter piles (5 ft to 12 ft) subjected to lateral loading.

The problem of a laterally loaded large diameter pile has been under investigation for some time, and various P-y curves have been proposed including Reese (1958, 1975), Matlock (1970), Randolph and Houlsby (1984), Jeanjean (2009), and Zhang et al. (2016). This project addresses the diameter effect from a database study point of view while using the most common P-y curves. The computer program LPILE developed by Ensoft is used to compare the predictions with measurements collected from field load tests. The P-y curves proposed by Matlock (1970) and Reese (1975) in clay and Reese et al. (1974) and American Petroleum Institute (API) (2010) in sand are used to make the predictions.

The database effort in this project consisted of collecting many load tests where piles had been subjected to lateral loading including small diameter piles (diameter $B < 5$ ft) and large diameter piles ($B \geq 5$ ft). More than 40 people were contacted in 10 countries, and a total of 89 load tests were collected, including 54 small diameter tests and 35 large diameter tests. Details about each load test including soil properties, pile properties, and the pile head displacement versus applied lateral load curves are presented. For all 89 load tests, the predictions are compared with the measured values. This comparison is analyzed to identify the diameter effect. In addition, a relatively new method called the Simple Approach for Lateral LOad on Piles (SALLOP) method (Briaud, 1997), which relies on pressuremeter results, is also used as a potential way to improve predictions. For all methods, the ratios of predicted over measured values are plotted versus pile diameter, and modifications to improve the predictions are suggested.

CHAPTER 2 DEFINITION AND BEHAVIOR

2.1 INTRODUCTION

Piles are structural members that are made of timber, concrete, or steel, usually used to contribute to the safety and serviceability of the superstructure. The list below identifies typical scenarios where pilings are used (Vesic, 1977; Figure 2-1):

- When the construction space is limited in an urban area. In this case, a shallow foundation may not have enough room to provide sufficient support for the superstructure or the bridge.
- When the bedrock is not encountered at a reasonable depth and one or more upper soil layers are highly compressible.
- When subjected to lateral forces such as waves on an offshore platform, vessel impact on a bridge pier, earthquake vibrations, and wind effects on a highway sign.
- When the soil is a shrink swell soil or a collapsible soil.
- When uplift forces are present such as for transmission towers, basement mats below the water table, and offshore platforms.
- When erosion or scour may take place near the ground surface.

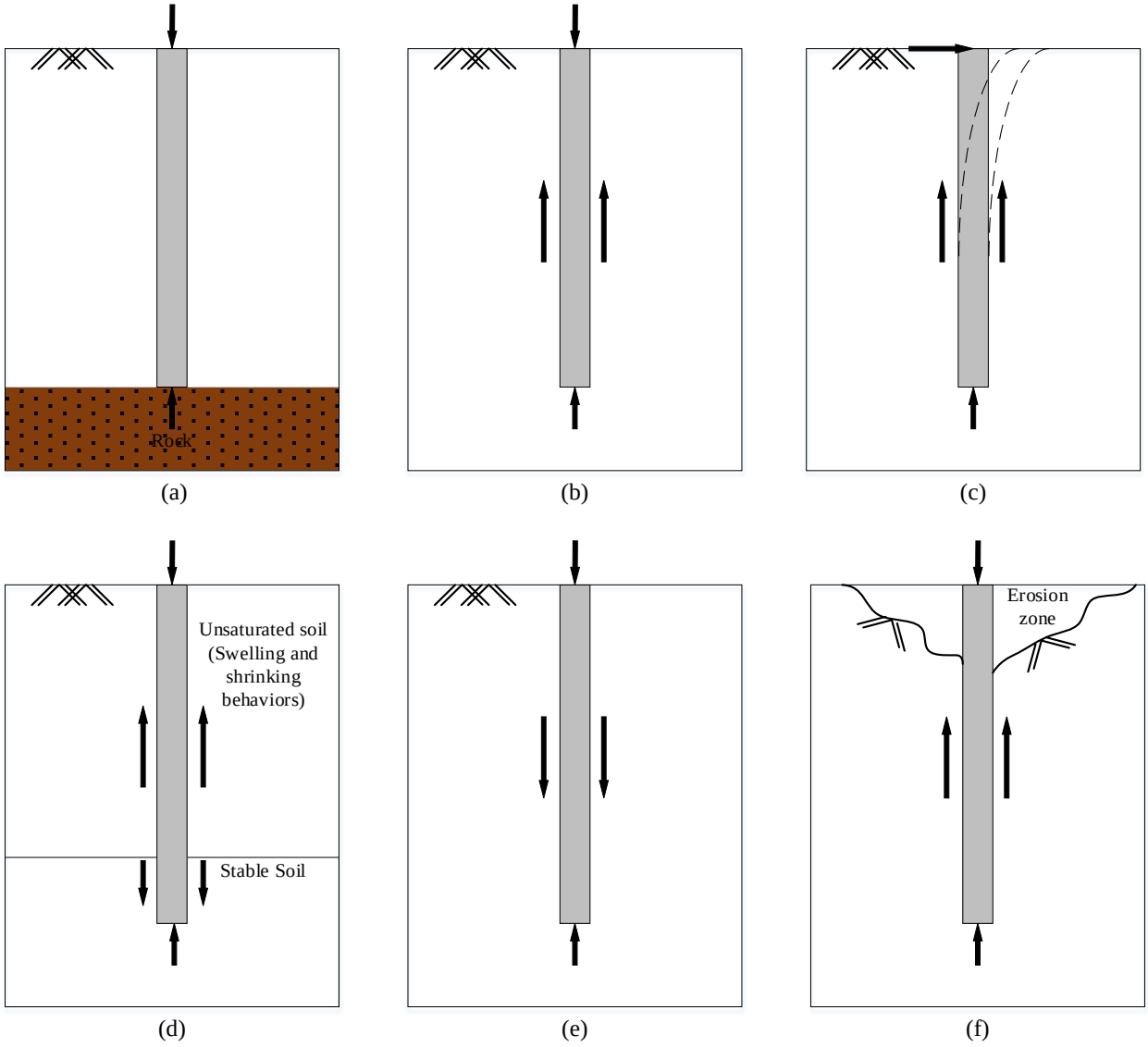

Figure 2-1. Different Soil/Rock Conditions with Embedded Pile (after Vesic, 1977).

2.2 LATERAL BEHAVIOR OF PILE FOUNDATIONS/DRILLED SHAFTS

Over the years, numerous analytical methods have been developed to predict the behavior of piles subjected to the lateral loading. Based on the method used in modeling, the analytical methods in the literature can be classified into the following groups:

- P-y method based on the Winkler model (e.g., Matlock, 1970; Reese et al., 1975).
- Soil continuum-based on elastic solutions (e.g., Poulos, 1971; Banerjee and Davies 1978; Randolph, 1981).

- Finite element or finite difference approaches (e.g., Comodromos and Pitilakis, 2005; Ahmed and Hawlader, 2016).
- Force and moment equilibrium-based solutions (e.g., Motta, 2012; Zhang and Ahmari, 2013).
- The strain wedge model (e.g., Ashour et al., 2002).

Although the P-y curve method has been used in practice for decades, its reliability and applicability are being challenged when applied to the design of larger diameter monopile. In this project, researchers focused on the behavior of large diameter single piles (B > 5 ft) subjected to monotonic lateral loading and the use of the P-y curve approach (Figure 2-2).

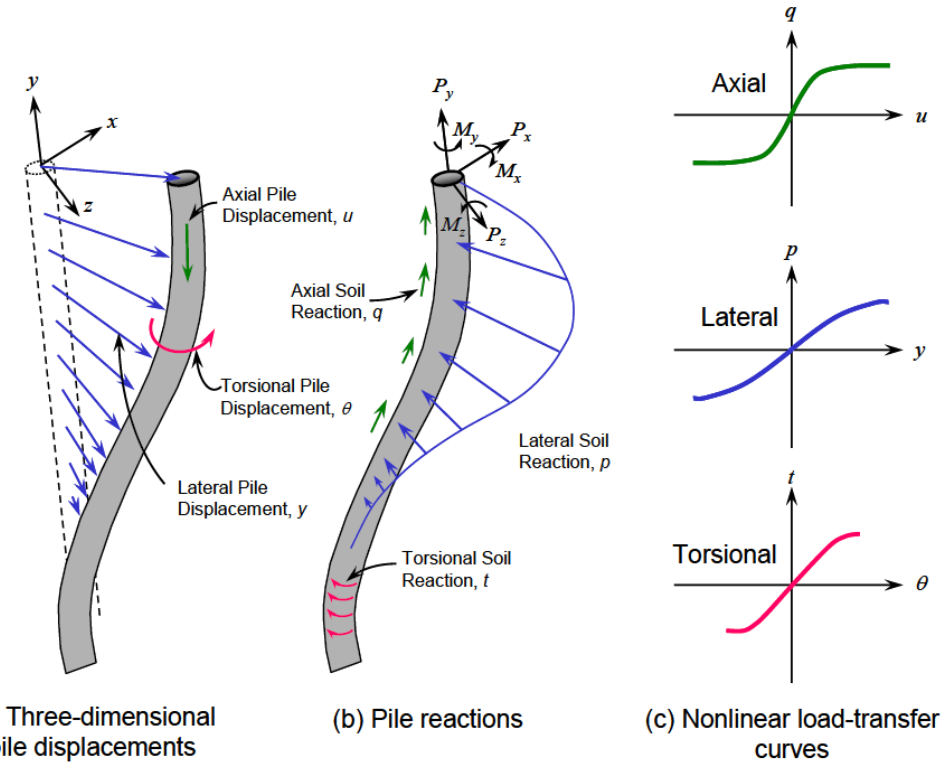

Figure 2-2. Three-Dimensional Soil-Pile Interaction (Isenhower and Wang, 2016).

CHAPTER 3 P-Y CURVES

3.1 INTRODUCTION

In this chapter, the P-y curves for cohesive and cohesionless soil are presented. Note that the P in the P-y curve represents the load per unit length of pile generated by the soil against the pile for a lateral deflection equal to y. The lower case p will refer to the average pressure generated by the line load P over the width B of the pile.

$$p = P/B \tag{1}$$

In the latest version of LPILE (2018) released by Ensoft Inc. in May 2018, there is a total of 16 different P-y curves available for the user. They are:

- Soft clay.
- API soft clay with user-defined J.
- Stiff clay with free water.
- Stiff clay without free water.
- Modified stiff clay without free water.
- Sand.
- API sand.
- Liquefied sand.
- Liquefied sand hybrid.
- Weak rock.
- Strong rock.
- Piedmont residual.
- Silt.
- Loess.
- Elastic subgrade.
- API soft clay with J and massive rock P-y.
- User input.

Recommendations from Matlock (1970) for soft clay (option 1), Reese et al. (1975) for stiff clay (option 4), Reese et al. (1974) for sand (option 6), and American Petroleum Institute (API, 2010) for sand (option 7) are described next.

A pile installed in the ground can be loaded vertically or laterally. A vertical pile load test gives a load-settlement curve as shown in Figure 3-1, while a lateral pile load test gives a curve as shown in Figure 3-2. The lateral load is H_o and the lateral deflection y_o. Lateral loads include waves on offshore foundations, vessel impact on bridge piers, earthquake vibrations, breaking forces from vehicles, and wind.

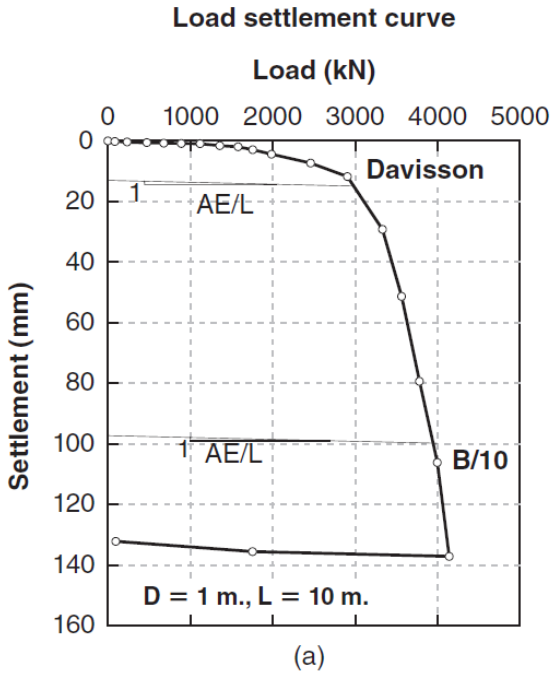

Figure 3-1. Load Settlement Curve (Briaud et al., 2013).

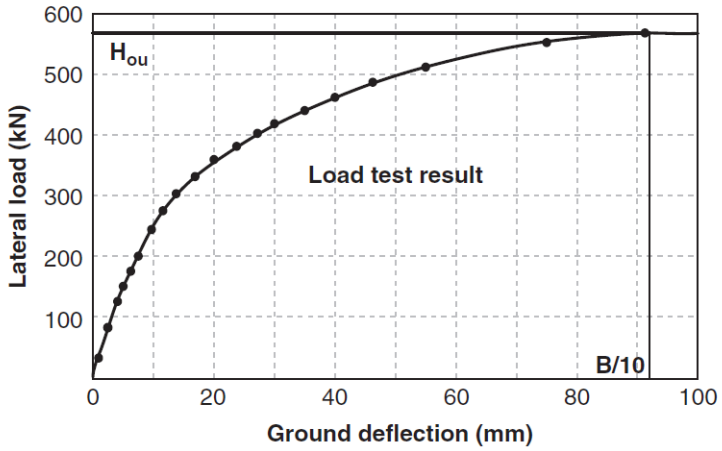

Figure 3-2. Example Load Test Result (Briaud, 1997).

The P-y curve method has become the most popular method for the analysis of laterally loaded piles. It seems to have originated in the mid-1950s (McClelland and Focht, 1956). At that time, the development of digital computers and associated programs for solving the nonlinear, fourth-order differential equation and the development of electrical resistance strain gauges to measure the bending moment in full-scale lateral pile load tests made implementation of the method possible. The P-y curves were established based on the analysis of the results of full-scale load tests on instrumented piles.

Looking at a pile cross section (Figure 3-3(a)), there is first a uniform distribution of stresses normal to the wall of the unloaded pile. When the pile is loaded laterally, the distribution of stresses becomes non-uniform (Figure 3-3(b)), where P is the line load resulting from the stress distribution and y represents the deflection of the pile.

The typical model in LPILE is shown in Figure 3-4 where the pile is subjected to an axial load, a lateral load, and an overturning moment. In LPILE, the axial load is included because it has an impact on bending and therefore lateral displacement. However, the vertical settlement is not calculated. The soil around the pile is represented as springs reflecting the nonlinear behavior of the soil resistance P as a function of pile deflection y. In Figure 3-4, the first curve shows that the pile may deflect a finite distance without soil resistance to simulate a possible gap between the pile and the soil at shallow depth. The subsequent curves show a gradual stiffening and strengthening of the soil with depth.

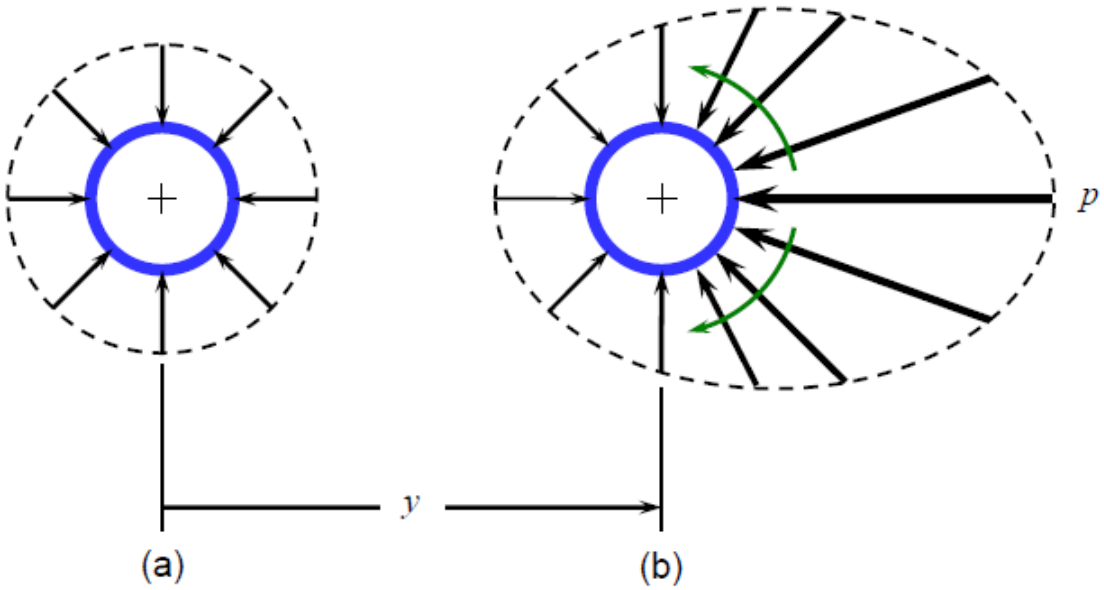

Figure 3-3. Distribution of Stresses Acting on a Pile, (a) before Lateral Deflection and (b) after Lateral Deflection (Isenhower and Wang, 2016).

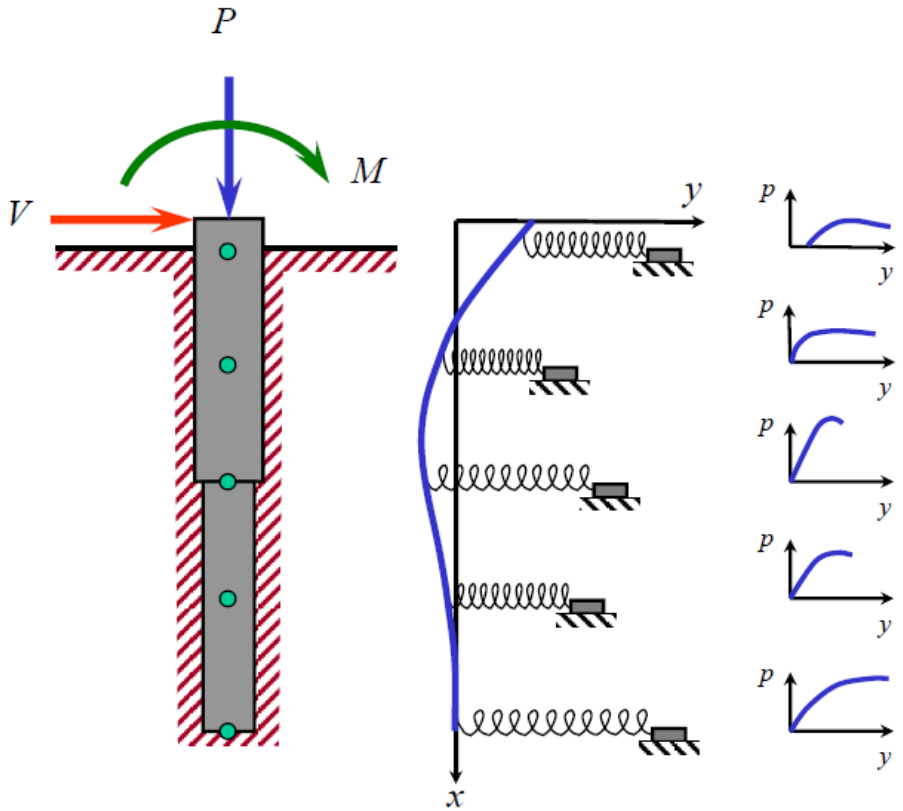

Figure 3-4. Model of a Pile under Lateral Loading and P-y Curves (Isenhower and Wang, 2016).

3.2 P-Y CURVE FOR COHESIVE SOILS

The P-y curves for a cohesive soil loaded monotonic by a pile are presented here. A typical P-y curve describes the lateral-load transfer along the pile as a function of depth and deflection. In either a uniform soil or a layered soil, the P-y curve changes with depth. The factors needed to prepare the P-y curve are the pile properties, the soil properties, and the loading type and magnitude.

Figure 3-5 shows a series of P-y curves for cohesive soils. In Figure 3-5, from the origin O to point a, the straight line reflects the linearity between p and y. Indeed it is often assumed that there is a linear relationship between p and y for small values of y. The portion of the curve in Figure 3-5(a) from point a to point b describes the nonlinearity associated with the nonlinear stress-strain behavior of the natural soil. There is no accepted analytical procedure to describe the a-b portion of the P-y curve (Isenhower and Wang, 2016). The lateral, straight-line portion of the P-y curve beyond point b in Figure 3-5(a) expresses that the soil behavior is plastic with no loss of shear strength with further displacement. This part of the curve corresponds to the ultimate resistance p_u, which is influenced by the pile properties, the soil properties, and the depth below the ground surface. At failure and close to the ground surface, the soil mass moves laterally and vertically. At failure and at large depth, the soil moves laterally only and the value of p_u is calculated differently.

The difference between Figure 3-5(a) and (b) is associated with strain softening at larger strains (point c to point d) that can be due to cyclic loading. The shaded area shows the loss of resistance, which depends on the number of cycles of loading. Figure 3-5(c) shows the possible effect of sustained, long-term loading. The decreasing value of p implies that the resistance is transferred to other soil zones along the pile as the pile head displacement increases under constant load. According to Isenhower and Wang (2016), the effect of sustained loading should be negligible at small displacement, for heavily overconsolidated clays, and for granular soils. The effect for soft clays can be significant and can be predicted based on a power law model (Briaud, 2013).

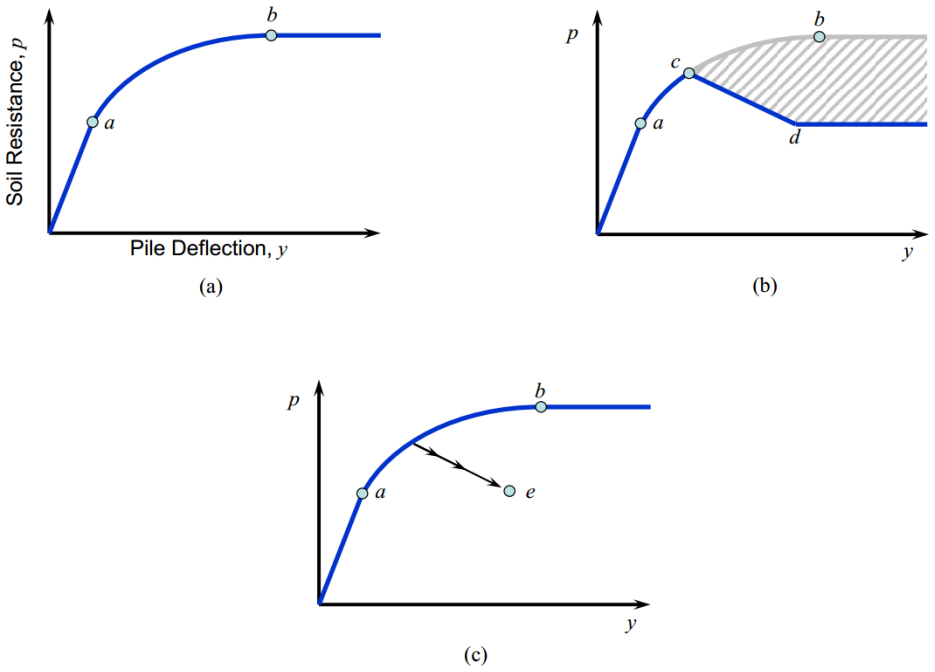

Figure 3-5. Conceptual P-y Curve (Isenhower and Wang, 2016).

3.2.1 The Ultimate Lateral Resistance

The ultimate lateral resistance P_u (force per unit length) of the soil in clay is a function of the lateral bearing capacity factor N_p, the undrained shear strength S_u, and the pile diameter B (Zhang and Ahmari, 2013):

$$P_u = N_p S_u B \tag{2}$$

$$\text{With } N_p = N_{P0} + N_{Pw} \leq N_{Pd} \tag{3}$$

Where N_{p0} is the bearing capacity factor associated with the ultimate resistance of a shallow passive pressure wedge in front of the pile assuming a weightless soil, N_{pw} is the bearing capacity factor due to the weight of that shallow wedge ($\gamma z/S_u$), and N_{pd} is the bearing capacity factor at large depth due to a flow mechanism around the pile shaft.

Several researchers have provided recommendations for N_p. Table 3-1 presents the historic development of the N_p starting with Reese (1958) all the way to Zhang et al. (2016). As an example, the value of N_p according to Jeanjean et al. (2017) is in the range of 3~5 at shallow depth and from 7~12 at larger depth (Figure 3-6). The ultimate values for sand are discussed in the section 3.3.

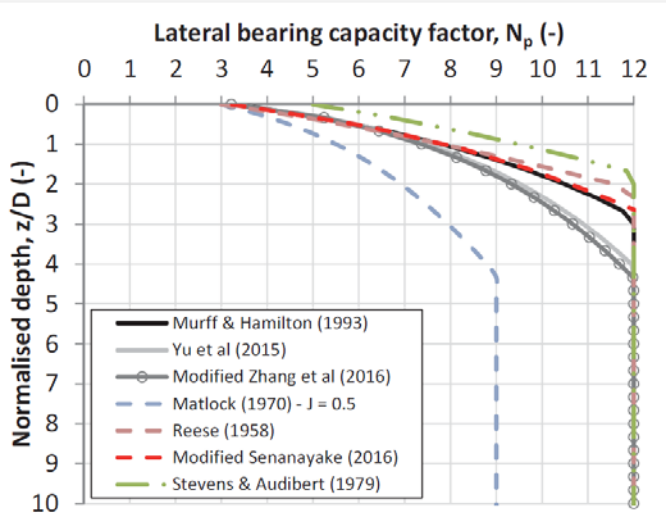

Figure 3-6. Comparison of Bearing Capacity Factors for B = 3 ft (Jeanjean et al., 2017).

Table 3-1. Summary of Recommendations for Lateral Bearing Capacity Factors (after Jeanjean et al., 2017).

Reference: Reese (1958)
$N_{p0} = 2 + 2.83(\frac{z}{D})$-smooth pile and $N_{pd} = 12$ $N_{p0} = 3 + 2.83(\frac{z}{D})$-rough pile and $N_{pd} = 12$ • Used with assumption of gapping on the back side. • Applicable to constant shear strength profiles. • N_{p0} derived from simplified wedge analysis with 45° wedge angle constant with depth. • N_{pd} calculated from limit equilibrium analysis of full flow mechanism around a rough square pile.
Reference: Matlock (1962, 1970)
$N_{p0} = 3 + J(\frac{z}{D})$ -smooth pile and $N_{pd} = 9$ • N_{p0} formulation implies a rough pile. • Used with assumption of gapping on the back side. • N_{p0} derived from 1-g field scale tests on soft clays at Lake Austin (s_u ~ 5.5psi (38 kPa)) and Sabine River (s_u ~ 1.7-2.9psi (12–20 kPa)). • J = 0.5 for linearly increasing shear strength profiles (Sabine River tests). J = 0.25 for constant shear strength profiles (Lake Austin tests). • N_{pd} assumed from industry consensus.
Reference: Reese et al. (1975)
$N_{p0} = 2 + 2.83(\frac{z}{D})$- and $N_{pd} = 11$ • Method derived from Reese (1958) for a smooth pile. • Used with assumption of gapping on the back side. • N_{p0} used to analyze 1-g field tests at Manor, TX, on stiff slickensided clays (~14.5psi (100 kPa) < su < ~29psi (200 kPa)). • N_{pd} harmonized from limit equilibrium analysis of full flow mechanism around a rough square pile and recommendations in McClelland and Focht (1958).

Reference: Stevens and Audibert (1979)

$N_{p0} = 5 + 2.5\left(\frac{z}{D}\right)$ and $N_{pd} = 12$

Expression of N_{p0} is based on Reese (1958) formulation.

Empirical recommendation based on range of measured values on seven series of 1 g tests on piles of diameter between 0.28 m and 1.5 m (11 in. and 59 in.)

Formulation implies gapping and a rough pile.

Reference: Sullivan et al. (1980)

N_{po} is the smaller of two following values:

$N_{p0} = 2 + 0.833\left(\frac{z}{D}\right)$- and $N_{p0} = 3 + 0.5\left(\frac{z}{D}\right)$ with $N_{pd} = 9$

- The total N_p factor is calculated by adding the weight of the wedge term only to the first equation. The total Np factor is therefore the smallest of $N_{p0} = 2 + 0.833\left(\frac{z}{D}\right) + \frac{\gamma}{S_u}$ and $N_{p0} = 3 + 0.5\left(\frac{z}{D}\right)$
- The first expression implies a smooth pile and gapping whereas the second expression implies a rough pile with gapping in a weightless soil. N_{pd} implies a smooth pile.

Reference: Randolph and Houlsby (1984)

$N_{pd} \sim 9 + 3\alpha$ or $N_{pd} \sim 9.14 + 4.1\alpha - 1.34\alpha^2$

- Used limit analysis of plane strain flow around cylindrical pile.
- No allowance for gapping on back side of pile and elastic deformation of soil.
- N_{pd} linear fit with α suggested for most engineering applications.
- N_{pd} quadratic fit with α provided in Randolph (2013).

Reference: Murff and Hamilton (1993)

$N_{p0} = N_{pd} - N_2 \exp(-\frac{\xi z}{D})$

$N_2 = 7 + 1.5\alpha$

$\xi = 0.25 + 0.05\lambda$ for $\lambda < 6$ and $\xi = 0.55$for $\lambda \geq 6$

$\lambda = \frac{s_{u1}}{s_{u1} D}$

$N_{pd} \sim 9 + 3\alpha$

- N_{p0} derived from upper bound analysis of 3D conical wedge collapse mechanism.
- Not a rigorous solution since some energy dissipation terms neglected and transition from wedge to flow around mechanism not continuous (Klar and Randolph, 2008).
- Developed for purely translating pile, but case of pile constrained to rotate about its tip gave identical results.
- N_{pd} taken from Randolph and Houlsby (1984).
- In the original publication, N_{pd} was noted as N_1.

Reference: Liang et al. (2007)

$P = \frac{y}{\frac{1}{K_i} + \frac{y}{P_{ult}}}$

$K_i = 0.943\left(\frac{Z}{Z_{ref}}\right)^{0.016}\left(\frac{D}{D_{ref}}\right) v_s^{-0.078} E_s^{1.036} E_p^{-0.031}$ and $Z_{ref} = 1.0\ m\ (3.28\ ft)$ and $D_{ref} = 1.0\ m\ (3.28\ ft)$

$N_p = N_{p0} + N_{pw} \leq N_{pd}$ and $N_{pd} = 10$

Reference: Jeanjean (2009)

$N_{p0} = N_{pd} - N_2 \exp(-\frac{\xi z}{D})$ with $N_2 = 4$ and $N_{pd} = 12$

$\xi = 0.25 + 0.05\lambda$ for $\lambda < 6$ and $\xi = 0.55$for $\lambda \geq 6$

$\lambda = \frac{s_{u0}}{s_{u1} D}$

Formulation used for no gapping case only. The expression is not N_{p0}. The expression of N_p includes the resistance of both the passive and active wedges.

Expression of N_p is modified from Murff and Hamilton (1993) formulation for N_{p0}.

Empirical recommendation based on range of values measured in centrifuges tests on soft kaolin clay and calculated from FEA. No gapping observed in tests.

Formulation implies a rough pile.

Reference: Yu et al. (2015)

$N_{p0} = N_1 - (1 - \alpha) - (N_1 - N_2)[1 - \left(\frac{z}{14.5}\right)^{0.6}]^{1.35}$

$N_1 = 11.94$; $N_2 = 3.22$

$N_{pd} \sim 9.14 + 2.8\alpha$

- N_{p0} derived from upper bound analysis of translating pile.
- Wedge collapse mechanism improved from Murff and Hamilton (1993) by assuming curved surface.
- Verified against 3D ALE adaptive remeshing FEA.
- N_{pd} taken from Randolph and Houlsby (1984).

Reference: Senanayake (2016)

$N_{p0} = 2 + \sqrt{2}\left(\frac{2S_{u0} + S_{u1} z}{S_{u0} + S_{u1} z}\right)\left(\frac{z}{D}\right)$

With $N_{pd} = 9$ for $\alpha = 0$ and 12 for $\alpha = 1$.

- Method applicable to constant and linearly increasing shear strength profiles.
- N_{p0} derived from Reese (1958) wedge geometry for smooth pile and with constant wedge angle ($\beta = 45°$).
- N_{pd} from Randolph and Houlsby (1984) limit analysis.

Reference: Jeanjean et al. (2017) labeled as "Modified Senanayake (2016)"

$N_{p0} = \frac{1}{sin\beta cos\beta} + \frac{\alpha\pi}{2} cot\beta + \frac{2S_{u0} + S_{u1} z}{(S_{u0} + S_{u1} z) cos\beta}\left(\frac{z}{D}\right)$ with $N_{pd} = 9 + 3\alpha$

- Method applicable to constant and linearly increasing shear strength profiles.
- N_{p0} derived from Reese (1958) wedge geometry for any pile adhesion, α, as a function of wedge angle, β.
- N_{p0} is calculated at each depth, z, by minimizing the value of N_{p0} with respect to β.
- N_{pd} from Randolph and Houlsby (1984) limit analysis.

Reference: Zhang et al. (2016)

$N_{p0} = N_1 - (1 - \alpha) - (N_1 - N_2)[1 - \left(\frac{z}{dD}\right)^{0.6}]^{1.35}$

$N_1 = 11.94$; $N_2 = 3.22$

$d = 16.8 - 2.3 \log_{10}(\lambda) \geq 14.5$

$N_{pd} \sim 9.14 + 2.8\alpha$

- Method adapted from Yu et al. (2015).
- Refined calibration of method against FEA with linear increasing strength profiles.

Reference: Jeanjean et al. (2017) labeled as "Modified Zhang et al. (2016)"
$N_{p0} = N_1 - (1-\alpha) - (N_1 - N_2)[1 - \left(\frac{z}{dD}\right)^{0.6}]^{1.35}$ $N_1 = 11.94$; $N_2 = 3.22$ $d = 16.8 - 2.3\log_{10}(\lambda) \geq 14.5$ $N_{pd} \sim 9 + 3\alpha$ Modified using N_{pd} linear fit with α suggested for most engineering applications by Randolph and Houlsby (1984).

3.2.2 Procedures for Computing P-y Curves in Clay

In this section, the P-y curve criteria developed by Matlock (1970) and Reese and Welch (1975) are described. Matlock's model was developed based on a series of lateral load tests on an instrumented steel-pipe pile that was 12.75 in. in diameter and 42 ft in length. The average undrained shear strength of the clay was about 800 psf. Reese and Welch (1975) performed a series of lateral load tests with a drilled shaft (bored pile) that was 36 in. in diameter. The average undrained shear strength of the clay was about 2200 psf in the upper 20 ft. The procedures to generate those two P-y curves are described below.

3.2.3 Soft Clay Criterion (Matlock)

The steps for computing the P-y curves in soft clay (Matlock) for static loading are listed:

1. Select the best possible estimate of the variation of undrained shear strength and effective unit weight with depth. Also obtain the value of ε_{50}, the normal strain corresponding to one-half the maximum principal stress difference in a triaxial test. If no stress-strain curves are available, typical values of ε_{50} are given in Table 3-2 (Isenhower and Wang, 2016).

Table 3-2. Representative Values of ε_{50} for Soft to Stiff Clays (Isenhower and Wang, 2016).

Consistency of Clay	ε_{50}
Soft	0.020
Medium	0.010
Stiff	0.005

2. Use conservative values of undrained shear strength to compute the ultimate soil resistance per unit length of pile as follows:

$$P_u = 9 \times S_u \times B \quad (4)$$

$$P_u = \left(3 + \frac{\gamma'_{avg}}{Su}x + \frac{J}{B}x\right) S_u \times B \quad (5)$$

Where

γ'_{avg} = average effective unit weight from the ground surface down to the P-y curve considered, pci (kN/m3).

x = depth from the ground surface to the P-y curve, in. (m).

S_u= undrained shear strength at depth x, psi (kN/m^2)

B = width of pile, ft (m)

J = 0.5 for soft clay, is a dimensionless fitting coefficient to better fit the observed data.

3. Compute the deflection corresponding to one-half the ultimate soil resistance, y_{50}, as follows:

$$y_{50} = 2.5 \times \epsilon_{50} \times B \quad (6)$$

4. Compute points describing the P-y curve from the origin up to 8 y_{50} using:

$$P = \frac{P_u}{2}\left(\frac{y}{y_{50}}\right)^{1/3} \quad (7)$$

The value of P remains constant for y values beyond 8 y_{50}.

3.2.4 Stiff Clay Criterion (Reese)

The steps for computing the P-y curves in stiff clay (Reese) for static loading without free water are:

1. Select the best possible estimate of the variation of undrained shear strength and effective unit weight with depth. Also obtain the value of ε_{50}, the normal strain corresponding to one-half the maximum principal stress difference in a triaxial test. If no stress-strain curves are available, typical values of ε_{50} are given in Table 3-2.
2. Use conservative values of undrained shear strength to compute the ultimate soil resistance per unit length of pile, given by Equations (3) and (4) in section 3.2.2, but with J = 0.25 for stiff clay.
3. Compute the deflection at one-half the ultimate soil resistance, y_{50}, from the following equation:

$$y_{50} = 2.5 \times \epsilon_{50} \times B \tag{8}$$

4. Compute points describing the P-y curve from the origin up to 16 y_{50} using:

$$\mathrm{P} = \frac{P_u}{2}\left(\frac{y}{y_{50}}\right)^{1/4} \tag{9}$$

The value of P remains constant for y values beyond 16 y_{50}.

3.2.5 Example Curve for Cohesive Soil

An example for generating a P-y curve in cohesive soil is presented below. Table 3-3 lists the parameters. The steps are as follows:

Table 3-3. Assumed Parameters for Generating P-y Curves in Clay.

Soil type	γ, pcf	B, ft	ε_{50}	Su, psf
Soft Clay	127.3	1.0	0.02	1044

1. From Table 3-3, ε_{50} = 0.02
2. For soft clay, J=0.5

$$P_u = \left[9 \times S_u \times B, \left(3 + \frac{\gamma'_{avg}}{Su}x + \frac{J}{B}x\right) S_u \times B\right]$$

$$= \left[9 \times 1044 \times 1.0, \left(3 + \frac{127.3}{1044} \times 1 + \frac{0.5}{1.0} \times 1.0\right) 1044 \times 1.0\right]$$

$$= [9336, 3781.3] = 3781.3\frac{\text{lb}}{\text{ft}} = 315.1 \text{ lbs/in}$$

3. $y_{50} = 2.5 \times \epsilon_{50} \times B = 2.5 \times 0.02 \times 1.0 \times 12 = 0.6\ in$
4. $\mathrm{P} = \frac{P_u}{2}\left(\frac{y}{y_{50}}\right)^{1/3}$, which means $\mathrm{y} = \mathrm{y}_{50}\left[2\left(\frac{P}{P_u}\right)\right]^3$

For several values of P the corresponding value of y is calculated:

P=0 lb, $\mathrm{y} = \mathrm{y}_{50}\left[2\left(\frac{P}{P_u}\right)\right]^3 = 0.6\left[2\left(\frac{0}{315.1}\right)\right]^3 = 0$ in

P=10 lb, $\mathrm{y} = 0.6\left[2\left(\frac{10}{315.1}\right)\right]^3 = 0.00015$ in

…

P=300 lbs, $y = 0.6\left[2\left(\frac{300}{315.1}\right)\right]^3 = 4.142\ in$

P=320 lbs,$y = 0.6\left[2\left(\frac{320}{315.1}\right)\right]^3 = 5.027\ in > 8\ y_{50}$, where $8\ y_{50} = 8 \times 0.6 = 4.8$ in

The value of P remains constant for y values beyond 8 y50 (P=315 lb in this case).

5. Plot the P-y curve based on Matlock (1970) recommendations with P on the vertical axis and y on the lateral axis as shown in Figure 3-7.

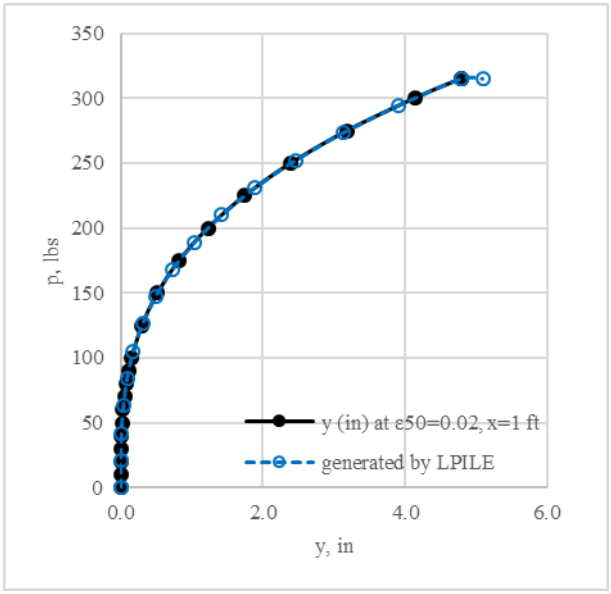

Figure 3-7. Example P-y Curve for Soft Clay with No Free Water, Static Loading by Following the Recommendations by Matlock (1970).

3.3 P-Y CURVE FOR COHESIONLESS SOILS

3.3.1 Procedures for Computing P-y Curves in Sand

Figure 3-8 shows the model used for computing the ultimate resistance for piles in sand at shallow depth. As shown in Figure 3-8(c), the total lateral force F_{pt} may be computed by subtracting the active force F_a from the passive force F_p. The force F_a is computed by use of Rankine theory, and F_p is computed by considering the wedge shown in Figure 3-8(a) and assuming that the Mohr-Coulomb failure condition is satisfied on the side planes ADE and BCF and on the sloping wedge surface AEFB. The directions of the resultant forces in the model can be found in Figure 3-8(b).

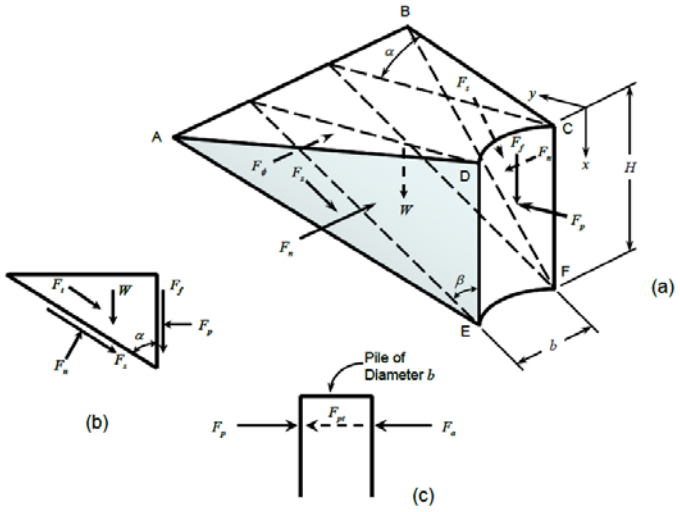

Figure 3-8. Geometry Assumed for Passive Wedge Failure for Pile in Sand (Isenhower and Wang, 2016).

The resulting equation for the total lateral force F_{pt} is:

$$F_{pt} = \gamma H^2 \left[\frac{K_0 H tan\phi tan\beta}{3\tan(\beta-\phi)\cos\alpha} + \frac{tan\beta}{\tan(\beta-\phi)}\left(\frac{\beta}{2} + \frac{H}{3}tan\beta tan\alpha\right)\right] + \gamma H^2\left[\frac{K_0 H tan\beta}{3}(tan\phi sin\beta - tan\alpha) - \frac{K_A B}{2}\right] \quad (10)$$

Where

α = the angle of the wedge in the lateral direction, degree.

β = is the angle of the wedge with the ground surface, degree.

B = is the pile diameter, ft (m).

H = the height of the wedge, ft (m).

K_0 = coefficient of earth pressure at rest.

K_A = coefficient of active earth pressure.

The ultimate soil resistance close to the ground surface per unit length of pile P_{usa} is obtained by differentiating Equation (9) with respect to the depth H:

$$P_{u_{sa}} = \gamma H\left[\frac{K_0 H tan\phi sin\beta}{\tan(\beta-\phi)\cos\alpha_s} + \frac{tan\beta}{\tan(\beta-\phi)}(B + H tan\beta tan\alpha)\right] + \gamma H[K_0 H tan\beta(tan\phi sin\beta - tan\alpha) - K_A B] \quad (11)$$

Bowman (1958) performed some model tests with a small flat plate in sand and suggested values of α equal to ϕ/3 to ϕ/2 for loose sand and ϕ for dense sand. The value of β is taken as:

$$\beta = 45° + \frac{\phi}{2} \tag{12}$$

The failure model at some distance below the ground surface is assumed to be as shown in Figure 3-9. Referring to this model, block 1 will fail in shear along the dashed line. Block 2 will also fail by shearing along the dashed line, and block 3 will slide laterally. Block 4 will fail by being pushed as shown in the figure, and block 5 will fail as the pile pushes against it. The stress σ_1 at the back of the pile cannot be less than the minimum active earth pressure, or the soil could slump from the ground surface against the pile. In Figure 3-9(b), the states of stress are assumed and the ultimate soil resistance for lateral movement of the soil may be computed as:

$$P_{u_{sb}} = K_A B\gamma H(tan^8\beta - 1) + K_0 B\gamma H tan\phi tan^4\beta \tag{13}$$

Where P_{usb} is the force per unit length with lateral flow around the pile.

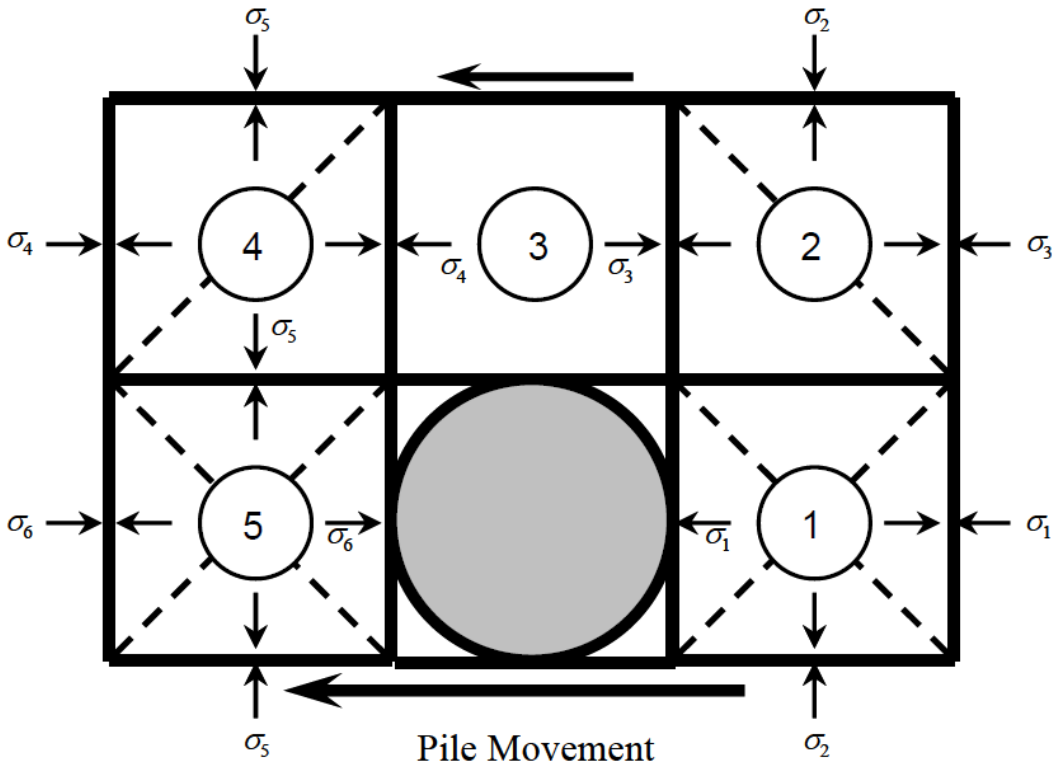

(a)

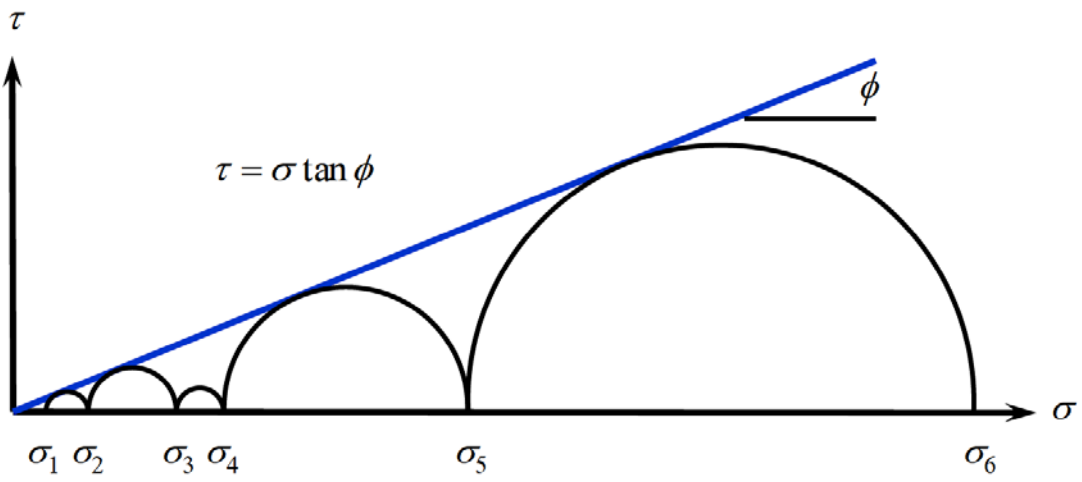

(b)

Figure 3-9. Assumed Mode of Soil Failure by Lateral Flow around Pile in Sand (a) Section though Pile, (b) Mohr-Coulomb Diagram (Isenhower and Wang, 2016).

The P-y curves developed by Reese and API are described in the following paragraphs.

3.3.2 Sand Criterion (Reese)

The steps for computing a P-y curve in sand are as follows (Reese et al., 1974):

1. For the depth x of the P-y curve considered, obtain the angle of internal friction Φ, effective unit weight of soil γ, and pile diameter B (Note: use the effective unit weight for sand below the water table and total unit weight for sand above the water table).
2. Compute the following parameters:

$$\alpha = \frac{\phi}{2} \tag{14}$$

$$\beta = 45° + \frac{\phi}{2} \tag{15}$$

$$K_A = \tan^2(45° - \frac{\phi}{2}) \tag{16}$$

3. Compute the ultimate soil resistance per unit length of pile, P_s, using the smaller of P_{st} or P_{sd}, where P_{st} is the soil resistance near the ground surface and P_{sd} is the soil resistance well below the ground surface:

$$P_s = \min[P_{st}, P_{sd}] \tag{17}$$

Where,

$$P_{st} = \gamma x \left[\frac{K_0 x tan\phi sin\beta}{\tan(\beta-\phi)\, cos\alpha} + \frac{tan\beta}{\tan(\beta-\phi)}(B + x tan\beta tan\alpha) + K_0 x tan\beta(tan\phi sin\beta - tan\alpha) - K_A B\right] \quad (18)$$

$$P_{sd} = K_A B\gamma x(\tan^8\beta - 1) + K_0 B\gamma x tan\phi \tan^4\beta \quad (19)$$

4. Compute the y_u value defining the abscissa of point u in Figure 3-10.

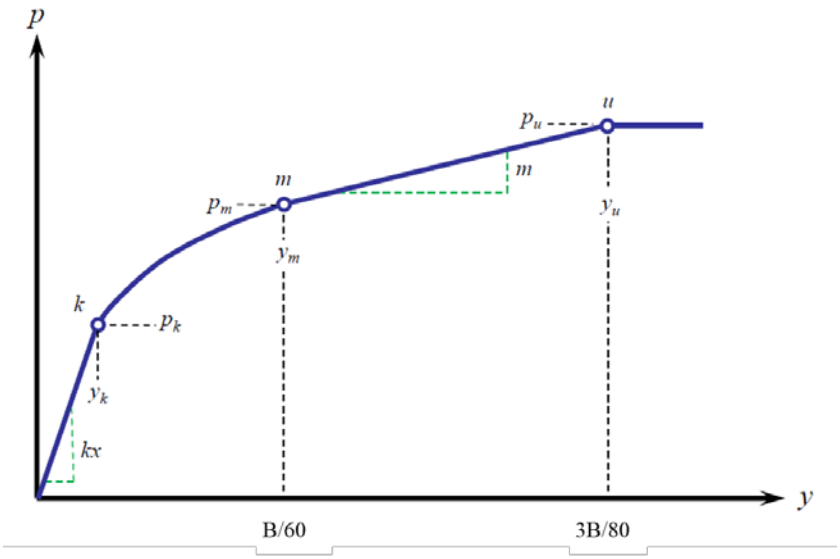

Figure 3-10. Characteristic Shape of P-y Curves for Static Loading in Sand (Isenhower and Wang, 2016).

$$y_u = \frac{3B}{80} \quad (20)$$

5. Compute the P_u value defining the ordinate of point u for static loading conditions using:

$$P_u = \overline{A_s} P_s \quad (21)$$

or for cyclic loading conditions using:

$$P_u = \overline{A_c}\, P_s \quad (22)$$

6. Obtain the appropriate value of As or Ac from Figure 3-11 as a function of the non-dimensional depth and the type of loading (either static or cyclic). Compute P_s using Equation (18) or (19).

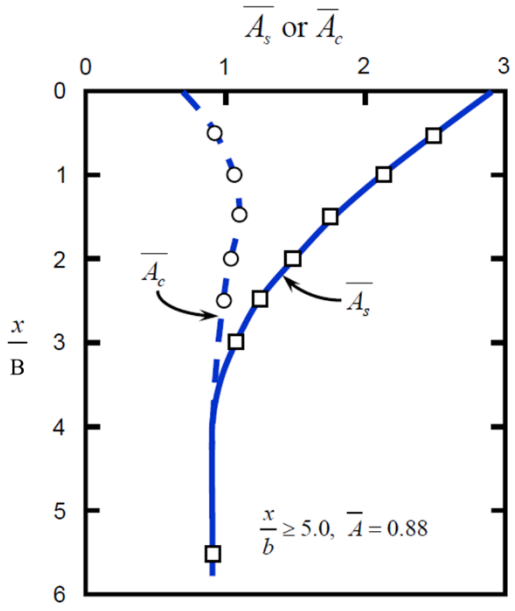

Figure 3-11. Values of Coefficients Ac and As for Cohesionless Soils (Isenhower and Wang, 2016).

7. Compute y at point m as shown in Figure 3-10 by using:

$$y_m = \frac{B}{60} \tag{23}$$

8. Compute p_m at point m for static loading conditions using:

$$p_m = B_s P_s \tag{24}$$

or for cyclic loading conditions using:

$$p_m = B_c P_s \tag{25}$$

9. Obtain the appropriate value of B_s or B_c from Figure 3-12 as a function of the nondimensional depth and the type of loading (either the static or cyclic). Use Equation (18) or Equation (19) to obtain values of P_s and keep the smallest one. The

two straight-line portions of the P-y curve beyond the point where y is equal to B/60 can now be determined.

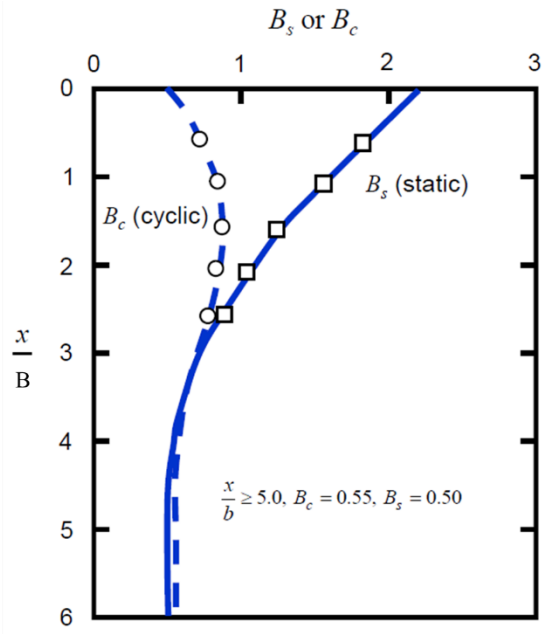

Figure 3-12. Values of Coefficients Bc and Bs for Cohesionless Soils (Isenhower and Wang, 2016).

10. Establish the initial straight-line portion of the P-y curve:

$$P = (kx)y \tag{26}$$

The constant k is introduced in the formula to obtain the modulus of deformation of the soil and allow it to increase with depth:

$$E_s = kx \tag{27}$$

Where k is a constant giving the variation of the soil modulus with depth, and x is the depth below the ground surface. Use the appropriate value of k from Table 3-2 and Table 3-3. If the k value is left equal to zero, the software LPILE will compute a default value using the curves shown in Figure 3-13 and the input friction angle. If the input value of ϕ is greater than 45°, a k value corresponding to 45° is used by LPILE. The sand will be considered to be below the water table if the effective unit weight is less than 77.76 pcf (12.225 kN/m^3).

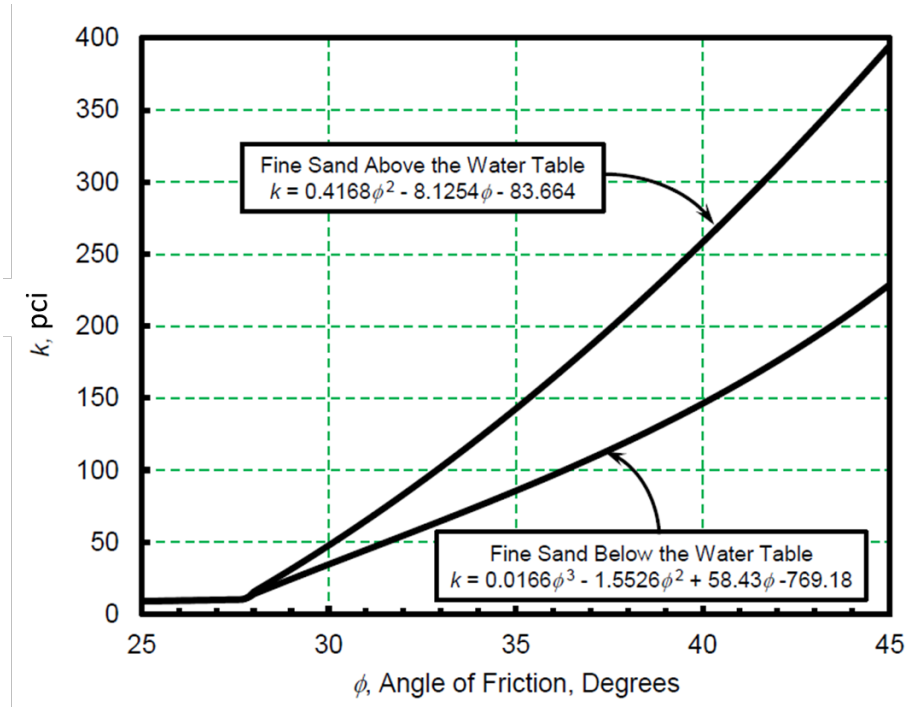

Figure 3-13. Value of k versus Friction Angle for Fine Sand Used in LPILE (Isenhower and Wang, 2016).

Table 3-4. Representative Values of k for Fine Sand below the Water Table for Static and Cyclic Loading (Isenhower and Wang, 2016).

Recommended k	Relative Density		
	Loose	Medium	Dense
MN/m^3 (pci)	5.4 (20.0)	16.3 (60.0)	34 (125.0)

Table 3-5. Representative Value of k for Fine Sand above Water Table for Static and Cyclic Loading (Isenhower and Wang, 2016).

Recommended k	Relative Density		
	Loose	Medium	Dense
MN/m^3 (pci)	6.8 (25.0)	24.4 (90.0)	61.0 (225.0)

If the sand is a coarse or a well-graded sand, the user may consider using a higher value of k than those suggested in Table 3-4 and Table 3-5. While there are very little experimental data for k in well-graded sands, using values that are 10 to 50 percent higher than those in the

tables may be appropriate in dense and very dense well-graded sands with no compressible minerals such as mica.

11. Fit the parabola between point k and point m as follows (Figure 3-10):

    a. Compute the slope of the P-y curve between point m and point u using:

$$\mathrm{m} = \frac{P_u - P_m}{y_u - y_m} \tag{28}$$

    b. Compute the power of the parabolic section using:

$$\mathrm{n} = \frac{P_m}{m y_m} \tag{29}$$

    c. Compute the coefficient $\bar{C}$ using:

$$\bar{C} = \frac{P_m}{y_m^{1/n}} \tag{30}$$

    d. Compute the y value defining point k using:

$$\mathrm{y_k} = \left(\frac{\bar{C}}{kx}\right)^{\frac{n}{n-1}} \tag{31}$$

    e. Compute the p_k value defining point k using:

$$\mathrm{P_k} = kx y_k \tag{32}$$

    f. Compute the p and y values along the parabolic section of the P-y curve between points k and m using:

$$\mathrm{P} = \bar{C} y^{1/n} \tag{33}$$

3.3.3 Sand Criterion (API)

For the API sand criterion, the steps are as follows:

1. Obtain the values for the angle of internal friction ϕ, the effective unit weight of soil, γ', and the pile diameter B.
2. Compute the ultimate soil resistance at the depth *x* of the P-y curve considered. The ultimate lateral bearing capacity (ultimate lateral resistance Pu) for sand has been found to vary from a value at shallow depths determined by Equation (34) to a value

at large depths determined by Equation (35). At a given depth, the value of Pu is the lesser of Pu at shallow depth, Pus, or Pu at larger depth, Pud, where:

$$P_{us} = (C_1 x + C_2 B)\gamma' x \tag{34}$$

$$P_{ud} = C_3 B \gamma' x \tag{35}$$

Where:

P_u = ultimate resistance (force/unit length), lb/in. (kN/m).

γ' = effective unit weight, pci (kN/m^3).

x = depth, in. (m).

ϕ' = angle of internal friction of sand, degrees.

C_1, C_2, C_3 = coefficients determined from Figure 3-14 as a function of ϕ, or from:

$$C_1 = tan\beta \left\{ K_p tan\alpha + K_0 \left[tan\phi sin\beta \left(\frac{1}{\cos \alpha} + 1 \right) - tan\alpha \right] \right\} \tag{36}$$

$$C_2 = K_p - K_A \tag{37}$$

$$C_3 = K_p^2 \left(K_p + K_0 tan\phi \right) - K_A \tag{38}$$

Where:

$K_p = \tan^2 \left(45° + \frac{\phi}{2} \right)$.

$K_0 = 0.4$.

B = average pile diameter from surface to depth, in. (m).

The factors C_1, C_2, C_3, are similar to bearing capacity factors in the general bearing capacity equation.

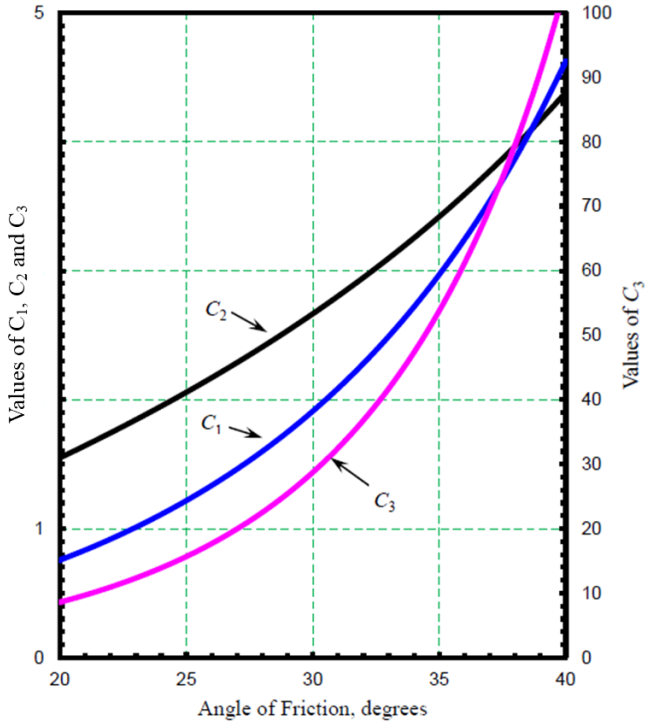

Figure 3-14. Coefficients C1, C2, and C3 versus Angle of Internal Friction (Isenhower and Wang, 2016).

3. Compute the P-y relationship for the sand. In the absence of more definite information, this relationship may be approximated at any specific depth x by the following expression:

$$p = Ap_u tanh\left(\frac{kx}{Ap_u}y\right) \quad (39)$$

Where:

A = factor to account for cyclic or static loading. Evaluated by:

A = 0.9 for cyclic loading.

$A = \left(3.0 - 0.8\frac{x}{B}\right) \geq 0.9$ for static loading.

P_u = smaller of the two values computed from step 2 in lb/in.,

k = initial modulus of subgrade reaction, pci. Determine *k* from Figure 3-13 as a function of the angle of internal friction, ϕ,

y = lateral deflection, in.

x = depth, in. (m).

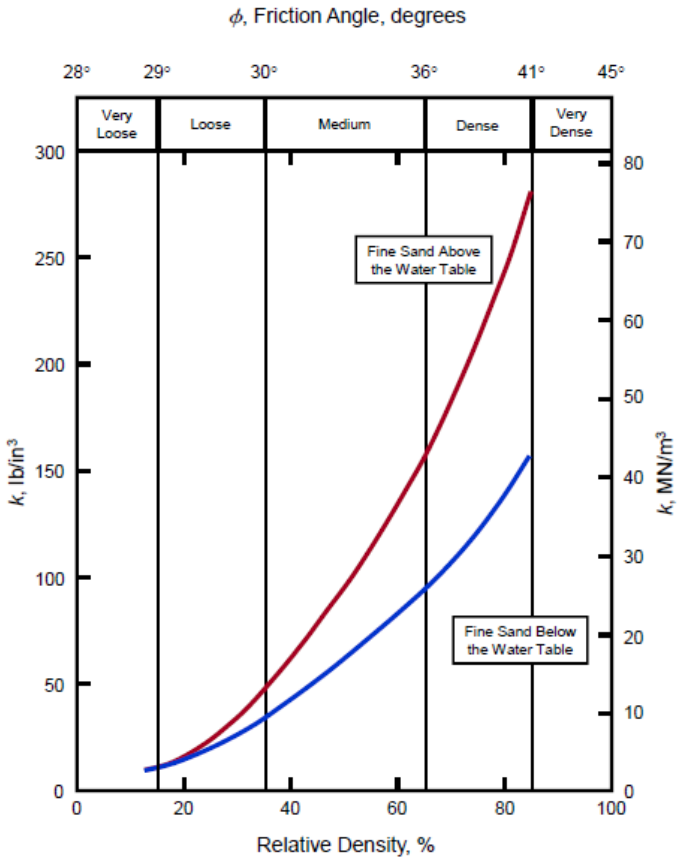

Figure 3-15. Value of k for API Sand Procedure (Isenhower and Wang, 2016).

3.3.4 Example Curve for Cohesionless Soil

This section presents an example for generating P-y curves in cohesionless soil for a monotonically loaded pile. Table 3-6 shows a set of assumed parameters.

Table 3-6. Assumed Parameters for Generating P-y Curves in Sand.

Soil Type	γ, pcf	B, ft	Φ, °	k, pci
Sand	127.3	1.0	30	60

4. Table 3-6 shows the soil and pile parameters:

   γ = 127.3 pcf

   B = 1.0 ft

   Φ = 30°

5. Obtain α and β to calculate K_a and K_o:

$$\alpha = \frac{\phi}{2} = \frac{30^\circ}{2} = 15^\circ$$

$$\beta = 45^\circ + \frac{\phi}{2} = 45^\circ + \frac{30^\circ}{2} = 60^\circ$$

$$K_A = \tan^2(45^\circ - \frac{\phi}{2}) = \tan^2\left(45^\circ - \frac{30^\circ}{2}\right) = 0.33$$

$$K_0 = 0.4$$

6. Compute the ultimate soil resistance per unit length of pile, P_s (Equation [17] and [18]) with x = 0.5 ft:

$$P_{st} = \gamma x\left[\frac{K_0 x tan\phi sin\beta}{\tan(\beta-\phi)cos\alpha} + \frac{tan\beta}{\tan(\beta-\phi)}(B + xtan\beta tan\alpha) + K_0 x tan\beta(tan\phi sin\beta - tan\alpha) - K_A B\right] = 127.3 \times 0.5\left[\frac{0.4\times0.5\times tan30^\circ sin60^\circ}{\tan(60^\circ-30^\circ)cos15^\circ} + \frac{tan60^\circ}{\tan(60^\circ-30^\circ)}(1.0 + 0.5 \times tan60^\circ tan15^\circ) + 0.4 \times 0.5 \times tan60^\circ(tan15^\circ sin60^\circ - tan15^\circ) - 0.33 \times 1.0\right] = 230.57\ lbs/ft$$

$$P_{sd} = K_A B\gamma x(\tan^8\beta - 1) + K_0 B\gamma x tan\phi \tan^4\beta = 0.33 \times 1.0 \times 20.0 \times 0.5 \times (\tan^8 60^\circ - 1) + 0.4 \times 1.0 \times 127.3 \times 0.5 \times tan30^\circ \tan^4 60^\circ = 1829.63\ lbs/ft$$

$$P_s = \min[P_{st}, P_{sd}] = \min[230.57, 1829.63] = 230.57\ lbs/ft$$

7. Compute the y_u value defining point u (Figure 3-10):

$$y_u = \frac{3B}{80} = \frac{3\times1.0}{80} = 0.0375\ ft = 0.45\ in$$

For $\frac{x}{B} = \frac{0.5}{1.0} = 0.5$, A_s can be found by using Figure 3-11,

$$A_s = 2.5$$

$$P_u = \overline{A_s} p_s = 2.5 \times 230.57 = 576.43\frac{lbs}{ft} = 48.04\frac{lb}{in}$$

8. Compute the y_m value at point m (Figure 3-10):

$$y_m = \frac{B}{60} = \frac{1.0}{60} = 0.0167\ ft = 0.2\ in$$

For $\frac{x}{B} = \frac{0.5}{1.0} = 0.5$, B_s can be found by using Figure 3-12,

$$B_s = 1.826$$

$$P_m = \overline{B_s} p_s = 1.826 \times 230.57 = 421.02\frac{lbs}{ft} = 35.09\frac{lbs}{in}$$

9. Establish the initial straight-line portion of the P-y curve:

   P = (kx)y, where k = 60 pci (from Table 3-4) and x = 0.5 ft,

   $P = (kx)y = 60 \times 0.5 \times 12 \times y = 360y$ (lbs/in)

10. Fit the parabola between point k and point m (Figure 3-10):

    i. Compute the slope of the P-y curve between point m and point u using:

    $m = \frac{P_u - P_m}{y_u - y_m} = \frac{48.04 - 35.09}{0.45 - 0.2} = 51.771$

    ii. Compute the power of the parabolic section using:

    $n = \frac{P_m}{m y_m} = \frac{35.09}{51.771 \times 0.2} = 3.3893$

    iii. Compute the coefficient $\bar{C}$ using:

    $\bar{C} = \frac{P_m}{y_m^{1/n}} = \frac{35.09}{0.2^{\frac{1}{3.3893}}} = 56.423$

    iv. Compute the y value defining point k (Figure 3-10) using:

    $y_k = \left(\frac{\bar{C}}{kx}\right)^{\frac{n}{n-1}} = \left(\frac{56.423}{60 \times 0.5 \times 12}\right)^{\frac{3.3893}{3.3893-1}} = 0.07216$

    v. Compute the p_k value defining point k (Figure 3-10) using:

    $p_k = kxy_k = 60 \times 0.5 \times 12 \times 0.07216 = 25.977$ lbs/in

    vi. Compute the p and y values along the parabolic section of the P-y curve between points k and m using:

    $P = \bar{C} y^{1/n} = 56.423 \times y^{1/3.3893}$

    for y = 0.2 in, $P = \bar{C} y^{1/n} = 56.423 \times y^{1/3.3893} = 56.423 \times 0.2^{1/3.3893} = 35.09$ lbs/in

11. Plot the P-y curve based on Reese et al. (1974) recommendations with P on the vertical axis and y on the lateral axis as shown in Figure 3-16.

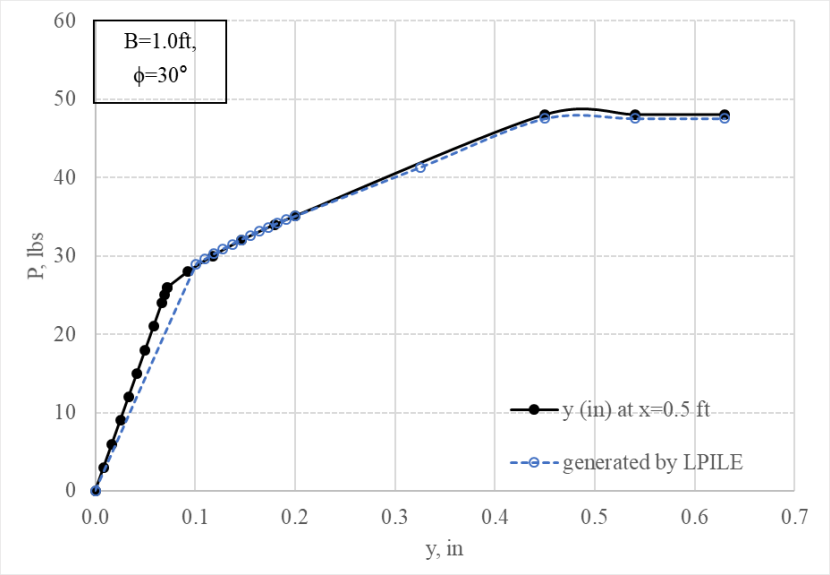

Figure 3-16. Example P-y Curve for Sand with below the Water Table, Static Loading by Following the Recommendations by Reese et al. (1974).

CHAPTER 4 LATERAL PILE LOAD TEST DATABASE

4.1 INTRODUCTION

To find quality lateral load tests on large diameter piles, including the soil properties, was critically important in this project. By contacting leading engineers from industries, professors from campuses, and researchers from all over the world, TTI researchers have collected 89 lateral pile load tests from 8 countries as shown in Figure 4-1 and Table 4-1.

A large diameter pile was defined as a pile with a diameter larger or equal to 5 ft (1.524 m). A small diameter pile was defined as a pile with a diameter smaller than 5 ft (1.524 m). As Table 4-2 shows, there are 54 small diameter pile load tests and 35 large diameter pile load tests in the database collected for this project. The pile length ranged from 5 ft (1.524 m) to 220 ft (67 m), and the diameter ranged from 1 ft (0.3 m) to 9.84 ft (3 m). The piles in the database included piles in layered soil; however, the cases were defined as sand or clay by considering the soil within the upper one-third of the pile length. The total number of piles can be further divided into 33 small diameter pile tests in sand, 21 small diameter pile tests in clay, 23 large diameter pile tests in sand, and 12 large diameter pile tests in clay (Table 4-2).

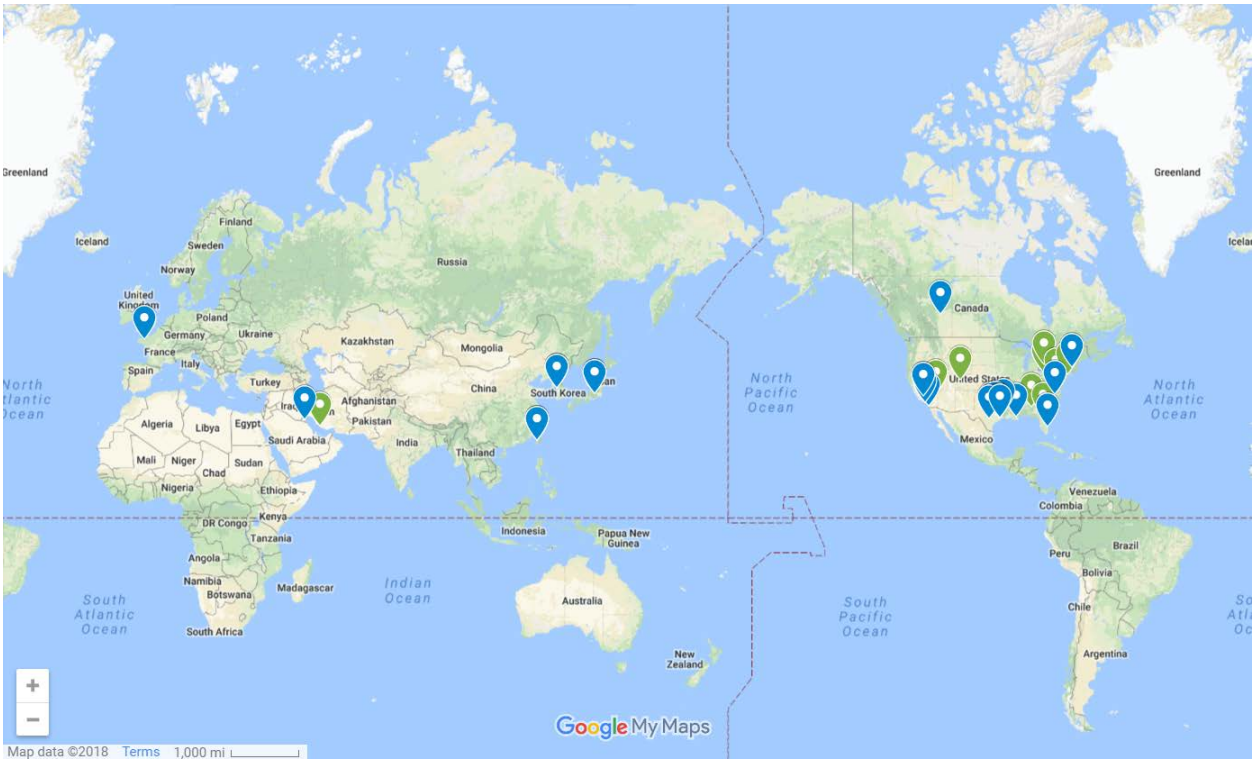

Figure 4-1. Map of Collected Lateral Pile Load Tests (Courtesy of Google Maps).

Table 4-1. Countries of Collected Lateral Pile Load Tests.

Country	Number of cases (B<5 ft)	Number of cases (B≥5 ft)	Number of cases
United States	36	21	57
Canada	6	2	8
France	1	0	1
Taiwan	3	0	3
South Korea	3	1	4
Japan	4	3	7
Kuwait	5	0	5
Iran	0	4	4

Table 4-2. Pile Length Range and Number of Cases in Sand and Clay.

Category		Pile Diameter B<5 ft	Pile Diameter B≥5 ft
Pile diameter range (ft)		1–5	5–9.84
Pile length range (ft)		5–120	7.5–220
Number of case		54	35
Soil type	Sand	33	23
	Clay	21	12

Each case includes the pile properties, the soil properties, and the load application details. The pile properties include diameter, length, type (bored pile, steel pile), elastic modulus of the pile material, moment of inertia, and wall thickness for steel pipe piles. Among the soil properties available for each case were: location of the water table, soil type of each soil layer, thickness of the soil layer, effective unit weight (γ), friction angle (ϕ) for sand, undrained shear strength (S_u) for clay, unconfined compressive strength for clay/rock (q_u), ε_{50}, SPT-N, plastic index, P_L (pressuremeter test), E_0 (pressuremeter test), and shear wave velocity. The 89 cases

collected were organized in an Excel spreadsheet with each case being assigned a record number (RN).

4.2 SMALL DIAMETER PILES—LATERAL LOAD TESTS

A total of 52 small diameter lateral load tests (RN 2, 3, 9, 10–50, 67-69, 80–82, and 86–89) was collected. There are 32 sand cases and 17 clay cases with a pile diameter ranging from 1 ft (0.32 m) to 4.92 ft (1.5 m) and a length ranging from 5 ft (1.524 m) to 120 ft (36.6 m). The two tests performed by Matlock and Reese in Sabine and Lake Austin were included among the 54 pile cases. Also included in the database are the 20 small diameter pile cases with pressuremeter data assembled by Briaud (1997). An additional 30 cases were collected during this project. The references for these 52 tests are from the United States (Matlock and Tucker, 1961; Woodward Clyde Consultants, 1979; Holloway et al., 1978; Kasch, 1977; Smith, 1983; Dunnavant and O'Neill, 1989; Tucker and Briaud, 1987; Little and Briaud, 1988; Huang et al., 1989; Ruesta and Townsend, 1997; Cho et al., 2001; Juirnarongrit and Ashford, 2004; Lemnitzer et al., 2010; Load Test Consulting, 2018), Canada (Donthireddy and Briaud, 1995; Adams and Radhakrishna, 1973), France (Baguelin et al., 1972), Taiwan (Huang et al., 2001), Kuwait (Ismael, 2009), South Korea (Jeong et al., 2007), and Japan (Ishikawa, 1985). Each of the 52 tests is presented next.

4.2.1 Chiayi, Taiwan Field Test

The Chiayi tests performed in Taiwan include two small diameter piles (B = 2.62 ft and 4.92 ft), and a series of a group pile tests (Huang et al., 2001). The pile lengths are 111.55 ft and 114.5 ft for pile diameter equals to 2.62 ft and 4.92 ft embedded in a layered soil that consists of fine sandy or clayey silt, silty fine sand, and silty clay. The maximum applied lateral load was 194 kips and caused a deflection of 11.61 in. at the pile head for smaller diameter pile while the maximum applied lateral load of 660 kips caused 5.03 in. of deflection at the pile head . The pile properties and the soil data for use in LPILE can be found in Table 4-2 (RN: 2) and Table 4-3 (RN: 3). Figure 4-2 and Figure 4-3 summarize the soil stratigraphy and the field test results with the LPILE predictions discussed in the following chapters.

Table 4-3. Pile and Soil Properties of Chiayi Test (RN: 2).

Record Number: 2

Chiayi Test, Taiwan							
Paper	Effects of construction on laterally loaded pile groups						
Reference	Huang, An-Bin, et al. "Effects of construction on laterally loaded pile groups." *Journal of Geotechnical and Geoenvironmental Engineering.* 127.5 (2001): 385-397.						
Pile Properties							
Pile type	B(ft)	L(ft)	f'c (psi)	f'y (psi)	E(psi)		
bored pile	4.92	114.5	3988.54	59697.64	2.898E+07		
Soil Properties used in LPILE							
P-y model	Depth		γ ' (pcf)	K (pci)	Su (psf)	φ (°)	ε_{50}
	Top	Bottom					
Reese/API Sand	0	9.9	120.95	99.98	n/a	35	n/a
Reese/API Sand	9.9	26.2	58.57	69.48	n/a	35	n/a
Matlock Soft Clay	26.2	39.4	58.57	n/a	1253.4	n/a	0.007
Reese/API Sand	39.4	55.8	59.84	67.49	n/a	34	n/a
Reese/ API Sand	55.8	82.0	58.57	75.01	n/a	34	n/a
Matlock Soft Clay	82.0	105.0	58.57	n/a	2402.35	n/a	0.005
Matlock Soft Clay	105.0	141.1	58.57	n/a	2533.96	n/a	0.005

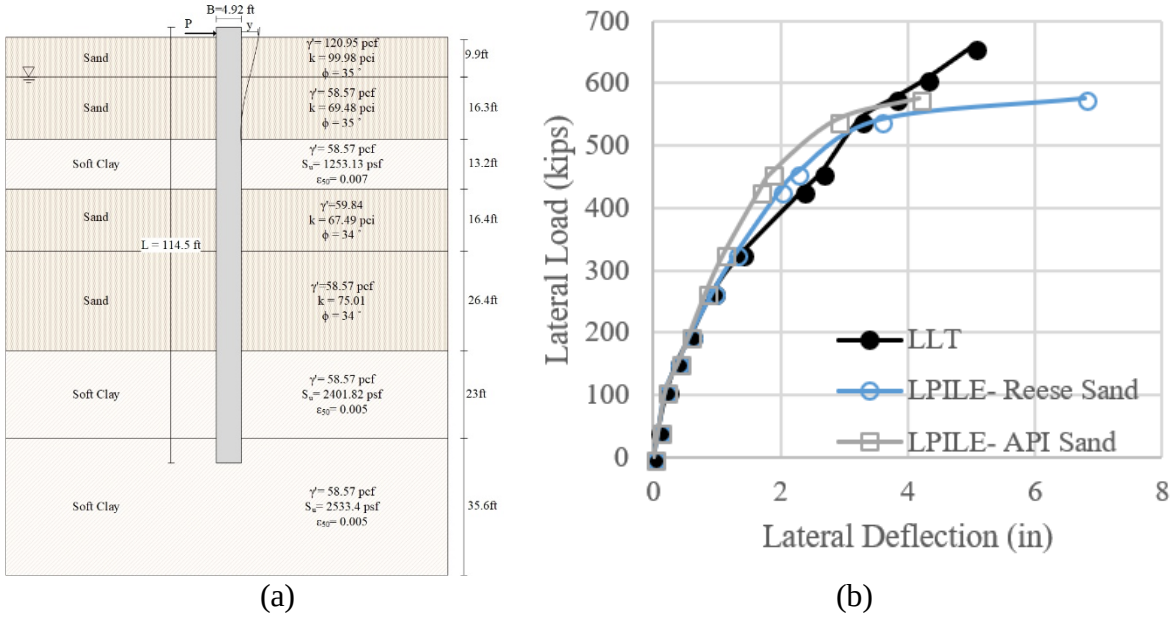

Figure 4-2. (a) Soil Stratigraphy, (b) Comparison between Measured and Predicted Lateral Deflection Curve of Chiayi.

Table 4-4. Pile and Soil Properties of Chiayi Test (RN: 3).

Record Number: 3

Chiayi, Taiwan						
Paper	Effects of construction on laterally loaded pile groups					
Reference	Huang, An-Bin, et al. "Effects of construction on laterally loaded pile groups." *Journal of Geotechnical and Geoenvironmental Engineerin.g* 127.5 (2001): 385-397.					
Pile properties used in LPILE						
B (ft)	L (ft)	f'c (psi)	f'y (psi)	E (psi)		
2.62	111.55	3988.45	59697.641	2.898E+07		
Soil Properties used in LPILE						
P-y model	Depth		γ ' (pcf)	K (pci)/ Su (psf)	φ (°)	ε_{50}
	Top	Bottom				
Reese/API Sand	0	9.9	120.95	99.98	35	n/a
Reese/API Sand	9.9	26.2	58.57	69.48	35	n/a
Matlock Soft Clay	26.2	39.4	58.57	1253.13	n/a	0.007
Reese/API Sand	39.4	55.8	59.84	67.49	34	n/a
Reese/API Sand	55.8	82.0	58.57	75.01	34	n/a
Matlock Soft Clay	82.0	105.0	58.57	2401.82	n/a	0.005
Matlock Soft Clay	105.0	141.1	58.57	2533.40	n/a	0.005

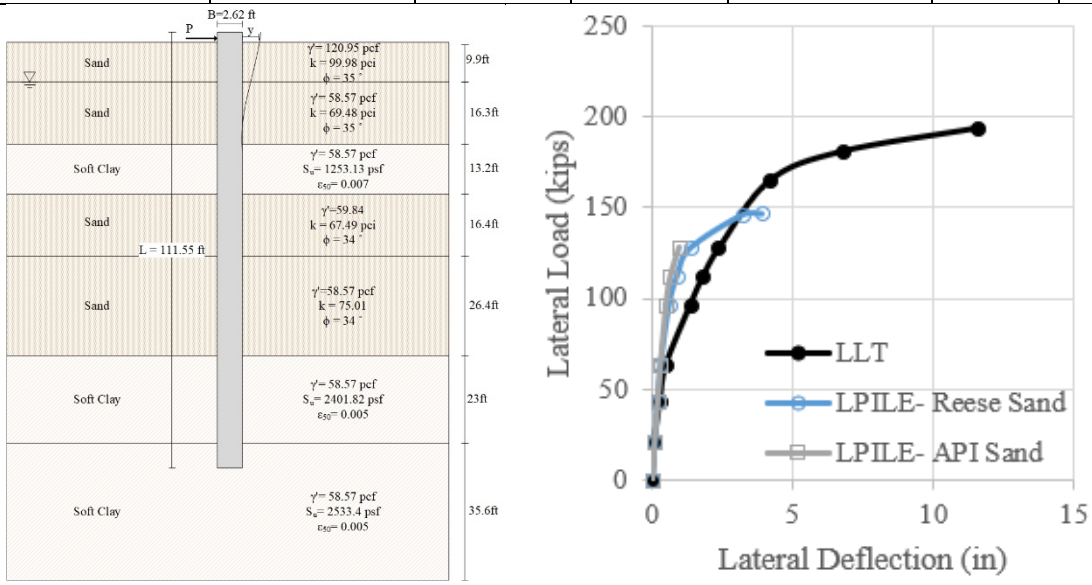

(a) (b)

Figure 4-3. (a) Soil Stratigraphy, (b) Comparison between Measured and Predicted Lateral Deflection Curve of Chiayi.

4.2.2 Edmonton, Alberta, Canada Test

There was a series of four 1.06 ft in diameter steel pipe piles with 0.37 in. in thickness and 78.7 ft in length that were embedded in a soft clay layer (Donthireddy and Briaud, 1995). The maximum applied lateral forces were up to 21 kips, 25 kips, 22 kips, and 26 kips and led to 1.35 in., 1.5 in., 1.44 in., and 1.46 in. of displacements at the pile top. Table 4-5, Table 4-6, Table 4-7, and Table 4-8 (RN: 9–12) summarize the pile properties and the soil properties used in LPILE. Figure 4-4, Figure 4-5, Figure 4-6, and Figure 4-7 show the soil stratigraphy and the field tests results.

4.2.3 New Orleans, Louisiana, Test

Three different types of piles were embedded in a sand layer in New Orleans (Donthireddy, 1995). The timber pile, the bored pile, and the steel pipe pile are all 1.17 ft in diameter and 68.9 ft in length. The maximum applied lateral loads were 27 kips, 27 kips, and 31 kips and led to 1.98 in., 0.84 in., and 1.34 in. of deflection at the pile top, respectively. Table 4-9, Table 4-10, and Table 4-11 list the pile properties and the soil data used in LPILE (RN: 13–15). Figure 4-8, Figure 4-9, and Figure 4-10 show the soil stratigraphy and the field test results.

4.2.4 Baytown, Texas, Test (Little)

The Baytown test in Texas included two tests (Little and Briaud, 1988). One steel pipe pile was 2 ft in diameter, 120 ft in length, and 0.6 in. in wall thickness, while the other one was a 1.67-ft diameter, 97.1-ft long bored concrete pile. The maximum applied lateral loads were 65 kips and 60 kips and caused 0.67 in. and 0.96 in. of deflection at the top of the pile, respectively. Table 4-12 and Table 4-13 (RN: 16–17) show the pile properties and the soil properties used in LPILE. Figure 4-11 and Figure 4-12 show the soil stratigraphy and field test results.

4.2.5 Sabine, Texas, Test

The Sabine test is one of the tests used by Matlock to the P-y curves for soft clay (Matlock and Tucker, 1961). The steel pipe pile was a 1.06 ft in diameter, 36 ft in length, and 0.6 in. in wall thickness embedded in soft clay. The maximum applied lateral force of 18 kips led to

2.5 in. of deflection at the pile head. Table 4-14 shows the pile properties and the soil properties (RN: 18), and Figure 4-13 shows the soil stratigraphy and field test results.

Table 4-5. Pile and Soil Properties of Edmonton Test (U4).

Record Number: 9

Edmonton, AB, Canada (U4)					
Paper	Simple pressuremeter approach to lateral loads on piles. Diss.				
Reference	Donthireddy, Srinivas. *Simple pressuremeter approach to lateral loads on piles*. Diss. Texas A&M University, 1995.				
Pile properties used in LPILE					
Pile type	B (ft)	L (ft)	t (in.)	I (in.^{4})	E (psi)
Steel Pipe pile	1.2	49.9	0.374	2.79E+02	2.90E+07
Soil Properties used in LPILE					
P-y model	Depth		γ ' (pcf)	Su (psf)	ε_{50}
	Top	Bottom			
Soft Clay	0	82.0	127.32	501.4	*

* automatically computed by LPILE

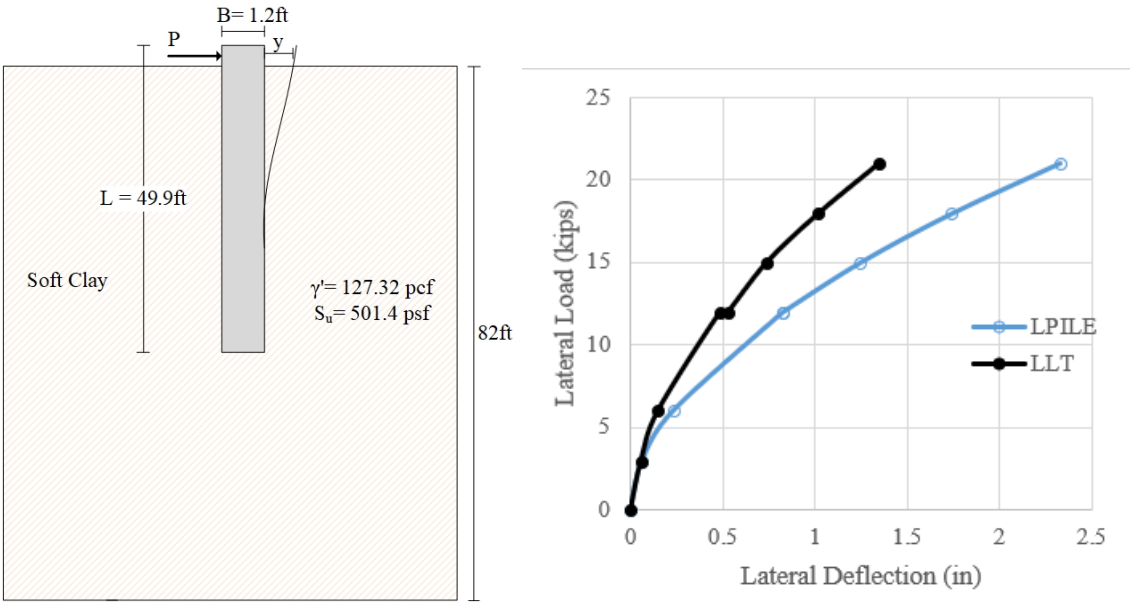

(a) (b)

Figure 4-4. (a) Soil Stratigraphy, (b) Comparison between Measured and Predicted Lateral Deflection Curve of Edmonton (U4).

Table 4-6. Pile and Soil Properties of Edmonton Test (C1).

Record Number: 10

Edmonton, AB, Canada (C1)					
Paper	Simple pressuremeter approach to lateral loads on piles. Diss.				
Reference	Donthireddy, Srinivas. *Simple pressuremeter approach to lateral loads on piles.* Diss. Texas A&M University, 1995.				
Pile properties used in LPILE					
Pile type	B (ft)	L (ft)	t (in.)	I (in.^{4})	E (psi)
Steel Pipe pile	1.2	49.9	0.374	2.79E+02	2.90E+07
Soil Properties used in LPILE					
P-y model	Depth		γ ' (pcf)	Su (psf)	ε_{50}
	Top	Bottom			
Soft Clay	0	82.0	127.32	501.4	*

* automatically computed by LPILE

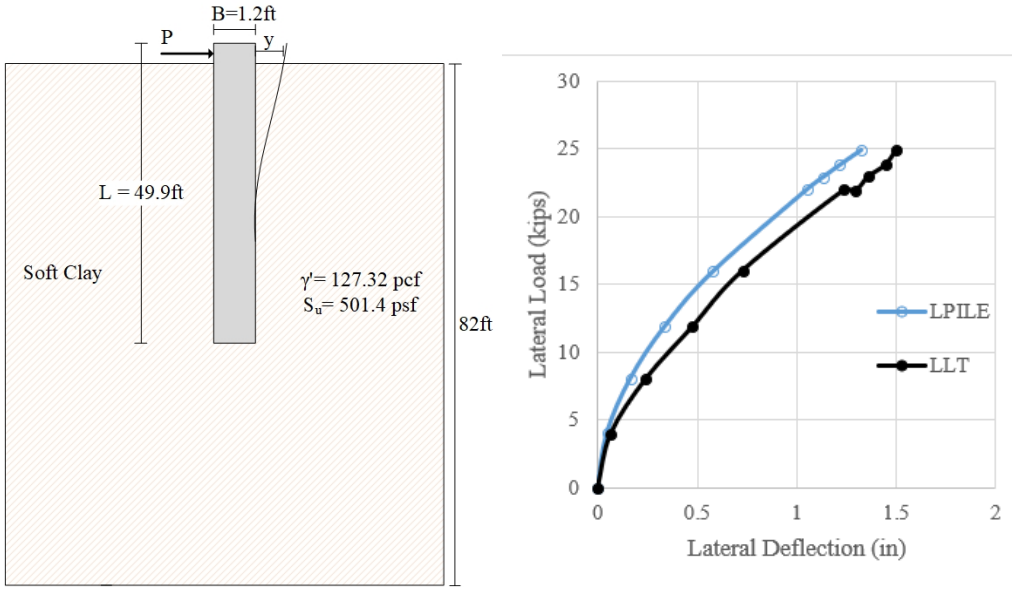

(a) (b)

Figure 4-5. (a) Soil Stratigraphy, (b) Comparison between Measured and Predicted Lateral Deflection Curve of Edmonton (C1).

Table 4-7. Pile and Soil Properties of Edmonton Test (C2).

Record Number: 11

Edmonton, AB, Canada (C2)					
Paper	Simple pressuremeter approach to lateral loads on piles. Diss.				
Reference	Donthireddy, Srinivas. *Simple pressuremeter approach to lateral loads on piles*. Diss. Texas A&M University, 1995.				
Pile properties used in LPILE					
Pile type	B (ft)	L (ft)	t (in.)	I (in.^{4})	E (psi)
Steel Pipe pile	1.2	49.9	0.374	2.79E+02	2.90E+07
Soil Properties used in LPILE					
P-y model	Depth		γ ' (pcf)	Su (psf)	ε_{50}
	Top	Bottom			
Soft Clay	0	82.0	127.32	501.4	*

* automatically computed by LPILE

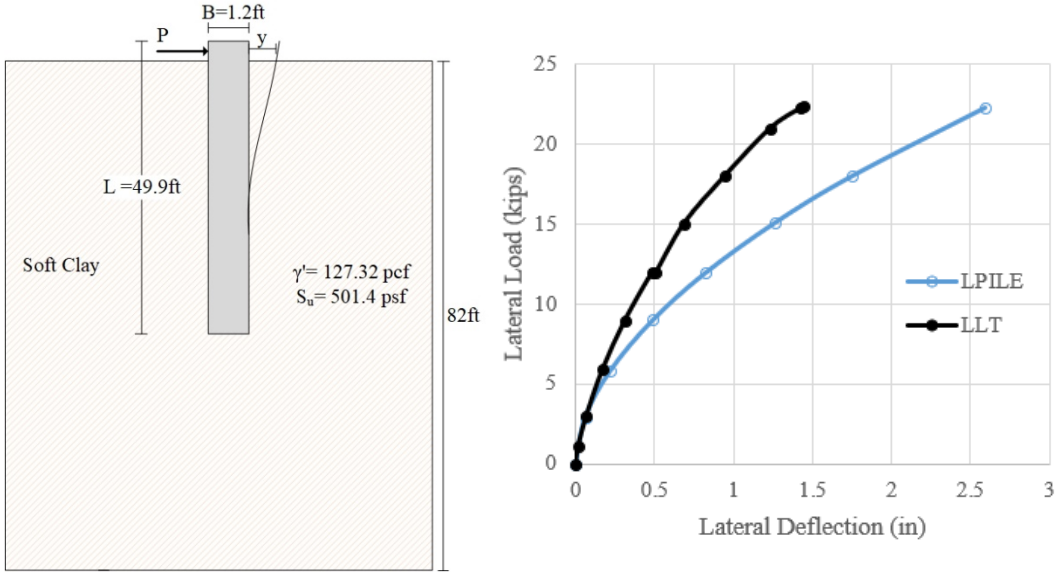

(a) (b)

Figure 4-6. (a) Soil Stratigraphy, (b) Comparison between Measured and Predicted Lateral Deflection Curve of Edmonton (C2).

Table 4-8. Pile and Soil Properties of Edmonton Test (C3).

Record Number: 12

Edmonton, AB, Canada (C3)					
Paper	Simple pressuremeter approach to lateral loads on piles. Diss.				
Reference	Donthireddy, Srinivas. *Simple pressuremeter approach to lateral loads on piles*. Diss. Texas A&M University, 1995.				
Pile properties used in LPILE					
Pile type	B (ft)	L (ft)	t (in.)	I (in.^{4})	E (psi)
Steel Pipe pile	1.063	78.74	0.374	2.79E+02	2.90E+07
Soil Properties used in LPILE					
P-y model	Depth		γ ' (pcf)	Su (psf)	ε_{50}
	Top	Bottom			
Soft Clay	0	82.0	127.32	501.4	*

* automatically computed by LPILE

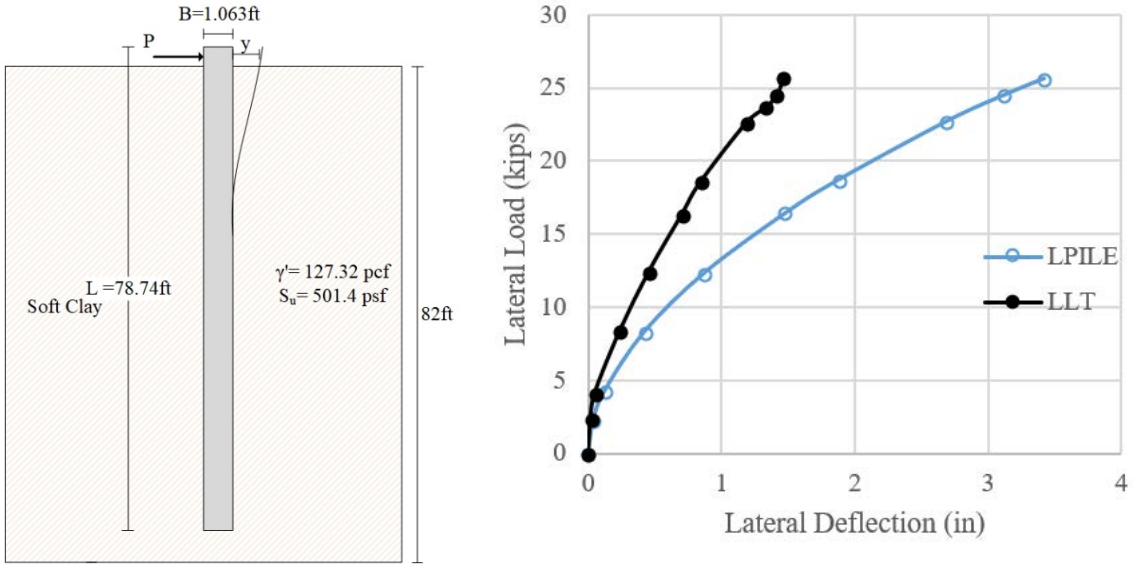

(a) (b)

Figure 4-7. (a) Soil Stratigraphy, (b) Comparison between Measured and Predicted Lateral Deflection Curve of Edmonton (C3).

Table 4-9. Pile and Soil Properties of New Orleans Test (RN: 13).

Record Number: 13

New Orleans, LA (TPU)					
Paper	Simple pressuremeter approach to lateral loads on piles. Diss.				
Reference	Donthireddy, Srinivas. *Simple pressuremeter approach to lateral loads on piles.* Diss. Texas A&M University, 1995.				
Pile properties used in LPILE					
Pile type	B (ft)		L (ft)	I (in.^{4})	E (psi)
Timber	1.17		68.9	1.89E+03	2.03E+06
Soil Properties used in LPILE					
P-y model	Depth		γ ' (pcf)	K (pci)	φ (°)
	Top	Bottom			
Sand	0	82.0	127.32	*	28

*automatically computed by LPILE

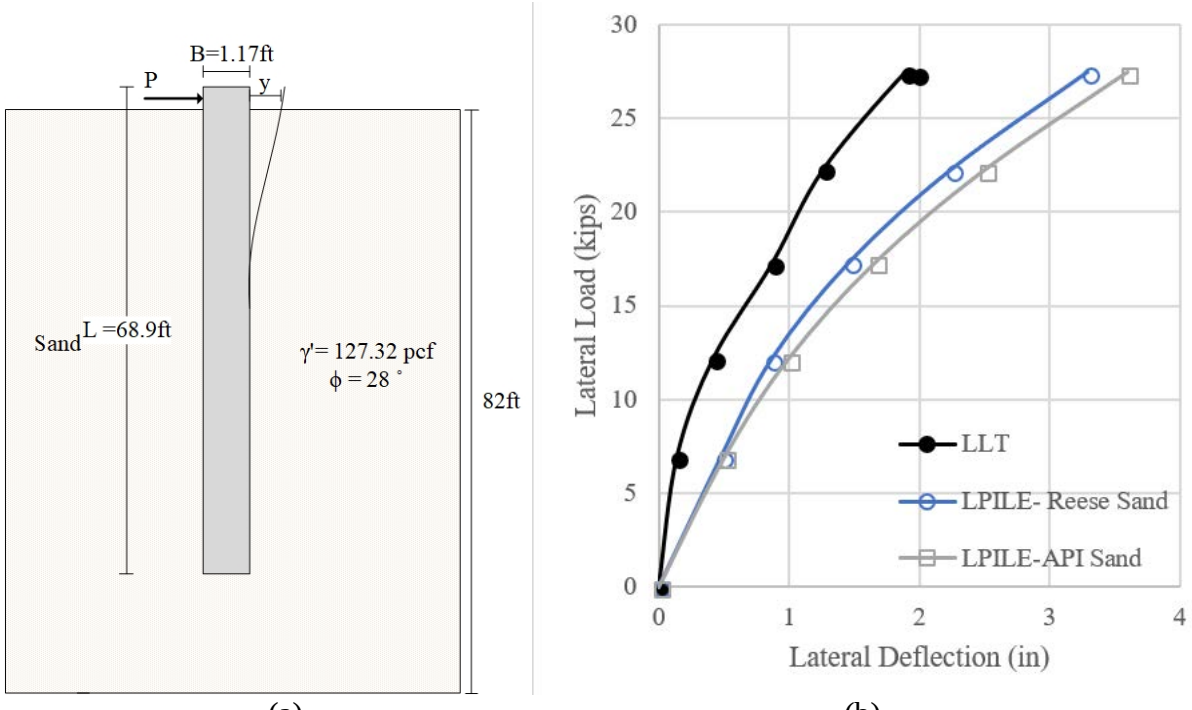

(a) (b)

Figure 4-8. (a) Soil Stratigraphy, (b) Comparison between Measured and Predicted Lateral Deflection Curve of New Orleans (RN: 13).

Table 4-10. Pile and Soil Properties of New Orleans Test (RN: 14).

Record Number: 14

New Orleans, LA (CPU)				
Paper	Simple pressuremeter approach to lateral loads on piles. Diss.			
Reference	Donthireddy, Srinivas. *Simple pressuremeter approach to lateral loads on piles.* Diss. Texas A&M University, 1995.			
Pile properties used in LPILE				
Pile type	B (ft)	L (ft)	I (in.^{4})	E (psi)
Driven pile circular	1.17	68.9	1.89E+03	2.90E+07
Soil Properties used in LPILE				
P-y model	Depth		γ ' (pcf)	K (pci)	φ (°)
	Top	Bottom			
Reese/API Sand	0	82.0	127.32	*	28

*automatically computed by LPILE

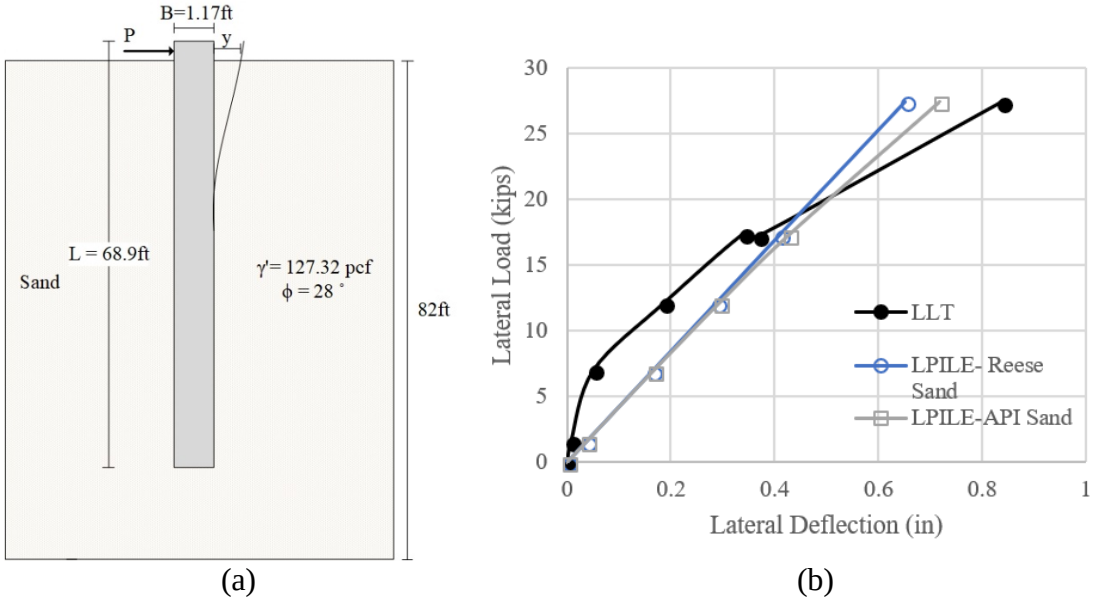

Figure 4-9. (a) Soil Stratigraphy, (b) Comparison between Measured and Predicted Lateral Deflection Curve of New Orleans (RN: 14).

Table 4-11. Pile and Soil Properties of New Orleans Test (RN: 15).

Record Number: 15

New Orleans, LA (CPI)					
Paper	Simple pressuremeter approach to lateral loads on piles. Diss.				
Reference	Donthireddy, Srinivas. *Simple pressuremeter approach to lateral loads on piles.* Diss. Texas A&M University, 1995.				
Pile properties used in LPILE					
Pile type	B (ft)	L (ft)	t (in.)	I (in.^{4})	E (psi)
Steel Pipe pile	1.17	68.9	0.39370	3.91E+02	3.92E+06
Soil Properties used in LPILE					
P-y model	Depth		γ ' (pcf)	K (pci)	φ (°)
	Top	Bottom			
Reese/API Sand	0	82	127.32	103.15	28

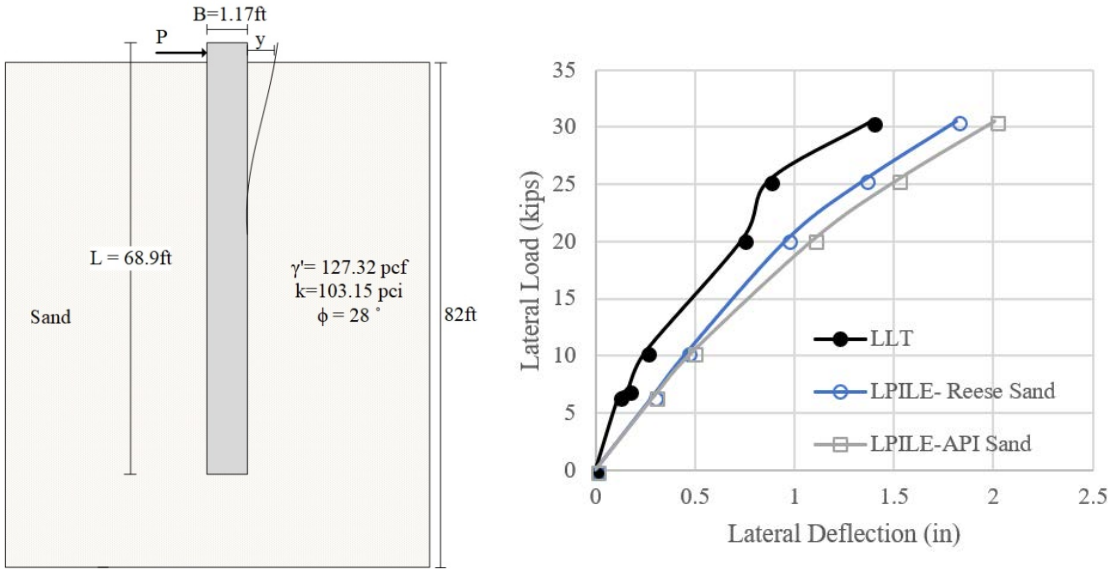

(a) (b)

Figure 4-10. (a) Soil Stratigraphy, (b) Comparison between Measured and Predicted Lateral Deflection Curve of New Orleans (RN: 15).

Table 4-12. Pile and Soil Properties of Baytown Test (Little) (RN: 16).

Record Number: 16

Baytown, Texas					
Paper	Full scale cyclic lateral load tests on six single piles in sand				
Reference	Little, Robert L., and Jean-Louis Briaud. *Full scale cyclic lateral load tests on six single piles in sand.* No. TAMU-RR-5640. Texas A&M Univeresity, College Station Department of Civil Engineering, 1988.				
Pile properties used in LPILE					
Pile type	B (ft)	L (ft)	t (in.)	I (in.^{4})	E (psi)
Steel Pipe pile	2.00	120	0.62992	3.17E+03	2.90E+07
Soil Properties used in LPILE					
P-y model	Depth		γ ' (pcf)	K (pci)	φ (°)
	Top	Bottom			
Reese/API Sand	0	131.2	127.32	*	30

*automatically computed by LPILE

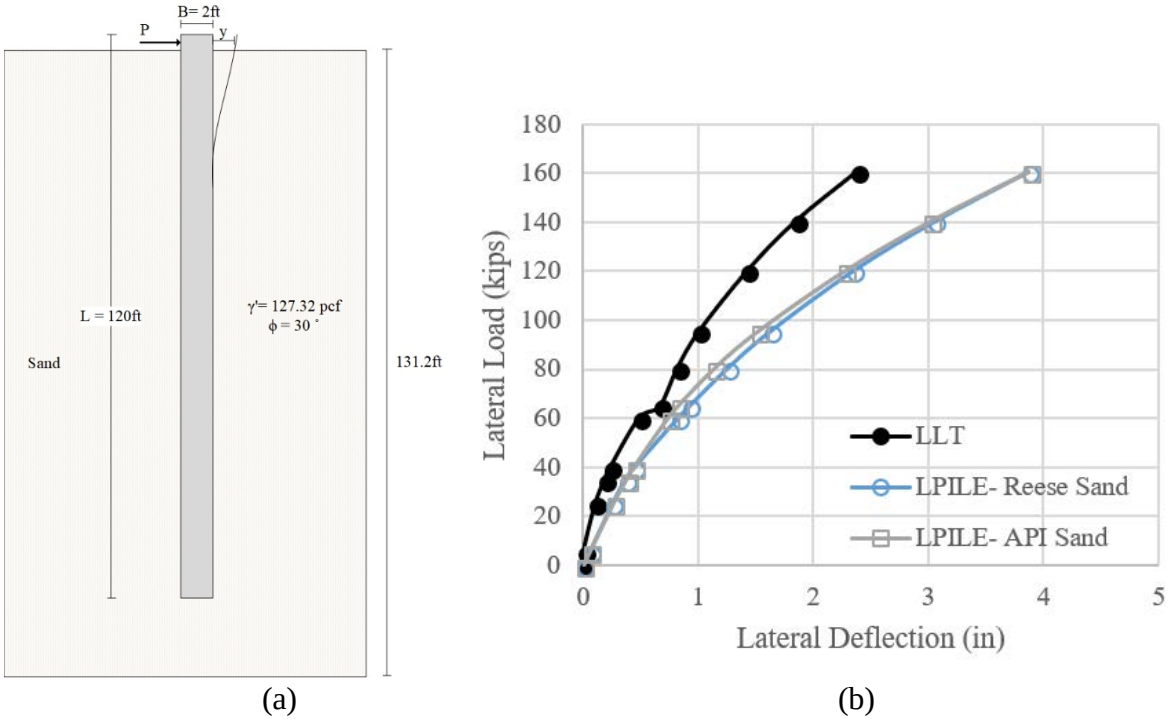

(a) (b)

Figure 4-11. (a) Soil Stratigraphy, (b) Comparison between Measured and Predicted Lateral Deflection Curve of Baytown (Little) (RN: 16).

Table 4-13. Pile and Soil Properties of Baytown Test (Little) (RN: 17).

Record Number: 17

Baytown, Texas				
Paper	Full scale cyclic lateral load tests on six single piles in sand			
Reference	Little, Robert L., and Jean-Louis Briaud. *Full scale cyclic lateral load tests on six single piles in sand*. No. TAMU-RR-5640. Texas A&M Univeresity, College Station Department of Civil Engineering, 1988.			
Pile properties used in LPILE				
Pile type	B (ft)	L (ft)	I (in.^{4})	E (psi)
Driven pile circular	1.67	97.1	7.98E+03	3.05E+06
Soil Properties used in LPILE				
P-y model	Depth		γ ' (pcf)	K (pci)	φ (°)
	Top	Bottom			
Reese/API Sand	0	114.8	127.32	*	30

*automatically computed by LPILE

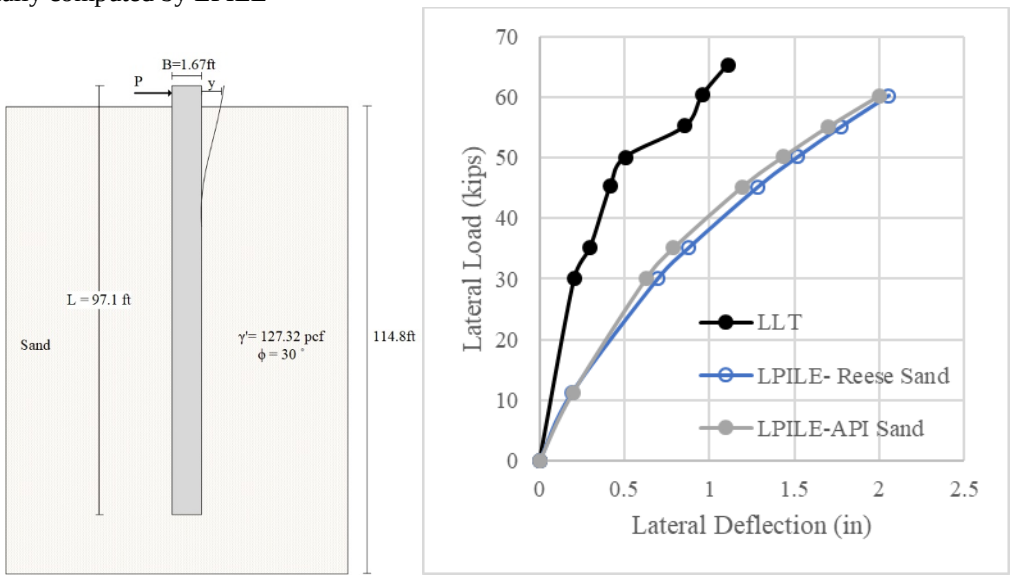

(a) (b)

Figure 4-12. (a) Soil Stratigraphy, (b) Comparison between Measured and Predicted Lateral Deflection Curve of Baytown (Little) (RN: 17).

Table 4-14. Pile and Soil Properties of Sabine Test.

Record Number: 18

Sabine, Texas					
Paper	Lateral-load tests of an instrumented pile at Sabine, Texas.				
Reference	Matlock, H., and R. L. Tucker. *Lateral-load tests of an instrumented pile at Sabine, Texas.* A Report to Shell Development Company, Houston (1961).				
Pile properties used in LPILE					
Pile type	B (ft)	L (ft)	t (in.)	I (in.^{4})	E (psi)
Steel Pipe pile	1.063	36.09	0.62992	4.42E+02	2.90E+07
Soil Properties used in LPILE					
P-y model	Depth		γ ' (pcf)	Su (psf)	ε_{50}
	Top	Bottom			
Soft Clay	0	49.2	127.32	300.0	*

*automatically computed by LPILE

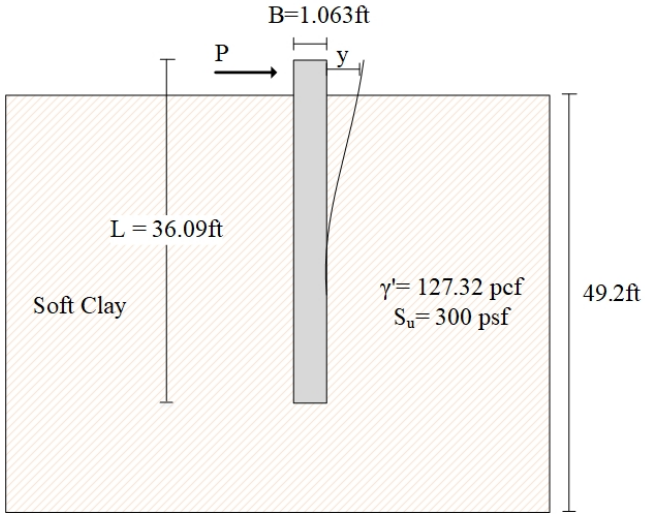

(a)

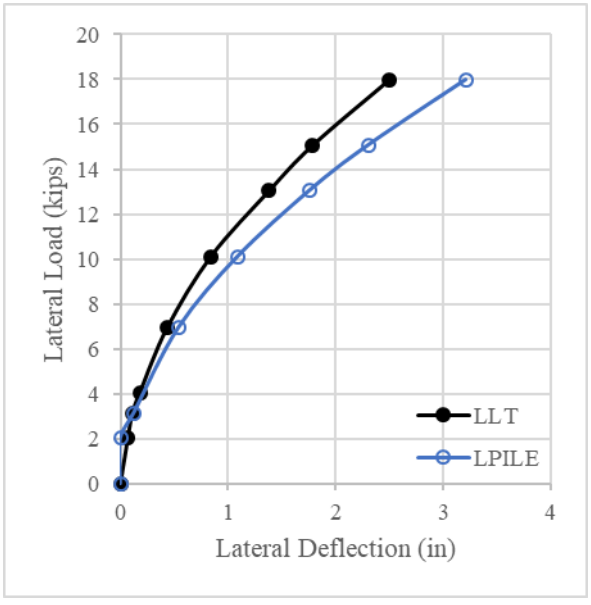

(b)

Figure 4-13. (a) Soil Stratigraphy, (b) Comparison between Measured and Predicted Lateral Deflection Curve of Sabine.

4.2.6 Lake Austin, Texas, Test

This test was performed at Lake Austin in Texas; one of the series tests was completed by Matlock in 1960s to develop P-y curves (Matlock, 1970). The size of the steel pipe pile was 1.06 ft in diameter, 40 ft in length, and 0.6 in thickness. A 23-kip maximum applied lateral load caused a 2 in. deflection at the top of the pile. Table 4-15 lists the pile properties and the soil data (RN: 19). Figure 4-14 shows the soil stratigraphy and the field test results.

4.2.7 Texas A&M University, Texas, Test

Two tests were completed in very stiff clay at Texas A&M University in College Station, Texas (Kasch, 1977; Holloway et al., 1978). The bored piles were both 3 ft in diameter, and 20 ft and 15 ft in length. The maximum applied lateral load of 170 kips and 152 kips led to 3.2 in. and 7.4 in. of deflection at the pile top, respectively. Table 4-16 and Table 4-17 summarize the pile dimensions and soil data used in LPILE (RN: 20–21). Figure 4-15 and Figure 4-16 show the soil stratigraphy and lateral load test results.

4.2.8 University of Houston, Texas, Test

This test was completed at the University of Houston in Houston, Texas, on a small diameter pile (B = 0.9 ft) (Briaud and Makarim, 1986). The steel pipe pile length was 38.7 ft with 0.37 in. wall thickness embedded in stiff clay. The maximum applied lateral load of 27 kips caused 3.26 in. of deflection at the pile top. Table 4-18 shows the pile properties and soil data used in LPILE (RN: 22). Figure 4-17 shows the soil stratigraphy and the field test results.

4.2.9 Lock and Dam 26, Illinois, Test

Four pile load tests were completed at Lock and Dam 26 in Illinois (Tucker and Briaud, 1987; Woodward Clyde Consultants, 1979). The three H pile (14×73) and one steel pipe pile were driven in sand; their length varied from 49.2 ft to 66.9 ft. The friction angle of the sand varied from 30° to 34°. The maximum applied lateral forces were 72 kips, 72 kips, 60 kips, and 50 kips, which led to 2.5 in., 1.91 in., 1.46 in., and 2.23 in. pile head displacements, respectively. Table 4-19, Table 4-20, Table 4-21, and Table 4-22 list the pile and soil data used in LPILE (RN: 23–26). Figure 4-18, Figure 4-19, Figure 4-20, and Figure 4-21 show the field load test results.

Table 4-15. Pile and Soil Properties of Lake Austin Test.

Record Number: 19

Lake Austin, Texas					
Paper	Lateral-load tests of an instrumented pile at Sabine, Texas.				
Reference	Matlock, Hudson. "Correlations for design of laterally loaded piles in soft clay." *Offshore Technology in Civil Engineering Hall of Fame Papers from the Early Years* (1970): 77-94.				
Pile properties used in LPILE					
Pile type	B (ft)	L (ft)	t (in.)	I (in.^{4})	E (psi)
Steel Pipe pile	1.063	40.03	0.59055	4.19E+02	2.90E+07
Soil Properties used in LPILE					
P-y model	Depth		γ ' (pcf)	Su (psf)	ε_{50}
	Top	Bottom			
Soft Clay	0	49.2	127.32	543.0	*

*automatically computed by LPILE

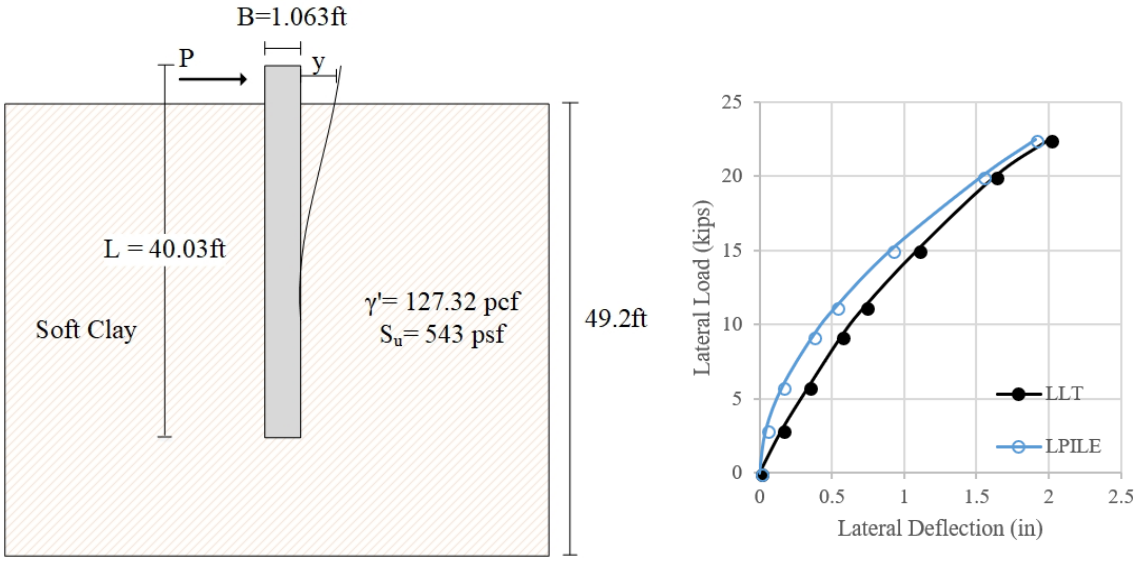

(a) (b)

Figure 4-14. (a) Soil Stratigraphy, (b) Comparison between Measured and Predicted Lateral Deflection Curve of Lake Austin.

Table 4-16. Pile and Soil Properties of Texas A&M University Test (RN: 20).

Record Number: 20

Texas A&M Uni., TX					
Paper	Lateral load test of a drilled shaft in clay				
Reference	Kasch, Vernon R., et al. *Lateral load test of a drilled shaft in clay*. No. FHWA-TX-77-211-1 Intrm Rpt. 1977				
Pile properties used in LPILE					
Pile type	B (ft)	L (ft)		I (in.^{4})	E (psi)
Driven pile circular	3.00	20.0		8.27E+04	3.05E+06
Soil Properties used in LPILE					
P-y model	Depth		γ ' (pcf)	Su (psf)	ε_{50}
	Top	Bottom			
Soft Clay	0	32.8	127.32	1388.9	*

*automatically computed by LPILE

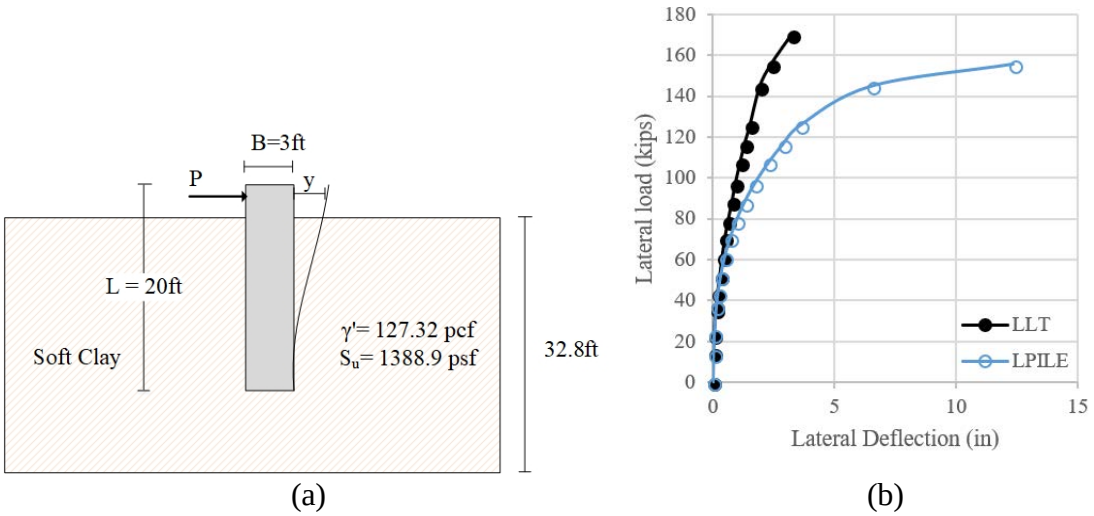

(a) (b)

Figure 4-15. (a) Soil Stratigraphy, (b) Comparison between Measured and Predicted Lateral Deflection Curve of Texas A&M University (RN: 20).

Table 4-17. Pile and Soil Properties of Texas A&M University Test (RN: 21).

Record Number: 21

Texas A&M Uni., TX					
Paper	Field test and preliminary design method for laterally loaded drilled shafts in clay				
Reference	Holloway, George L., et al. *Field test and preliminary design method for laterally loaded drilled shafts in clay*. No. FHWATX78-211-2 Intrm Rpt. 1978				
Pile properties used in LPILE					
Pile type	B (ft)	L (ft)	I (in.^{4})	E (psi)	
Bored pile circular	3.00	15.1	8.27E+04	3.05E+06	
Soil Properties used in LPILE					
P-y model	Depth		γ ' (pcf)	Su (psf)	ε_{50}
	Top	Bottom			
Soft Clay	0	32.8	127.32	1388.9	*

*automatically computed by LPILE

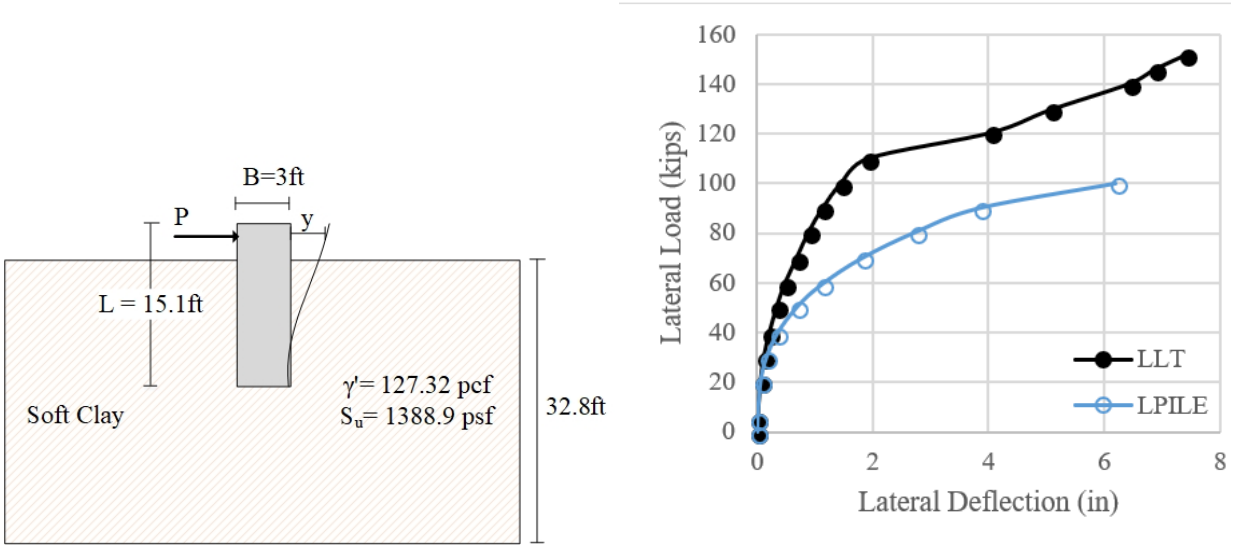

(a) (b)

Figure 4-16. (a) Soil Stratigraphy, (b) Comparison between Measured and Predicted Lateral Deflection Curve of Texas A&M University (RN: 21).

Table 4-18. Pile and Soil Properties of University of Houston Test.

Record Number: 22

Uni. Of Houston, TX				
Paper	Pressuremeter Method for Single Piles Subjected to Cyclic Lateral Loads in Overconsolidated Clay			
Reference	Makarim, Chaidir Anwar. *Pressuremeter Method for Single Piles Subjected to Cyclic Lateral Loads in Overconsolidated Clay*. (1986): 4991-4991.			
Pile properties used in LPILE				
Pile type	B (ft)	L (ft)	I (in.^{4})	E (psi)
Steel pipe pile	0.896	38.7	1.61E+02	2.90E+07
Soil Properties used in LPILE				

P-y model	Depth		γ ' (pcf)	Su (psf)	ε_{50}
	Top	Bottom			
Soft Clay	0	49.2	127.32	731.2	*

*automatically computed by LPILE

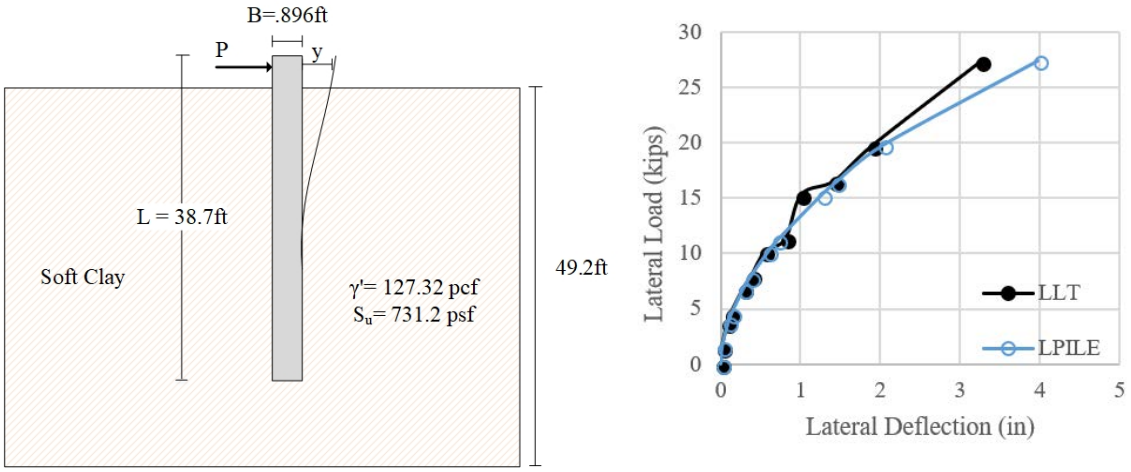

(a) (b)

Figure 4-17. (a) Soil Stratigraphy, (b) Comparison between Measured and Predicted Lateral Deflection Curve of University of Houston.

Table 4-19. Pile and Soil Properties of Lock and Dam Test (RN: 23).

Record Number: 1

Lock and Dam, IL (3-12)					
Paper	Analysis of the pile load test program at the lock and dam 26 replacement project				
Reference	Tucker, Larry M., and Jean-Louis Briaud. *Analysis of the pile load test program at the lock and dam 26 replacement project.* No. TAMU-RR-4690F. Texas A&M Univ College Station Dept of Civil Engineering, 1988.				
Pile properties used in LPILE					
Pile type	H-P Flange Width (in.)	H-P Depth (in.)	L (ft)	E (psi)	
H pile 14x73	14.5	13.6	66.9	2.90E+07	
Soil Properties used in LPILE					
P-y model	Depth		γ ' (pcf)	K (pci)	φ (°)
	Top	Bottom			
Reese/API Sand	0	82.0	115.99	*	34

*automatically computed by LPILE

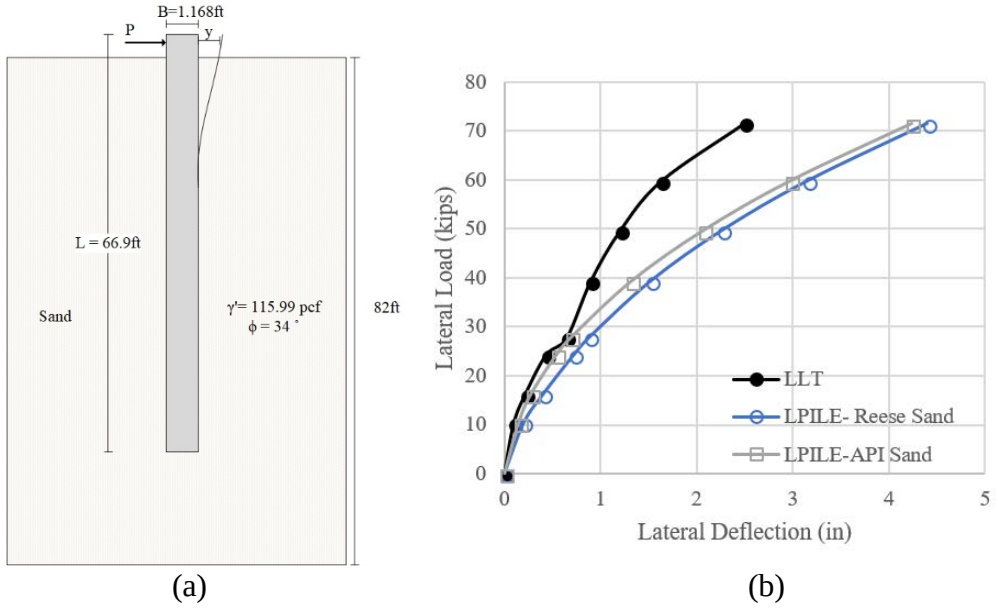

(a) (b)

Figure 4-18. (a) Soil Stratigraphy, (b) Comparison between Measured and Predicted Lateral Deflection Curve of Lock and Dam (RN: 23).

Table 4-20. Pile and Soil Properties of Lock and Dam Test (RN: 24).

Record Number: 24

Lock and Dam, IL (3-13)					
Paper	Analysis of the pile load test program at the lock and dam 26 replacement project				
Reference	Tucker, Larry M., and Jean-Louis Briaud. *Analysis of the pile load test program at the lock and dam 26 replacement project.* No. TAMU-RR-4690F. Texas A&M Univ College Station Dept of Civil Engineering, 1988.				
Pile properties used in LPILE					
Pile type	H-P Flange Width (in.)	H-P Depth (in.)	L (ft)	E (psi)	
H pile 14x73	14.5	13.6	66.9	2.90E+07	
Soil Properties used in LPILE					
P-y model	Depth		γ ' (pcf)	K (pci)	φ (°)
	Top	Bottom			
Reese/API Sand	0	82.0	115.99	*	34

*automatically computed by LPILE

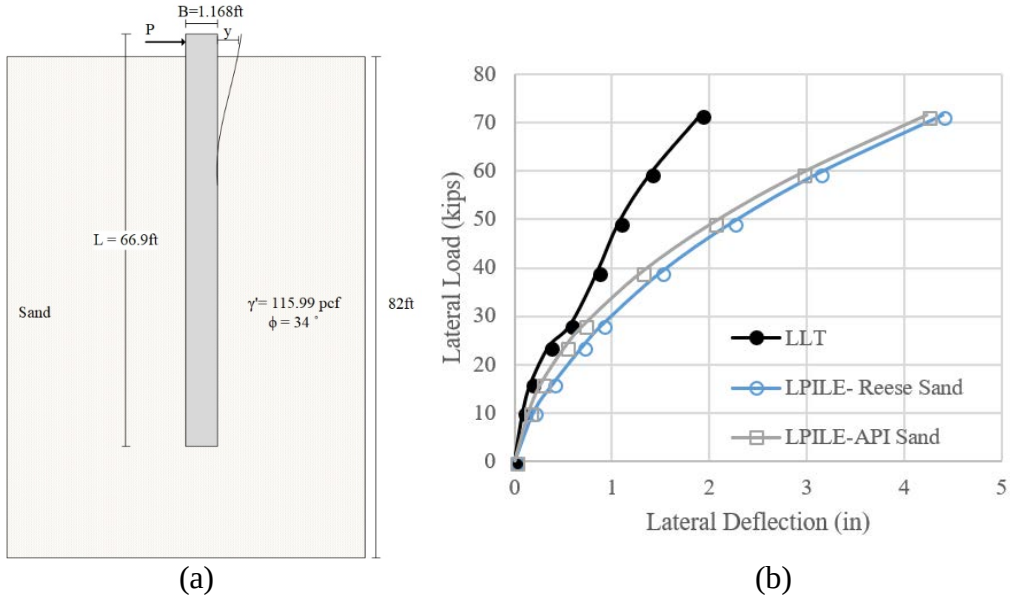

(a) (b)

Figure 4-19. (a) Soil Stratigraphy, (b) Comparison between Measured and Predicted Lateral Deflection Curve of Lock and Dam (RN: 24).

Table 4-21. Pile and Soil Properties of Lock and Dam Test (RN: 25).

Record Number: 25

Lock and Dam, TX (T3)				
Paper	Pressuremeter design method for single piles subjected to static lateral load			
Reference	Smith, Trevor David. *Pressuremeter design method for single piles subjected to static lateral load*. Diss. Texas A&M University, 1983.			
Pile properties used in LPILE				
Pile type	H-P Flange Width (in.)	H-P Depth (in.)	L (ft)	E (psi)
H pile 14x73	14.5	13.6	49.2	2.90E+07
Soil Properties used in LPILE				
P-y model	Depth		γ ' (pcf)	K (pci)	φ (°)
	Top	Bottom			
Reese/API Sand	0	65.6	127.32	*	30

*automatically computed by LPILE

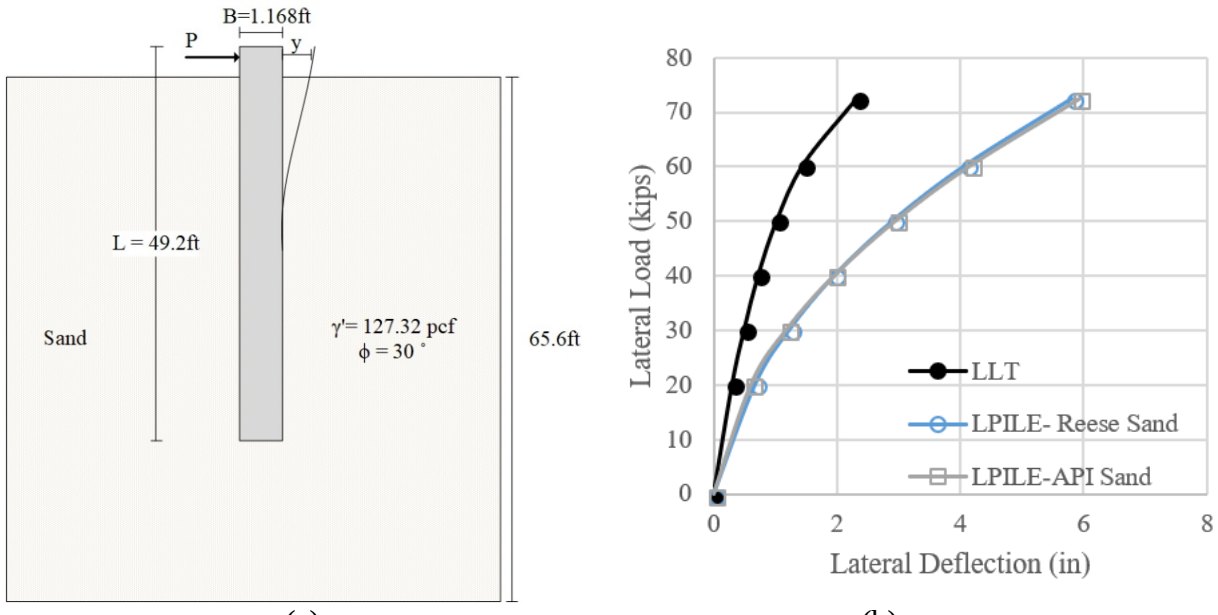

(a) (b)

Figure 4-20. (a) Soil Stratigraphy, (b) Comparison between Measured and Predicted Lateral Deflection Curve of Lock and Dam (RN: 25).

Table 4-22. Pile and Soil Properties of Lock and Dam Test (RN: 26).

Record Number: 26

Lock and Dam, TX (T4)					
Paper	Pressuremeter design method for single piles subjected to static lateral load				
Reference	Smith, Trevor David. *Pressuremeter design method for single piles subjected to static lateral load*. Diss. Texas A&M University, 1983.				
Pile properties used in LPILE					
Pile type	B (ft)	L (ft)	t (in.)	I (in.^{4})	E (psi)
Steel Pipe pile	1.17	49.9	0.3740	373.15	2.90E+07
Soil Properties used in LPILE					
P-y model	Depth		γ ' (pcf)	K (psi)	φ (°)
	Top	Bottom			
Reese/API Sand	0	65.6	127.32	*	30

*automatically computed by LPILE

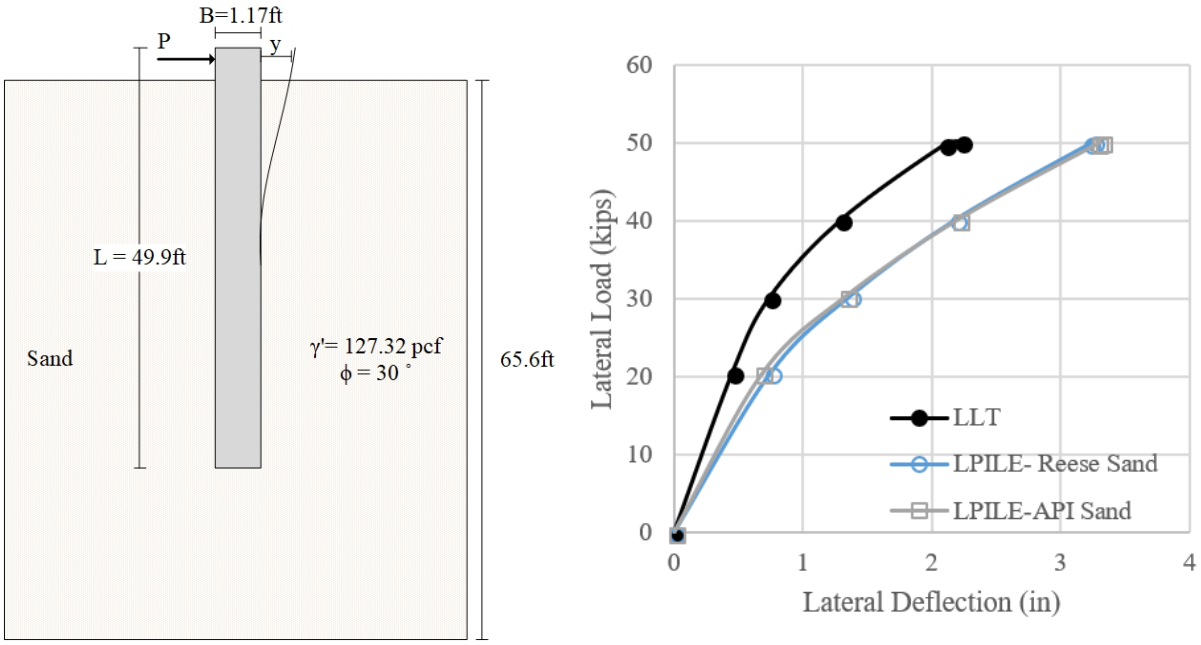

(a) (b)

Figure 4-21. (a) Soil Stratigraphy, (b) Comparison between Measured and Predicted Lateral Deflection Curve of Lock and Dam (RN: 26).

4.2.10 Baytown, Texas, Test (Smith)

This pile load test was performed near Baytown, Texas, and reported by Smith (1983) on a 2 ft diameter and 39 ft length pile. The maximum applied lateral load of 67 kips led a deflection of 3.41 in. at the pile head. Table 4-23 lists the pile and soil data used in LPILE (RN: 27). Figure 4-22 shows the soil stratigraphy and the field load test results.

4.2.11 Plancoet, France Test

An H-pile was embedded in soft clay in Plancoet, France (Baguelin et al., 1972). The pile was 20 ft long and tested by applying a series of lateral loads up to 14 kips. Table 4-24 describes the pile and soil data used in LPILE (RN: 28). Figure 4-23 shows the soil stratigraphy and the field test results.

4.2.12 Stuart, Florida, Test

There were two 2.5 ft diameter steel pipe piles with 0.374 in. wall thickness driven in sand and tested at Stuart, Florida (Ruesta and Townsend, 1997). The maximum applied lateral load for those two tests were 71 kips and 75 kips and both caused 4 in. of lateral deflection at the top of the piles. Figure 4-24 and Figure 4-25 show the soil stratigraphy and the field test results. Table 4-25 and Table 4-26 describe the data for the piles and for the soil used as input in LPILE (RN: 29, 30).

4.2.13 Rocky Mount, North Carolina, Test

Two full-scale lateral load tests were conducted in Rocky Mount, North Carolina, in a layered soil and rock (Cho et al., 2001). The bored piles were both 2.5 ft in diameter, one was 13.1 ft long and the other one was 16 ft long. The maximum applied lateral loads were 221 kips and 220 kips, which caused 1.4 in. and 1.38 in. lateral deflection at the top of piles. Figure 4-26 and Figure 4-27 show the soil stratigraphy and the field test results. Table 4-27 and Table 4-28 describe the data for the piles and soils used as input in LPILE (RN: 31, 32).

Table 4-23. Pile and Soil Properties of Baytown Test (Smith).

Record Number: 27

Baytown, Texas					
Paper	Pressuremeter design method for single piles subjected to static lateral load				
Reference	Smith, Trevor David. *Pressuremeter design method for single piles subjected to static lateral load*. Diss. Texas A&M University, 1983.				
Pile properties used in LPILE					
Pile type	B (ft)	L (ft)		I (in.^{4})	E (psi)
Bored pile circular	2.00	39.04		1.63E+04	3.05E+06
Soil Properties used in LPILE					
P-y model	Depth		γ ' (pcf)	Su (psf)	ε_{50}
	Top	Bottom			
Soft Clay	0	49.2	127.32	668.3	*

*automatically computed by LPILE

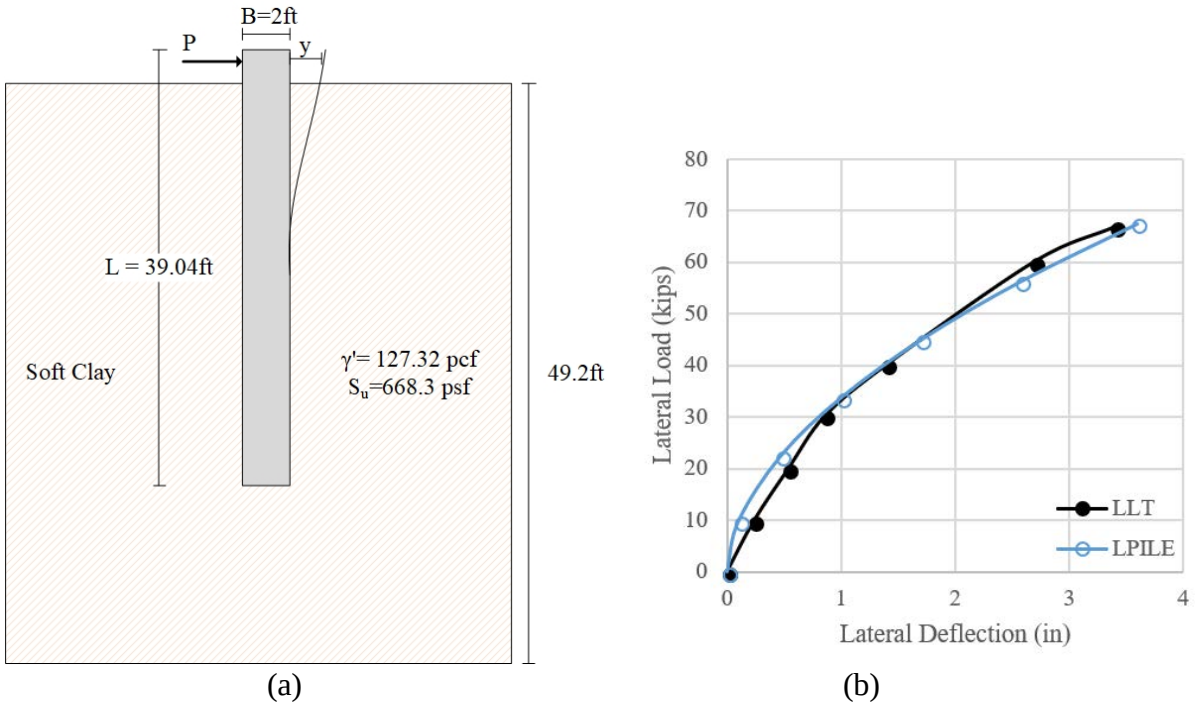

(a) (b)

Figure 4-22. (a) Soil stratigraphy, (b) Comparison between Measured and Predicted Lateral Deflection Curve of Baytown.

Table 4-24. Pile and Soil Properties of Plancoet Test.

Record Number: 28

Plancoet, France					
Paper	Expansion of cylindrical probes in cohesive soils				
Reference	Baguelin, Francois, et al. "Expansion of cylindrical probes in cohesive soils." *Journal of Soil Mechanics and Foundations* Div 98. Sm 11 (1972).				
Pile properties used in LPILE					
Pile type	H-P Flange Width (in.)	H-P Depth (in.)	L (ft)	E (psi)	
H pile 14x73	14.5	13.6	20.0	2.90E+07	
Soil Properties used in LPILE					
P-y model	Depth		γ ' (pcf)	Su (psf)	ε_{50}
	Top	Bottom			
Soft Clay	0	32.8	127.32	430.6	*

*automatically computed by LPILE

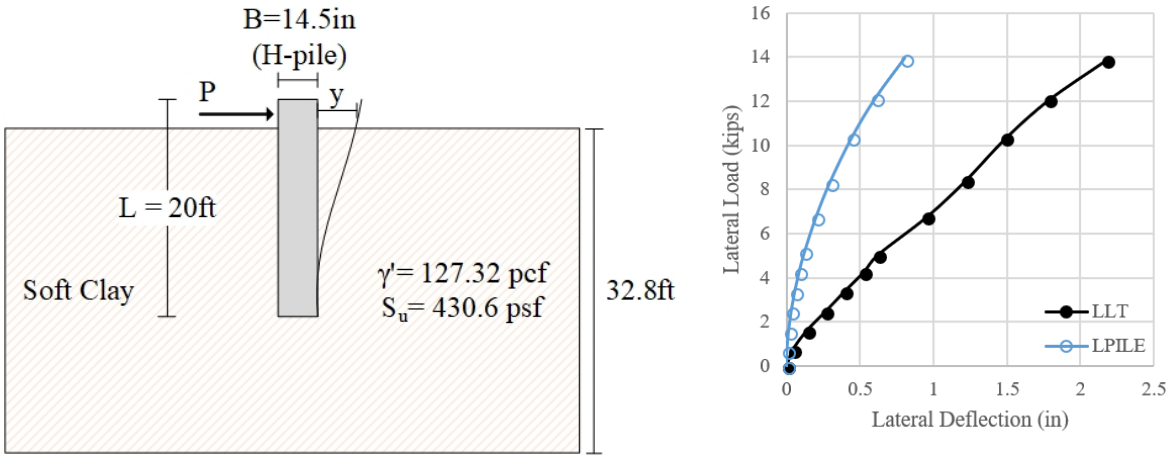

(a) (b)

Figure 4-23. (a) Soil Stratigraphy, (b) Comparison between Measured and Predicted Lateral Deflection Curve Plancoet.

Table 4-25. Pile and Soil Properties of Stuart Test (RN: 29).

Record Number: 29

Stuart, FL (a)					
Paper	Evaluation of laterally loaded pile group at Roosevelt Bridge				
Reference	Ruesta, Pedro F., and Frank C. Townsend. "Evaluation of laterally loaded pile group at Roosevelt Bridge." *Journal of Geotechnical and Geoenvironmental Engineering* 123.12 (1997): 1153-1161.				
Pile properties used in LPILE					
Pile type	B (ft)	L (ft)	t (in.)	I (in.^{4})	E (psi)
Steel Pipe pile	2.49	54.1	0.3740	3.80E+03	2.90E+07
Soil Properties used in LPILE					
P-y model	Depth		γ ' (pcf)	K (pci)	φ (°)
	Top	Bottom			
Reese/API Sand	0	13.1	56.66	60.05	32
Reese/API Sand	13.1	65.6	70.66	125.25	42

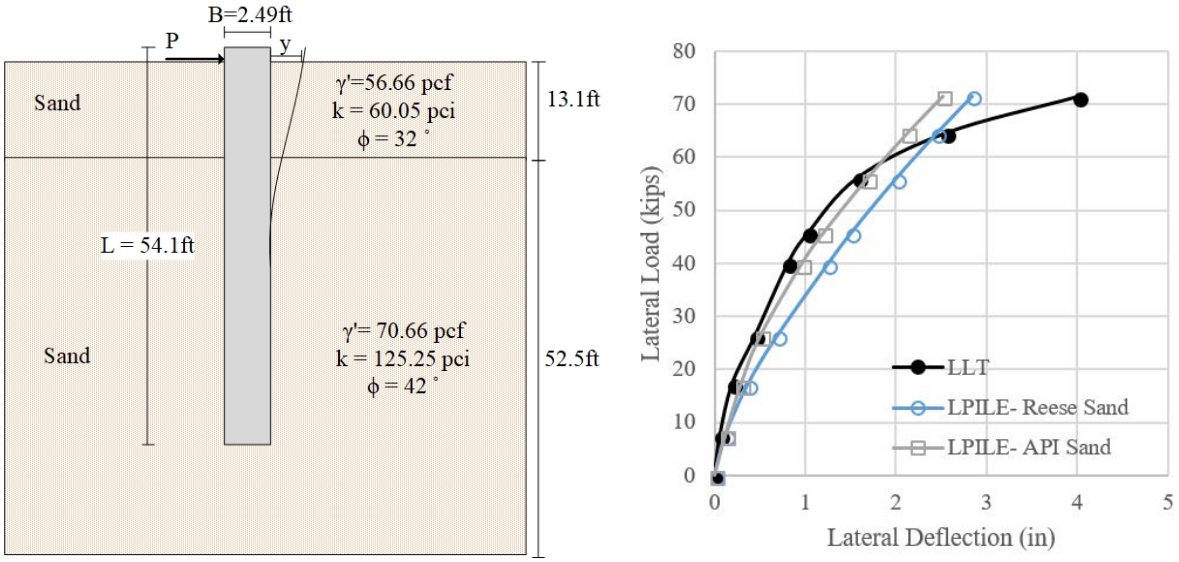

(a) (b)

Figure 4-24. (a) Soil Stratigraphy, (b) Comparison between Measured and Predicted Lateral Deflection Curve of Stuart (RN: 29).

Table 4-26. Pile and Soil Properties of Stuart Test (RN: 30).

Record Number: 30

Stuart, FL (b)					
Paper	Evaluation of laterally loaded pile group at Roosevelt Bridge				
Reference	Ruesta, Pedro F., and Frank C. Townsend. "Evaluation of laterally loaded pile group at Roosevelt Bridge." *Journal of Geotechnical and Geoenvironmental Engineering* 123.12 (1997): 1153-1161.				
Pile properties used in LPILE					
Pile type	B (ft)	L (ft)	t (in.)	I (in.^{4})	E (psi)
Steel Pipe pile	2.49	54.1	0.374	3.80E+03	2.90E+07
Soil Properties used in LPILE					
P-y model	Depth		γ ' (pcf)	K (pci)	φ (°)
	Top	Bottom			
Reese/API Sand	0	13.1	56.66	60.05	32
Reese/API Sand	13.1	45.9	70.66	125.25	42

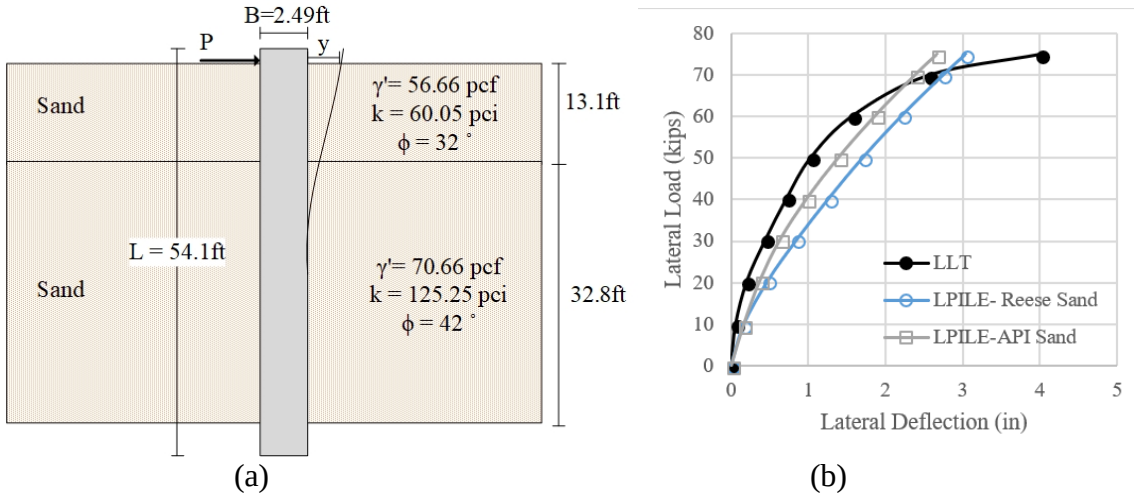

(a) (b)

Figure 4-25. (a) Soil Stratigraphy, (b) Comparison between Measured and Predicted Lateral Deflection Curve of Stuart (RN: 30).

Table 4-27. Pile and Soil Properties of Rocky Mount Test (RN: 31).

Record Number: 31

Rocky Mount, North Carolina (Short)									
Paper	Laterally loaded drilled shafts embedded in soft rock								
Reference	Cho, K. H., Clark, S. C., Keaney, B. D., Gabr, M. A., and Borden, R. H. (2001). "Laterally loaded drilled shafts embedded in soft rock." *Transportation Research Record: Journal of the Transportation Research Board*, 1772(1), 3-11.								
Pile properties used in LPILE									
Pile type	B (ft)		L (ft)		I (in.^{4})		E (psi)		
Bored pile circular	2.49		13.1		3.97E+04		3.05E+06		
Soil Properties used in LPILE									
P-y model	Depth		γ ' (pcf)	K (pci)	Su(psf)	qu (pcf)	φ (°)	ε_{50}	Rock mass modulus (kPa)
	Top	Bottom							
Soft Clay	0	4.9	127.32	n/a	294.72	n/a	n/a	*	n/a
Reese/API Sand	4.9	6.6	127.32	*	n/a	n/a	32	n/a	n/a
Reese Weak Rock	6.6	19.7	63.66	n/a	n/a	2800	n/a	n/a	223000

*automatically computed by LPILE

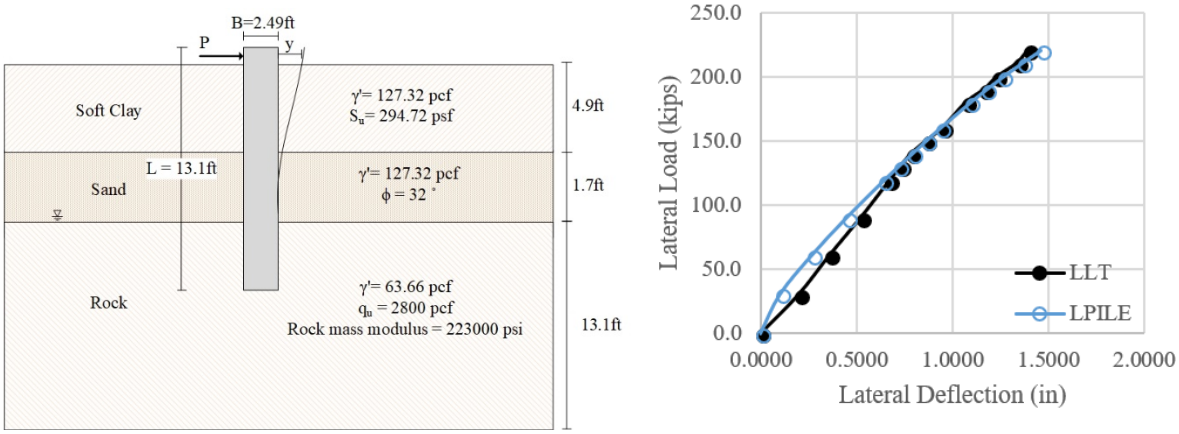

(a) (b)

Figure 4-26. (a) Soil Stratigraphy, (b) Comparison between Measured and Predicted Lateral Deflection Curve of Rocky Mount (RN: 31).

Table 4-28. Pile and Soil Properties of Rocky Mount Test (RN: 32).

Record Number: 32

Rocky Mount, North Carolina (Long)									
Paper	Laterally loaded drilled shafts embedded in soft rock								
Reference	Cho, K. H., Clark, S. C., Keaney, B. D., Gabr, M. A., and Borden, R. H. (2001). "Laterally loaded drilled shafts embedded in soft rock." *Transportation Research Record: Journal of the Transportation Research Board*, 1772(1), 3-11.								
Pile properties used in LPILE									
Pile type	B (ft)		L (ft)		I (in.^{4})		E (psi)		
Bored pile circular	2.49		16.1		39760.78		3.05E+06		
Soil Properties used in LPILE									
P-y model	Depth		γ ' (pcf)	K (pci)	Su (psf)	qu (pcf)	φ (°)	ε_{50}	Rock mass modulus (psi)
	Top	Bottom							
Soft Clay	0	4.9	127.32	n/a	294.72	n/a	n/a	*	n/a
Reese/API Sand	4.9	6.6	127.32	*	n/a	n/a	32	n/a	n/a
Reese Weak Rock	6.6	19.7	63.66	n/a	n/a	2800	n/a	n/a	223000

*automatically computed by LPILE

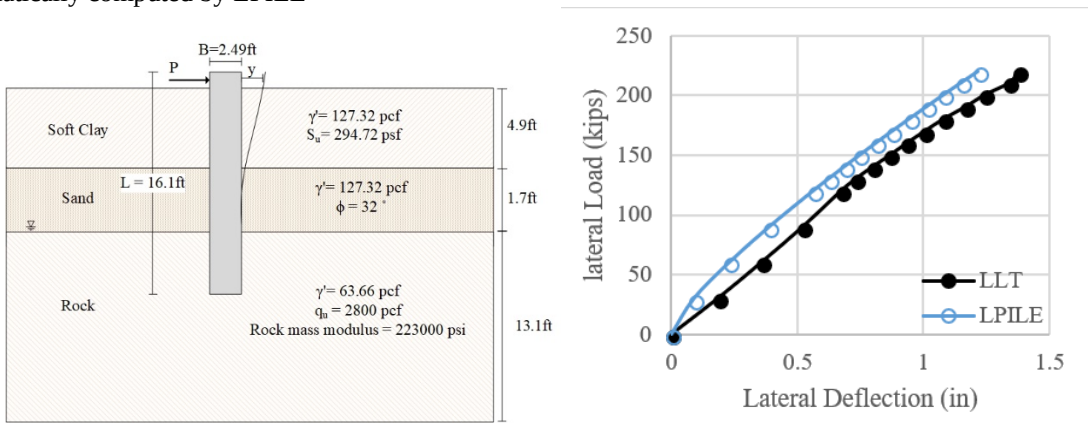

(a) (b)

Figure 4-27. (a) Soil Stratigraphy, (b) Comparison between Measured and Predicted Lateral Deflection Curve of Rocky Mount (RN: 32).

4.2.14 Jleeb Al-Shuyoukh, Kuwait Test

Five bored piles were constructed and tested in sand in Jleeb Al-Shuyoukh near the six-ring road, Kuwait, and reported by Ismael (2009). The maximum applied lateral loads in this series of tests were 34 kips, 38 kips, 45 kips, 54 kips, and 55 kips, which led to 0.98 in lateral deflection at the top of the piles for all the cases within the projects. The bored piles had diameters varying between 1 and 2 ft and some of them were tapered (RN: 33–37). The length varied but was approximately 17.5 ft on average. Figure 4-28, Figure 4-29, Figure 4-30, Figure 4-31, and Figure 4-32 show the soil stratigraphy and the field test results. Table 4-29 and Table 4-30, Table 4-31, Table 4-32, and Table 4-33 describe the data for the piles and the soil used as input in LPILE (RN: 33–37).

4.2.15 University of California, San Diego, California, Test (UCSD Test)

A series of four bored piles was installed to a depth 59 ft below the ground surface at a test site at the University of California, San Diego, California (Juirnarongrit and Ashford, 2004). The four piles were 1.31 ft, 1.97 ft, 2.95 ft, and 3.94 ft in diameter, and 14.8 ft, 39.4 ft, 39.4 ft, and 39.4 ft in length, respectively. The maximum applied lateral loads were 41 kips, 85 kips, 264 kips, and 526 kips, and caused a pile head deflection of 3.14 in., 2.99 in., 3.5 in., and 3.37 in., respectively. Figure 4-33, Figure 4-34, Figure 4-35, and Figure 4-36 show the soil stratigraphy and the field test results. Table 4-34, Table 4-35, Table 4-36, and Table 4-37 describe the data for piles and soils (RN: 38–41).

4.2.16 Hawthorne, California, Test (Lemnitzer)

There were two 2 ft in diameter bored circular piles installed in sand and laterally tested at Hawthorne, California (Lemnitzer et al., 2010). The maximum applied load within the tests were 275 kips for the free-head case and 28 kips for the flagpole case, which led to 3 in. and 1.62 in. of lateral deflection at the top of the piles, respectively. Figure 4-37 and Figure 4-38 show the soil stratigraphy and the field test results. Table 4-38 and Table 4-39 describe the data for the piles and soils used as input in LPILE (RN: 42–43).

Table 4-29. Pile and Soil Properties of Jleeb Al-Shuyoukh Test (RN: 33).

Record Number: 33

Jleeb Al-Shuyoukh near six-ring road, Kuwait					
Paper	Behavior of Step Tapered Bored Piles in Sand under Static Lateral Loading				
Reference	Ismael, N. F. (2009). "Behavior of Step Tapered Bored Piles in Sand under Static Lateral Loading." *Journal of Geotechnical and Geoenvironmental Engineering*, 136(5), 669-676.				
Pile properties used in LPILE					
Pile type	B (ft)	L (ft)	E (psi)	Area (in.^{2})	I (in.^{4})
bored pile	0.984	17.4	2.901E+07	109.56	9.553E+02
Soil Properties used in LPILE					

P-y model	Depth		γ ' (pcf)	K (pci)	φ (°)
	Top	Bottom			
Reese/API Sand	0	16.4	117.77	*	31
Reese/API Sand	16.4	26.2	114.59	*	40

*automatically computed by LPILE

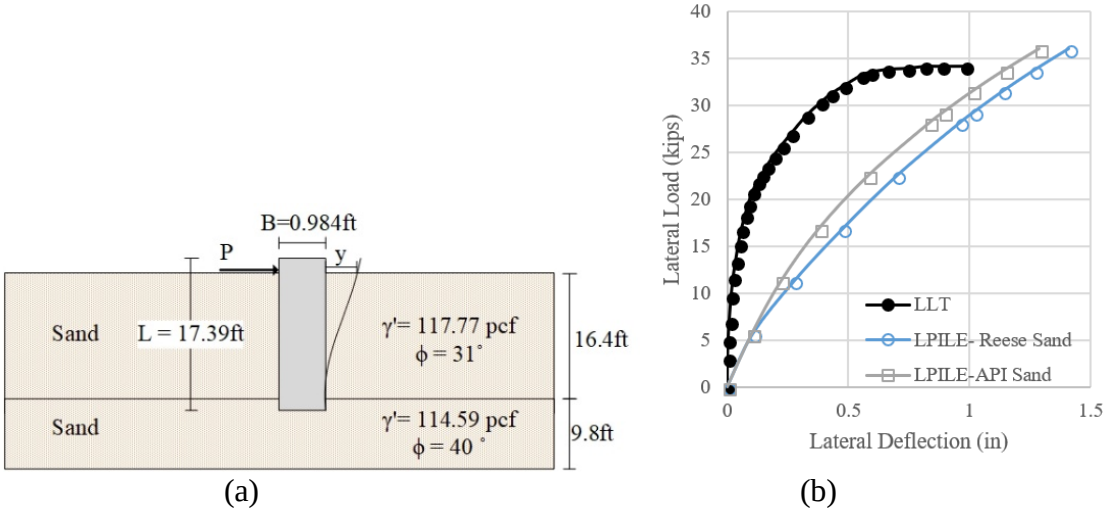

(a) (b)

Figure 4-28. (a) Soil Stratigraphy, (b) Comparison between Measured and Predicted Lateral Deflection Curve of Jleeb Al-Shuyoukh (RN: 33).

Table 4-30. Pile and Soil Properties of Jleeb Al-Shuyoukh Test (RN: 34).

Record Number: 34

Jleeb Al-Shuyoukh near six-ring road, Kuwait						
Paper		Behavior of Step Tapered Bored Piles in Sand under Static Lateral Loading				
Reference		Ismael, N. F. (2009). "Behavior of Step Tapered Bored Piles in Sand under Static Lateral Loading." *Journal of Geotechnical and Geoenvironmental Engineering*, 136(5), 669-676.				
Pile properties used in LPILE						
Pile type	pile section	B (ft)	L (ft)	E (psi)	Area (in.^{2})	I (in.^{4})
bored pile	1	1.64	2.62	2.901E+07	304.34	7.371E+03
	2	0.984	14.8	2.901E+07	109.56	9.553E+02

Soil Properties used in LPILE					
P-y model	Depth		γ ' (pcf)	K (pci)	φ (°)
	Top	Bottom			
Reese/API Sand	0	16.4	117.77	*	31
Reese/API Sand	16.4	26.2	114.59	*	40

*automatically computed by LPILE

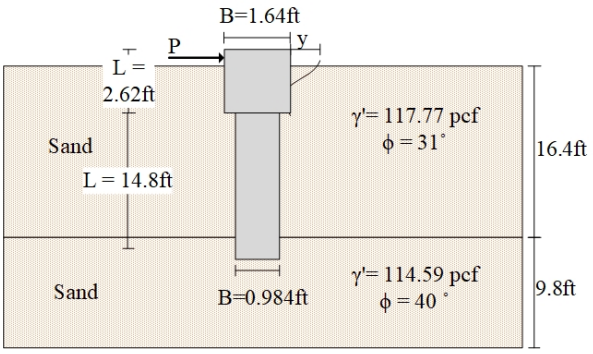

(a)

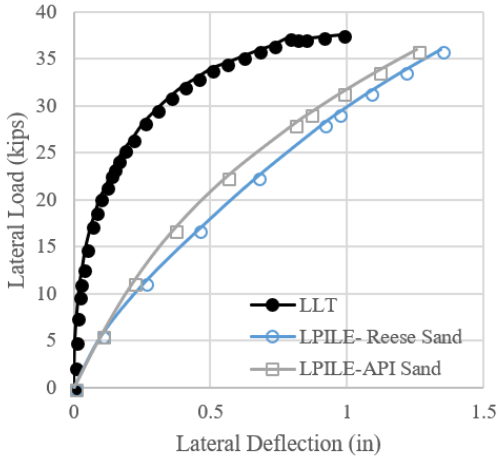

(b)

Figure 4-29. (a) Soil Stratigraphy, (b) Comparison between Measured and Predicted Lateral Deflection Curve of Jleeb Al-Shuyoukh (RN: 34).

Table 4-31. Pile and Soil Properties of Jleeb Al-Shuyoukh Test (RN: 35).

Record Number: 35

Jleeb Al-Shuyoukh near six-ring road, Kuwait						
Paper		Behavior of Step Tapered Bored Piles in Sand under Static Lateral Loading				
Reference		Ismael, N. F. (2009). "Behavior of Step Tapered Bored Piles in Sand under Static Lateral Loading." *Journal of Geotechnical and Geoenvironmental Engineering*, 136(5), 669-676.				
Pile properties used in LPILE						
Pile type	pile section	B (ft)	L (ft)	E (psi)	Area (in.^{2})	I (in.^{4})
bored pile	1	1.64	4.27	2.901E+07	304.34	7.361E+03
	2	0.98	13.1	2.901E+07	109.56	9.553E+02

Soil Properties used in LPILE					
P-y model	Depth		γ ' (pcf)	K (pci)	φ (°)
	Top	Bottom			
Reese/API Sand	0	16.4	117.77	*	31
Reese/API Sand	16.4	26.2	114.59	*	40

*automatically computed by LPILE

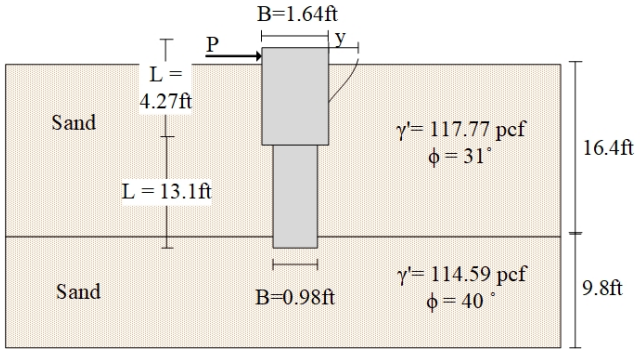

(a)

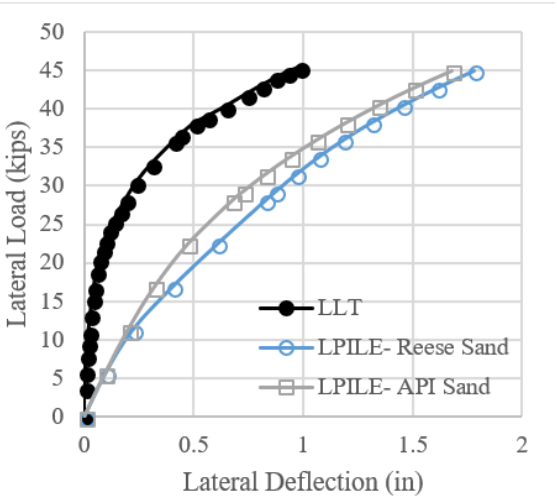

(b)

Figure 4-30. (a) Soil Stratigraphy, (b) Comparison between Measured and Predicted Lateral Deflection Curve of Jleeb Al-Shuyoukh (RN: 35).

Table 4-32. Pile and Soil Properties of Jleeb Al-Shuyoukh Test (RN: 36).

Record Number: 36

Jleeb Al-Shuyoukh near six-ring road, Kuwait						
Paper		Behavior of Step Tapered Bored Piles in Sand under Static Lateral Loading				
Reference		Ismael, N. F. (2009). "Behavior of Step Tapered Bored Piles in Sand under Static Lateral Loading." *Journal of Geotechnical and Geoenvironmental Engineering*, 136(5), 669-676.				
Pile properties used in LPILE						
Pile type	pile section	B (ft)	L (ft)	E (psi)	Area (in.^{2})	I (in.^{4})
bored pile	1	1.64	7.55	2.901E+07	304.34	7.371E+03
	2	0.98	9.84	2.901E+07	109.56	9.553E+02

Soil Properties used in LPILE					
P-y model	Depth		γ ' (pcf)	K (pci)	φ (°)
	Top	Bottom			
Reese/API Sand	0	16.4	117.77	*	31
Reese/API Sand	16.4	26.2	114.59	*	40

*automatically computed by LPILE

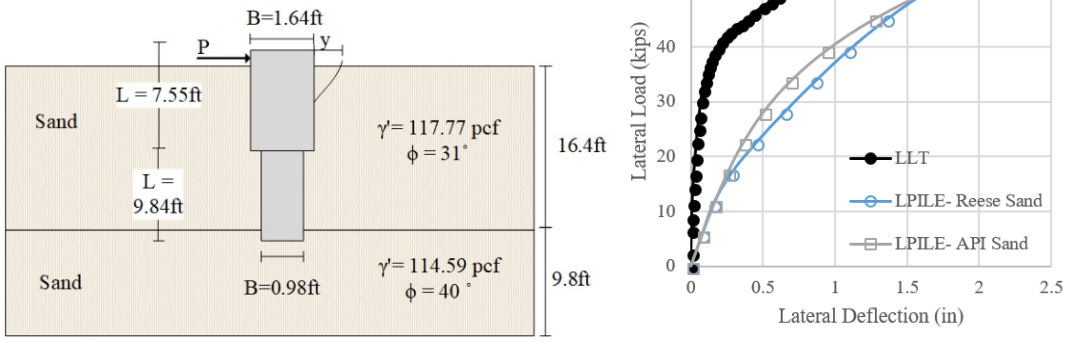

(a) (b)

Figure 4-31. (a) Soil Stratigraphy, (b) Comparison between Measured and Predicted Lateral Deflection Curve of Jleeb Al-Shuyoukh (RN: 36).

Table 4-33. Pile and Soil Properties of Jleeb Al-Shuyoukh Test (RN: 37).

Record Number: 37

Jleeb Al-Shuyoukh near six-ring road, Kuwait					
Paper	Behavior of Step Tapered Bored Piles in Sand under Static Lateral Loading				
Reference	Ismael, N. F. (2009). "Behavior of Step Tapered Bored Piles in Sand under Static Lateral Loading." *Journal of Geotechnical and Geoenvironmental Engineering*, 136(5), 669-676.				
Pile properties used in LPILE					
Pile type	B (ft)	L (ft)	E (psi)	Area (in.^{2})	I (in.^{4})
bored pile	1.64	17.4	2.901E+07	304.34	7.37E+03
Soil Properties used in LPILE					
P-y model	Depth		γ ' (pcf)	K (pci)	φ (°)
	Top	Bottom			
Reese/API Sand	0	16.4	117.77	*	31
Reese/API Sand	16.4	26.2	114.59	*	40

*automatically computed by LPILE

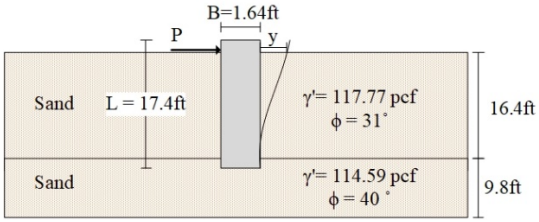

(a)

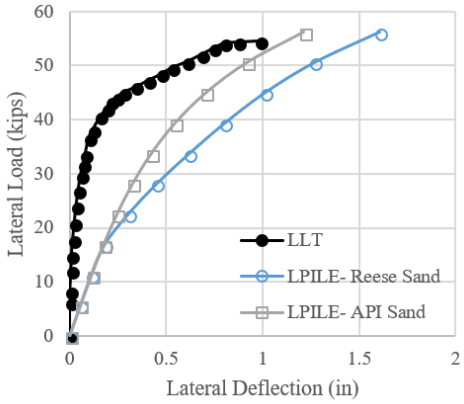

(b)

Figure 4-32. (a) Soil Stratigraphy, (b) Comparison between Measured and Predicted Lateral Deflection Curve of Jleeb Al-Shuyoukh (RN: 37).

Table 4-34. Pile and Soil Properties of University of California Test (RN: 38).

Record Number: 38

University of California, San Diego					
Paper	Lateral load behavior of cast-in-drilled-hole piles in weakly cemented sand				
Reference	Juirnarongrit, T., and Ashford, S. A. (2004). "Lateral load behavior of cast-in-drilled-hole piles in weakly cemented sand." *Transportation Research Record: Journal of the Transportation Research Board,* 1868(1), 190-198.				
Pile properties used in LPILE					
Pile type	B (ft)	L (ft)	f'c (psi)	f'y (psi)	E (psi)
bored pile	1.31	14.8	4061.06	60915.96	2.959E+07
Soil Properties used in LPILE					
P-y model	Depth		γ ' (pcf)	K (pci)	φ (°)
	Top	Bottom			
Reese/API Sand	0	19.7	127.32	*	42
Reese/API Sand	19.7	59.0	127.32	*	45

*automatically computed by LPILE

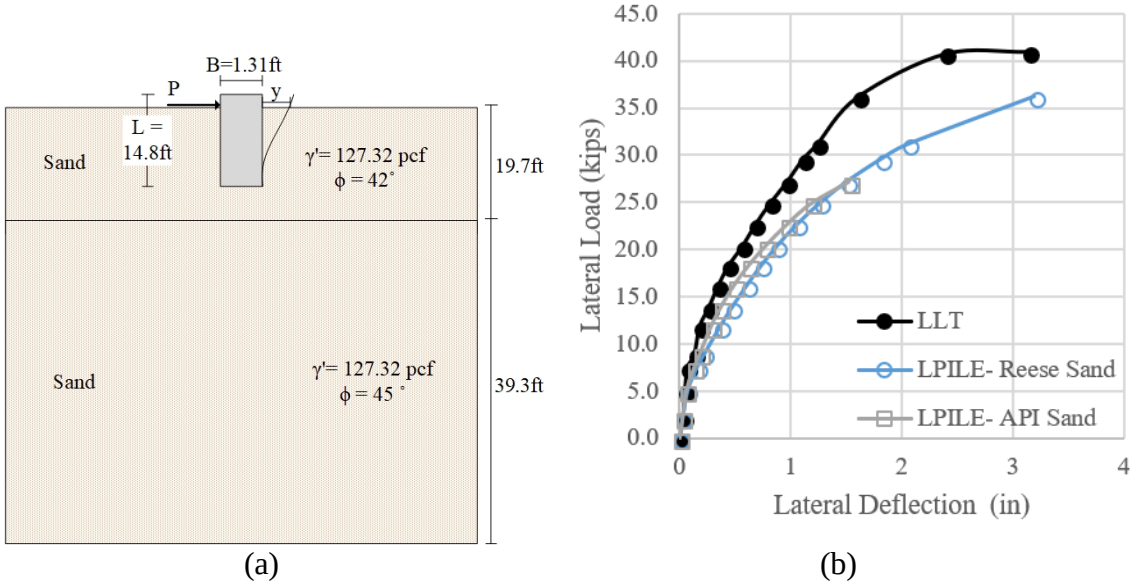

(a) (b)

Figure 4-33. (a) Soil Stratigraphy, (b) Comparison between Measured and Predicted Lateral Deflection Curve of University of California (RN: 38).

Table 4-35. Pile and Soil Properties of University of California Test (RN: 39).

Record Number: 39

University of California, San Diego					
Paper	Lateral load behavior of cast-in-drilled-hole piles in weakly cemented sand				
Reference	Juirnarongrit, T., and Ashford, S. A. (2004). "Lateral load behavior of cast-in-drilled-hole piles in weakly cemented sand." *Transportation Research Record: Journal of the Transportation Research Board*, 1868(1), 190-198.				
Pile properties used in LPILE					
Pile type	B (ft)	L (ft)	f'c (psi)	f'y (psi)	E (psi)
bored pile	1.97	39.4	4061.1	6.09E+04	2.959E+07
Soil Properties used in LPILE					
P-y model	Depth		γ ' (pcf)	K (pci)	φ (°)
	Top	Bottom			
Reese/API Sand	0	19.7	127.32	*	42
Reese/API Sand	19.7	59.0	127.32	*	45

*automatically computed by LPILE

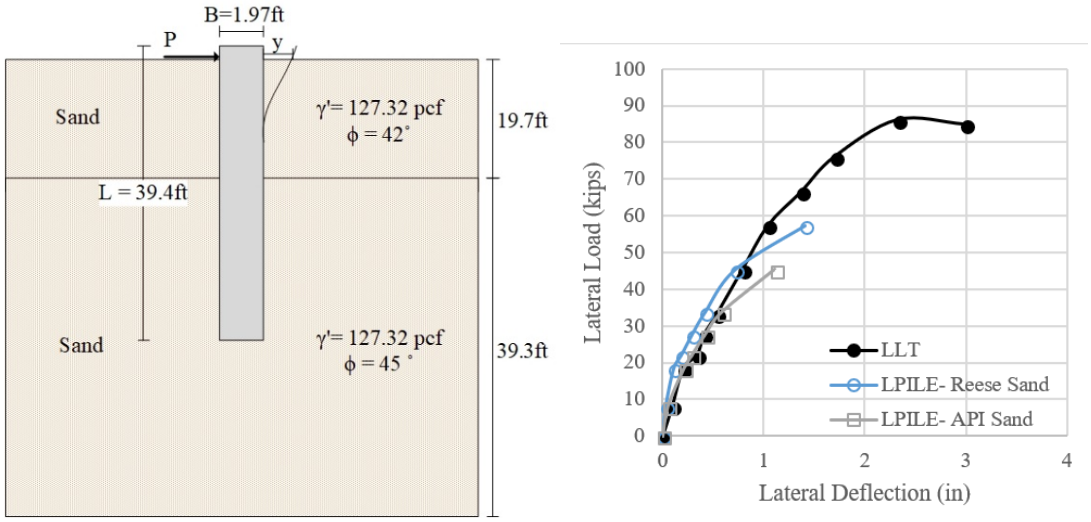

(a) (b)

Figure 4-34. (a) Soil Stratigraphy, (b) Comparison between Measured and Predicted Lateral Deflection Curve of University of California (RN: 39).

Table 4-36. Pile and Soil Properties of University of California Test (RN: 40).

Record Number: 40

University of California, San Diego					
Paper	Lateral load behavior of cast-in-drilled-hole piles in weakly cemented sand				
Reference	Juirnarongrit, T., and Ashford, S. A. (2004). "Lateral load behavior of cast-in-drilled-hole piles in weakly cemented sand." *Transportation Research Record: Journal of the Transportation Research Board*, 1868(1), 190-198.				
Pile properties used in LPILE					
Pile type	B (ft)	L (ft)	f'c (kPa)	f'y (kPa)	E (kN/m^2)
bored pile	2.95	39.4	4061.06	60915.96	2.959E+07
Soil Properties used in LPILE					
P-y model	Depth		γ ' (pcf)	K (Pci)	φ (°)
	Top	Bottom			
Reese/API Sand	0	19.7	127.32	*	42
Reese/API Sand	19.7	59.0	127.32	*	45

*automatically computed by LPILE

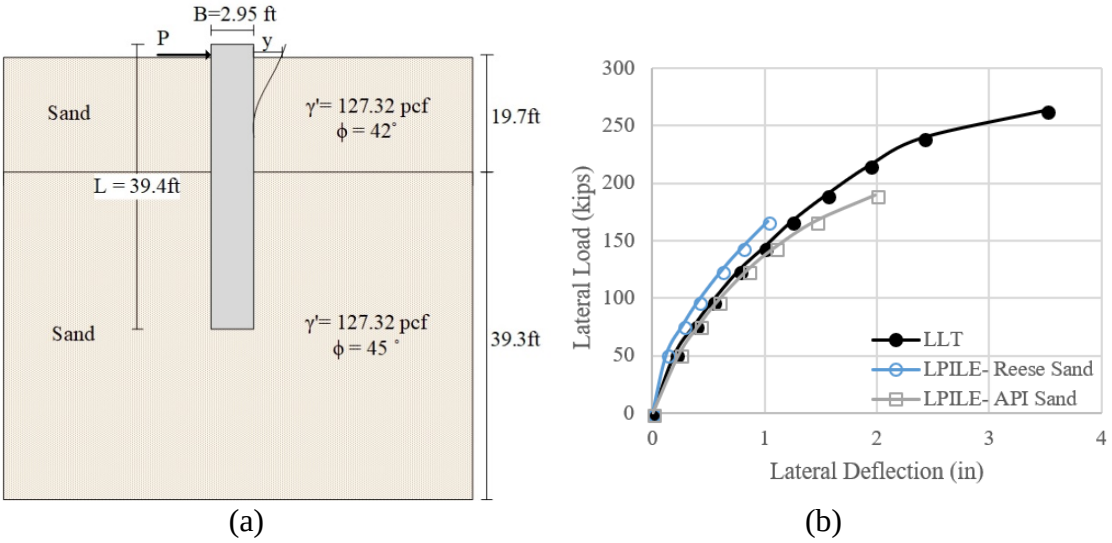

(a) (b)

Figure 4-35. (a) Soil Stratigraphy, (b) Comparison between Measured and Predicted Lateral Deflection Curve of University of California (RN: 40).

Table 4-37. Pile and Soil Properties of University of California Test (RN: 41).

Record Number: 41

University of California, San Diego					
Paper	Lateral load behavior of cast-in-drilled-hole piles in weakly cemented sand				
Reference	Juirnarongrit, T., and Ashford, S. A. (2004). "Lateral load behavior of cast-in-drilled-hole piles in weakly cemented sand." *Transportation Research Record: Journal of the Transportation Research Board*, 1868(1), 190-198.				
Pile properties used in LPILE					
Pile type	B (ft)	L (ft)	f'c (psi)	f'y (psi)	E (psi)
bored pile	3.94	39.4	4061.06	60915.96	2.959E+07
Soil Properties used in LPILE					

P-y model	Depth		γ ' (pcf)	K (pci)	φ (°)
	Top	Bottom			
Reese/API Sand	0	19.7	127.32	*	42
Reese/API Sand	19.7	59.0	127.32	*	45

*automatically computed by LPILE

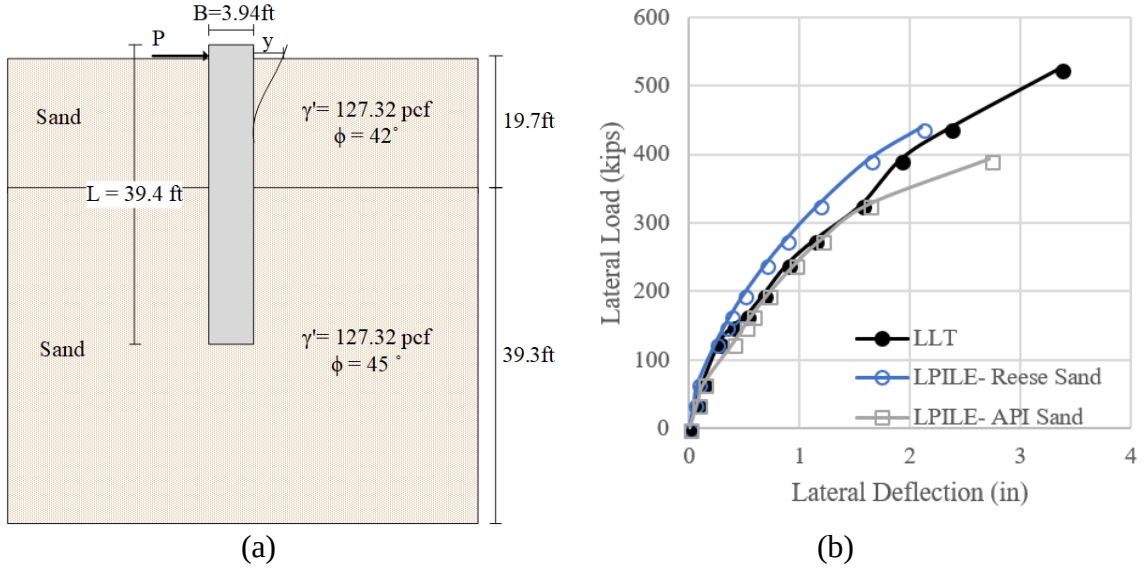

(a) (b)

Figure 4-36. (a) Soil Stratigraphy, (b) Comparison between Measured and Predicted Lateral Deflection Curve of University of California (RN: 41).

Table 4-38. Pile and Soil Properties of Hawthorne Test (Lemnitzer) (RN: 42).

Record Number: 42

Hawthorne, California (Fixed Head)							
Paper	Nonlinear efficiency of bored pile group under lateral loading						
Reference	Lemnitzer, Anne, et al. "Nonlinear efficiency of bored pile group under lateral loading." *Journal of Geotechnical and Geoenvironmental Engineering*. 136.12 (2010): 1673-1685.						
Pile properties used in LPILE							
Pile type	B (ft)	L (ft)	E (psi)	Area (in^2)	I (in^4)		
bored pile	2.0	38.3	3.046E+07	4.530E+02	1.63E+04		
Soil Properties used in LPILE							
P-y model	Depth		γ ' (pcf)	K (pci)	Su(psf)	φ (°)	ε_{50}
	Top	Bottom					
Reese/API Sand	0.0	14.8	127.32	*	n/a	28	n/a
Soft Clay	14.8	31.2	127.32	n/a	3759.38	n/a	*
Reese/API Sand	31.2	41.0	127.32	*	n/a	30	n/a
Soft Clay	41.0	70.5	127.32	n/a	3759.38	n/a	*
Reese/API Sand	70.5	86.9	127.32	*	n/a	33	n/a

*automatically computed by LPILE

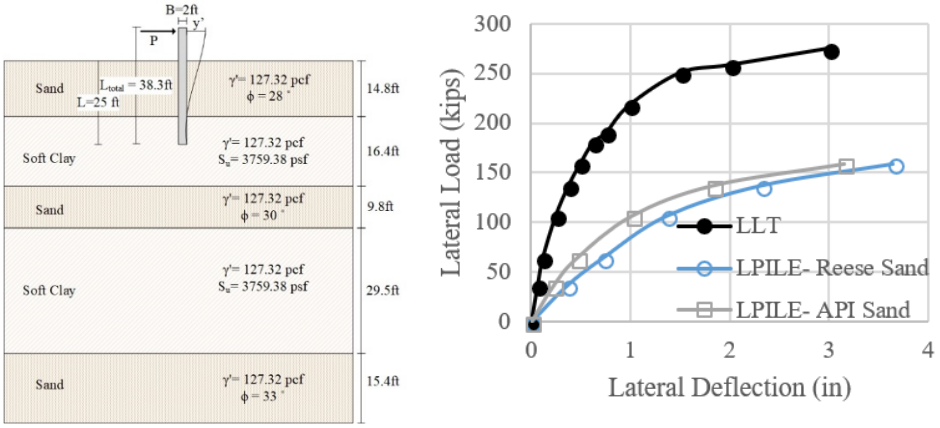

(a) (b)

Figure 4-37. (a) Soil Stratigraphy, (b) Comparison between Measured and Predicted Lateral Deflection Curve of Hawthorne (Lemnitzer) (RN: 42).

Table 4-39. Pile and Soil Properties of Hawthorne Test (Lemnitzer) (RN: 43).

Record Number: 43

Hawthorne, California (FlagPole)						
Paper	Nonlinear efficiency of bored pile group under lateral loading					
Reference	Lemnitzer, Anne, et al. "Nonlinear efficiency of bored pile group under lateral loading." *Journal of Geotechnical and Geoenvironmental Engineering*. 136.12 (2010): 1673-1685.					
Pile properties used in LPILE						
Pile type	B (ft)	L (ft)	E (psi)	Area (in^2)	I (in^4)	
bored pile	2.0	25.0	3.046E+07	4.530E+02	1.63E+04	
Soil Properties used in LPILE						
P-y model	Depth		γ ' (pcf)	K (pci)	Su(psf)	φ (°)	ε_{50}
	Top	Bottom					
Reese/API Sand	0.0	14.8	127.32	*	n/a	28	n/a
Soft Clay	14.8	31.2	127.32	n/a	3759.38	n/a	*
Reese/API Sand	31.2	41.0	127.32	*	n/a	30	n/a
Soft Clay	41.0	70.5	127.32	n/a	3759.38	n/a	*
Reese/API Sand	70.5	86.9	127.32	*	n/a	33	n/a

*automatically computed by LPILE

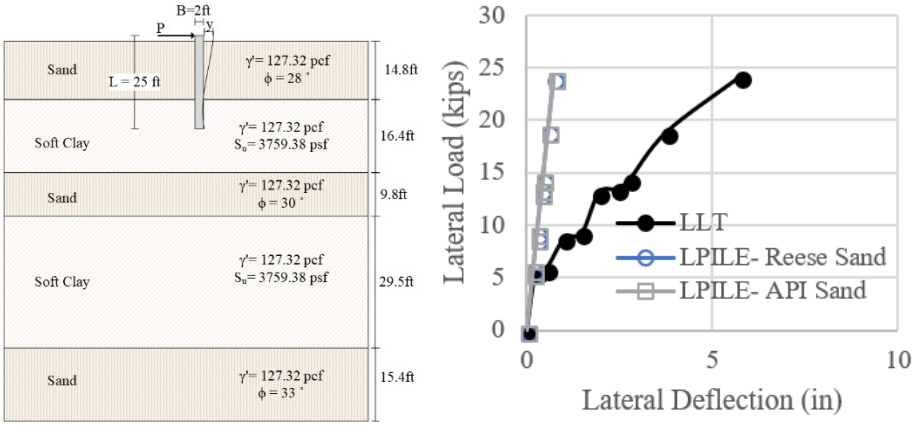

(a) (b)

Figure 4-38. (a) Soil Stratigraphy, (b) Comparison between Measured and Predicted Lateral Deflection Curve of Hawthorne (Lemnitzer) (RN: 43).

4.2.17 University of Massachusetts Campus in Amherst, Massachusetts, Test (UMass Amherst Test)

A series of full-scale pile load tests in sand was conducted at the University of Massachusetts in Amherst, Massachusetts (Lutenegger and Miller, 1993). The applied lateral load went up to about 15 kips and caused 2.17 in., 0.482 in., 1.72 in., and 0.61 in., respectively, at the top of those short piles. The four drilled-shafts were 1.67 ft in diameter for the first two, 2.0 ft in diameter for the other two and 5 ft, 8 ft, 5 ft, and 8 ft in length. Figure 4-39, Figure 4-40, Figure 4-41, and Figure 4-42 show the soil stratigraphy and the field test results. Table 4-40, Table 4-41, Table 4-42, and Table 4-43 describe the data for the piles and the soils used as input in LPILE (RN: 44–47).

4.2.18 Incheon, South Korea Test (Small)

Four full-scale lateral pile load tests were performed on two different size piles in clay at the Incheon Bridge in Incheon, South Korea (Jeong et al., 2007). Three of them were 3.3 ft in diameter and 87 ft in length. The other pile is a large diameter pile that will be presented in the next section. The maximum lateral deflection at the top of the piles were 6.9 in., 6.9 in., and 5.9 in. caused by the maximum lateral loads of 203 kips, 203 kips, and 180 kips, respectively. Figure 4-43, Figure 4-44, and Figure 4-45 show the soil stratigraphy and the field test results. Table 4-44, Table 4-45, and Table 4-46 describe the data for the piles and the soils used as input in LPILE (RN: 48–50).

4.2.19 Japan Test (Small)

Several lateral load tests were performed on piles in Japan and reported by Ishikawa (1985). The three tests on piles smaller than 5 ft in diameter are introduced here, and the rest will be discussed in the next section. The three, small diameter drilled-shafts were 4 ft in diameter and 118 ft in length at the C site, 3.33 ft in diameter and 112 ft in length at the D site and 4.92 ft in diameter and 135 ft in length at the E site. The soil profile at the C site consisted of 131.2 ft of coarse to fine sand and silt. The soil profile at the D site consisted of 114.8 ft of clay, silt, gravel with sand, and fine sand. The soil profile at site E consists of 157.5 ft of fine sand with clay, gravel with sand, and volcanic fine sand. Figure 4-46, Figure 4-47 and Figure 4-48 show the soil stratigraphy and the field test results. Table 4-47, Table 4-48 and Table 4-49 describe the data for the piles and the soils used as input in LPILE (RN: 67–69).

Table 4-40. Pile and Soil Properties of the University of Massachusetts Test (RN: 44).

Record Number: 44

University of Massachusetts campus in Amherst, Massachusetts (0.51x1.52)						
Paper	Behavior of laterally loaded drilled shafts in stiff soil					
Reference	Lutenegger, Alan J., and Gerald A. Miller. "Behavior of laterally loaded drilled shafts in stiff soil." (1993)					
Pile properties used in LPILE						
Pile type	B (ft)	L (ft)	I (in.^{4})	E (psi)		
Bored Pile	1.67	5.0	7978.40	3.05E+06		
Soil Properties used in LPILE						
P-y model	Depth		γ ' (pcf)	K (pci)	Su(psf)	φ (°)	ε_{50}
	Top	Bottom					
Reese/API Sand	0.0	3.9	127.32	*	n/a	30	n/a
Soft Clay	3.9	9.84	127.32	n/a	1253.13	n/a	*
Soft Clay	9.84	16.4	127.32	n/a	1253.13	n/a	*

*automatically computed by LPILE

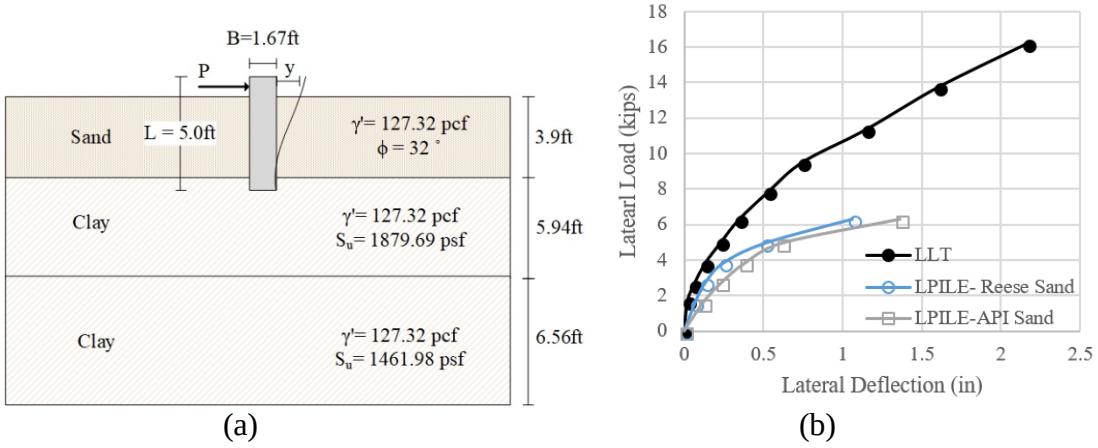

Figure 4-39. (a) Soil Stratigraphy, (b) Comparison between Measured and Predicted Lateral Deflection Curve of the University of Massachusetts (RN: 44).

Table 4-41. Pile and Soil Properties of the University of Massachusetts Test (RN: 45).

Record Number: 45

University of Massachusetts campus in Amherst, Massachusetts (0.51x2.44)							
Paper	Behavior of laterally loaded drilled shafts in stiff soil						
Reference	Lutenegger, Alan J., and Gerald A. Miller. "Behavior of laterally loaded drilled shafts in stiff soil." (1993)						
Pile properties used in LPILE							
Pile type	B (ft)		L (ft)		I (in.^{4})	E (psi)	
Bored Pile	1.67		8.0		7978.40	3.05E+06	
Soil Properties used in LPILE							
P-y model	Depth		γ ' (pcf)	K (pci)	Su(psf)	φ (°)	ε_{50}
	Top	Bottom					
Reese/API Sand	0.0	3.9	127.32	*	n/a	32	n/a
Soft Clay	3.9	9.84	127.32	n/a	1879.69	n/a	*
Soft Clay	9.84	16.4	127.32	n/a	1461.98	n/a	*

*automatically computed by LPILE

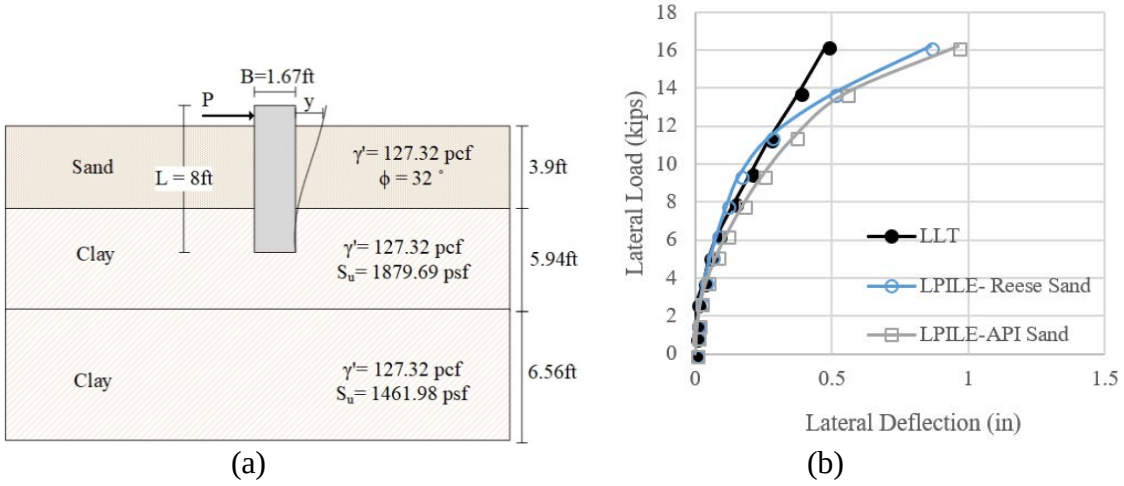

Figure 4-40. (a) Soil Stratigraphy, (b) Comparison between Measured and Predicted Lateral Deflection Curve of the University of Massachusetts (RN: 45).

Table 4-42. Pile and Soil Properties of the University of Massachusetts Test (RN: 46).

Record Number: 46

University of Massachusetts campus in Amherst, Massachusetts (0.61x1.52)							
Paper	Behavior of laterally loaded drilled shafts in stiff soil						
Reference	Lutenegger, Alan J., and Gerald A. Miller. "Behavior of laterally loaded drilled shafts in stiff soil." (1993)						
Pile properties used in LPILE							
Pile type	B (ft)		L (ft)	I (in.^{4})		E (psi)	
Bored Pile	2.0		5.0	16328.8		3.05E+06	
Soil Properties used in LPILE							
P-y model	Depth		γ ' (pcf)	K (pci)	Su(psf)	φ (°)	ε_{50}
	Top	Bottom					
Reese/API Sand	0.0	3.9	127.32	*	n/a	32	n/a
Soft Clay	3.9	9.84	127.32	n/a	1879.69	n/a	*
Soft Clay	9.84	16.4	127.32	n/a	1461.98	n/a	*

*automatically computed by LPILE

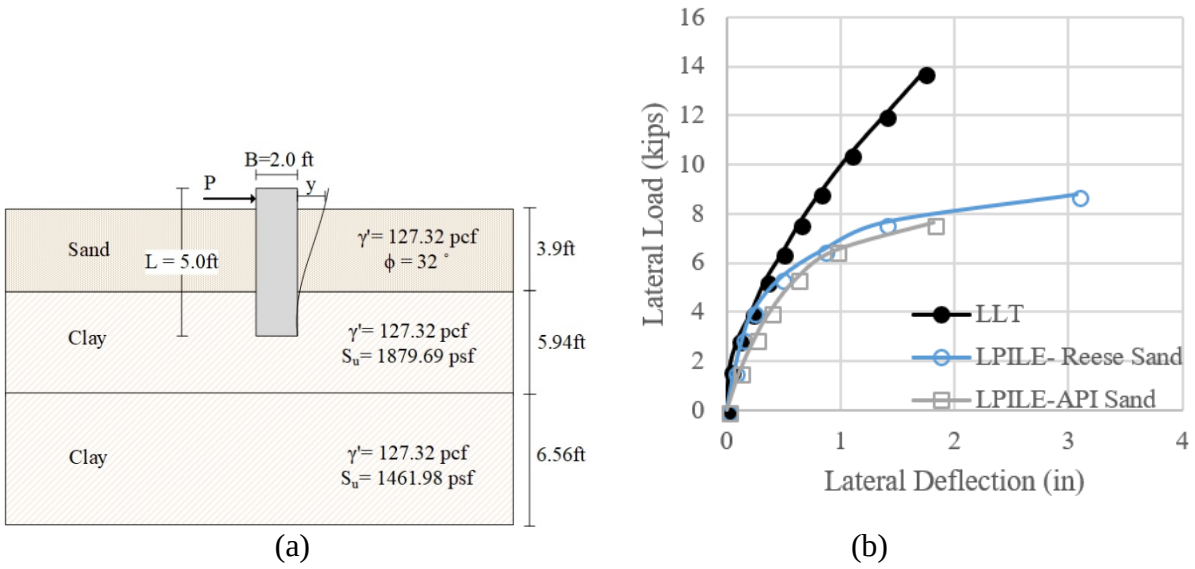

(a) (b)

Figure 4-41. (a) Soil Stratigraphy, (b) Comparison between Measured and Predicted Lateral Deflection Curve of the University of Massachusetts (RN: 46).

Table 4-43. Pile and Soil Properties of the University of Massachusetts Test (RN: 47).

Record Number: 47

University of Massachusetts campus in Amherst, Massachusetts (0.61x2.44)							
Paper	Behavior of laterally loaded drilled shafts in stiff soil						
Reference	Lutenegger, Alan J., and Gerald A. Miller. "Behavior of laterally loaded drilled shafts in stiff soil." (1993)						
Pile properties used in LPILE							
Pile type	B (ft)	L (ft)	I (in.^{4})	E (psi)			
Bored Pile	2.0	8.0	16328.80	3.05E+06			
Soil Properties used in LPILE							
P-y model	Depth		γ ' (pcf)	K (pci)	Su(psf)	φ (°)	ε_{50}
	Top	Bottom					
Reese/API Sand	0.0	3.9	127.32	*	n/a	32	n/a
Soft Clay	3.9	9.84	127.32	n/a	1879.69	n/a	*
Soft Clay	9.84	16.4	127.32	n/a	1461.98	n/a	*

*automatically computed by LPILE

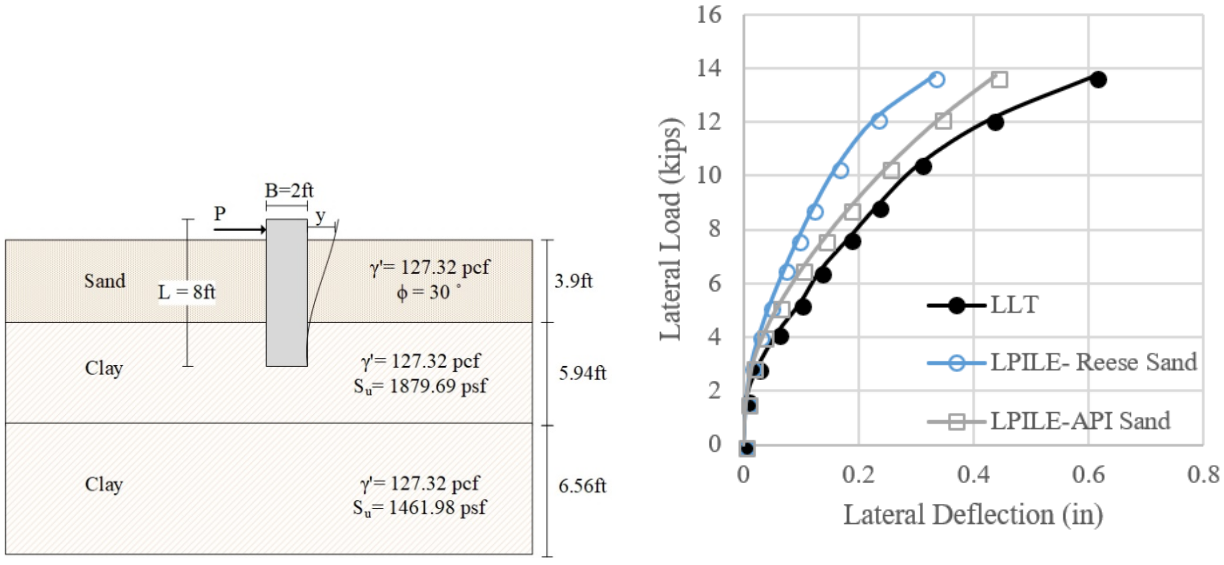

(a) (b)

Figure 4-42. (a) Soil Stratigraphy, (b) Comparison between Measured and Predicted Lateral Deflection Curve of the University of Massachusetts (RN: 47).

Table 4-44. Pile and Soil Properties of Incheon Bridge Test (RN: 48).

Record Number: 48

Incheon Birdge, Incheon, South Korea (LT1)							
Paper	Cyclic lateral load tests of offshore large diameter piles of Incheon Bridge in marine clay						
Reference	Jeong, Sangseom, et al. "Cyclic lateral load tests of offshore large diameter piles of Incheon Bridge in marine clay." The Seventeenth International Offshore and Polar Engineering Conference. International Society of Offshore and Polar Engineers, 2007.						
Pile properties used in LPILE							
Pile type	B (ft)	L (ft)	t (in.)	I (in.^{4})	E (psi)		
Steel pipe pile	3.33	87.3	0.63	15135.81	2.90E+07		
Soil Properties used in LPILE							
P-y model	Depth		γ ' (pcf)	K (pci)	Su(psf)	φ (°)	ε_{50}
	Top	Bottom					
Soft Clay	0	59.1	111.40	n/a	375.94	n/a	*
Reese Sand	59.1	72.2	113.31	*	n/a	24	n/a
Reese Sand	72.2	98.4	113.31	*	n/a	34	n/a
Reese Sand	98.4	121.4	128.59	*	n/a	32	n/a
Reese Sand	121.4	147.6	130.5	*	n/a	33	n/a

*automatically computed by LPILE

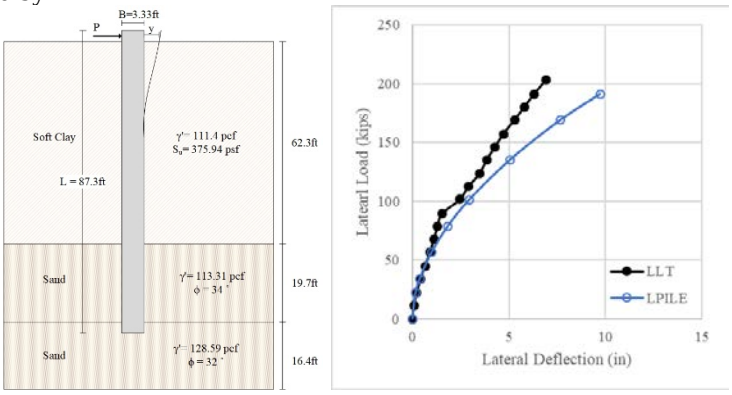

(a) (b)

Figure 4-43. (a) Soil Stratigraphy, (b) Comparison between Measured and Predicted Lateral Deflection Curve Incheon Bridge (RN: 48).

Table 4-45. Pile and Soil Properties of Incheon Bridge Test (RN: 49).

Record Number: 49

Incheon Birdge, Incheon, South Korea (LT2)							
Paper	Cyclic lateral load tests of offshore large diameter piles of Incheon Bridge in marine clay						
Reference	Jeong, Sangseom, et al. "Cyclic lateral load tests of offshore large diameter piles of Incheon Bridge in marine clay." The Seventeenth International Offshore and Polar Engineering Conference. International Society of Offshore and Polar Engineers, 2007.						
Pile properties used in LPILE							
Pile type	B (ft)	L (ft)	t (in.)	I (in.^{4})	E (psi)		
Steel pipe pile	3.33	87.3	0.63	15135.81	2.90E+07		
Soil Properties used in LPILE							
P-y model	Depth		γ ' (pcf)	K (pci)	Su(psf)	φ (°)	ε_{50}
	Top	Bottom					
Soft Clay	0	62.3	111.40	n/a	375.94	n/a	*
Reese Sand	62.3	82.0	113.31	*	n/a	34	n/a
Reese Sand	82.0	98.4	128.59	*	n/a	32	n/a

*automatically computed by LPILE

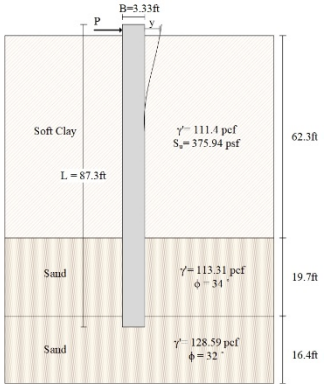

(a)

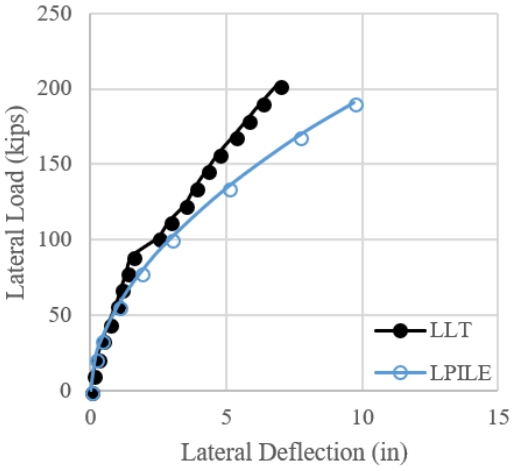

(b)

Figure 4-44. (a) Soil Stratigraphy, (b) Comparison between Measured and Predicted Lateral Deflection Curve Incheon Bridge (RN: 49).

Table 4-46. Pile and Soil Properties of Incheon Bridge Test (RN: 50).

Record Number: 50

Incheon Bridge, Incheon, South Korea (LT3)							
Paper	Cyclic lateral load tests of offshore large diameter piles of Incheon Bridge in marine clay						
Reference	Jeong, Sangseom, et al. "Cyclic lateral load tests of offshore large diameter piles of Incheon Bridge in marine clay." The Seventeenth International Offshore and Polar Engineering Conference. International Society of Offshore and Polar Engineers, 2007.						
Pile properties used in LPILE							
Pile type	B (ft)	L (ft)	t (in.)	I (in.^{4})	E (psi)		
Steel pipe pile	3.33	87.3	0.63	15135.81	2.90E+07		
Soil Properties used in LPILE							
P-y model	Depth		γ ' (pcf)	K (pci)	Su (psf)	φ (°)	ε_{50}
	Top	Bottom					
Soft Clay	0	62.3	111.40	n/a	375.94	n/a	*
Reese Sand	62.3	82.0	113.31	*	n/a	34	n/a
Reese Sand	82.0	98.4	128.59	*	n/a	32	n/a

*automatically computed by LPILE

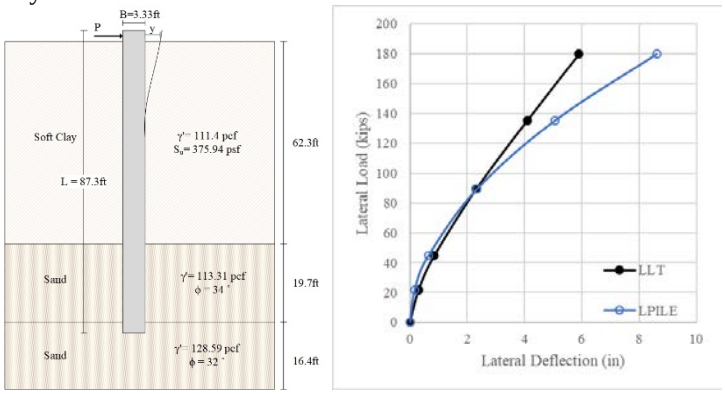

(a) (b)

Figure 4-45. (a) Soil Stratigraphy, (b) Comparison between Measured and Predicted Lateral Deflection Curve Incheon Bridge (RN: 50).

Table 4-47. Pile and Soil Properties of Japan Site C Test (RN: 67).

Record Number: 67

Japan Test (C site)					
Paper	Study on lateral resistance of large diameter pile				
Reference	Ishikawa (1985). "Study on lateral resistance of large diameter pile," 土木試驗所月報. (In Japanese)				
Pile properties used in LPILE					
Pile type	B (ft)	L (ft)	t (in.)	I (in.^{4})	E (psi)
Pipe Pile	4.0	118.1	0.551	2.31E+04	2.98E+07
Soil Properties used in LPILE					

P-y model	Depth		γ ' (pcf)	K (Pci)	φ (°)
	Top	Bottom			
Reese/API Sand	0	32.8	127.32	*	30
Reese/API Sand	32.8	62.7	127.32	*	26
Reese/API Sand	62.7	73.8	127.32	*	41
Reese/API Sand	73.8	83.7	120.95	*	28
Reese/API Sand	83.7	95.1	127.32	*	30
Reese/API Sand	95.1	131.2	140.05	*	41

*automatically computed by LPILE

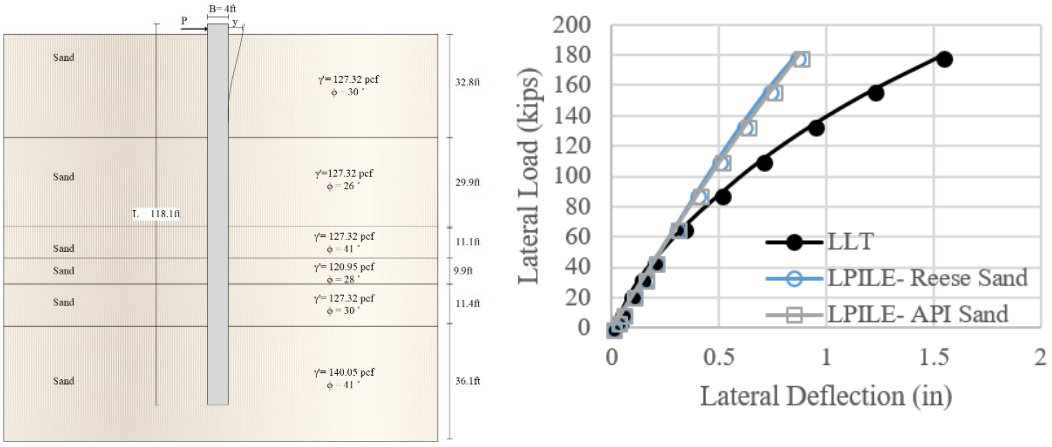

(a) (b)

Figure 4-46. (a) Soil Stratigraphy, (b) Comparison between Measured and Predicted Lateral Deflection Curve of Japan Site C.

Table 4-48. Pile and Soil Properties of Japan Site D Test (RN: 68).

Record Number: 68

Japan Test (D site)							
Paper	Study on lateral resistance of large diameter pile						
Reference	Ishikawa (1985). “Study on lateral resistance of large diameter pile,” 土木試驗所月報. (In Japanese)						
Pile properties used in LPILE							
Pile type	B (ft)	L (ft)	t (in.)	I (in.^{4})	E (psi)		
Pipe Pile	3.33	111.5	0.472	1.51E+12	2.98E+07		
Soil Properties used in LPILE							
P-y model	Depth		γ ' (pcf)	K (pci)/Su (psf)	φ (°)	ε_{50}	
	Top	Bottom					
Reese Sand	0	13.1	127.32	*	28	n/a	
Soft Clay	13.1	62.3	127.32	626.7	n/a	*	
Soft Clay	62.3	73.5	127.32	1044.5	n/a	*	
Reese Sand	73.5	90.9	127.32	*	32	n/a	
Reese Sand	90.9	95.8	127.32	*	32	n/a	
Reese Sand	95.8	102.0	127.32	*	37	n/a	
Reese Sand	102.0	114.8	133.68	*	41	n/a	

*automatically computed by LPILE

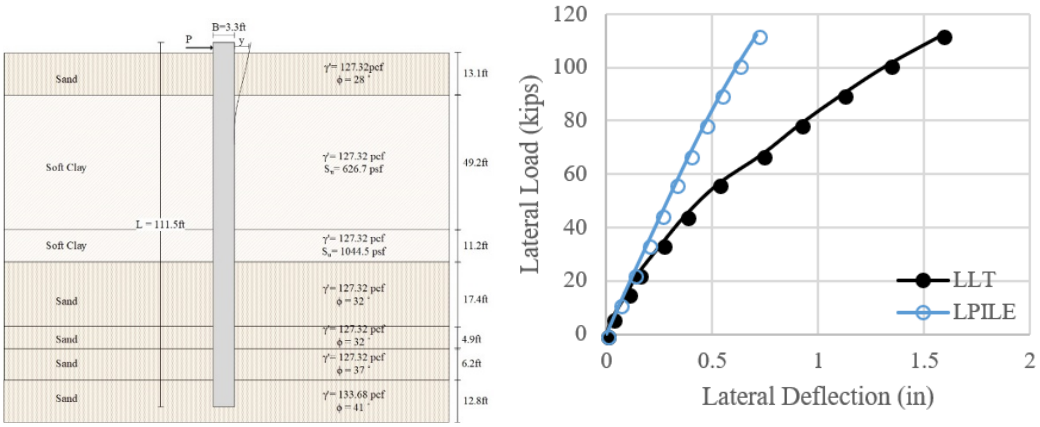

(a) (b)

Figure 4-47. (a) Soil stratigraphy, (b) Comparison between Measured and Predicted Lateral Deflection Curve Japan Site D.

Table 4-49. Pile and Soil Properties of Japan Site E Test (RN: 69).

Record Number: 69

Japan Test (E site)				
Paper	Study on lateral resistance of large diameter pile			
Reference	Ishikawa (1985). "Study on lateral resistance of large diameter pile," 土木試驗所月報. (In Japanese)			
Pile properties used in LPILE				
Pile type	B (ft)	L (ft)	I (in.^{4})	E (psi)
bored pile	4.92	134.5	8.24E+13	4.33E+06

Soil Properties used in LPILE					
P-y model	Depth		γ ' (pcf)	K (Pci)	φ (°)
	Top	Bottom			
Reese/API Sand	0	26.2	133.68	*	30
Reese/API Sand	26.2	95.1	127.32	*	28
Reese/API Sand	95.1	118.1	133.68	*	36
Reese/API Sand	118.1	157.5	127.32	*	33

*automatically computed by LPILE

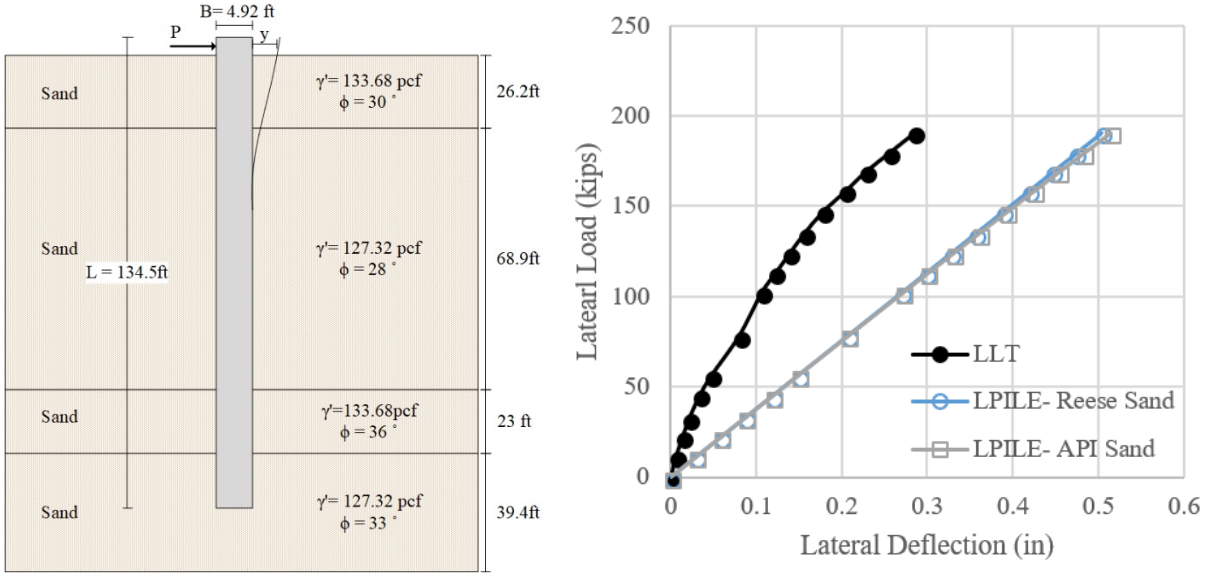

(a) (b)

Figure 4-48. (a) Soil Stratigraphy, (b) Comparison between Measured and Predicted Lateral Deflection Curve of Japan (RN: 69).

4.2.20 Kern County, California, Test (Small)

There were four pile load tests performed at Kern County, California (Load Test Consulting, 2018). Three of them were constructed and tested as small diameter pile (B=3.25 ft ATS-2/Test pile, 4.25 ft ATS-2/React pile, and 4.75 ft ATS-3/Test pile). One was 5.75 ft in diameter and will be discussed in the later section. For ATS-2/Test shaft, the maximum applied lateral load of 352 kips caused 4 in. deflection at the pile top. For ATS-2/React shaft, the maximum applied lateral load of 352 kips led to 1.06 in. displacement at the pile head. For ATS-3/Test shaft, the maximum applied lateral load of 541 kips caused 3.78 in. deflection at the pile top. The soil profile consists of 158 ft of sand and clay soil. Figure 4-49, Figure 4-50, and Figure 4-51 show the soil stratigraphy and the field test results. Table 4-50, Table , and Table 4-52 describe the data for piles and soils are described in (RN: 80–82).

4.2.21 Massena, New York, Test

A series of four lateral load tests was conducted in Massena, New York. The piles were 0.5 ft in diameter for the first two and 5 ft and 10 ft in length while the other two were 1.0 ft in diameter and 5 ft and 10 ft in length. The soil profile consisted of 13.1 ft of stiff clay close to the ground and soft clay underneath. A maximum lateral load of 2.02 kips led to 0.22 in. and 0.29 in. deflection at the pile top for the first two tests, respectively, while a maximum lateral load 4.61 kips caused 0.21 and 0.31 in. deflection at the pile head for the other two. Figure 4-52, Figure 4-53, Figure 4-54, and Figure 4-55 show the soil stratigraphy and the field test results. Table 4-53, Table 4-54, Table 4-55, and Table 4-56 describe the data for the piles and the soils used as input in LPILE (RN: 86–89).

Table 4-50. Pile and Soil Properties of Kern County Test (RN: 80).

Record Number: 80

Kern County, CA (ATS-2/Test)							
Report	LTC Data Report - Lateral Load Test Results for ATS-2, Merced Avenue Overpass						
Reference	Load Test Consulting, Ltd. (2018) "LTC Data Report - Lateral Load Test Results for ATS-2, Merced Avenue Overpass." Load Test Consulting load test report.						
Pile properties used in LPILE							
Pile type	B(ft)	L(ft)		I(in^4)		E(psi)	
bored pile	3.250	50		1.14E+05		3.05E+06	
Soil Properties used in LPILE							
P-y model	Depth		γ ' (pcf)	K (pci)	Su (psf)	φ (°)	ε_{50}
	Top	Bottom					
Reese Sand	0	30.0	119.60	*	n/a	32	n/a
Reese Sand	30.0	43.0	103.10	*	n/a	38	n/a
Stiff Clay	43.0	56.1	117.90	n/a	7518.76	n/a	*
Reese Sand	56.1	73.2	113.40	*	n/a	41	n/a
Stiff Clay	73.2	80.1	113.40	n/a	3341.67	n/a	*

*automatically computed by LPILE

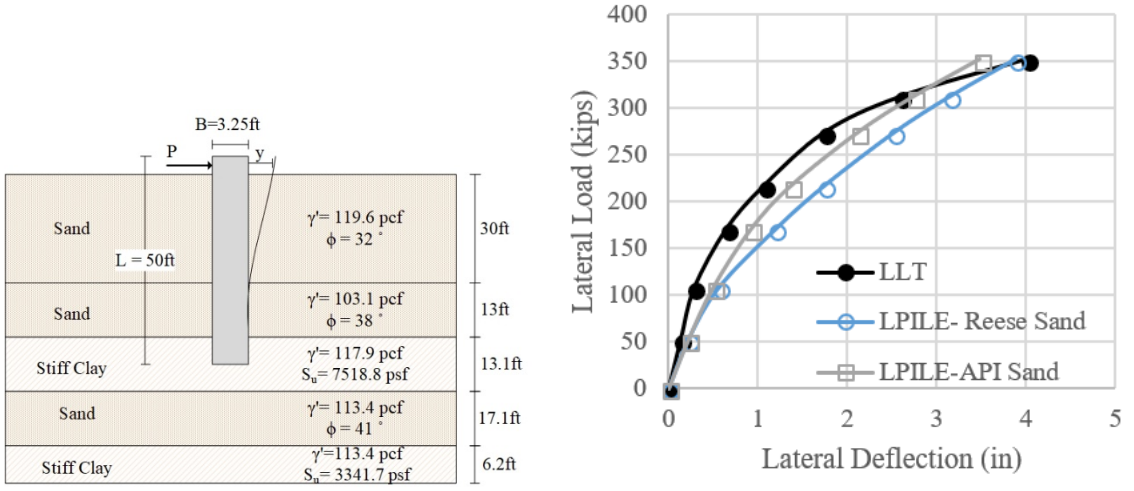

(a) (b)

Figure 4-49. (a) Soil Stratigraphy, (b) Comparison between Measured and Predicted Lateral Deflection Curve of Kern County (RN: 80).

Table 4-51. Pile and Soil Properties of Kern County Test (RN: 81).

Record Number: 81

Kern County, CA (ATS-2/React)							
Report	LTC Data Report - Lateral Load Test Results for ATS-2, Merced Avenue Overpass						
Reference	Load Test Consulting, Ltd. (2018) "LTC Data Report - Lateral Load Test Results for ATS-2, Merced Avenue Overpass." Load Test Consulting load test report.						
Pile properties used in LPILE							
Pile type	B(ft)	L(ft)	$I(in^4)$	E(psi)			
bored pile	4.249	65.62	3.32E+05	3.05E+06			
Soil Properties used in LPILE							
P-y model	Depth		γ ' (pcf)	K (pci)	Su (psf)	φ (°)	ε_{50}
	Top	Bottom					
Reese Sand	0	30.0	119.60	*	n/a	32	n/a
Reese Sand	30.0	43.0	103.10	*	n/a	38	n/a
Stiff Clay	43.0	56.1	117.90	n/a	7518.8	n/a	*
Reese Sand	56.1	73.2	113.40	*	n/a	41	n/a
Stiff Clay	73.2	79.4	113.40	n/a	3341.7	n/a	*

*automatically computed by LPILE

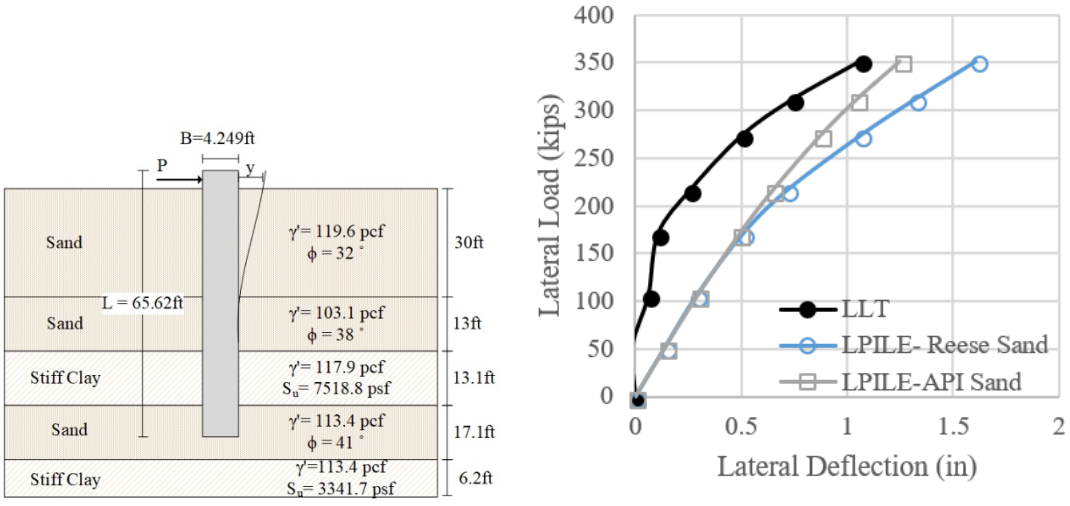

(a) (b)

Figure 4-50. (a) Soil Stratigraphy, (b) Comparison between Measured and Predicted Lateral Deflection Curve of Kern County (RN: 81).

Table 4-52. Pile and Soil Properties of Kern County Test (RN: 82).

Record Number: 82

Kern County, CA (ATS-3/Test)							
Report	LTC Data Report - Lateral Load Test Results for ATS-3, Merced Avenue Overpass						
Reference	Load Test Consulting, Ltd. (2018) "LTC Data Report - Lateral Load Test Results for ATS-3, Merced Avenue Overpass." Load Test Consulting load test report.						
Pile properties used in LPILE							
Pile type	B(ft)	L(ft)	$I(in^4)$	E(psi)			
bored pile	4.751	82.05	5.18E+05	3.05E+06			
Soil Properties used in LPILE							
P-y model	Depth		γ ' (pcf)	K (pci)	Su (psf)	φ (°)	ε_{50}
	Top	Bottom					
Reese Sand	0	13.1	115.20	*	n/a	29	n/a
Reese Sand	13.1	27.9	119.30	*	n/a	36	n/a
Stiff Clay	27.9	43.0	106.40	n/a	3759.4	n/a	*
Reese Sand	43.0	53.1	106.40	*	n/a	41	n/a
Stiff Clay	53.1	67.9	113.20	n/a	6892.2	n/a	*
Reese Sand	67.9	101.4	121.10	*	n/a	41	n/a

*automatically computed by LPILE

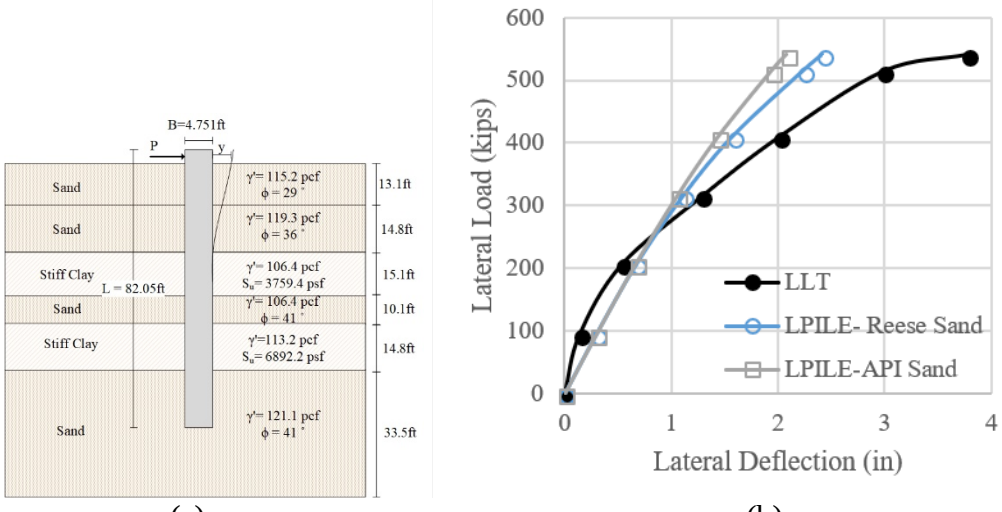

(a) (b)

Figure 4-51. (a) Soil Stratigraphy, (b) Comparison between Measured and Predicted Lateral Deflection Curve of Kern County (RN: 82).

Table 4-53. Pile and Soil Properties of Massena Test (RN: 86).

Record Number: 86

Massena, New York					
Paper	Analysis of Laterally Loaded Drilled Shafts Using In Situ Test Results				
Reference	Huang, A. B., et al. "Analysis of Laterally Loaded Drilled Shafts Using In Situ Test Results." *Transportation Research Record* 1235 (1989): 60-67.				
Pile properties used in LPILE					
Pile type	B(ft)	L(ft)	I(in^4)	E(psi)	
bored pile	0.5	5	6.3E+05	3.05E+06	
Soil Properties used in LPILE					
P-y model	Depth		γ ' (pcf)	Su (psf)	ε_{50}
	Top	Bottom			
Stiff Clay	0	3.3	127.32	1775.65	0.012
Soft Clay	3.3	4.9	127.32	1086.2	0.01

*automatically computed by LPILE

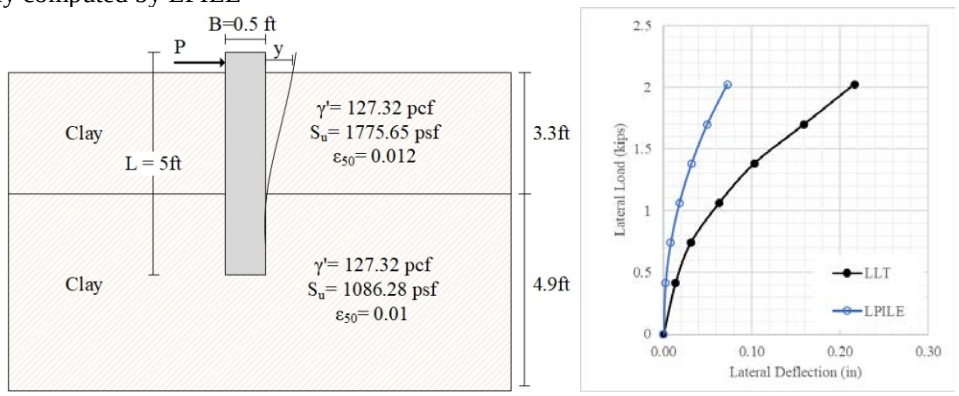

(a) (b)

Figure 4-52. (a) Soil Stratigraphy, (b) Comparison between Measured and Predicted Lateral Deflection Curve of Massena (RN: 86).

Table 4-54. Pile and Soil Properties of Massena Test (RN: 87).

Record Number: 87

Massena, New York					
Paper	Analysis of Laterally Loaded Drilled Shafts Using In Situ Test Results				
Reference	Huang, A. B., et al. "Analysis of Laterally Loaded Drilled Shafts Using In Situ Test Results." *Transportation Research Record* 1235 (1989): 60-67.				
Pile properties used in LPILE					
Pile type	B(ft)	L(ft)	$I(in^4)$	E(psi)	
bored pile	0.5	10	6.3E+05	3.05E+06	
Soil Properties used in LPILE					
P-y model	Depth		γ ' (pcf)	Su (psf)	ε_{50}
	Top	Bottom			
Stiff Clay	0	3.3	127.32	1775.65	0.012
Stiff Clay	3.3	4.9	127.32	1086.2	0.01
Soft Clay	4.9	8.2	127.32	1086.2	0.01
Soft Clay	8.2	9.8	127.32	1462.3	0.009
Soft Clay	9.8	11.5	127.32	1044.5	0.008
Soft Clay	11.5	13.1	127.32	1462.3	0.008

*automatically computed by LPILE

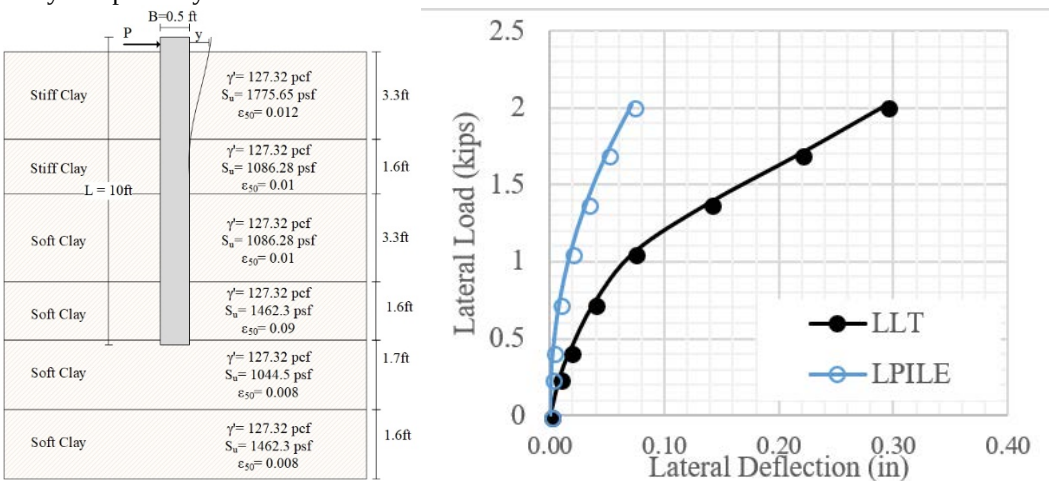

(a) (b)

Figure 4-53. (a) Soil Stratigraphy, (b) Comparison between Measured and Predicted Lateral Deflection Curve of Massena (RN: 87).

Table 4-55. Pile and Soil Properties of Massena Test (RN: 88).

Record Number: 88

Massena, New York					
Paper	Analysis of Laterally Loaded Drilled Shafts Using In Situ Test Results				
Reference	Huang, A. B., et al. "Analysis of Laterally Loaded Drilled Shafts Using In Situ Test Results." *Transportation Research Record* 1235 (1989): 60-67.				
Pile properties used in LPILE					
Pile type	B(ft)	L(ft)	I(in^4)	E(psi)	
bored pile	1	5	1.02E+07	3.05E+06	
Soil Properties used in LPILE					
P-y model	Depth		γ ' (pcf)	Su (psf)	ε_{50}
	Top	Bottom			
Stiff Clay	0	3.3	127.32	1775.65	0.012
Stiff Clay	3.3	4.9	127.32	1086.2	0.01
Soft Clay	4.9	8.2	127.32	1086.2	0.01
Soft Clay	8.2	9.8	127.32	1462.3	0.009
Soft Clay	9.8	11.5	127.32	1044.5	0.008
Soft Clay	11.5	13.1	127.32	1462.3	0.008

*automatically computed by LPILE

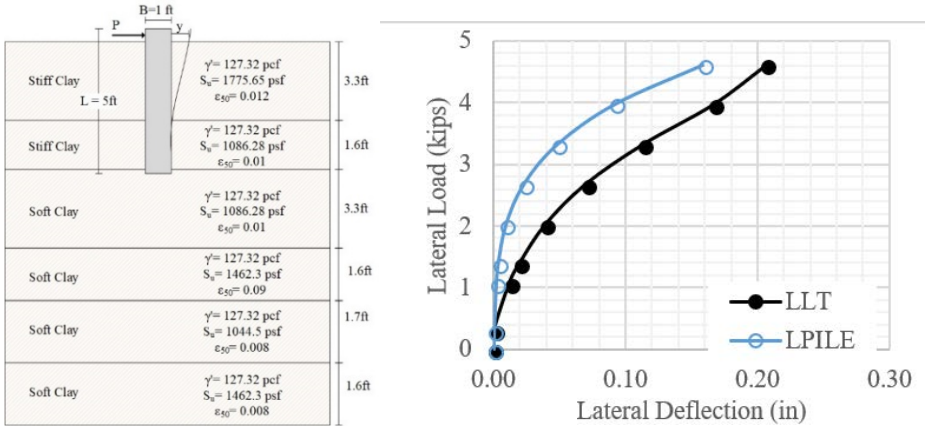

(a) (b)

Figure 4-54. (a) Soil Stratigraphy, (b) Comparison between Measured and Predicted Lateral Deflection Curve of Massena (RN: 88).

Table 4-56. Pile and Soil Properties of Massena Test (RN: 89).

Record Number: 89

Massena, New York					
Paper	Analysis of Laterally Loaded Drilled Shafts Using In Situ Test Results				
Reference	Huang, A. B., et al. "Analysis of Laterally Loaded Drilled Shafts Using In Situ Test Results." *Transportation Research Record* 1235 (1989): 60-67.				
Pile properties used in LPILE					
Pile type	B(ft)	L(ft)	I(in^4)	E(psi)	
bored pile	1	10	1.02E+05	3.05E+06	
Soil Properties used in LPILE					
P-y model	Depth		γ ' (pcf)	Su (psf)	ε_{50}
	Top	Bottom			
Stiff Clay	0	3.3	127.32	1775.65	0.012
Stiff Clay	3.3	4.9	127.32	1086.2	0.01
Soft Clay	4.9	8.2	127.32	1086.2	0.01
Soft Clay	8.2	9.8	127.32	1462.3	0.009
Soft Clay	9.8	11.5	127.32	1044.5	0.008
Soft Clay	11.5	13.1	127.32	1462.3	0.008

*automatically computed by LPILE

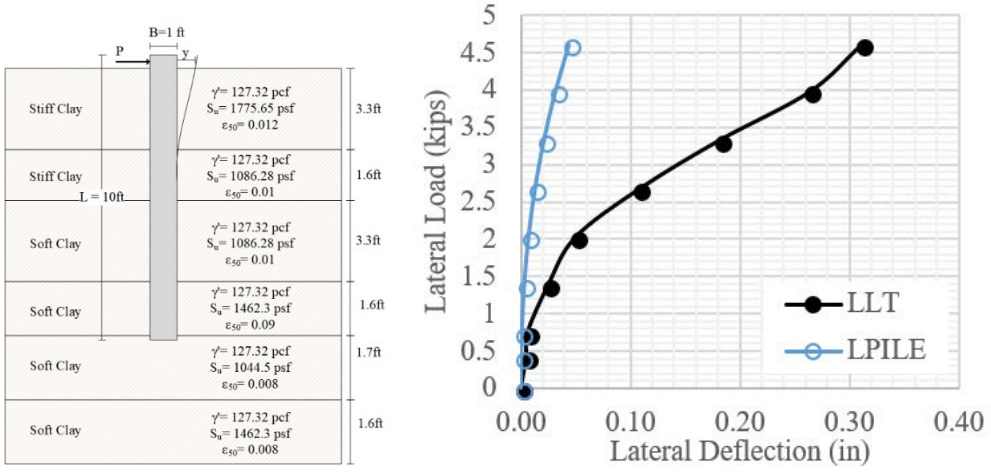

(a) (b)

Figure 4-55. (a) Soil Stratigraphy, (b) Comparison between Measured and Predicted Lateral Deflection Curve of Massena (RN: 89).

4.3 LARGE DIAMETER PILES—LATERAL LOAD TESTS

Researchers collected a total of 35 large diameter lateral load tests (RN: 1, 4–8, 51–66, 70–79, and 83–85). There are 23 sand cases and 12 clay cases with a pile diameter in the range of 5 ft (1.524 m) to 9.8 ft (3.0 m) and a pile length in the range of 7.5 ft (2.3 m) to 220 ft (67 m). The tests took place in the United States (Liang et al., 2007; Naramore and Feng, 1990; Rinne et al., 1996; Macklin and Chou, 1988; Kahle and Brown, 2002; Castelli and Fan, 2002; Billiet and Sewell, 2014; Daugiala, 2015; Load Test Consultant, 2018), Taiwan (Huang et al., 2001), South Korea (Joeng et al., 2007), Iran (Hokmabadi et al., 2012), and Japan (Ishikawa, 1985). They are described one by one in the following.

4.3.1 Inner Belt Bridge, Ohio, Test

The test was performed on a 6 ft in diameter pile in Cleveland, Ohio (Liang et al., 2007). A maximum lateral load of 798 kips applied to a 148 ft in length pile caused 4.56 in. of deflection at the pile top. The soil profile consists of 157.5 ft of silty or hard clay and gravel; the undrained shear strengths were from 1107 psf to 5326 psf. Figure 4-56 shows the soil stratigraphy and the field test results. Table 4-57 describes the data for piles and soils (RN: 1).

4.3.2 Hawthorne, California, Test (Janoyan)

A bored pile was load tested in Hawthorne, California (Janoyan et al., 2006). The pile was 6.56 ft in diameter and 48 ft in length. The maximum applied lateral load of 307 kips led to 40 in. of deflection (cracking of the pile). The soil profile consisted of 50 ft of silty sandy clay, silty clayey sand, or silty medium to fine-grained sand. Figure 4-57 shows the soil stratigraphy and the field test results. Table 4-58 describes the data for the pile and the soils used as input in LPILE (RN: 4).

Table 4-57. Pile and Soil Properties of Inner Belt Bridge USA Test (RN: 1).

Record Number: 1

Bridge CUY-90-1524 (Inner Belt Bridge, Cleveland, Ohio)					
Paper	Hyperbolic P-Y Criterion for Cohesive Soils				
Reference	Liang, R., Ehab S. Shatnawi, and Jamal Nusairat. "Hyperbolic P-y criterion for cohesive soils." *Jordan J. Civ. Eng* 1.1 (2007): 38-58.				
Pile properties used in LPILE					
Pile type	B(ft)	L(ft)	f'c (psi)	f'y (psi)	E(psi)
bored pile	6.00	147.64	4061.06	60915.96	3.19E+06
Soil Properties					

P-y model	Depth		γ' (pcf)	Su (psf)	ε_{50}
	Top	Bottom			
Soft Clay	0	13.1	120.95	1106.9	0.007
Stiff Clay w/o W	13.1	39.4	57.29	1357.6	0.007
Stiff Clay w/o W	39.4	52.5	70.03	1733.5	0.006
Stiff Clay w/o W	52.5	124.7	63.66	5221.4	0.005
Stiff Clay w/o W	124.7	157.5	70.03	5325.8	0.004

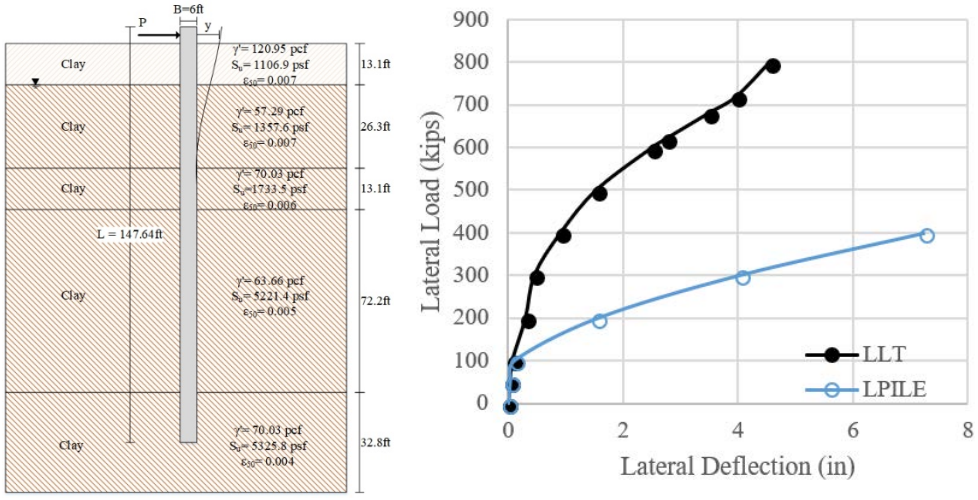

(a) (b)

Figure 4-56. (a) Soil Stratigraphy, (b) Comparison between Measured and Predicted Lateral Deflection Curve of Inner Belt Bridge.

Table 4-58. Pile and Soil Properties of Hawthorne USA Test (Janoyan) (RN: 4).

Record Number: 4

Hawthorne, California							
Paper		Full-Scale Cyclic Lateral Load Test of Reinforced Concrete Pier-Column					
Reference		Janoyan, Kerop D., John W. Wallace, and Jonathan P. Stewart. "Full-scale cyclic lateral load test of reinforced concrete pier-column." *ACI Structural Journal.* 103.2 (2006): 178. APA					
Pile Properties used in LPILE							
Pile type	B(ft)	L (ft)	f'c (psi)	f'y (psi)	E (psi)		
bored pile	6.56	88.0	6091.6	71068.62	2.900E+07		
Soil Properties							
P-y model	Depth		γ ' (pcf)	K (pci)	Su (psf)	φ (°)	ε_{50}
	Top	Bottom					
Reese Sand	0	4.9	127.32	55.26	n/a	33	n/a
Matlock Soft Clay	4.9	13.1	127.32	n/a	3274.93	n/a	0.004
Reese Sand	13.1	15.1	127.32	92.1	n/a	34	n/a
Matlock Soft Clay	15.1	24.9	127.32	n/a	1000.84	n/a	0.007
Reese Sand	24.9	28.9	127.32	147.36	n/a	35	n/a
Matlock Soft Clay	28.9	49.9	127.32	n/a	3349.4	n/a	0.004

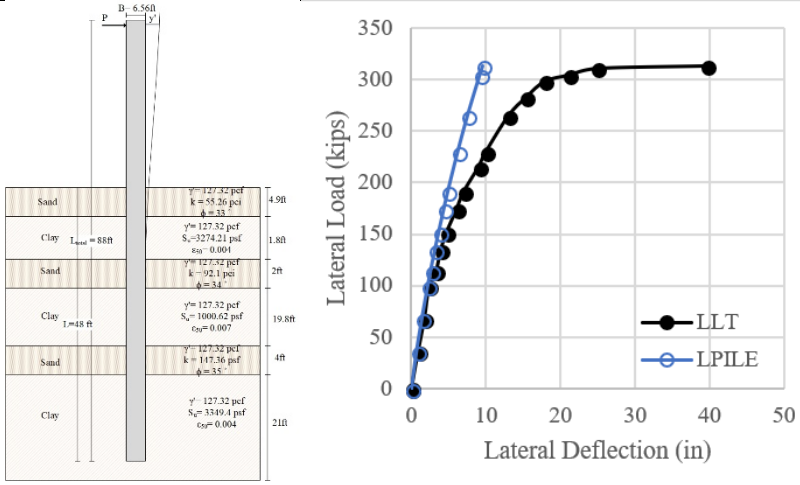

(a) (b)

Figure 4-57. (a) Soil Stratigraphy, (b) Comparison between Measured and Predicted Lateral Deflection Curve of Hawthorne (Janoyan).

4.3.3 Asalouyeh, Iran Test

Four load tests were performed in Pars Special Economic Energy Zone Area of Asalouyeh in Iran (Hokmabadi et al., 2012). The steel pipe piles were 5.8 ft in diameter for pile 1 and 3, 6.25 ft in diameter for piles 2 and 4; all piles were 131 ft in length with 1 in. wall thickness. Piles 1 and 2 were embedded 45.93 ft under the sea bed, while piles 3 and 4 were embedded 55.77 ft under the sea bed. The maximum applied lateral load of 202 kips for piles 1 and 2 led to 12.6 in. and 8.7 in. of deflection at the pile top, while the maximum applied lateral load of 141 kips for piles 3 and 4 led to 30.95 and 23.03 in. of deflection at the pile top. Figure 4-58, Figure 4-59, Figure 4-60, and Figure 4-61 show the soil stratigraphy and the field test results. Table 4-59, Table 4-60, Table 4-61, and Table 4-62 describe the data for the piles and the soils used as input in LPILE (RN: 5–8).

4.3.4 Incheon, South Korea Test (Large)

Four lateral load tests were performed on two different size piles in clay at Incheon Bridge in Incheon, South Korea (Jeong et al., 2007). The smaller three are described in section 4.2.18. The large pile was a bored pile 7.87 ft in diameter and 148 ft in length. The maximum lateral deflection at the top of the piles was 0.47 in. caused by a maximum applied lateral load of 224 kips. Figure 4-62 shows the soil stratigraphy and the field test results. Table 4-63 describes the data for the pile and the soil used as input in LPILE (RN: 51).

4.3.5 Hawthorne, California, Test (Naramore)

A Caltrans funded project included two lateral pile load tests in clay on 7.87 ft diameter bored piles in Hawthorne, California (Naromore and Feng, 1990). Shaft A and Shaft B were both 60 ft in length, constructed by reinforced concrete. The soil profile consisted of 167 ft of clay, and silt overlaying a thick sand layer. The maximum applied lateral load was 800 kips and caused deflections equal to 0.52 in. and 0.81 in., respectively. Figure 4-63 and Figure 4-64 show the soil stratigraphy and the field test results. Table 4-64 and Table 4-65 describe the data for the piles and the soils used as input in LPILE (RN: 52–53).

Table 4-59. Pile and Soil Properties of Asalouyeh Test (RN: 5).

Record Number: 5

Pars Special Economic Energy Zone Area, Asalouyeh, Iran						
Paper		Full scale lateral behaviour of monopiles in granular marine soils				
Reference		Hokmabadi, A. S., A. Fakher, and B. Fatahi. "Full scale lateral behaviour of monopiles in granular marine soils." *Marine Structures* 29.1 (2012): 198-210.				
Pile Properties						
Pile type	No. pile	B (ft)	L (ft)	t (in.)	f'y (psi)	E (psi)
Steel pipe pile	#1	5.83	131.23	1.00	52213.68	3.046E+07
Soil Properties used in LPILE						
P-y model		Depth		γ ' (pcf)	K (pci)	φ (°)
		Top	Bottom			
Reese /API Sand		0	26.2	127.32	110.52	38
Reese/API Sand		26.2	68.9	133.68	165.78	40
Reese/API Sand		68.9	98.4	133.68	202.62	43

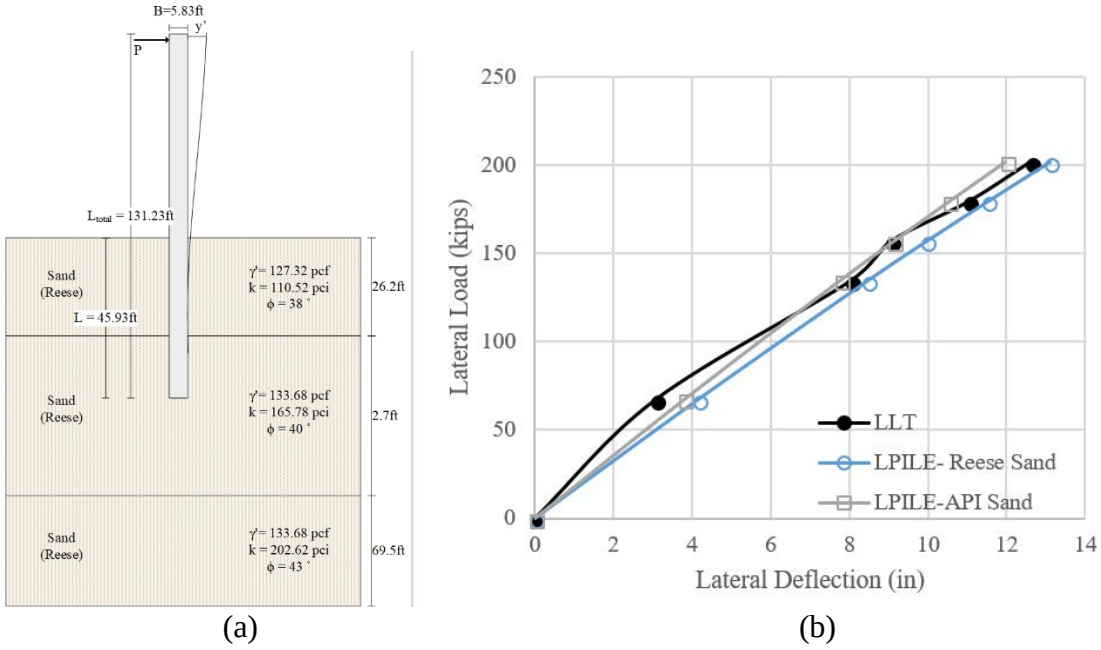

(a) (b)

Figure 4-58. (a) Soil Stratigraphy, (b) Comparison between Measured and Predicted Lateral Deflection Curve of Asalouyeh (RN: 5).

Table 4-60. Pile and Soil Properties of Asalouyeh Test (RN: 6).

Record Number: 6

Pars Special Economic Energy Zone Area, Asalouyeh, Iran						
Paper		Full scale lateral behaviour of monopiles in granular marine soils				
Reference		Hokmabadi, A. S., A. Fakher, and B. Fatahi. "Full scale lateral behaviour of monopiles in granular marine soils." *Marine Structures* 29.1 (2012): 198-210.				
Pile Properties						
Pile type	No. pile	B (ft)	L (ft)	t (in.)	f'y (psi)	E (psi)
Steel pipe pile	#2	6.266	131.23	1.00	52213.68	3.046E+07
Soil Properties used in LPILE						

P-y model	Depth		γ ' (pcf)	K (pci)	φ (°)
	Top	Bottom			
Reese/API Sand	0	26.2	127.32	110.52	38
Reese/API Sand	26.2	68.9	133.68	165.78	40
Reese/API Sand	68.9	98.4	133.68	202.62	43

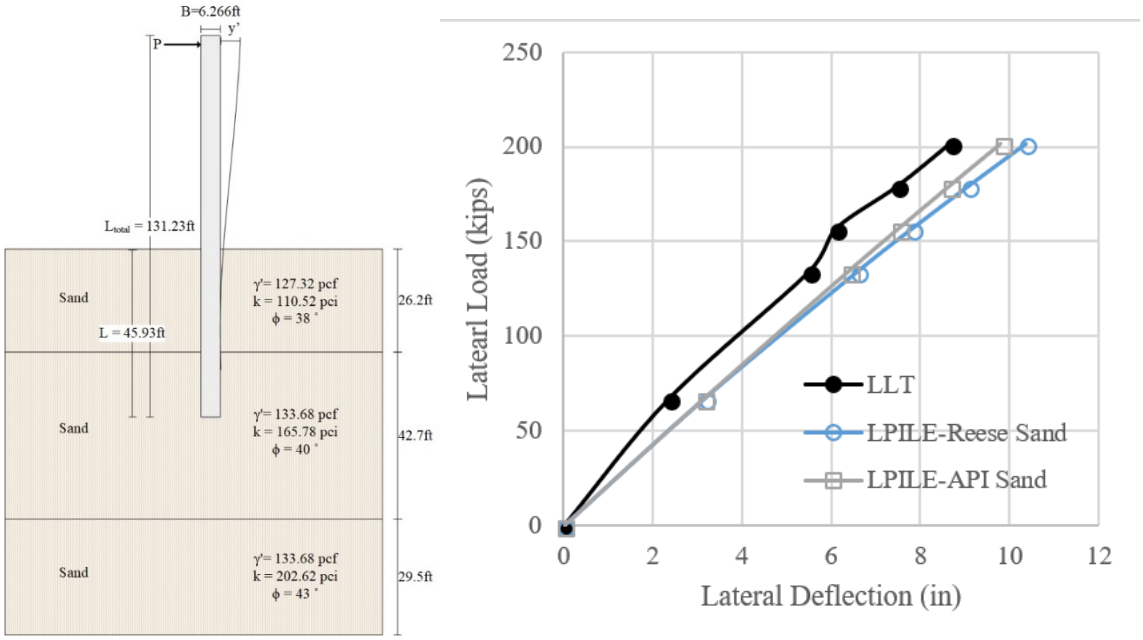

(a) (b)

Figure 4-59. (a) Soil Stratigraphy, (b) Comparison between Measured and Predicted Lateral Deflection Curve of Asalouyeh (RN: 6).

Table 4-61. Pile and Soil Properties of Asalouyeh Test (RN: 7).

Record Number: 7

Pars Special Economic Energy Zone Area, Asalouyeh, Iran						
Paper		Full scale lateral behaviour of monopiles in granular marine soils				
Reference		Hokmabadi, A. S., A. Fakher, and B. Fatahi. "Full scale lateral behaviour of monopiles in granular marine soils." *Marine Structures* 29.1 (2012): 198-210.				
Pile Properties						
Pile type	No. pile	B (ft)	L (ft)	t (in.)	f'y (psi)	E (psi)
Steel pipe pile	#3	5.866	131.23	1.00	52213.68	3.046E+07
Soil Properties used in LPILE						

P-y model	Depth		γ ' (pcf)	K (pci)	φ (°)
	Top	Bottom			
Reese/API Sand	0	26.2	127.32	110.52	38
Reese/API Sand	26.2	68.9	133.68	165.78	40
Reese/API Sand	68.9	98.4	133.68	202.62	43

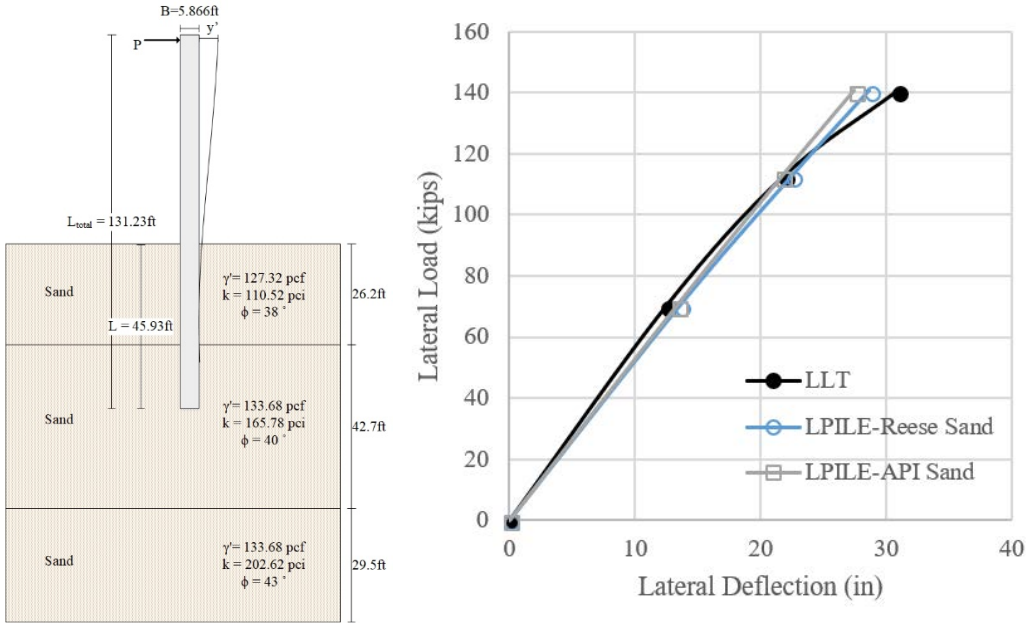

(a) (b)

Figure 4-60. (a) Soil Stratigraphy, (b) Comparison between Measured and Predicted Lateral Deflection Curve of Asalouyeh (RN: 7).

Table 4-62. Pile and Soil Properties of Asalouyeh Test (RN: 8).

Record Number: 8

Pars Special Economic Energy Zone Area, Asalouyeh, Iran						
Paper		Full scale lateral behaviour of monopiles in granular marine soils				
Reference		Hokmabadi, A. S., A. Fakher, and B. Fatahi. "Full scale lateral behaviour of monopiles in granular marine soils." *Marine Structures* 29.1 (2012): 198-210.				
Pile Properties						
Pile type	No. pile	B (ft)	L (ft)	t (in.)	f'y (psi)	E (psi)
Steel pipe pile	#4	6.266	131.23	1.0	52213.68	3.046E+07
Soil Properties used in LPILE						

P-y model	Depth		γ ' (pcf)	K (pci)	φ (°)
	Top	Bottom			
Reese/API Sand	0	26.2	127.32	110.52	38
Reese/API Sand	26.2	68.9	133.68	165.78	40
Reese/API Sand	68.9	98.4	133.68	202.62	43

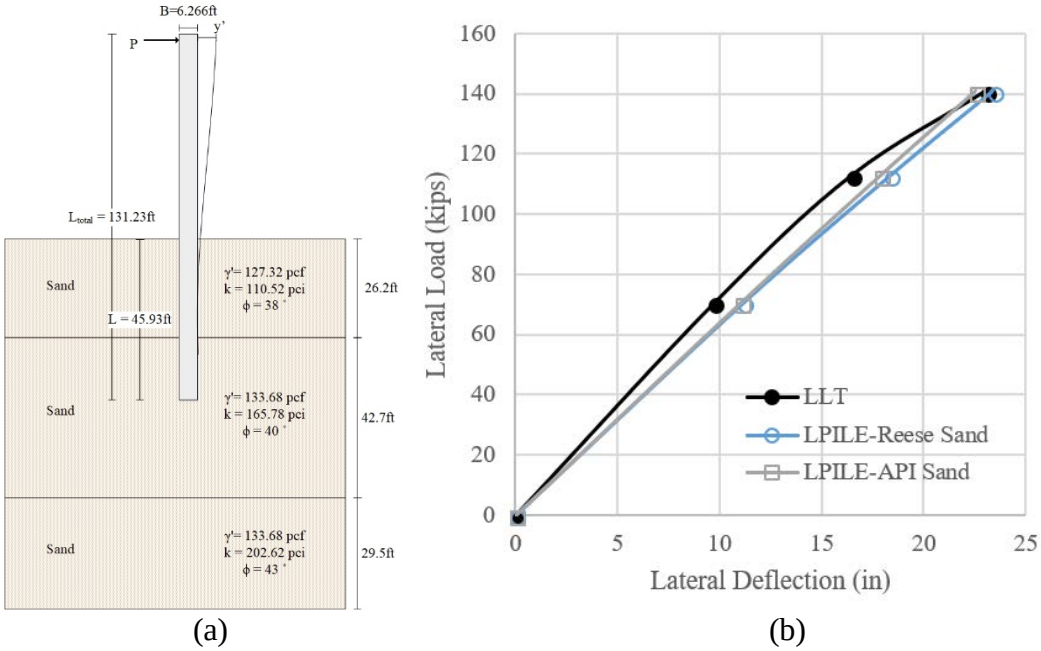

(a) (b)

Figure 4-61. (a) Soil Stratigraphy, (b) Comparison between Measured and Predicted Lateral Deflection Curve of Asalouyeh (RN: 8).

Table 4-63. Pile and Soil Properties of Incheon Test.

Record Number: 51

Incheon Bridge, Incheon, South Korea							
Paper	Cyclic lateral load tests of offshore large diameter piles of Incheon Bridge in marine clay						
Reference	Jeong, Sangseom, et al. "Cyclic lateral load tests of offshore large diameter piles of Incheon Bridge in marine clay." The Seventeenth International Offshore and Polar Engineering Conference. International Society of Offshore and Polar Engineers, 2007.						
Pile properties used in LPILE							
Pile type	B (ft)	L (ft)	ε_s (%)	f'y (psi)	E (psi)		
bored pile	7.87	147.6	1.1	71068.62	3.046E+07		
Soil Properties used in LPILE							
P-y model	Depth		γ ' (pcf)	K (pci)	Su(psf)	φ (°)	ε_{50}
	Top	Bottom					
Matlock Soft Clay	0	59.1	111.40	n/a	375.94	n/a	0.01
Reese Sand	59.1	72.2	113.31	55.26	n/a	24	n/a
Reese Sand	72.2	98.4	114.59	110.52	n/a	34	n/a
Reese Sand	98.4	121.4	128.59	147.36	n/a	32	n/a
Reese Sand	121.4	147.6	149.60	184.20	n/a	35	n/a

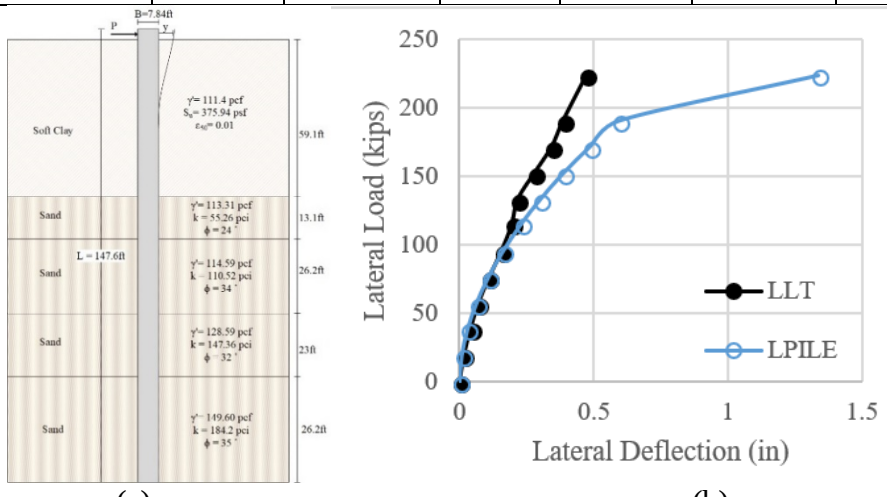

(a) (b)

Figure 4-62. (a) Soil Stratigraphy, (b) Comparison between Measured and Predicted Lateral Deflection Curve Incheon.

Table 4-64. Pile and Soil Properties of Hawthorne Test (Naramore) (RN: 52).

Record Number: 52

Hawthorne, California (Shaft A)							
Paper	Field tests of large diameter drilled shafts part I-lateral loads						
Reference	Naramore, S. A., and F. Y. Feng. *Field tests of large diameter drilled shafts part I-lateral loads*. ReportNo. FHWA/CA/SD-88/02, California Department of Transportation, Sacramento, California (1990).						
Pile properties used in LPILE							
Pile type	B (ft)	L (ft)	I (in.^{4})	E (psi)			
Bored pile circular	7.87	60.0	391273.1	3.05E+06			
Soil Properties used in LPILE							
P-y model	Depth		γ ' (pcf)	K (pci)	Su(psf)	φ (°)	ε_{50}
	Top	Bottom					
Stiff Clay	0	19.0	125.00	n/a	2798.65	n/a	*
Reese Sand	19.0	43.0	127.32	*	n/a	43	n/a
Stiff Clay	43.0	50.9	112.04	n/a	2401.82	n/a	*
Reese Sand	50.9	69.9	110.13	*	n/a	31	n/a

*automatically computed by LPILE

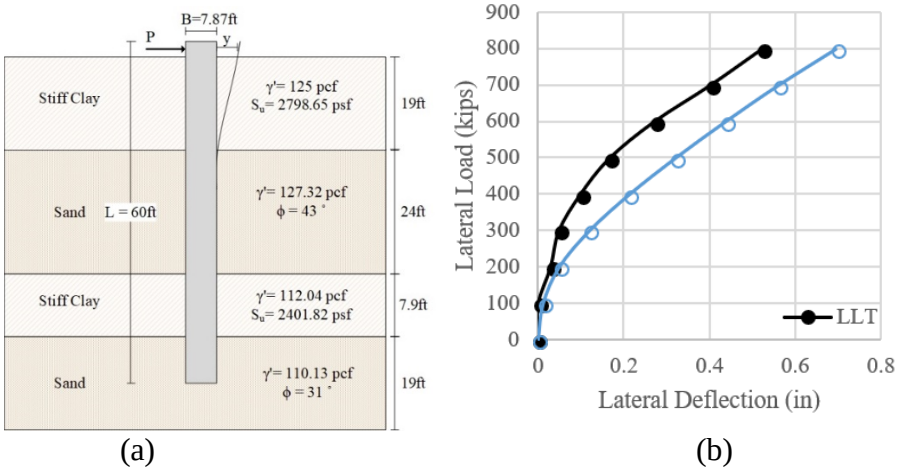

(a) (b)

Figure 4-63. (a) Soil Stratigraphy, (b) Comparison between Measured and Predicted Lateral Deflection Curve of Hawthorne (Naramore) (RN: 52).

Table 4-65. Pile and Soil Properties of Hawthorne Test (Naramore) (RN: 53).

Record Number: 53

Hawthorne, California (Shaft B)							
Paper	Field tests of large diameter drilled shafts part I-lateral loads						
Reference	Naramore, S. A., and F. Y. Feng. *Field tests of large diameter drilled shafts part I-lateral loads.* ReportNo. FHWA/CA/SD-88/02, California Department of Transportation, Sacramento, California (1990).						
Pile properties used in LPILE							
Pile type	B (ft)	L (ft)	I (in.^{4})	E (psi)			
Bored pile circular	7.87	60	391273.1	3.05E+06			
Soil Properties used in LPILE							
P-y model	Depth		γ ' (pcf)	K (pci)	Su(psf)	φ (°)	ε_{50}
	Top	Bottom					
Stiff Clay	0	12.5	124.00	n/a	2005.00	n/a	*
Reese Sand	12.5	18.0	128.33	*	n/a	43	n/a
Stiff Clay	18.0	53.5	119.33	n/a	3101	n/a	*
Reese Sand	53.5	69.9	110.00	*	n/a	31	n/a

*automatically computed by LPILE

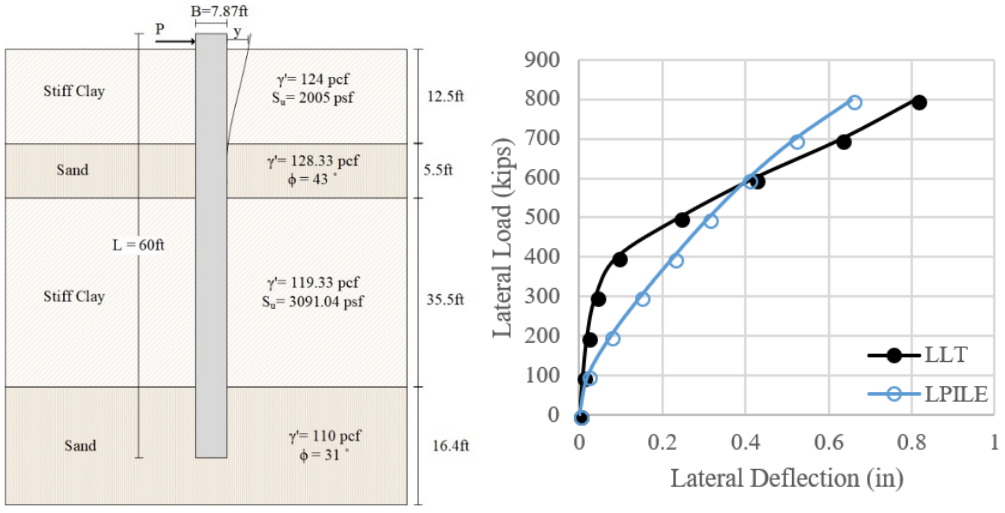

(a) (b)

Figure 4-64. (a) Soil Stratigraphy, (b) Comparison between Measured and Predicted Lateral Deflection Curve of Hawthorne (Naramore) (RN: 53).

4.3.6 Spring Villa, Alabama, Test

A series of lateral load tests was performed at Spring Villa, Alabama (Kahle and Brown, 2002). Drilled shafts C2, C3, C4, F2, F3, and F4 were all 5 ft in diameter, and 7.5 ft in length for C2 and F2, 5 ft in length for C3 and F3, and 2.5 ft in length for C4 and F4. The applied maximum forces at the pile top were 334 kips, 221 kips, 89 kips, 332 kips, 220 kips, and 89 kips, which caused 2.37 in., 2.31 in., 1.26 in., 1.13 in., 1.20 in., and 1.52 in. displacements, respectively. Figure 4-65, Figure 4-66, Figure 4-67, Figure 4-68, Figure 4-69, and Figure 4-70 show the soil stratigraphy and the field test results. Table 4-66, Table 4-67, Table 4-68, Table 4-69, Table 4-70, and Table 4-71 describe the data for the piles and the soils used as input for LPILE (RN: 54–59).

4.3.7 Las Vegas, Nevada, Test

The Las Vegas test was performed on an 8-ft diameter, 32-ft long drilled shaft in a stiff clay (Rinne et al., 1996). The applied load was 1663 kips and caused a 1.37 in. deflection at the top of the pile. The soil profile consisted of 121 ft of stiff clay, caliche, and soft clay. Figure 4-71 shows the soil stratigraphy and the field test results. Table 4-72 describes the data for the pile and the soils used as input in LPILE (RN: 60).

4.3.8 Glenwood Canyon, Colorado, Test

Lateral load tests were performed on two 7.87 ft diameter bored piles at Glenwood Canyon, Colorado (Macklin and Chou, 1988). The length were 32.2 ft and 35.4 ft. The maximum lateral load applied was 401 kips and caused 0.17 and 0.12 in. of deflection at the pile head, respectively. These two piles were embedded in a 40 ft thick layer of very dense sand, gravel, and cobbles. Figure 4-72 and Figure 4-73 show the soil stratigraphy and the field test results. Table 4-73 and Table 4-74 describe the data for piles and the soils used as input in LPILE (RN: 61–62).

Table 4-66. Pile and Soil Properties of Spring Villa Test (RN: 54).

Record Number: 54

Spring Villa, Alabama (C2)								
Paper	Performance of Laterally Loaded Drilled Sockets Founded in Weathered Quartzite							
Reference	Kahle, Kevin James, and Dan A. Brown. "Performance of Laterally Loaded Drilled Sockets Founded in Weathered Quartzite." (2002).							
Pile properties used in LPILE								
Pile type	B (ft)	L (ft)	I (in.^{4})	E (psi)				
Bored pile circular	5.00	9.75	636172.5	3.05E+06				
Soil Properties used in LPILE								
P-y model	Depth		γ ' (pcf)	Su (psf)	qu (psf)	ε_{50}	Rock mass modulus (psf)	krm
	Top	Bottom						
Stiff Clay	0	1.64	127.32	7205.5	n/a	*	n/a	n/a
Reese Weak Rock	1.64	4.92	127.32	n/a	14410.9	n/a	1148697	0.0004

*automatically computed by LPILE

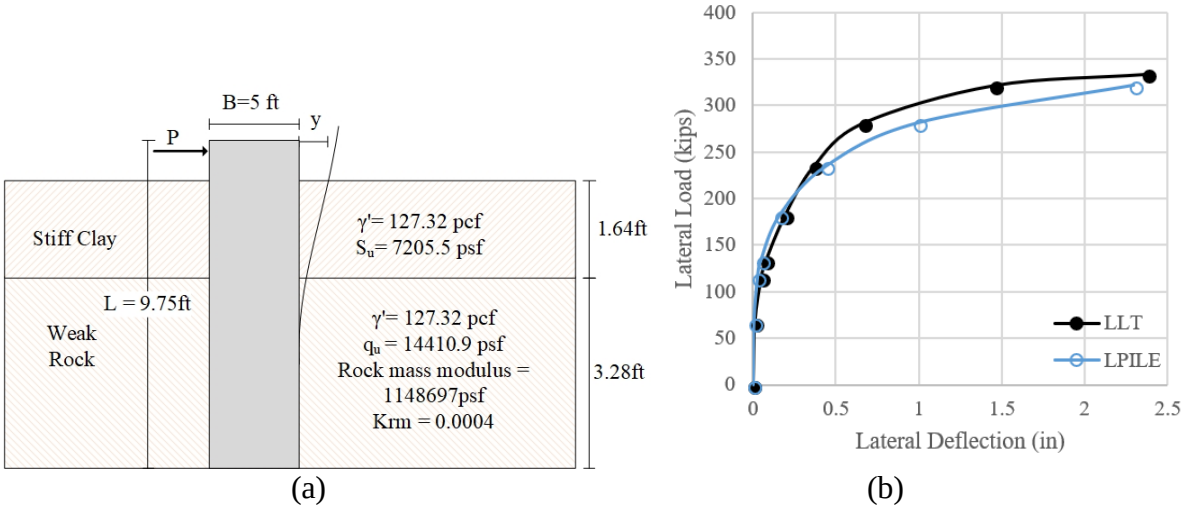

(a) (b)

Figure 4-65. (a) Soil Stratigraphy, (b) Comparison between Measured and Predicted Lateral Deflection Curve of Spring Villa (RN: 54).

Table 4-67. Pile and Soil Properties of Spring Villa Test (RN: 55).

Record Number: 55

Spring Villa, Alabama (C3)								
Paper	Performance of Laterally Loaded Drilled Sockets Founded in Weathered Quartzite							
Reference	Kahle, Kevin James, and Dan A. Brown. "Performance of Laterally Loaded Drilled Sockets Founded in Weathered Quartzite." (2002).							
Pile properties used in LPILE								
Pile type	B (ft)		L (ft)		I (in.^{4})		E (psi)	
Bored pile circular	5.0		5.0		636172.5		3.05E+06	
Soil Properties used in LPILE								
P-y model	Depth		γ ' (pcf)	Su (psf)	qu (psf)	ε_{50}	Rock mass modulus (psf)	krm
	Top	Bottom						
Stiff Clay	0	1.64	127.32	4594.8	n/a	*	n/a	-
Reese Weak Rock	1.64	4.92	127.32	n/a	11278.1	n/a	1148697	0.0004

*automatically computed by LPILE

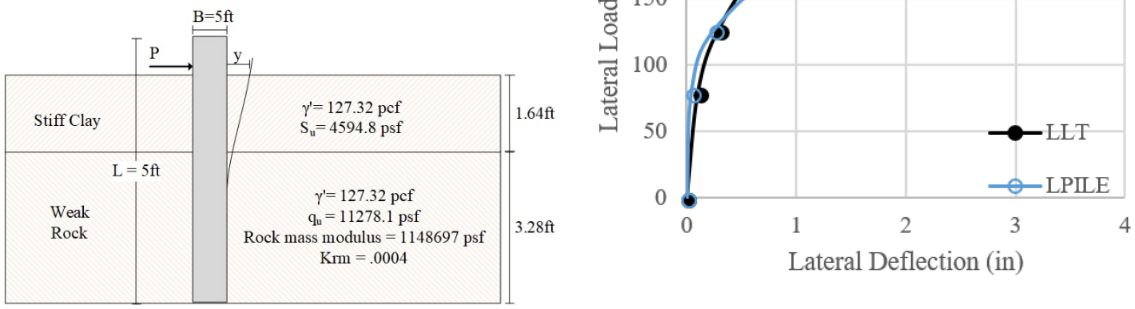

(a) (b)

Figure 4-66. (a) Soil Stratigraphy, (b) Comparison between Measured and Predicted Lateral Deflection Curve of Spring Villa (RN: 55).

Table 4-68. Pile and Soil Properties of Spring Villa Test (RN: 56).

Record Number: 56

Spring Villa, Alabama (C4)								
Paper	Performance of Laterally Loaded Drilled Sockets Founded in Weathered Quartzite							
Reference	Kahle, Kevin James, and Dan A. Brown. "Performance of Laterally Loaded Drilled Sockets Founded in Weathered Quartzite." (2002).							
Pile properties used in LPILE								
Pile type	B (ft)		L (ft)	I (in.^{4})		E (psi)		
Bored pile circular	5.0		2.5	636172.5		3.05E+06		
Soil Properties used in LPILE								
P-y model	Depth		γ ' (pcf)	Su (psf)	qu (psf)	ε_{50}	Rock mass modulus (psf)	krm
	Top	Bottom						
Stiff Clay	0	1.64	127.32	3759.4	n/a	*	n/a	n/a
Reese Weak Rock	1.64	4.92	127.32	n/a	5221.4	n/a	1148698	0.0004

*automatically computed by LPILE

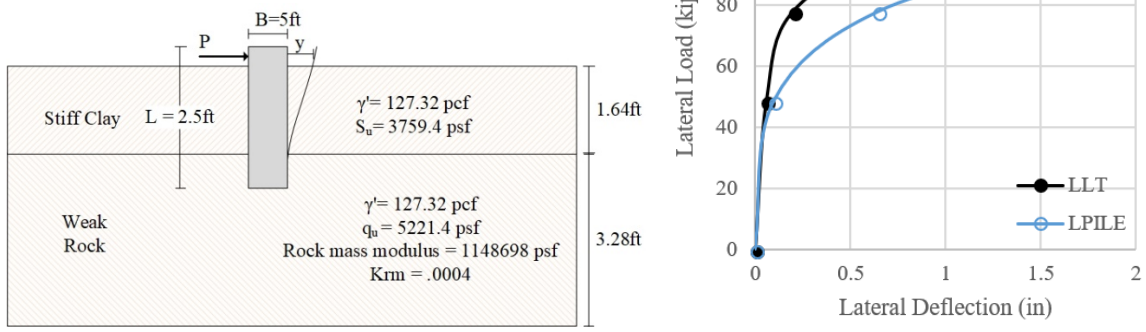

(a) (b)

Figure 4-67. (a) Soil Stratigraphy, (b) Comparison between Measured and Predicted Lateral Deflection Curve of Spring Villa (RN: 56).

Table 4-69. Pile and Soil Properties of Spring Villa Test (RN: 57).

Record Number: 57

Spring Villa, Alabama (F2)								
Paper	Performance of Laterally Loaded Drilled Sockets Founded in Weathered Quartzite							
Reference	Kahle, Kevin James, and Dan A. Brown. "Performance of Laterally Loaded Drilled Sockets Founded in Weathered Quartzite." (2002).							
Pile properties used in LPILE								
Pile type	B (ft)	L (ft)	I (in.^{4})	E (psi)				
Bored pile circular	5.0	7.5	636172.5	3.05E+06				
Soil Properties used in LPILE								
P-y model	Depth		γ ' (pcf)	Su (psf)	qu (psf)	ε_{50}	Rock mass modulus (psf)	krm
	Top	Bottom						
Stiff Clay	0	1.64	127.32	3759.4	n/a	*	n/a	n/a
Reese Weak Rock	1.64	4.92	127.32	n/a	5221.4	n/a	1148698.8	0.0004

*automatically computed by LPILE

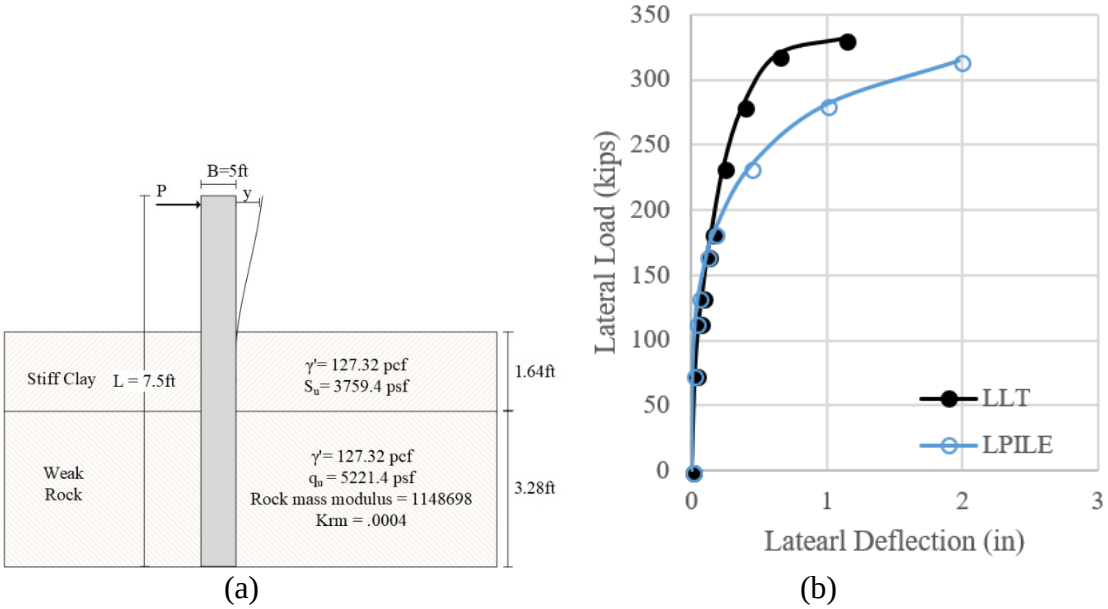

(a) (b)

Figure 4-68. (a) Soil Stratigraphy, (b) Comparison between Measured and Predicted Lateral Deflection Curve of Spring Villa (RN: 57).

Table 4-70. Pile and Soil Properties of Spring Villa Test (RN: 58).

Record Number: 58

Spring Villa, Alabama (F3)								
Paper	Performance of Laterally Loaded Drilled Sockets Founded in Weathered Quartzite							
Reference	Kahle, Kevin James, and Dan A. Brown. "Performance of Laterally Loaded Drilled Sockets Founded in Weathered Quartzite." (2002).							
Pile properties used in LPILE								
Pile type	B (ft)	L (ft)	I (in.^{4})	E (psi)				
Bored pile circular	5.0	5	636172.5	3.05E+06				
Soil Properties used in LPILE								
P-y model	Depth		γ ' (pcf)	Su (psf)	qu (psf)	ε_{50}	Rock mass modulus (psf)	krm
	Top	Bottom						
Stiff Clay	0	1.64	127.32	11487	n/a	*	n/a	n/a
Reese Weak Rock	1.64	4.92	127.32	n/a	11487	n/a	1148699	0.0004

*automatically computed by LPILE

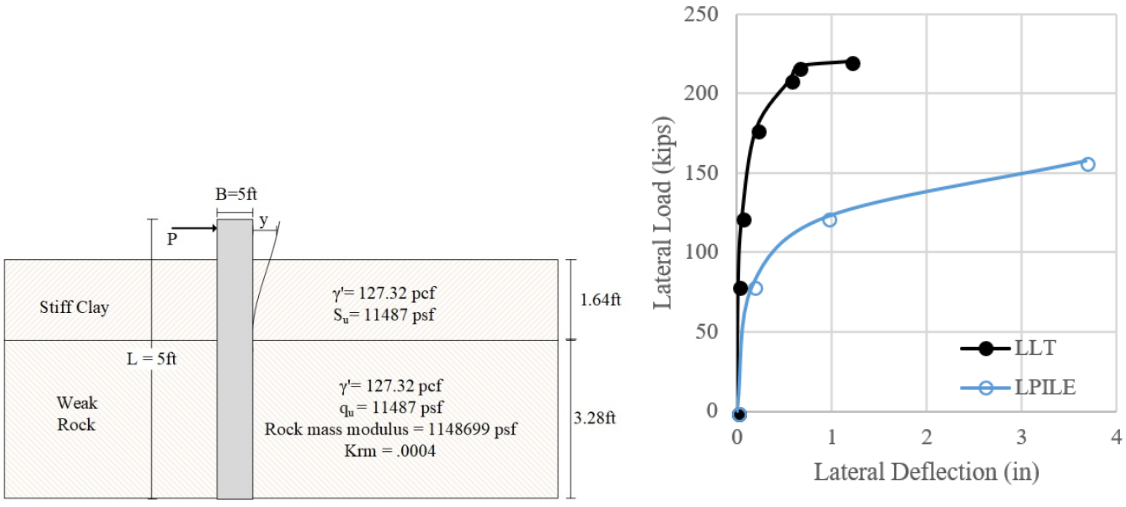

(a) (b)

Figure 4-69. (a) Soil Stratigraphy, (b) Comparison between Measured and Predicted Lateral Deflection Curve of Spring Villa (RN: 58).

Table 4-71. Pile and Soil Properties of Spring Villa Test (RN: 59).

Record Number: 59

Spring Villa, Alabama (F4)								
Paper	Performance of Laterally Loaded Drilled Sockets Founded in Weathered Quartzite							
Reference	Kahle, Kevin James, and Dan A. Brown. "Performance of Laterally Loaded Drilled Sockets Founded in Weathered Quartzite." (2002).							
Pile properties used in LPILE								
Pile type	B (ft)	L (ft)	I (in.^{4})	E (psi)				
Bored pile circular	5.0	2.5	636172.5	3.05E+06				
Soil Properties used in LPILE								
P-y model	Depth		γ ' (pcf)	Su (kPa)	qu (kPa)	ε_{50}	Rock mass modulus (psf)	Krm
	Top	Bottom						
Stiff Clay	0	1.64	127.32	11487	n/a	*	n/a	n/a
Reese Weak Rock	1.64	4.92	127.32	n/a	11487	n/a	1148699	0.0004

*automatically computed by LPILE

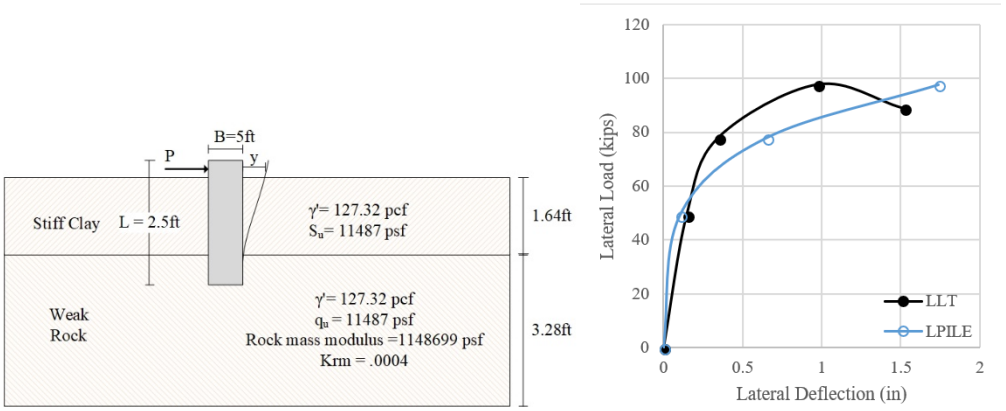

(a) (b)

Figure 4-70. (a) Soil Stratigraphy, (b) Comparison between Measured and Predicted Lateral Deflection Curve of Spring Villa (RN: 59).

Table 4-72. Pile and Soil Properties of Las Vegas Test.

Record Number: 60

I-15/U.S. 95 Load Test Program Las Vegas, Nevada					
Paper	I-15/U.S. 95 Load Test Program Las Vegas, Nevada, Proj. No. 31-215903-07A				
Reference	Rinne, E., Thompson, J., and Vanderpool, W. (1996). "I-15/U.S. 95 Load Test Program Las Vegas, Nevada," Proj. No. 31-215903-07A, Kleinfelder, Inc.				
Pile properties used in LPILE					
Pile type	B (ft)	L (ft)	f'c	f'y (psi)	E (psi)
bored pile	8.0	32.0	6300.01	71068.62	2.90E+07
Soil Properties used in LPILE					

P-y model	Depth		γ ' (pcf)	Su (psf)	ε_{50}
	Top	Bottom			
Stiff Clay w/o W	0	16.4	120.3	1600	0.007
Stiff Clay w/o W	16.4	29.53	124.8	3000	0.005
Stiff Clay w/o W	29.5	44.29	120.3	2000	0.0063

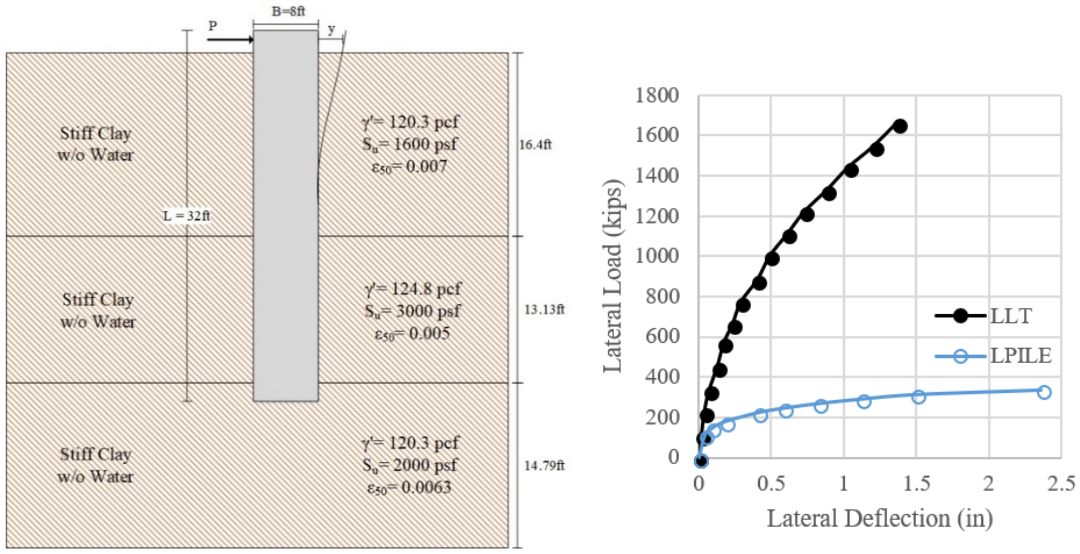

(a) (b)

Figure 4-71. (a) Soil Stratigraphy, (b) Comparison between Measured and Predicted Lateral Deflection Curve of Las Vegas.

Table 4-73. Pile and Soil Properties of Glenwood Canyon Test (RN: 61).

Record Number: 61

Glenwood Canyon (East), Colorado					
Paper	A Lateral Load Test on Seven Foot Diameter Caissons				
Reference	Macklin, P. and Chou, N. (1988). "A Lateral Load Test on Seven Foot Diameter Caissons," *Foundation Engineering*, Vol. 2, 1122-1131.				
Pile properties used in LPILE					
Pile type	B (ft)	L (ft)	f'c	f'y (psi)	E (psi)
bored pile	7.87	32.2	5221.37	71068.62	2.90E+07
Soil Properties used in LPILE					

P-y model	Depth		γ ' (pcf)	K (pci)	φ (°)
	Top	Bottom			
Reese/API Sand	0	39.4	134.96	151.04	42

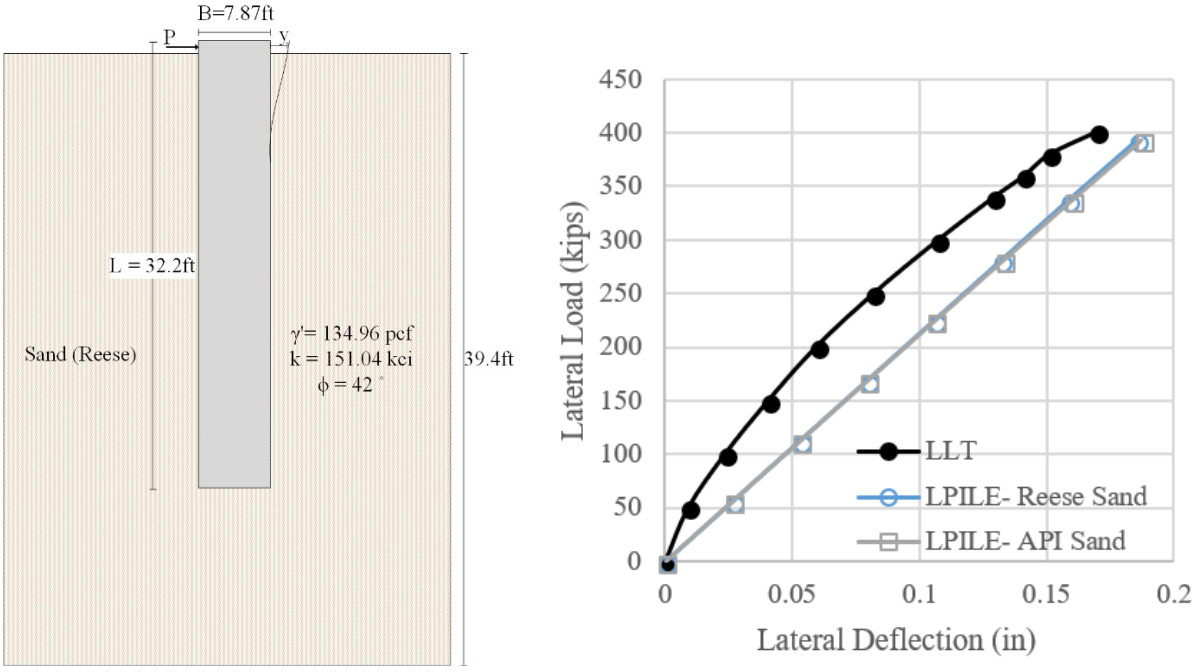

(a) (b)

Figure 4-72. (a) Soil Stratigraphy, (b) Comparison between Measured and Predicted Lateral Deflection Curve of Glenwood Canyon (RN: 61).

Table 4-74. Pile and Soil Properties of Glenwood Canyon Test (RN: 62).

Record Number: 62

Glenwood Canyon (West), Colorado					
Paper	A Lateral Load Test on Seven Foot Diameter Caissons				
Reference	Macklin, P. and Chou, N. (1988). "A Lateral Load Test on Seven Foot Diameter Caissons," *Foundation Engineering*, Vol. 2, 1122-1131.				
Pile properties used in LPILE					
Pile type	B(ft)	L(ft)	f'c	f'y (psi)	E(psi)
bored pile	7.87	35.4	5221.37	71068.62	3.345
Soil Properties used in LPILE					

P-y model	Depth		γ ' (pcf)	K (pci)	φ (°)
	Top	Bottom			
Reese/API Sand	0	39.4	134.96	151.04	42

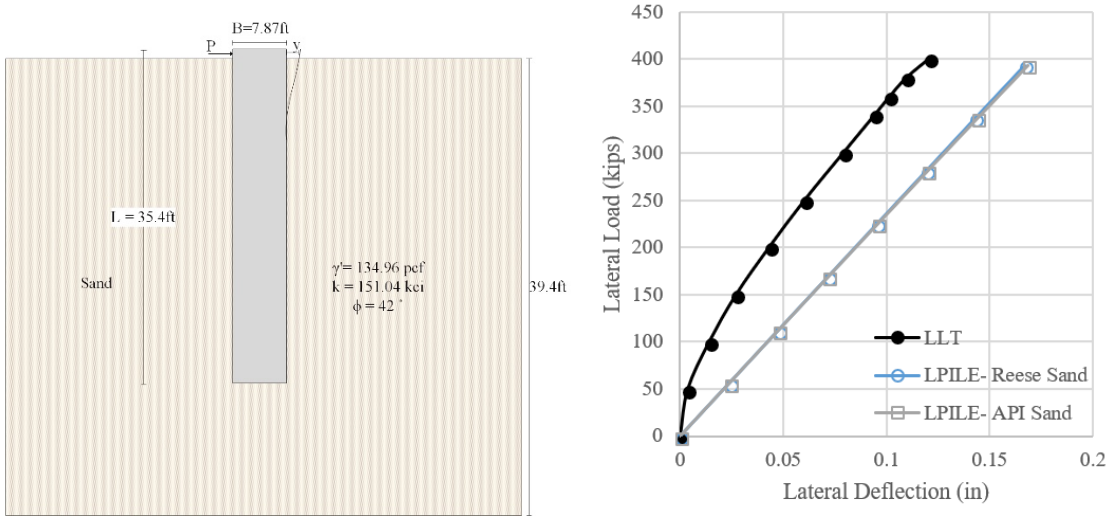

(a) (b)

Figure 4-73. (a) Soil Stratigraphy, (b) Comparison between Measured and Predicted Lateral Deflection Curve of Glenwood Canyon (RN: 62).

4.3.9 London, Ontario, Canada Test

Two lateral load tests were performed in sand in London, Ontario, Canada and reported by Adams and Radhakishna (1973). The two bored piles were 5 ft in diameter and 30 ft in length, and the soil consisted of loose silty sand and compact fine to medium sand. The maximum lateral loads applied were 24 kips and 25 kips and led to 0.27 in. and 0.07 in. of deflection at the top of the pile, respectively. Figure 4-74 and Figure 4-75 show the soil stratigraphy and the field test results. Table 4-75 and Table 4-76 describe the data for the piles and the soils used as input in LPILE (RN: 63–64).

4.3.10 Japan Test (Large)

Several lateral load tests were performed on piles in Japan and are reported by Ishikawa (1985). The tests on the two smaller diameter drilled-shafts were presented in section 4.2.19. The three large piles were 9.8 ft in diameter and 66 ft in length at site A, 9.78 ft in diameter and 88 ft in length at site B, and 6.56 ft in diameter and 220 ft in length at site F. The soil profile at site A consists of 66 ft of gravel, sand stone, weathered shale, and shale. The soil profile at site B consists of 90 ft silt, gravel, and medium sand overlaying a thick layer of fine sand. The soil profile at site C consists of 131.2 ft of coarse to fine sand, silt, and overlaying on a sandy stone layer. The soil profile at site D consists of 114.8 ft of clay, silt, gravel with sand, and fine sand. The soil profile at site F consists of 256 ft of gravel with sand and fine to medium sand overlaying on a tuff layer. Figure 4-76, Figure 4-77, and Figure 4-78 show the soil stratigraphy and the field test results. Table 4-77, Table 4-78, and Table 4-79 describe the data for the piles and the soils used as input for LPILE (RN: 65–66, 70).

Table 4-75. Pile and Soil Properties of London, Ontario, Test (RN: 63).

Record Number: 63

London (Sand), Ontario					
Paper	The Lateral Capacity of Deep Augered Footings				
Reference	Adams, J. and Radhakrishna, H. (1973). "The Lateral Capacity of Deep Augered Footings," Proc. 8th Intl. Conf. on Soil Mechanics and Foundation Engineering, Moscow, Vol. 2.1, 1-8				
Pile properties used in LPILE					
Pile type	B (ft)	L (ft)	f'c	f'y (psi)	E (psi)
bored pile	5	30.0	5221.37	71068.62	2.90E+07

Soil Properties used in LPILE					
P-y model	Depth		γ ' (pcf)	K (Pci)	φ (°)
	Top	Bottom			
Reese/API Sand	0	4.9	127.32	*	29
Reese/API Sand	4.9	32.0	127.32	*	32

*automatically computed by LPILE

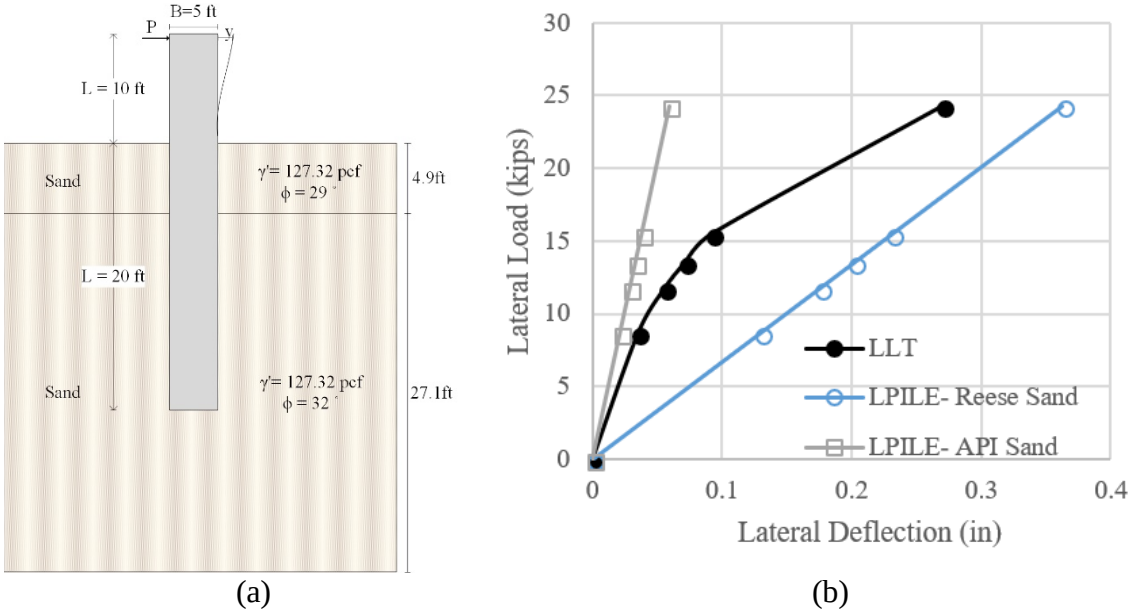

(a) (b)

Figure 4-74. (a) Soil Stratigraphy, (b) Comparison between Measured and Predicted Lateral Deflection Curve of London, Ontario (RN: 63).

Table 4-76. Pile and Soil Properties of London, Ontario, Test (RN: 64).

Record Number: 64

London (Till), Ontario					
Paper	The Lateral Capacity of Deep Augered Footings				
Reference	Adams, J. and Radhakrishna, H. (1973). "The Lateral Capacity of Deep Augered Footings," Proc. 8th Intl. Conf. on Soil Mechanics and Foundation Engineering, Moscow, Vol. 2.1, 1-8				
Pile properties used in LPILE					
Pile type	B (ft)	L (ft)	f'c	f'y (psi)	E (psi)
bored pile	5	30.0	5221.37	71068.62	2.90E+07
Soil Properties used in LPILE					

P-y model	Depth		γ ' (pcf)	K (Pci)	φ (°)
	Top	Bottom			
Reese/API Sand	0	4.0	127.32	*	35
Reese/API Sand	4.0	30.0	127.32	*	43

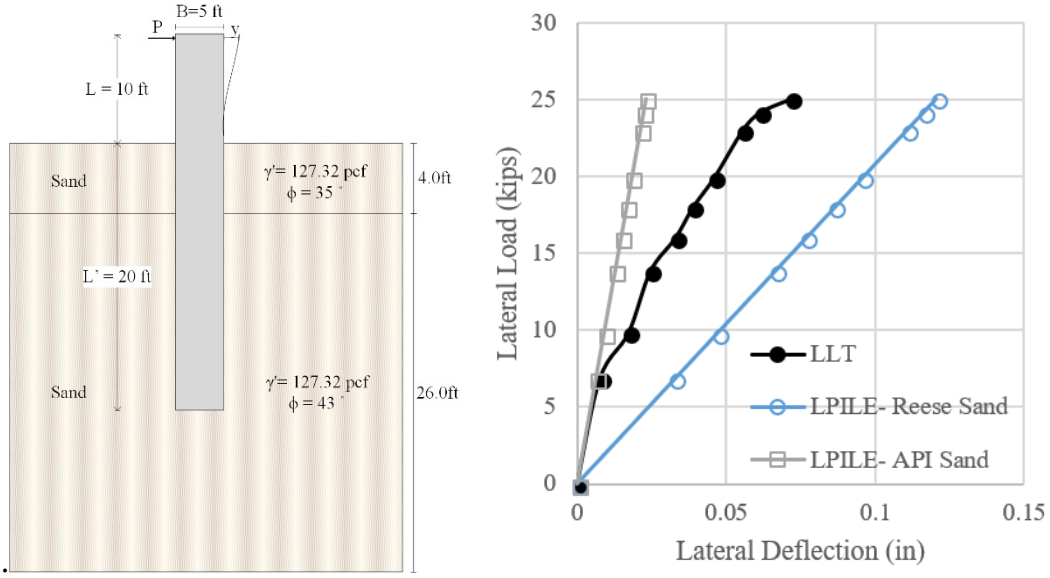

(a) (b)

Figure 4-75. (a) Soil Stratigraphy, (b) Comparison between Measured and Predicted Lateral Deflection Curve of London, Ontario (RN: 64).

Table 4-77. Pile and Soil Properties of Japan Test (RN: 65).

Record Number: 65

Japan Test (A site)					
Paper	Study on lateral resistance of large diameter pile				
Reference	Ishikawa (1985). "Study on lateral resistance of large diameter pile," 土木試驗所月報. (In Japanese)				
Pile properties used in LPILE					
Pile type	B (ft)	b (ft)	L (ft)	I (in.^{4})	E (psi)
bored pile	9.84	4.59	65.6	9.10E+06	3.806E+06
Soil Properties used in LPILE					

P-y model	Depth		γ ' (pcf)	K (Pci)	φ (°)
	Top	Bottom			
Reese/API Sand	0	13.1	140.05	*	43
Reese/API Sand	13.1	19.7	133.68	*	41
Reese/API Sand	19.7	36.1	127.32	*	38
Reese/API Sand	36.1	65.6	127.32	*	38

*automatically computed by LPILE

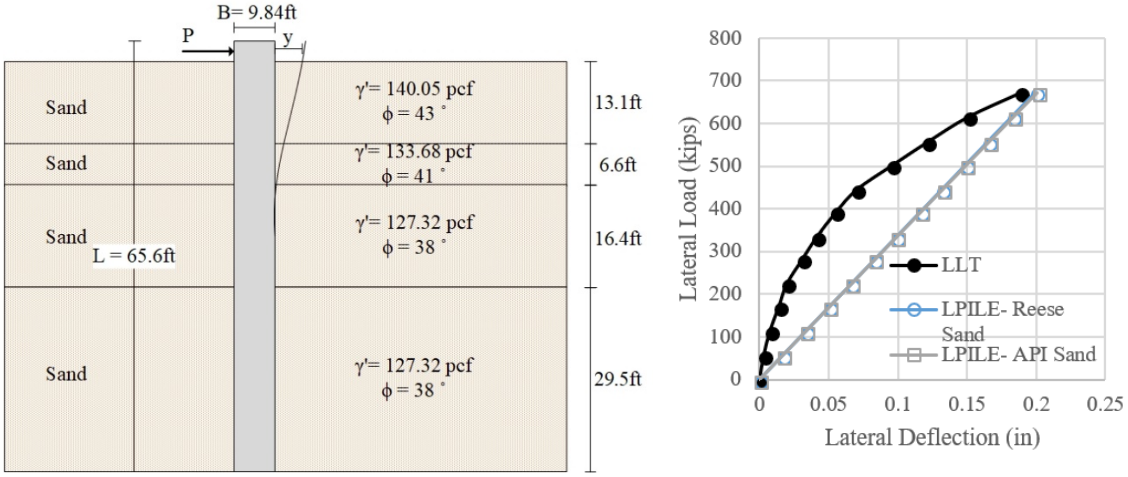

(a) (b)

Figure 4-76. (a) Soil Stratigraphy, (b) Comparison between Measured and Predicted Lateral Deflection Curve of Japan (RN: 65).

Table 4-78. Pile and Soil Properties of Japan Test (RN: 66).

Record Number: 66

Japan Test (B site)					
Paper	Study on lateral resistance of large diameter pile				
Reference	Ishikawa (1985). “Study on lateral resistance of large diameter pile,” 土木試驗所月報. (In Japanese)				
Pile properties used in LPILE					
Pile type	B (ft)	L (ft)	I (in.^{4})	E (psi)	
bored pile	9.78	88.5	5.53E+14	5.97E+06	
Soil Properties used in LPILE					
P-y model	Depth		γ ' (pcf)	K (Pci)	φ (°)
	Top	Bottom			
Reese/API Sand	0	7.2	127.32	*	28
Reese/API Sand	7.2	11.5	133.68	*	41
Reese/API Sand	11.5	17.1	127.32	*	32
Reese/API Sand	17.1	23.3	133.68	*	41
Reese/API Sand	23.3	35.1	127.32	*	30
Reese/API Sand	35.1	44.3	127.32	*	26
Reese/API Sand	44.3	98.4	127.32	*	33

*automatically computed by LPILE

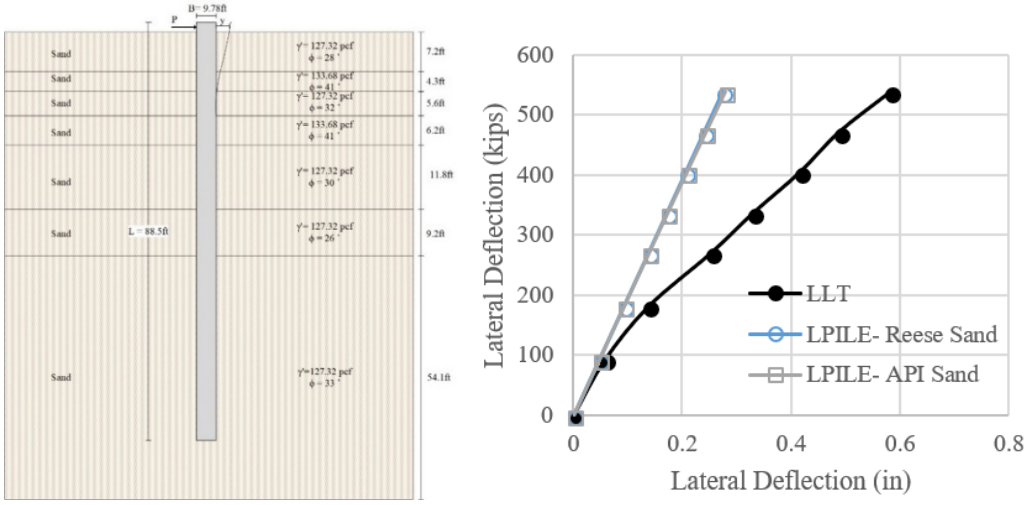

(a) (b)

Figure 4-77. (a) Soil Stratigraphy, (b) Comparison between Measured and Predicted Lateral Deflection Curve of Japan (RN: 66).

Table 4-79. Pile and Soil Properties of Japan Test (RN: 70).

Record Number: 70

Japan Test (F site)							
Paper	Study on lateral resistance of large diameter pile						
Reference	Ishikawa (1985). "Study on lateral resistance of large diameter pile," 土木試驗所月報. (In Japanese)						
Pile properties used in LPILE							
Pile type	B (ft)	L (ft)		I (in.^{4})		E (psi)	
bored pile	6.56	219.8		1.89E+06		5.36E+06	
Soil Properties used in LPILE							
P-y model	Depth		γ ' (pcf)	K (pci)	Su (psf)	φ (°)	ε_{50}
	Top	Bottom					
Reese/API Sand	0	39.4	140.05	*	n/a	28	n/a
Reese/API Sand	39.4	65.6	127.32	*	n/a	30	n/a
Reese/API Sand	65.6	91.9	127.32	*	n/a	33	n/a
Soft Clay	91.9	114.8	127.32	n/a	2610.68	n/a	*
Reese/API Sand	114.8	219.8	146.41	*	n/a	33	n/a
Reese/API Sand	219.8	255.9	146.41	*	n/a	38	n/a

*automatically computed by LPILE

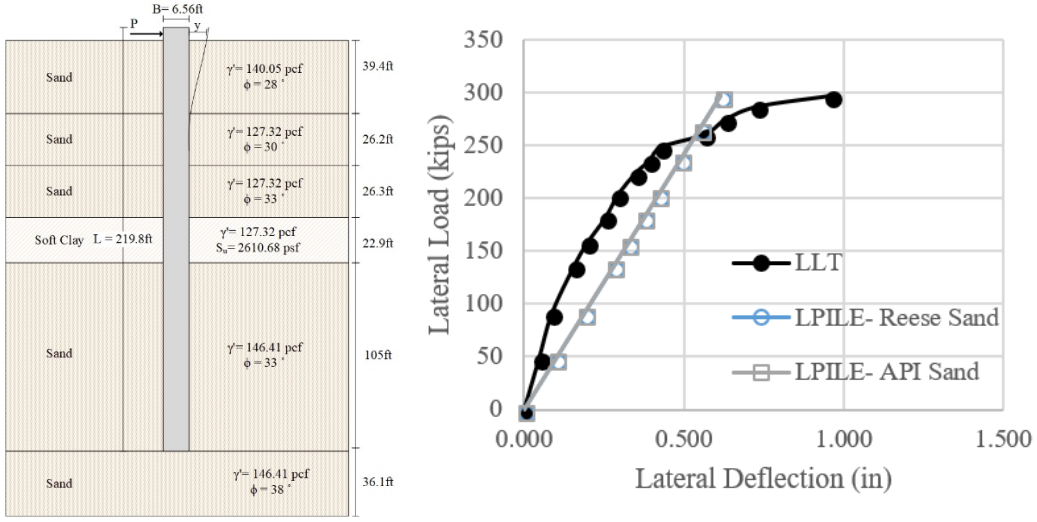

(a) (b)

Figure 4-78. (a) Soil Stratigraphy, (b) Comparison between Measured and Predicted Lateral Deflection Curve of Japan (RN: 70).

4.3.11 Sterling, Virginia Test

Three lateral load tests were performed on large diameter piles in Sterling, Virginia (Billiet and Sewell, 2014). Pile LTS-1 was 6 ft in diameter and 54 ft in length, pile LTS-2 was 6 ft in diameter and 34 in length, and pile LTS-3 was 6 ft in diameter and 31 in length. The maximum applied lateral load of 1101 kips caused 1.83 in. deflection at the top of LTS-1, the maximum applied lateral load of 1118 kips led to a 0.72 in. displacement at the top of LTS-2, and the maximum applied lateral load of 1127 kips caused a 0.6 in. deflection at the top of LTS-3. The soil profile in this project consists of 30 ft to 55 ft layers of sand overlaying weak rock. Figure 4-79, Figure 4-80, and Figure 4-81 show the soil stratigraphy and the field test results. Table 4-80, Table 4-81, and Table 4-82 describe the data for the piles and the soils used as input in LPILE (RN: 71–73).

4.3.12 Jacksonville, Florida Test

Two lateral load tests were performed in Jacksonville, Florida (Castelli and Fan, 2002). Drilled shaft LLT-1 and LLT-2 were both 6 ft in diameter and 115 ft in length embedded in a soil consisting of dense clayey silty fine or silty fine sand. The maximum applied lateral load of 73 kips led to an 8.34 in. deflection at the top of shaft LLT-1 and caused 9.12 in. of displacement at the top of shaft LLT-2. Figure 4-82 and Figure 4-83 show the soil stratigraphy and the field test results. Table 4-83 and Table 4-84 describe the data for the piles and the soils used as input in LPILE (RN: 74–75).

4.3.13 New York City, New York Test

Several lateral load tests for the Kosciuszko Bridge project were completed on 7 ft diameter bored piles in the city of New York (Daugiala, 2015). Pile S3 and pile S4 were tested two times, the first and the second maximum applied load of 666 kips and 784 kips led to 0.36 in. and 0.52 in. deflections at the top of pile S3, respectively, while the first and the second maximum applied force of 761 kips and 782 kips caused 0.46 in. and 0.51 in. displacements at the top of pile S4. The soil profile consists of 200 ft of clay and sand overlaying a 30 ft rock layer. Figure 4-84, Figure 4-85, Figure 4-86, and Figure 4-87 show the soil stratigraphy and the field test results. Table 4-85, Table 4-86, Table 4-87, and Table 4-88 describe the data for the piles and the soils used as input in LPILE (RN: 76–79).

Table 4-80. Pile and Soil Properties of Sterling Test (RN: 71).

Record Number: 71

Loudon and Fairfax County, Virginia							
Paper	Dulles Corridor Metrorail Project – Phase 2 Package A						
Reference	William Billiet and Jeffrey Sewell (2014). "Dulles Corridor Metrorail Project – Phase 2 Package A." Load Test Report of Aerial Guideway Load Test Program, Loudon and Fairfax County, Virginia						
Pile Properties used in LPILE							
Pile type Pile section	B (ft)	L (ft)	f'c (psi)	f'y (psi)	E (psi)		
bored pile with casing	6.0	49.9	27600	4003.05	2.90E+07		
Casing Properties used in LPILE							
t (in)	B (ft)	L (ft)	f'y-casing (psi)	E (psi)			
0.6252	6.11	25.0	35969.4	2.90E+07			
Soil Properties used in LPILE							
P-y model	Depth (ft)		γ ' (pcf)	K (pci)	qu (psf)	φ (°)	Rock mass modulus (psf)
	Top	Bottom					
Reese/API Sand	0.0	10.0	120.00	65.94	n/a	32	n/a
Reese/API Sand	10.0	18.5	140.00	260.0	n/a	38	n/a
Reese/API Sand	18.5	24.5	77.60	150.0	n/a	38	n/a
Reese weak rock	24.6	55.0	82.60	n/a	2000	n/a	603291.26

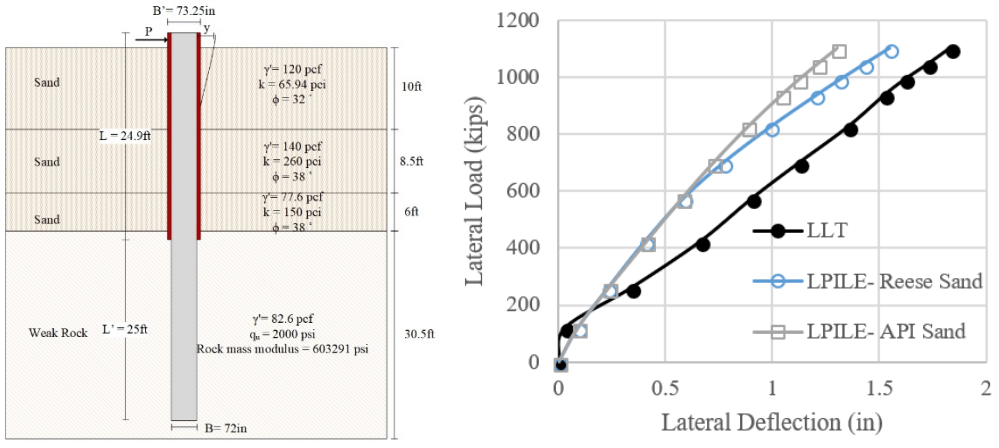

(a) (b)

Figure 4-79. (a) Soil Stratigraphy, (b) Comparison between Measured and Predicted Lateral Deflection Curve of Sterling (RN: 71).

Table 4-81. Pile and Soil Properties of Sterling Test (RN: 72).

Record Number: 72

Loudon and Fairfax County, Virginia					
Paper	Dulles Corridor Metrorail Project – Phase 2 Package A				
Reference	William Billiet and Jeffrey Sewell (2014). "Dulles Corridor Metrorail Project – Phase 2 Package A." Load Test Report of Aerial Guideway Load Test Program, Loudon and Fairfax County, Virginia				
Pile Properties used in LPILE					
Pile type Pile section	B (ft)	L (ft)	f'c (psi)	f'y (psi)	E (psi)
bored pile with casing	6.00	20.0	27600	4003.05	2.90E+07

Casing Properties used in LPILE				
t (in)	B (ft)	L (ft)	f'y-casing (psi)	E (psi)
0.6252	6.10	10.0	35969.4	2.90E+07

Soil Properties used in LPILE							
P-y model	Depth (ft)		γ ' (pcf)	K (pci)	qu (psf)	φ (°)	Rock mass modulus (psf)
	Top	Bottom					
Reese/API Sand	0.0	8	130.00	60.0	n/a	32	n/a
Reese/API Sand	8	10	140.00	260.0	n/a	38	n/a
Reese weak rock	10	35	82.60	n/a	4000.0	n/a	375000

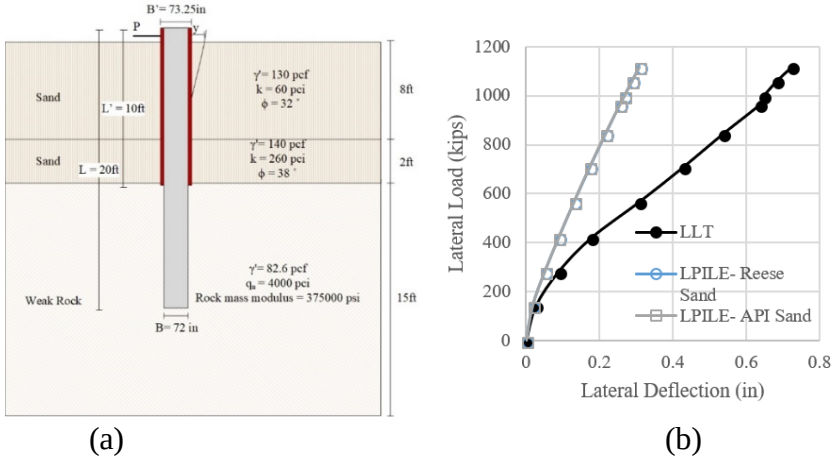

(a) (b)

Figure 4-80. (a) Soil Stratigraphy, (b) Comparison between Measured and Predicted Lateral Deflection Curve of Sterling (RN: 72).

Table 4-82. Pile and Soil Properties of Sterling Test (RN: 73).

Record Number: 73

Loudon and Fairfax County, Virginia						
Paper	Dulles Corridor Metrorail Project – Phase 2 Package A					
Reference	William Billiet and Jeffrey Sewell (2014). "Dulles Corridor Metrorail Project – Phase 2 Package A." Load Test Report of Aerial Guideway Load Test Program, Loudon and Fairfax County, Virginia					
Pile Properties used in LPILE						
Pile type Pile section	B (ft)	L (ft)	f'c (psi)	f'y (psi)	E (psi)	
bored pile with casing	6.0	19.5	4003.05	60045.7	2.90E+07	
Casing Properties used in LPILE						
t (in)	B (ft)	L (ft)	f'y-casing (psi)	E (psi)		
0.625	6.11	7.5	35969.4	2.90E+07		

Soil Properties used in LPILE

P-y model	Depth (ft)		γ ' (pcf)	K (pci)	qu (psf)	φ (°)	Rock mass modulus (psf)
	Top	Bottom					
Reese/API Sand	0.0	3.6	130.00	60.0	n/a	32	n/a
Reese/API Sand	3.6	7.5	140.00	260.0	n/a	38	n/a
Reese weak rock	7.5	10.5	82.60	n/a	2000.0	n/a	87500
Reese weak rock	10.5	29.9	82.60	n/a	4000.0	n/a	375000

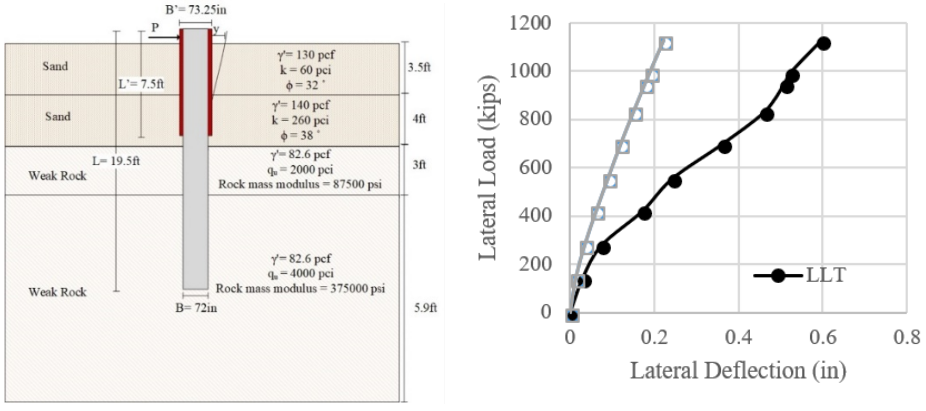

(a) (b)

Figure 4-81. (a) Soil Stratigraphy, (b) Comparison between Measured and Predicted Lateral Deflection Curve of Sterling (RN: 73).

Table 4-83. Pile and Soil Properties of Jacksonville Test (RN: 74).

Record Number: 74

Jacksonville, Florida (LLT-1)					
Paper	Lateral Load Test Results on Drilled Shafts in Marl at Jacksonville, Florida				
Reference	Castelli, Raymond J., and Ke Fan. "Lateral Load Test Results on Drilled Shafts in Marl at Jacksonville, Florida." Deep Foundations 2002: An International Perspective on Theory, Design, Construction, and Performance. 2002. 824-835				
Pile properties used in LPILE					
Pile type	B (ft)	L (ft)		I (in.^{4})	E (psi)
bored pile	6.004	115		1.32E+06	3.05E+06
Soil Properties used in LPILE					
P-y model	Depth		γ ' (pcf)	K (pci)	φ (°)
	Top	Bottom			
Reese/API Sand	0	6.6	127.32	*	37
Reese/API Sand	6.6	19.7	133.68	*	42
Reese/API Sand	19.7	36.1	127.32	*	36

*automatically computed by LPILE

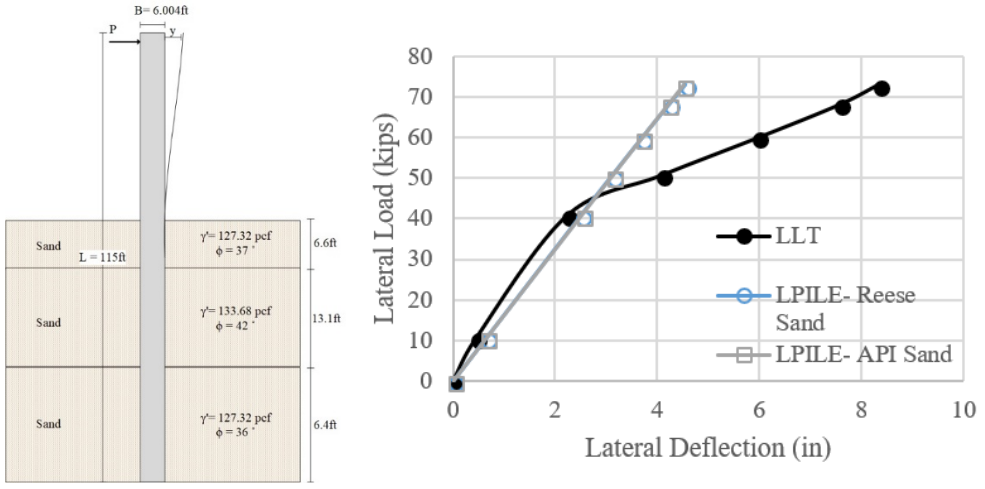

(a) (b)

Figure 4-82. (a) Soil Stratigraphy, (b) Comparison between Measured and Predicted Lateral Deflection Curve of Jacksonville (RN: 74).

Table 4-84. Pile and Soil Properties of Jacksonville Test (RN: 75).

Record Number: 75

Jacksonville, Florida (LLT-2)					
Paper	Lateral Load Test Results on Drilled Shafts in Marl at Jacksonville, Florida				
Reference	Castelli, Raymond J., and Ke Fan. "Lateral Load Test Results on Drilled Shafts in Marl at Jacksonville, Florida." Deep Foundations 2002: An International Perspective on Theory, Design, Construction, and Performance. 2002. 824-835				
Pile properties used in LPILE					
Pile type	B (ft)	L (ft)		I (in.^{4})	E (psi)
bored pile	6.004	115		1.32E+06	3.05E+06
Soil Properties used in LPILE					
P-y model	Depth		γ ' (pcf)	K (pci)	φ (°)
	Top	Bottom			
Reese/API Sand	0	6.6	127.32	*	37
Reese/API Sand	6.6	19.7	133.68	*	42
Reese/API Sand	19.7	36.1	127.32	*	36

*automatically computed by LPILE

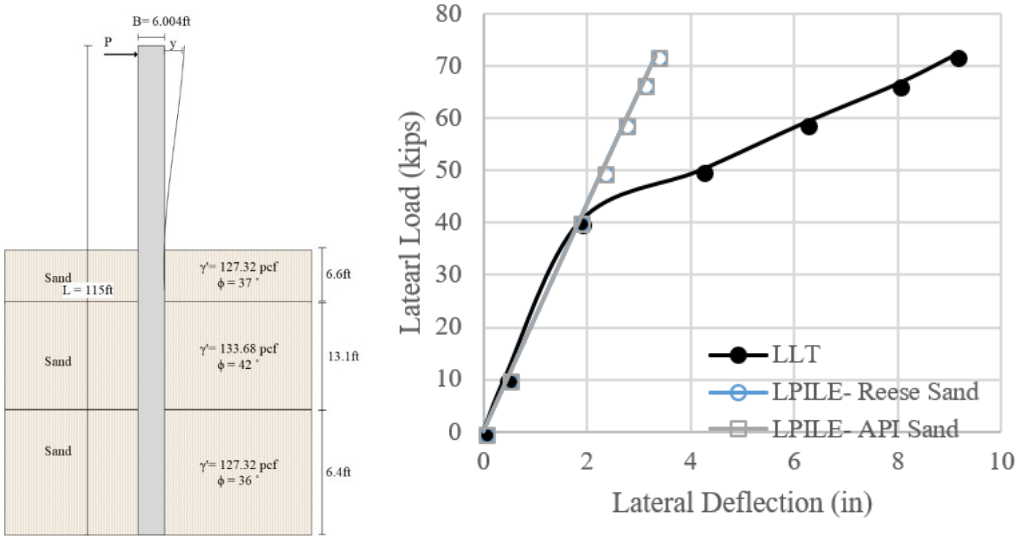

(a) (b)

Figure 4-83. (a) Soil Stratigraphy, (b) Comparison between Measured and Predicted Lateral Deflection Curve of Jacksonville (RN: 75).

Table 4-85. Pile and Soil Properties of New York City Test (RN: 76).

Record Number: 76

New York City (S3R1)						
Report	Geotechnical Nominal Resistance Test Results for Lateral Test on Drilled Shafts S-3 and S-4 for the Kosciuszko Bridge Project – Phase 1					
Reference	Alfredas Daugiala (2015). "Geotechnical Nominal Resistance Test Results for Lateral Test on Drilled Shafts S-3 and S-4 for the Kosciuszko Bridge Project – Phase 1." Report No. 0042-TI-002-001. New York City.					
Pile properties used in LPILE						
Pile type	B (ft)	L (ft)	I (in.^{4})	E (psi)		
Bored pile with Casing	6.988	177	2.43E+06	3.05E+06		
Casing properties used in LPILE						
Casing t(in)	Casing diameter(ft)	Casing length(ft)				
0.6252	7.087	166.77				
Soil Properties used in LPILE						
P-y model	Depth		γ ' (pcf)	K (pci)	Su (psf)	φ (°)	ε_{50}
	Top	Bottom					
Reese/API Sand	0	30.0	127.32	*	n/a	33	n/a
Stiff Clay	30.0	40.0	105.00	n/a	1670.8	n/a	*
Reese/API Sand	40.0	60.0	127.32	*	n/a	30	n/a
Stiff Clay	60.0	75.0	127.32	n/a	1879.7	n/a	*
Reese/API Sand	75.0	90.0	127.32	*	n/a	35	n/a
Stiff Clay	90.0	120.0	127.32	n/a	3759.4	n/a	*
Reese/API Sand	120.0	160	127.32	*	n/a	36	n/a
Reese/API Sand	160	200.0	127.32	*	n/a	41	n/a

*automatically computed by LPILE

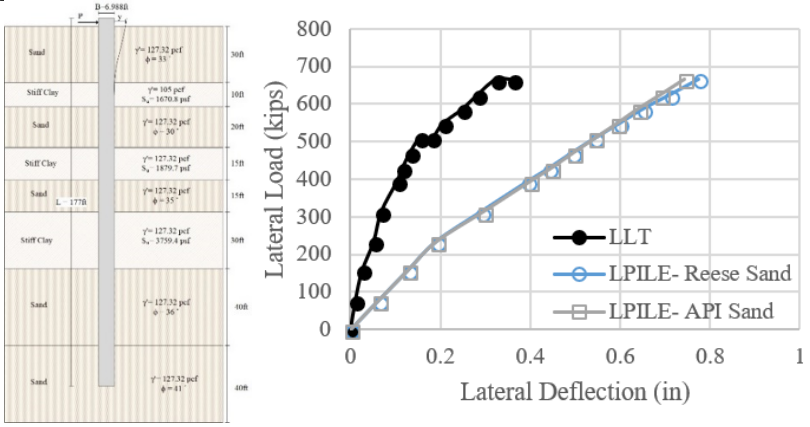

(a) (b)

Figure 4-84. (a) Soil Stratigraphy, (b) Comparison between Measured and Predicted Lateral Deflection Curve of New York City (RN: 76).

Table 4-86. Pile and Soil Properties of New York City Test (RN: 77).

Record Number: 77

New York City (S4R1)						
Report	Geotechnical Nominal Resistance Test Results for Lateral Test on Drilled Shafts S-3 and S-4 for the Kosciuszko Bridge Project – Phase 1					
Reference	Alfredas Daugiala (2015). "Geotechnical Nominal Resistance Test Results for Lateral Test on Drilled Shafts S-3 and S-4 for the Kosciuszko Bridge Project – Phase 1." Report No. 0042-TI-002-001. New York City.					
Pile properties used in LPILE						
Pile type	B (ft)	L (ft)	I (in.^{4})	E (psi)		
Bored pile with Casing	6.988	177	2.43E+06	3.05E+06		
Casing properties used in LPILE						
Casing t (in.)	Casing diameter (ft)	Casing length (ft)				
0.625	7.087	166.77				
Soil Properties used in LPILE						
P-y model	Depth		γ ' (pcf)	K (pci)	Su (psf)	φ (°)	ε_{50}
	Top	Bottom					
Reese/API Sand	0	30.0	127.32	*	n/a	33	n/a
Stiff Clay	30.0	40.0	105.00	n/a	1670.8	n/a	*
Reese/API Sand	40.0	60.0	127.32	*	n/a	30	n/a
Stiff Clay	60.0	75.0	127.32	n/a	1879.7	n/a	*
Reese/API Sand	75.0	90.0	127.32	*	n/a	35	n/a
Stiff Clay	90.0	120.0	127.32	n/a	3759.4	n/a	*
Reese/API Sand	120.0	160	127.32	*	n/a	36	n/a
Reese/API Sand	160	200.0	127.32	*	n/a	41	n/a

*automatically computed by LPILE

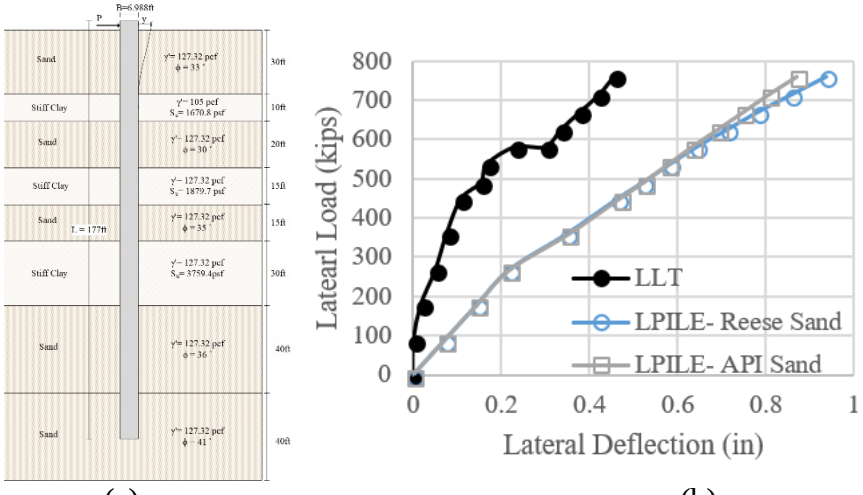

(a) (b)

Figure 4-85. (a) Soil Stratigraphy, (b) Comparison between Measured and Predicted Lateral Deflection Curve of New York City (RN: 77).

Table 4-87. Pile and Soil Properties of New York City Test (RN: 78).

Record Number: 78

New York City (S3R2)						
Report	Geotechnical Nominal Resistance Test Results for Lateral Test on Drilled Shafts S-3 and S-4 for the Kosciuszko Bridge Project – Phase 1					
Reference	Alfredas Daugiala (2015). "Geotechnical Nominal Resistance Test Results for Lateral Test on Drilled Shafts S-3 and S-4 for the Kosciuszko Bridge Project – Phase 1." Report No. 0042-TI-002-001. New York City.					
Pile properties used in LPILE						
Pile type	B (ft)	L (ft)	I (in.^{4})	E (psi)		
Bored pile with Casing	6.988	177	2.43E+06	3.05E+06		
Casing properties used in LPILE						
Casing t (in.)	Casing diameter (ft)	Casing length (ft)				
0.625	7.087	166.77				
Soil Properties used in LPILE						
P-y model	Depth		γ ' (pcf)	K (pci)	Su (psf)	φ (°)	ε_{50}
	Top	Bottom					
Reese/API Sand	0	30.0	127.32	*	n/a	33	n/a
Stiff Clay	30.0	40.0	105.00	n/a	1670.8	n/a	*
Reese/API Sand	40.0	60.0	127.32	*	n/a	30	n/a
Stiff Clay	60.0	75.0	127.32	n/a	1879.7	n/a	*
Reese/API Sand	75.0	90.0	127.32	*	n/a	35	n/a
Stiff Clay	90.0	120.0	127.32	n/a	3759.4	n/a	*
Reese/API Sand	120.0	160	127.32	*	n/a	36	n/a
Reese/API Sand	160	200.0	127.32	*	n/a	41	n/a

*automatically computed by LPILE

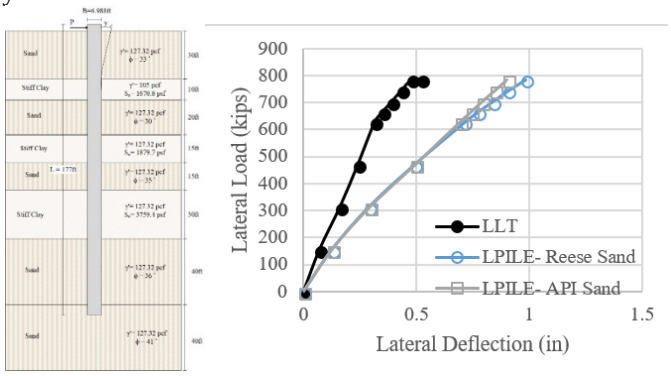

(a) (b)

Figure 4-86. (a) Soil Stratigraphy, (b) Comparison between Measured and Predicted Lateral Deflection Curve of New York City (RN: 78).

Table 4-88. Pile and Soil Properties of New York City Test (RN: 79).

Record Number: 79

New York City (S4R1)						
Report	Geotechnical Nominal Resistance Test Results for Lateral Test on Drilled Shafts S-3 and S-4 for the Kosciuszko Bridge Project – Phase 1					
Reference	Alfredas Daugiala (2015). "Geotechnical Nominal Resistance Test Results for Lateral Test on Drilled Shafts S-3 and S-4 for the Kosciuszko Bridge Project – Phase 1." Report No. 0042-TI-002-001. New York City.					
Pile properties used in LPILE						
Pile type	B (ft)	L (ft)	I (in.^{4})	E (psi)		
Bored pile with Casing	6.988	177	2.43E+06	3.05E+06		
Casing properties used in LPILE						
Casing t (in.)	Casing diameter (ft)	Casing length (ft)				
0.625	7.087	166.77				
Soil Properties used in LPILE						
P-y model	Depth		γ ' (pcf)	K (pci)	Su (psf)	φ (°)	ε_{50}
	Top	Bottom					
Reese/API Sand	0	30.0	127.32	*	n/a	33	n/a
Stiff Clay	30.0	40.0	105.00	n/a	1670.8	n/a	*
Reese/API Sand	40.0	60.0	127.32	*	n/a	30	n/a
Stiff Clay	60.0	75.0	127.32	n/a	1879.7	n/a	*
Reese/API Sand	75.0	90.0	127.32	*	n/a	35	n/a
Stiff Clay	90.0	120.0	127.32	n/a	3759.4	n/a	*
Reese/API Sand	120.0	160	127.32	*	n/a	36	n/a
Reese/API Sand	160	200.0	127.32	*	n/a	41	n/a

*automatically computed by LPILE

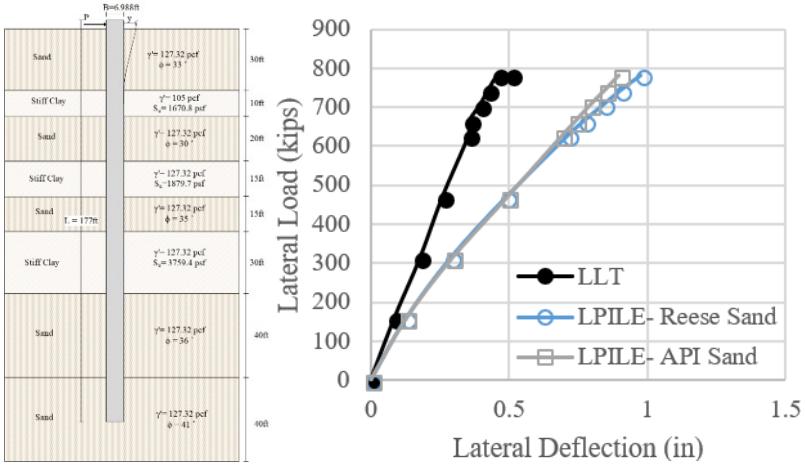

(a) (b)

Figure 4-87. (a) Soil Stratigraphy, (b) Comparison between Measured and Predicted Lateral Deflection Curve of New York City (RN: 79).

4.3.14 Kern County, California, Test (Large)

Four lateral pile load tests were performed in Kern County, California (Load Test Consulting, 2018). One of them was carried out on a large diameter (B = 5.75 ft) pile. The soil was primarily a sand deposit. The AST/React pile had a maximum deflection of 1.5 in. at about 540 kips. Figure 4-88 shows the soil stratigraphy and the field test results. Table 4-89 describes the data for the piles and the soils used as input in LPILE (RN: 83).

4.3.15 Mount Pleasant, South Carolina, Test

Two lateral load tests were performed on large diameter piles at Mount Pleasant, South Carolina (Ashour et al., 2008). Pile MP-1 was Cast-in-Steel-Shell, 8.2 ft in diameter, and 38 ft in length while Pile MP-2 was Cast-in Drilled Hole, 8.5 ft in diameter, and 38 ft in length. The soil profile consisted of 120 ft of sandy clay, slightly clayey, very clayey, or silty sand overlaying the cooper marl. The maximum applied lateral load of 970 kips led to a 5.0 in. deflection at the top of pile MP-1 while the maximum applied lateral force of 1003 kips caused 3.98 in. of displacement at the top of pile MP-2. Figure 4-89 and Figure 4-90 show the soil stratigraphy and the field test results. Table 4-90 and Table 4-91 describe the data for the piles and the soils used as input in LPILE (RN: 84–85).

Table 4-89. Pile and Soil Properties of Kern County Test.

Record Number: 2

Kern County, CA (ATS-3/React)							
Report	LTC Data Report - Lateral Load Test Results for ATS-2, Merced Avenue Overpass						
Reference	Load Test Consulting, Ltd. (2018) "LTC Data Report - Lateral Load Test Results for ATS-2, Merced Avenue Overpass." Load Test Consulting load test report.						
Pile properties used in LPILE							
Pile type	B (ft)	L (ft)	I (in.^{4})	E (psi)			
bored pile	5.751	98.4	1.11E+06	3.05E+06			
Soil Properties used in LPILE							
P-y model	Depth		γ ' (pcf)	K (pci)	Su (psf)	φ (°)	ε_{50}
	Top	Bottom					
Reese/API Sand	0	13.1	115.20	*	n/a	29	n/a
Reese/API Sand	13.1	27.9	119.30	*	n/a	36	n/a
Stiff Clay	27.9	43.0	106.40	n/a	3760.2	n/a	*
Reese/API Sand	43.0	53.1	106.40	*	n/a	41	n/a
Stiff Clay	53.1	67.9	113.20	n/a	6893.7	n/a	*
Reese/API Sand	67.9	101.4	121.10	*	n/a	41	n/a

*automatically computed by LPILE

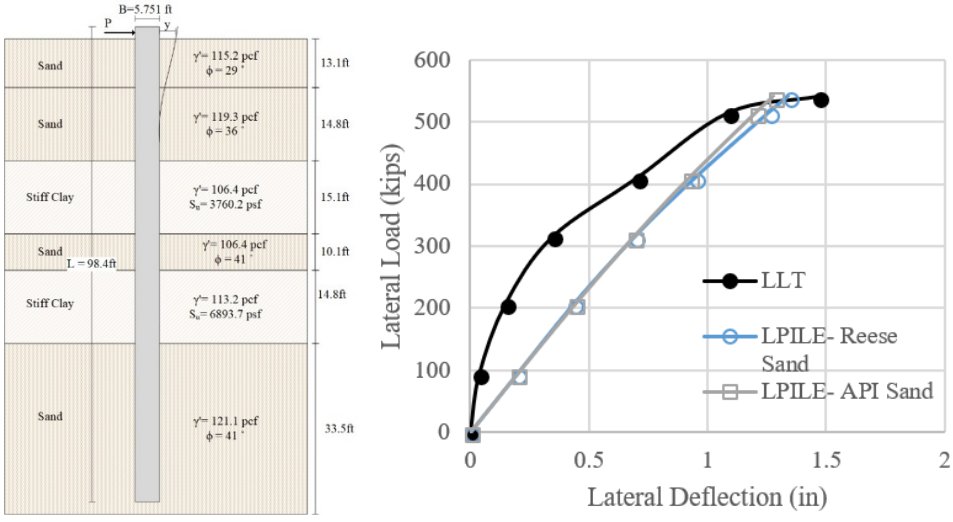

(a) (b)

Figure 4-88. (a) Soil Stratigraphy, (b) Comparison between Measured and Predicted Lateral Deflection Curve of Kern County.

Table 4-90. Pile and Soil Properties of Mt. Pleasant Test (RN: 84).

Record Number: 84

Mt. Pleasant, South Carolina							
Paper	Analysis of laterally loaded long or intermediate drilled shafts of small or large diameter in layered soil						
Reference	Ashour, Mohamed, Gary Norris, and Sherif Elfass. *Analysis of laterally loaded long or intermediate drilled shafts of small or large diameter in layered soil.* No. CA04-0252. California. Dept. of Transportation. Division of Research and Innovation, 2008.						
Pile properties used in LPILE							
Pile type	B (ft)	L (ft)	I (in.^{4})	E (psi)			
Cast-in steel shell	8.2	38	4.61E+06	3.05E+06			
Soil Properties used in LPILE							
P-y model	Depth		γ ' (pcf)	K (psi)	Su (psf)	φ (°)	ε_{50}
	Top	Bottom					
Sand	0	4	120	*	n/a	34	n/a
Sand	4	13	62	*	n/a	30	n/a
Sand	13	29	62	*	n/a	32	n/a
Sand	29	38	62	*	n/a	30	n/a
Clay	38	117.8	65	n/a	4300.8	n/a	*

*automatically computed by LPILE

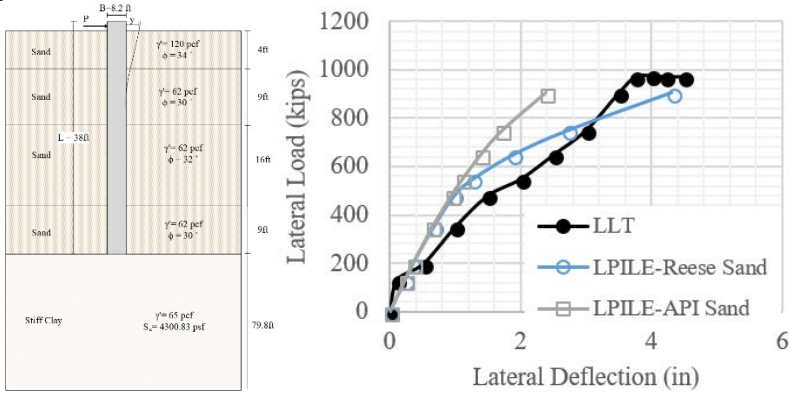

(a) (b)

Figure 4-89. (a) Soil Stratigraphy, (b) Comparison between Measured and Predicted Lateral Deflection Curve of Mt. Pleasant (RN: 84).

Table 4-91. Pile and Soil Properties of Mt. Pleasant Test (RN: 85).

Record Number: 85

Mt. Pleasant, South Carolina							
Paper	Analysis of laterally loaded long or intermediate drilled shafts of small or large diameter in layered soil						
Reference	Ashour, Mohamed, Gary Norris, and Sherif Elfass. *Analysis of laterally loaded long or intermediate drilled shafts of small or large diameter in layered soil.* No. CA04-0252. California. Dept. of Transportation. Division of Research and Innovation, 2008.						
Pile properties used in LPILE							
Pile type	B (ft)	L (ft)	I (in.^{4})	E (psi)			
Cast-in steel shell	8.5	38	5.39E+06	3.05E+06			
Soil Properties used in LPILE							
P-y model	Depth		γ ' (pcf)	K (psi)	Su (psf)	φ (°)	ε_{50}
	Top	Bottom					
Sand	0	4	120	*	n/a	34	n/a
Sand	4	13	62	*	n/a	30	n/a
Sand	13	29	62	*	n/a	32	n/a
Sand	29	38	62	*	n/a	30	n/a
Clay	38	117.8	65	n/a	4300.8	n/a	*

*automatically computed by LPILE

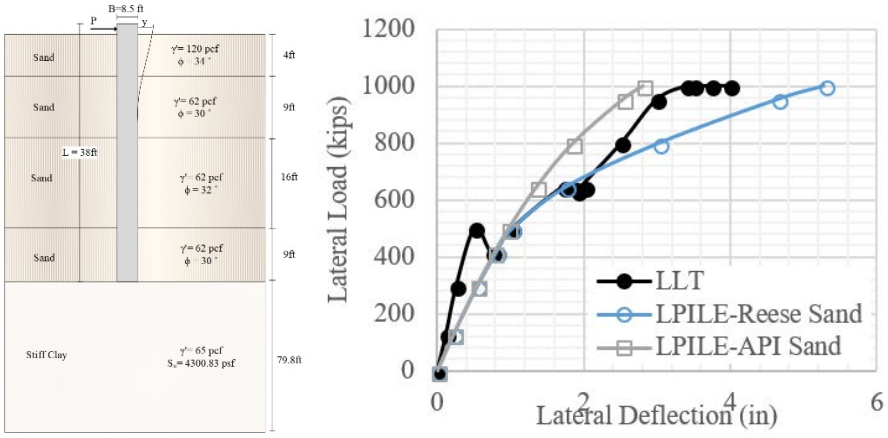

(a) (b)

Figure 4-90. (a) Soil Stratigraphy, (b) Comparison between Measured and Predicted Lateral Deflection Curve of Mt. Pleasant (RN: 85).

CHAPTER 5 PREDICTING LATERAL PILE BEHAVIOR

5.1 INTRODUCTION

There are several ways to predict the behavior of laterally loaded piles. Yegian and Wright (1973) and Thompson (1977) used the finite element method to compare measured and predicted behavior. Briaud (1997) developed a SALLOP method by using the experimental data from pressuremeter test to predict the lateral behavior of piles. Others assumed an elastic pile and soil (Terzaghi, 1955), a rigid pile and plastic/spring modeled soil (Broms, 1965; DiGioa et al., 1989) (Figure 5-1), and a nonlinear pile and soil represented by P-y curves (Isenhower and Wang, 2016).

The nonlinear pile and P-y soil model method shown in Figure 5-1 and the SALLOP method shown in Figure 5-2 are the two methods used to provide a comparison between the full-scale experimental results and the calculated values called predictions.

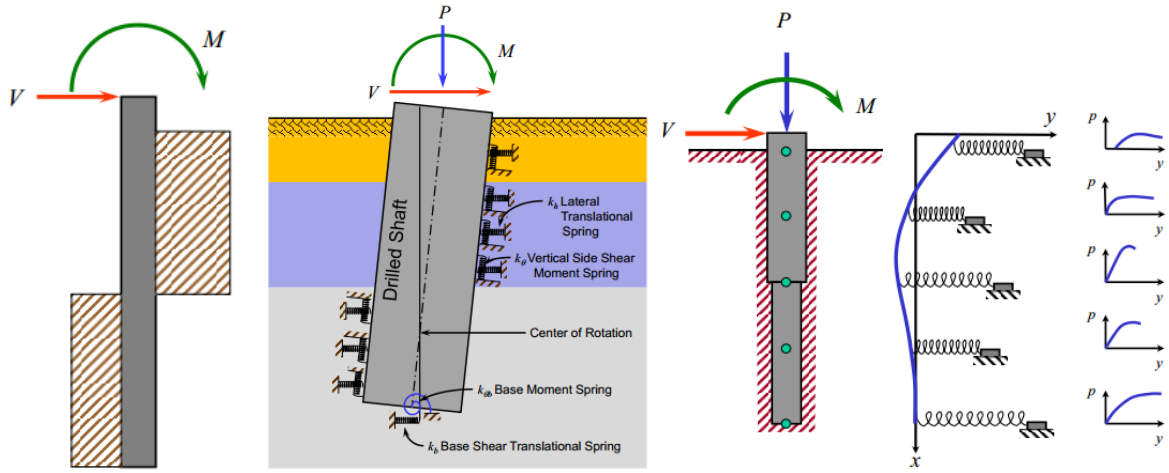

(a) (b) (c)

Figure 5-1. Models of Piles under Lateral Loading (a) Broms' Model (Broms, 1965), (b) DiGioa's Model (DiGioa, 1989), and (c) P-y Curves (Isenhower and Wang, 2016).

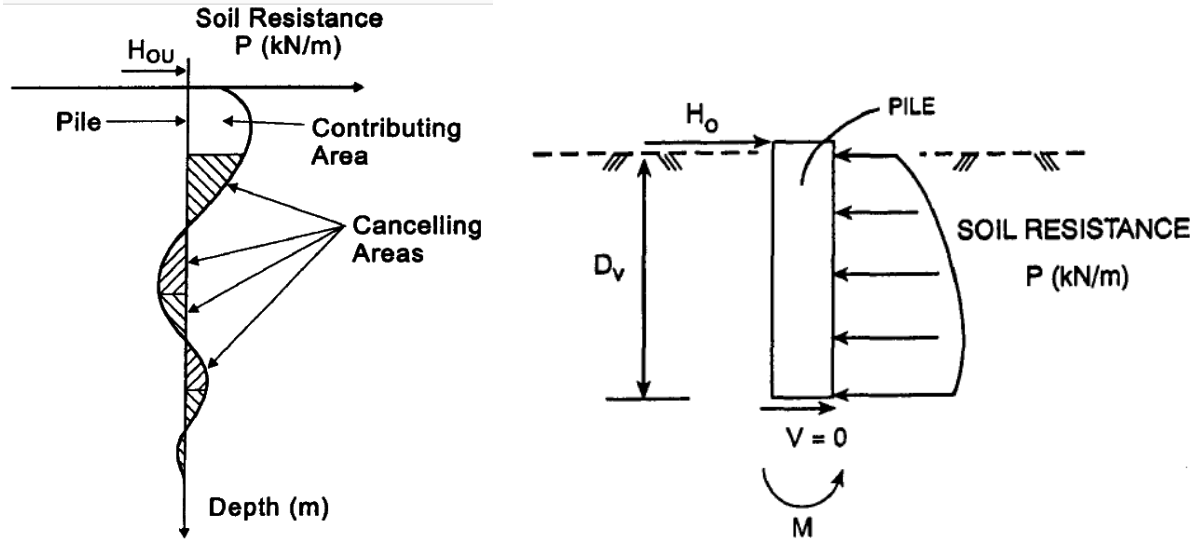

(a) (b)

Figure 5-2. (a) Concept of SALLOP method (b) Free body diagram of pile down to Zero-Shear depth (Briaud, 1997)

In this section, a total of 54 small diameter (B < 5 ft) cases will be discussed. LPILE 2018 (LPILE, 2018) was used to predict the load deflection curve at the pile head and compared with the lateral load test results. The P-y criteria included the sand criterion (Reese et al., 1974; API, 2010) and the clay criterion (Matlock, 1970; Reese and Welch, 1975).

5.2.1 Chiayi, Taiwan Field Test

A series of lateral loads was applied to the pile head in LPILE to predict the behavior of the pile in this Taiwan project. Figure 4-2(b) and Figure 4-3(b) show the comparison between the measured and predicted results.

5.2.2 Edmonton, Alberta, Canada Test

Figure 4-4(b), Figure 4-5(b), Figure 4-6(b), and Figure 4-7(b) show the comparison between the LPILE prediction results and the measurements for the project in Edmonton, Canada.

5.2.3 New Orleans, Louisiana, Test

In this case, the API sand P-y criterion and the Reese sand P-y criterion were used in the LPILE simulations. Figure 4-8(b), Figure 4-9(b), and Figure 4-10(b) present the comparison of

load-deflection curves between the load test results and the computed results for pile TPU(Timber pile), pile CPU(Concrete pile), and pile CIP (Cast-in-place).

5.2.4 Baytown, Texas, Test (Little)

Figure 4-11(b) and Figure 4-12(b) show the comparison between the measured load-displacement curves and the predicted load displacement curves with LPILE using Reese and API sand criteria.

5.2.5 Sabine, Texas, Test

Figure 4-13(b) shows the comparison between the measured and LPILE predicted load-deflection curves.

5.2.6 Lake Austin, Texas, Test

Figure 4-14(b) shows the comparison between the load test and the LPILE prediction.

5.2.7 Texas A&M University, Texas, Test

Figure 4-15(b) and Figure 4-16(b) compare the measured load displacement curve and LPILE predicted load displacement curve.

5.2.8 University of Houston, Texas, Test

Figure 4-17(b) shows the field test results and the LPILE predictions.

5.2.9 Lock and Dam 26, Illinois, Test

Figure 4-18(b) and Figure 4-19(b) show the comparison between the measured results and the predictions by LPILE using the Reese and API sand criteria.

5.2.10 Baytown, Texas, Test (Smith)

Figure 4-20(b) shows the comparison between the load-deflection curves for the full-scale test and for the LPILE predictions.

5.2.11 Plancoet, France Test

Figure 4-21(b) shows the load-deflection comparison between the full-scale test in France and the LPILE simulation.

5.2.12 Stuart, Florida, Test

The predicted load-deflection curves at the pile head were compared with the measured ones; Figure 4-22(b) and Figure 4-23(b) show the comparison for pile a and pile b.

5.2.13 Rocky Mount, North Carolina, Test

Table 4-27 and Table 4-28 show the parameters used for simulating the lateral pile behaviors in LPILE. Figure 4-24(b) and Figure 4-25(b) show the comparisons between the LPILE predictions and the measured curves.

5.2.14 Kuwait Test

Figure 4-26(b), Figure 4-27(b), Figure 4-28(b), Figure 4-29(b), and Figure 4-30(b) show the comparisons between the measured load-displacement curves and the predicted curves. Table 4-29, Table 4-30, Table 4-31, Table 4-32, and Table 4-33 list the pile load tests including two straight piles and three tapered piles, where the parameters were used in the LPILE simulations.

5.2.15 University of California, San Diego, Test (UCSD Test)

Table 4-34, Table 4-35, Table 4-36, and Table 4-37 summarize the parameters used for the LPILE predictions. Figure 4-33(b), Figure 4-34(b), Figure 4-35(b), and Figure 4-36(b) show the load-deflection curves for the load tests and the LPILE predictions.

5.2.16 Hawthorne, California, Test (Lemnitzer)

Table 4-38 and Table 4-39 summarize the parameters used for LPILE predictions. Figure 4-37(b) and Figure 4-38(b) show the comparison between the measured and LPILE predicted load-displacement curves.

5.2.17 University of Massachusetts Campus in Amherst Test (UMass Amherst Test)

A series of four small diameter pile load tests was completed at the University of Massachusetts campus in Amherst. Figure 4-39(b), Figure 4-40(b), Figure 4-41(b), and Figure 4-42(b) compare the load-deflection curves from the field tests with the LPILE predicted curves. Table 4-40, Table 4-41, Table 4-42, and Table 4-43 contain the parameters used for LPILE simulations.

5.2.18 Incheon, South Korea Test (Small)

Table 4-44, Table 4-45, and Table 4-46 summarize the parameters used for the LPILE predictions. Figure 4-43(b), Figure 4-44(b), and Figure 4-45(b) show the comparison results.

5.2.19 Japan Test (Small)

Three of the six full-scale tests completed in Japan were classified as small diameter piles. Table 4-47 Table 4-48 and Table 4-49 list the parameters used in LPILE. Figure 4-46(b), Figure 4-47(b) and Figure 4-48(b) present the comparison of load-deflection curves.

5.2.20 Kern County, California, Test (Small)

Table 4-50, Table , and Table 4-52 summarize the parameters used in LPILE. The predicted load-deflection curve at the pile head are compared with the measured curves in Figure 4-49(b), Figure 4-50(b), and Figure 4-51(b).

5.2.21 Massena, New York, Test

Table 4-53, Table 4-54, Table 4-55, and Table 4-56 summarize the parameters used in LPILE. Figure 4-52(b), Figure 4-53(b), Figure 4-54(b), and Figure 4-55(b) present the comparison between the measured load-deflection curves and the LPILE predicted curves.

5.3 PREDICTING LARGE DIAMETER PILES BEHAVIOR

In this section, researchers analyzed a total of 35 lateral load tests on large diameter (B > 5 ft) piles (RN: 1, 4–8, 51–66, 70–79, and 83). The predictions according to LPILE (LPILE, 2018) are performed and compared to the measured results in the load test. The P-y criteria included the sand criterion (Reese et al., 1974; API, 2010) and the clay criterion (Matlock, 1970; Reese and Welch, 1975).

5.3.1 Inner Belt Bridge, Ohio, Test

The Matlock P-y curves were used in the LPILE computer program to compute the response of the test piles under the applied lateral loads in Inner belt bridge case. Table 4-57 summarizes the pile was considered as an elastic member and the parameters used in the LPILE simulation. Figure 4-56(b) presents the predicted load-deflection curve at the pile head and the measured curve.

5.3.2 Hawthorne, California, Test (Janoyan)

In this simulation, the Reese sand and Matlock clay P-y curves were used in the LPILE computer program to compute the response of the test pile under the applied lateral loads. The pile was considered as an elastic member. Table 4-58 summarizes the parameters used in the LPILE simulation. Figure 4-57(b) compares the predicted and measured curves.

5.3.3 Iran Test

These offshore lateral load tests were completed at Pars Special Economic Energy Zone Area near Asalouyeh in Iran and simulated by using the Reese sand and API sand P-y curves in the LPILE computer program to predict the behaviors of the test piles under the applied lateral loads. Table 4-59, Table 4-60, Table 4-61, and Table 4-62 summarize the parameters used in the LPILE simulation. Figure 4-58(b), Figure 4-59(b), Figure 4-60(b), and Figure 4-61(b) compare the predicted load-displacement curves at the top of the pile the measured curves for pile 1 to pile 4, respectively.

5.3.4 Incheon, South Korea Test (Large)

This large pile load test was one of four performed in Incheon, South Korea. Table 4-63 summarizes the parameters used in the LPILE simulation. Figure 4-62(b) presents the measured and predicted load-deflection curves for this large diameter pile.

5.3.5 Hawthorne, California, Test (Naramore)

Table 4-64 and Table 4-65 summarize the parameters used in the LPILE simulation. Figure 4-63(b) and Figure 4-64(b) present the measured and predicted load-deflection curves for the shaft A and shaft B.

5.3.6 Spring Villa, Alabama, Test

The Matlock clay and Reese weak rock P-y curves were used in the LPILE computer program to predict the behavior of the test piles. The piles were considered as elastic members. Table 4-66, Table 4-67, Table 4-68, Table 4-69, Table 4-70, and Table 4-71 describe the parameters used in the LPILE simulations. Figure 4-65(b), Figure 4-66(b), Figure 4-67(b), Figure

4-68(b), Figure 4-69(b), and Figure 4-70(b) compare the predicted load-deflection curves at the top of the pile with the measured curves.

5.3.7 Las Vegas, Nevada, Test

Table 4-72 summarizes the parameters used in the LPILE simulation. Figure 4-71(b) compares the measured load-deflection curves of the pile with those predicted using LPILE with the Matlock clay P-y curves.

5.3.8 Glenwood Canyon, Colorado, Test

The Reese sand and API sand P-y curves were used in the LPILE computer program to predict the behavior of the test piles under the applied lateral forces. The pile was considered as an elastic member. Figure 4-72(b) and Figure 4-73(b) present the measured and predicted load-deflection curves for the East case and West case.

5.3.9 London, Ontario, Canada Test

The Reese sand and API sand P-y curves were used in the LPILE computer program to compute the behaviors of the test piles under the applied lateral loads. In the Reese sand criterion, the k value was computed from Figure 3-5 and Figure 3-6 while using a friction angle obtained from the API sand criterion. The pile was considered as an elastic member. Figure 4-74(b) and Figure 4-75(b) compare the predicted and measured load displacement curves.

5.3.10 Japan Test (Large)

There were three simulations completed by using the Reese sand, API sand, and Matlock P-y curves of LPILE computer program to predict the responses of the test piles under the applied lateral loads. The values of the friction angle were determined by conversion from the SPT-N values provided from the publication (Ishikawa, 1985). Table 4-77, Table 4-78, and Table 4-79 summarize the parameters used in the LPILE simulation. The predicted load-deflection curves at the pile head are compared with the measured curves in Figure 4-76(b), Figure 4-77(b) and Figure 4-78(b) for piles at site A, site B and site F, respectively.

5.3.11 Sterling, Virginia, Test

The criteria used in LPILE were the Reese sand, API sand, and Reese weak rock P-y curves. Table 4-80, Table 4-81, and Table 4-82 describe the parameters used in the LPILE simulation. Figure 4-79(b), Figure 4-80(b), and Figure 4-81(b) present the measured and predicted load-deflection curves for the Sterling test.

5.3.12 Jacksonville, Florida, Test

The Reese sand and API sand P-y curves were used in the LPILE computer program to compute the response of the test piles under the applied lateral loads. Table 4-83 and Table 4-84 summarize the piles were considered as elastic members and the parameters used in the LPILE simulation. Figure 4-82(b) and Figure 4-83(b) compare the predicted load-deflection curves at the pile top with the measured ones.

5.3.13 New York City, New York, Test

Table 4-85, Table 4-86, Table 4-87, and Table 4-88 summarize the parameters used in the LPILE simulation. Figure 4-84(b), Figure 4-85(b), Figure 4-86(b), and Figure 4-87(b) compare the measured load-deflection curves of the pile with those predicted using LPILE with the Reese sand, API sand and Matlock clay P-y curves.

5.3.14 Kern County, California, Test (Large)

The Reese sand, API sand, and Matlock clay P-y curves were used to compute the response of the test pile under different applied lateral loads. Table 4-89 describes the parameters used in LPILE simulations. Figure 4-88(b) shows the measured and predicted load-deflection curve.

5.3.15 Mount Pleasant, South Carolina, Test

There were two simulations completed by using the Reese sand, API sand, and Matlock P-y curves to predict the responses of the test piles under the applied lateral loads. Table 4-90 and Table 4-91 summarize the parameters used in the LPILE simulation. Figure 4-89(b) and Figure 4-90(b) compare the predicted load-deflection curves to the measured ones.

CHAPTER 6 COMPARING THE PREDICTIONS WITH THE MEASUREMENTS

6.1 INTRODUCTION

This chapter presents the comparison between the field test results and the prediction results for different pile diameters. The 89 load test results were compared with the LPILE predicted results from two viewpoints. The first one compared the load at different pile top deflection levels, and the second one compared the deflection at different pile top load levels. The levels of pile head deflection were 0.25, 0.5, 1.0, and 2.0 in.; the levels of pile head load were 10 percent, 25 percent, 33 percent, and 50 percent of the ultimate load capacity defined as the load corresponding to 10 percent of the pile diameter.

Also, a comparison was performed between the load test ultimate load at 10 percent of the pile diameter and the one predicted by the SALLOP method (Briaud, 1997).

The last part of the chapter discusses the relative number of times (probability) that the predictions are on the unsafe side. This unsafe side is taken as an overprediction of the load for a chosen deflection or an underprediction of the deflection for a given load as a percent of ultimate.

6.2 COMPARISON BETWEEN THE PREDICTIONS AND THE MEASUREMENTS

In this section, the comparison is first presented as the ratio of the predicted over measured load for a given deflection plotted against the pile diameter and predicted versus measured scatter plots. The selected pile head deflections were 0.25, 0.5, 1.0, and 2.0 in. The comparison is done for the two types of soil—sand and clay. For the sands, the Reese sand P-y curves (Reese et. al., 1974) is selected, and for the clays the soft clay P-y curves (Matlock, 1970) and the stiff clay with no free water P-y curves (Reese and Welch, 1975) were chosen. For layered soils, the case was classified as sand or clay by selecting the dominant soil type within the top third of the pile length.

Secondly, the comparison is presented as the ratio of the predicted over measured deflection for a given load expressed as a percent of the ultimate load and plotted against the pile diameter as well as predicted versus measured scatter plots. The ultimate load was taken as the load at a pile-head displacement corresponding to 0.1B where B is the pile diameter (Briaud,

2013). The comparison is presented for lateral loads equal to 10 percent, 25 percent, 33 percent, and 50 percent of the ultimate lateral load.

Then the ultimate load predicted by the SALLOP method was compared to the measured ultimate load for all cases where pressuremeter data were available.

6.3 THE PREDICTIONS OF LPILE COMPUTER PROGRAM AND THE MEASUREMENTS

The 89 cases were split into four groups: comparison based on loads in sand, comparison based on loads in clay, comparison based on deflections in sand, and comparison based on deflections in clay. They can be found next in sections 6.3.1 to 6.3.4.

6.3.1 Comparison of Loads in Sand

Figure 6-1, Figure 6-3, Figure 6-5, and Figure 6-7 present the comparison between the ratio of the predicted and measured load at lateral pile head displacements of 0.25 in., 0.50 in., 1.0 in., and 2.0 in., respectively, and the pile diameter. The average predicted over measured load ratio is equal to 0.77, 0.79, 0.85, 0.89 in sand for the 0.25 in., 0.50 in., 1.0 in., and 2.0 in., respectively; thus the load corresponding to these deflections is underpredicted on average. Also and in all cases, the predicted over measured ratio increases with the pile diameter with the average ratio becoming closer to 1 for large diameter piles.

Figure 6-2, Figure 6-4, Figure 6-6, and Figure 6-8 show the frequency distribution curves of the ratio of predicted load L_p over measured load L_m. The mean value of the load ratio (L_p/L_m) for the group of small diameter piles (B<5ft) were 0.71, 0.75, 0.77, and 0.85 for the 0.25 in., 0.50 in., 1.0 in., and 2.0 in., respectively. The mean value of the load ratio (L_p/L_m) for the group of large diameter pile (B>5 ft) were 0.85, 0.86, 0.97, and 0.96 for the 0.25 in, 0.50 in, 1.0 in., and 2.0 in. deflections, respectively. The scale effect does not make a significant difference in the predictions by LPILE when using the Reese-Sand P-y curve criterion to predict the lateral deflection of the piles in the database. Figure 6-9 regroups all the results in sand presented as the ratio L_p/L_m as a function of the pile diameter. While the average ratio L_p/L_m is relatively close to 1 and indicates a good prediction on the average, the scatter is quite large and is reflected in the low R^2, which varies between 0.09 and 0.29, and in the coefficient of variation of the ratio L_p/L_m, which is between 0.5 and 0.2. Note that the coefficient of variation decreases as the predicted deflection becomes larger. In other words, the larger the prediction, the better the prediction.

Overall one can expect to have an L_p/L_m ratio between 0.4 and 1.6 for piles in sand with better predictions for larger diameter piles. Again these results are for piles in sand.

Figure 6-10, Figure 6-11, Figure 6-12, and Figure 6-13 show the predicted versus measured loads at lateral pile head displacements of 0.25 in., 0.50 in., 1.0 in., and 2.0 in. in sand, respectively. They confirm the observations made on the predicted versus measured load ratio.

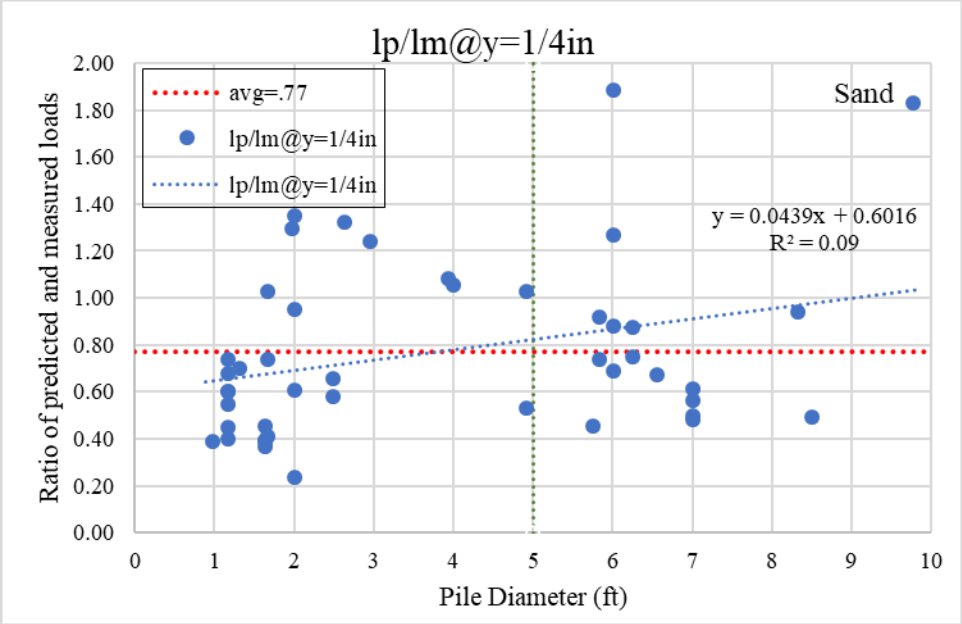

Figure 6-1. Comparison between the Ratio of Predicted and Measured Load versus Pile Diameter at Pile Top Displacement Equals to 0.25 in. in Sand.

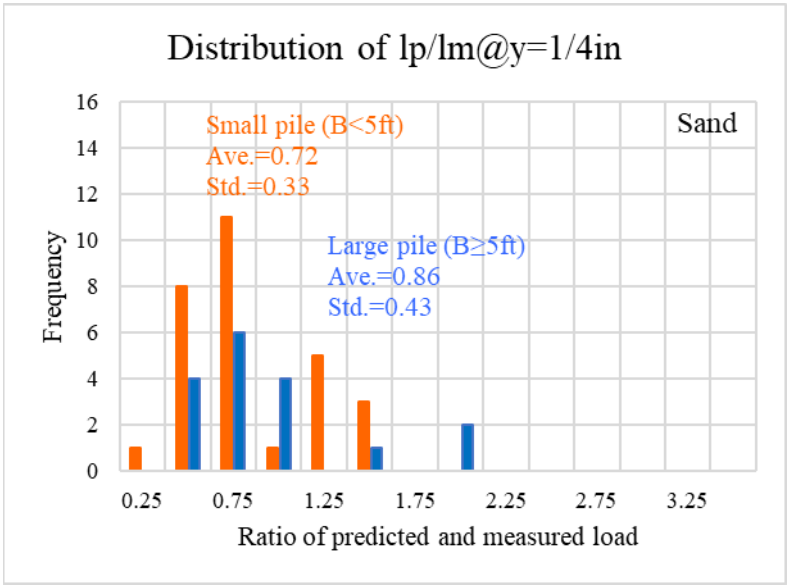

Figure 6-2. Distribution of lp/lm at y = ¼ in. in Sand.

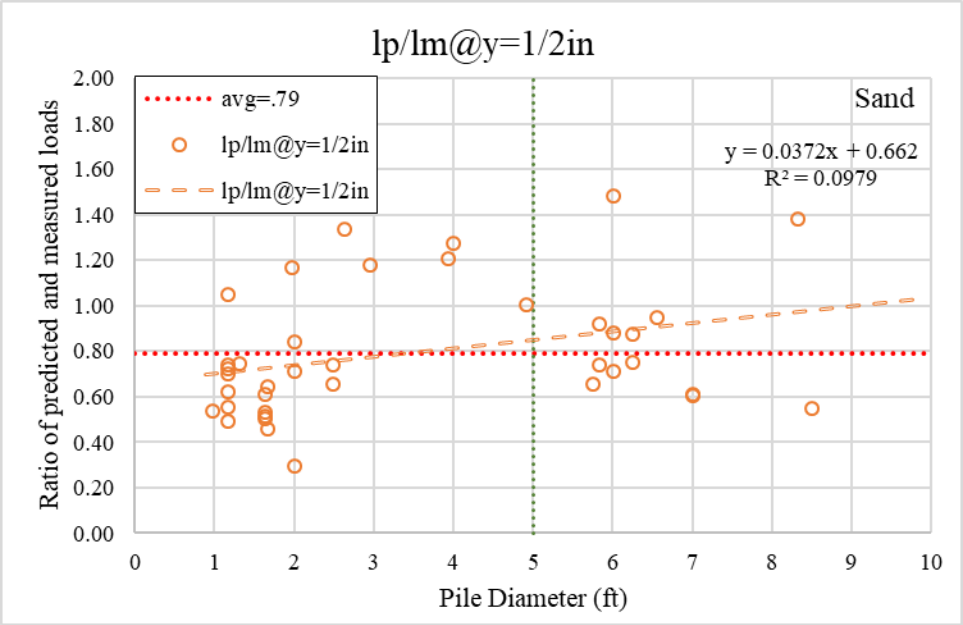

Figure 6-3. Comparison between the Ratio of Predicted and Measured Load versus Pile Diameter at Pile Top Displacement Equals to 0.5 in. in Sand.

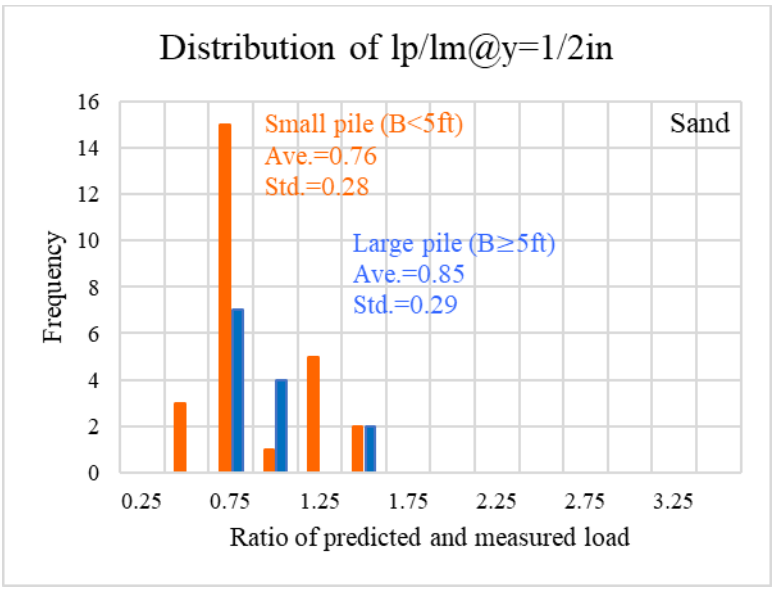

Figure 6-4. Distribution of lp/lm at y = ½ in. in Sand.

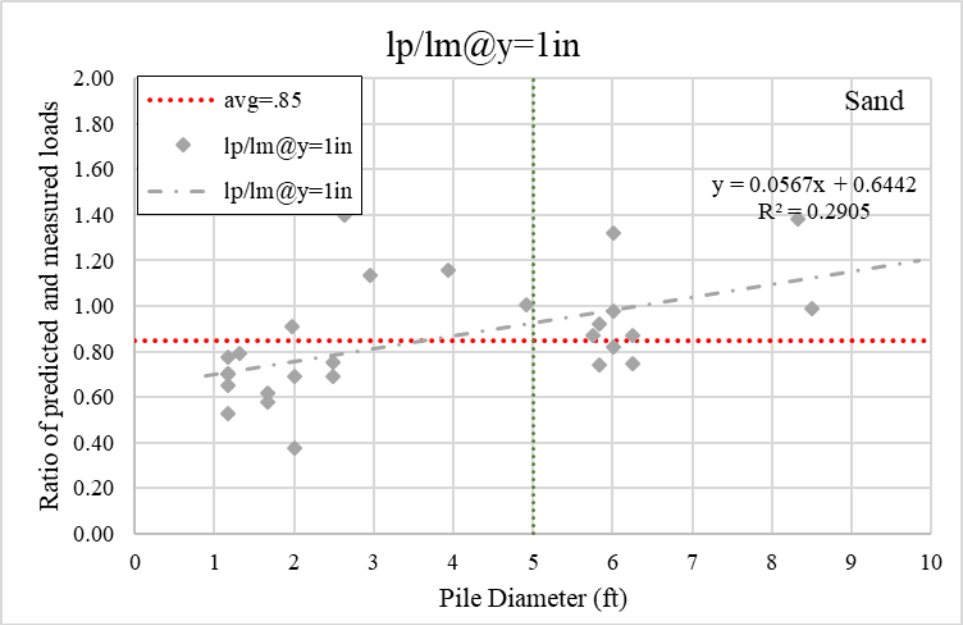

Figure 6-5. Comparison between the Ratio of Predicted and Measured Load versus Pile Diameter at Pile Top Displacement Equals to 1.0 in. in Sand.

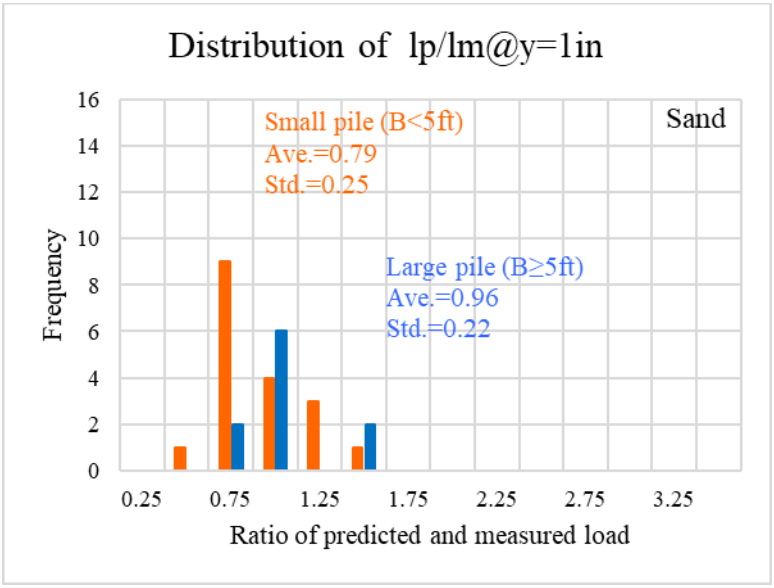

Figure 6-6. Distribution of lp/lm at y = 1 in. in Sand.

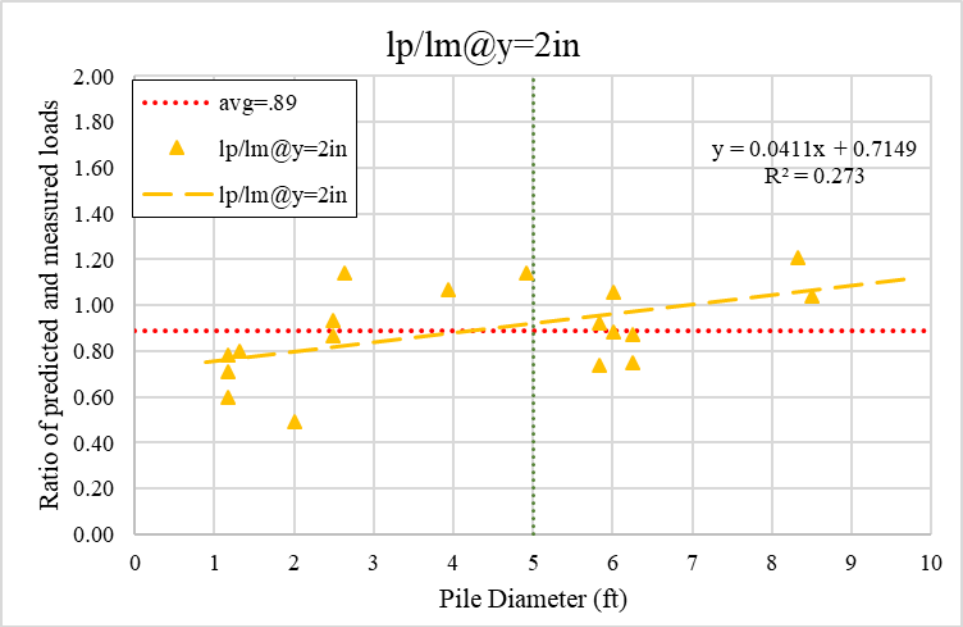

Figure 6-7. Comparison between the Ratio of Predicted and Measured Load versus Pile Diameter at Pile Top Displacement Equals to 2.0 in. in Sand.

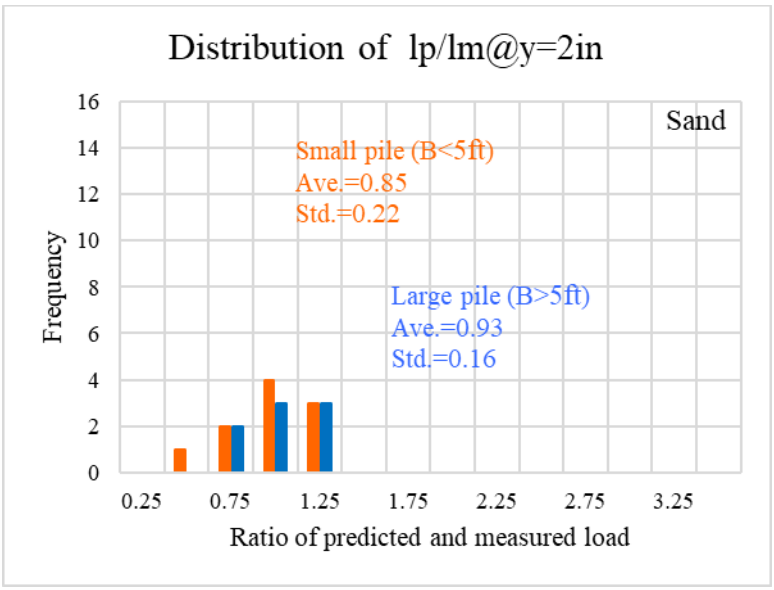

Figure 6-8. Distribution of lp/lm at y = 2 in. in Sand.

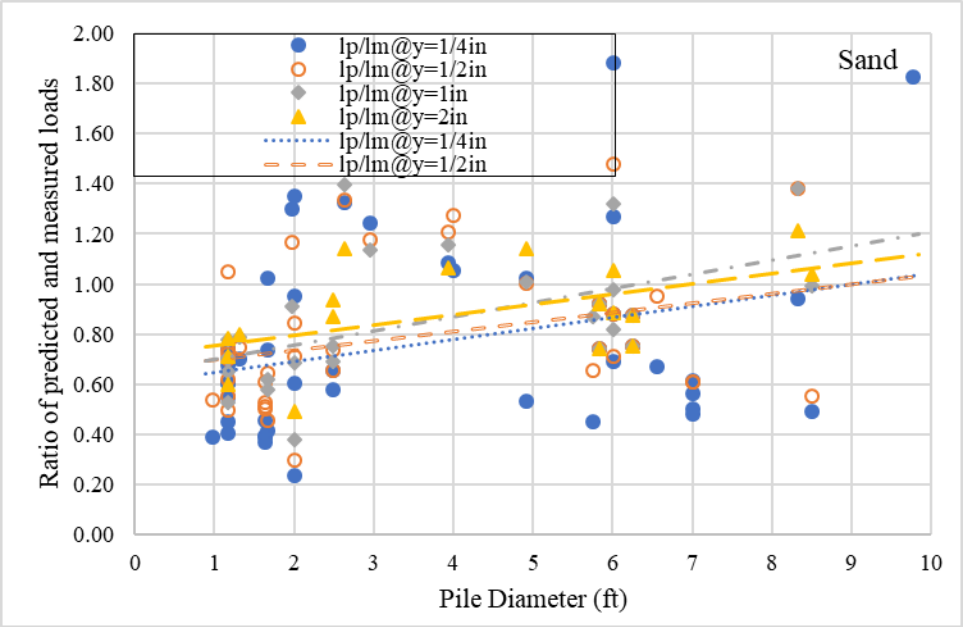

Figure 6-9. Comparison between the Ratio of Predicted and Measured Load versus Pile Diameter at Pile Top Displacement Equals to 0.25, 0.5, 1.0 in. and 2.0 in. in Sand.

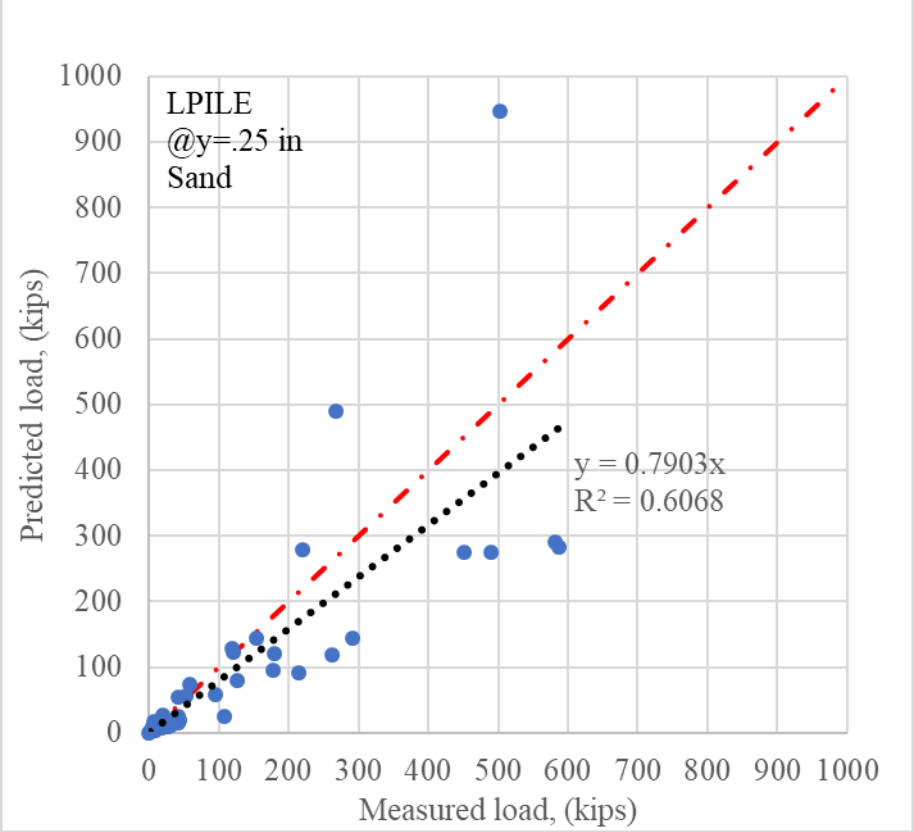

Figure 6-10. LPILE Predictions versus Measurements at Pile Top Displacement Equals to 0.25 in. in Sand.

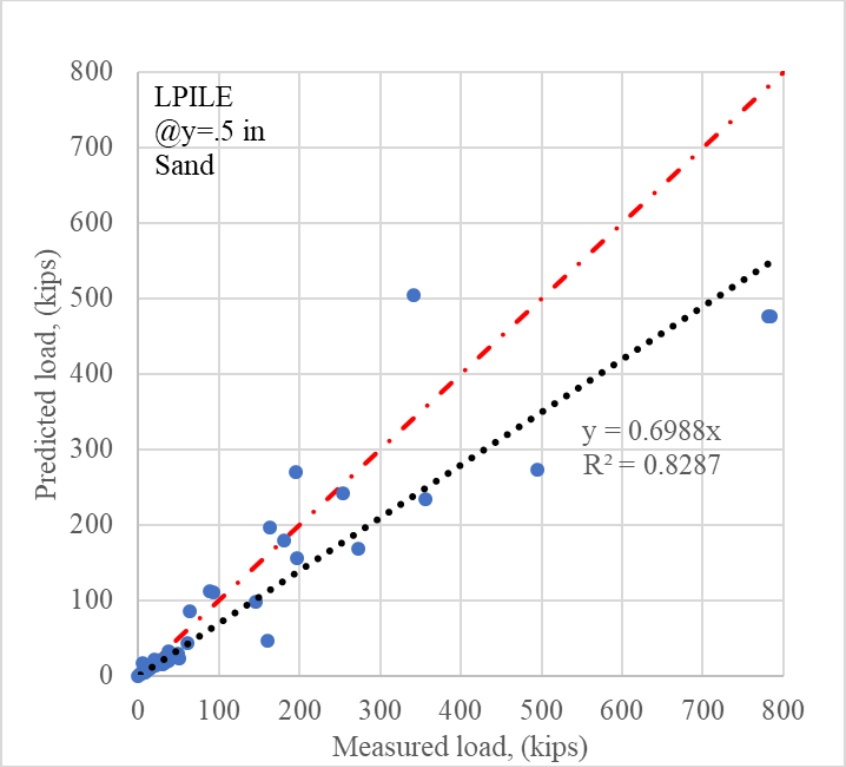

Figure 6-11. LPILE Predictions versus Measurements at Pile Top Displacement Equals to 0.5 in. in Sand.

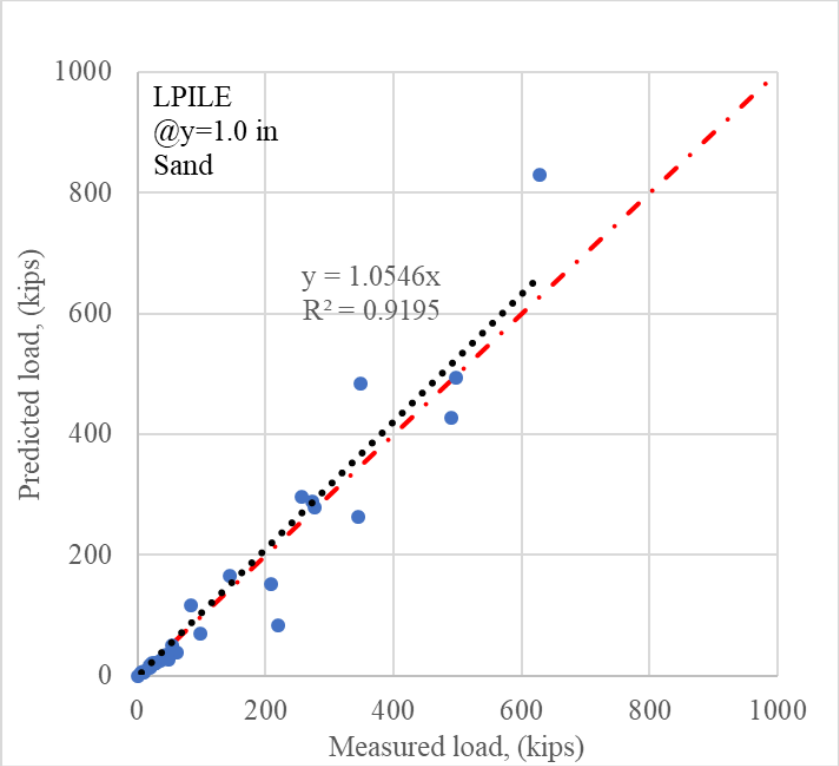

Figure 6-12. LPILE Predictions versus Measurements at Pile Top Displacement Equals to 1.0 in. in Sand.

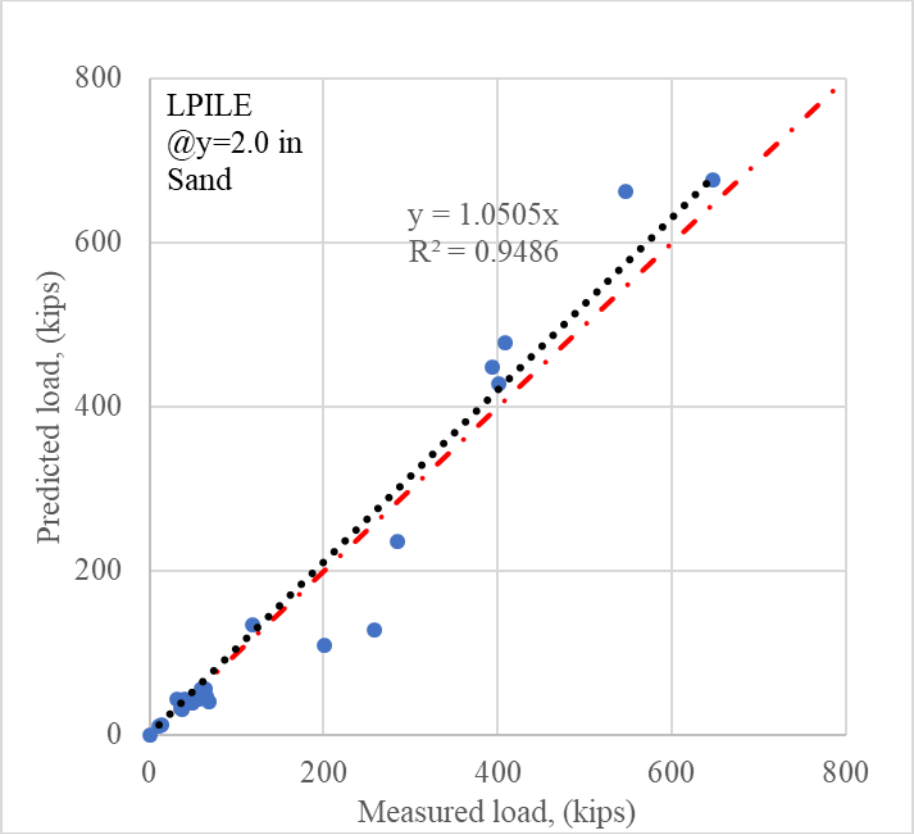

Figure 6-13. LPILE Predictions versus Measurements at Pile Top Displacement Equals to 2.0 in. in Sand.

6.3.2 Comparison of Loads in Clay

Figure 6-14, Figure 6-16, Figure 6-18, and Figure 6-20 plot the ratio of the predicted over the measured load L_p/L_m at lateral pile head displacements of 0.25 in., 0.50 in., 1.0 in., and 2.0 in., respectively, on one hand and the pile diameter on the other. The average predicted over measured load ratio is equal to 1.09, 1.01, 0.86, 0.83 in clay for the 0.25 in., 0.50 in., 1.0 in., and 2.0 in., displacement, respectively. Therefore the predicted over measured load ratio is close to 1 in all cases and decreases with the pile diameter; the load ratio approaches 0.5 for large diameter piles. These results are for piles in clay and the decreasing trend of L_p/L_m with increasing diameter for piles in clay is the opposite of the case of piles in sand.

Figure 6-15, Figure 6-17, Figure 6-19, and Figure 6-21 show the frequency distribution curves of the ratio L_p/L_m. The mean value of the load ratio L_p/L_m for the group of small diameter pile (B<5 ft) were 1.3, 1.17, 0.95, and 0.86, for the 0.25 in., 0.50 in., 1.0 in., and 2.0 in. deflections, respectively. The mean value of the load ratio L_p/L_m for the group of large diameter pile (B>5 ft) were 0.76, 0.74, 0.71, and 0.75 for the 0.25 in., 0.50 in., 1.0 in., and 2.0 in.

deflections, respectively. The scale effect is more pronounced in clay than in sand when using the soft clay P-y curve criterion (Matlock, 1970) and stiff clay P-y curve criterion (Reese and Welch, 1975) without free water to predict the lateral deflection of the piles in the database. Figure 6-18 regroups all the results in clay presented as the ratio L_p/L_m as a function of the pile diameter. As can be seen, the ratio L_p/L_m drops significantly with increasing diameter and reaches an average of 0.5 for very large diameters (10 ft). The scatter is quite large and is reflected in the low R^2, which varies between 0.18 and 0.27 and in the coefficient of variation of the ratio L_p/L_m, which is between 0.44 and 0.16. For small diameter piles, the coefficient of variation decreases as the deflection increases, but the reverse trend is observed for large diameter piles. Overall one can expect to have an L_p/L_m ratio most of the time between 0.4 and 1.6 for piles in clay with under predictions for large diameter piles. Again these results are for piles in clay.

Figure 6-23, Figure 6-24, Figure 6-25, and Figure 6-26 show the predicted versus measured loads at lateral pile head displacements of 0.25 in., 0.50 in., 1.0 in., and 2.0 in. in clay, respectively. They confirm the observations made on the predicted versus measured load ratio.

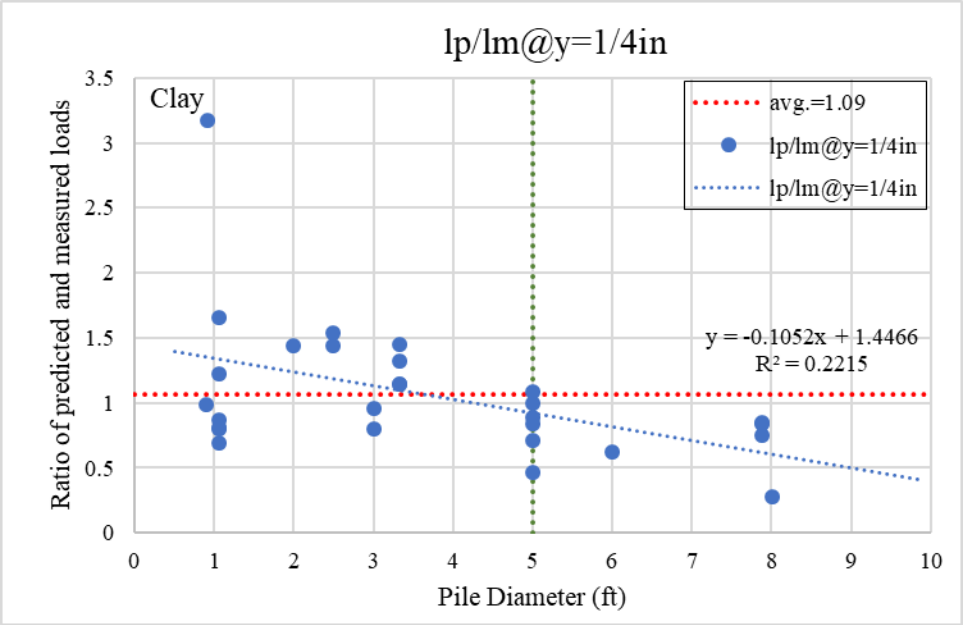

Figure 6-14. Comparison between the Ratio of Predicted and Measured Load versus Pile Diameter at Pile Top Displacement Equals to 0.25 in. in Clay.

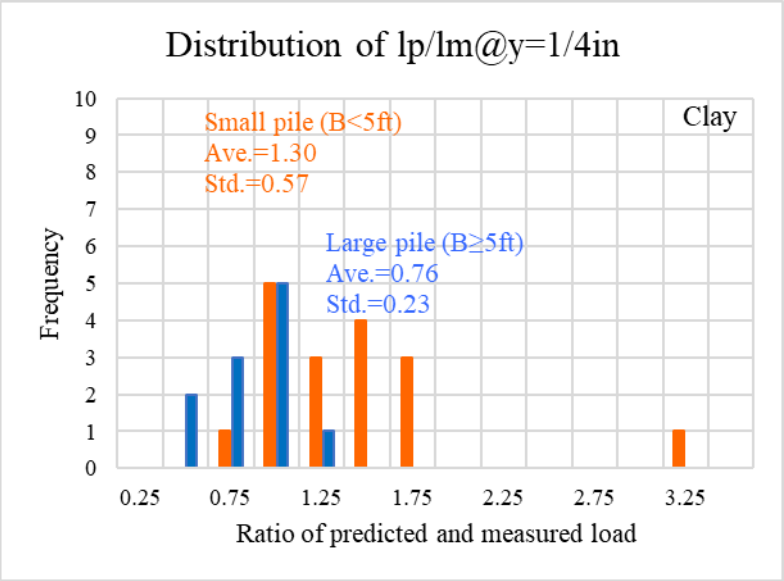

Figure 6-15. Distribution of lp/lm at y = ¼ in. in Clay.

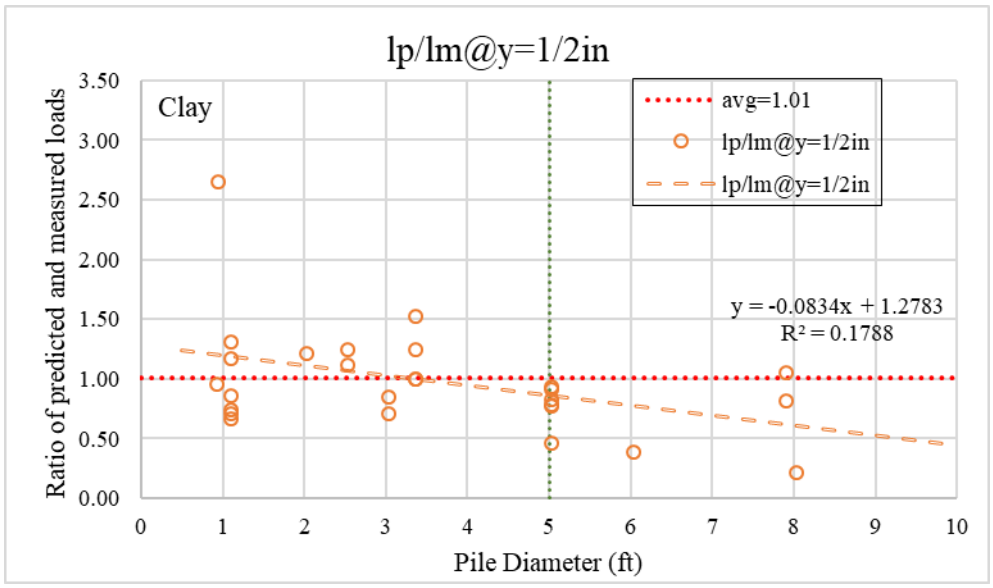

Figure 6-16. Comparison between the Ratio of Predicted and Measured Load versus Pile Diameter at Pile Top Displacement Equals to 0.5 in. in Clay.

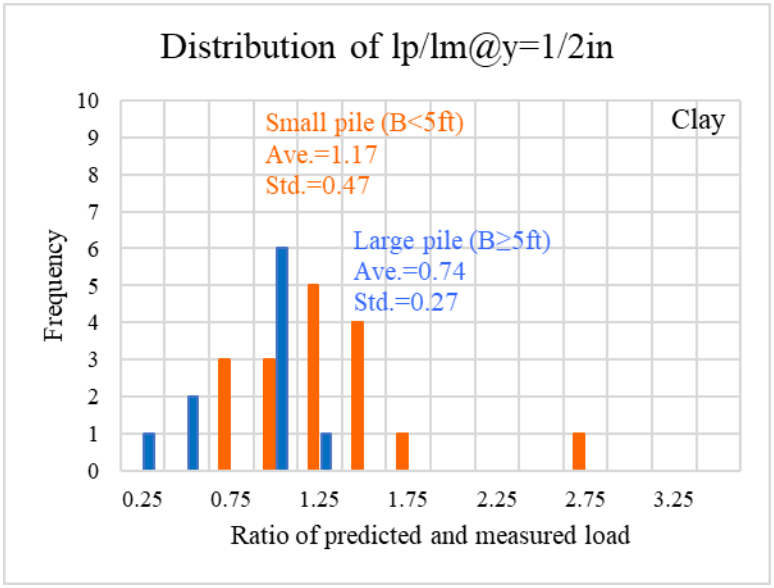

Figure 6-17. Distribution of lp/lm at y = ½ in. in Clay.

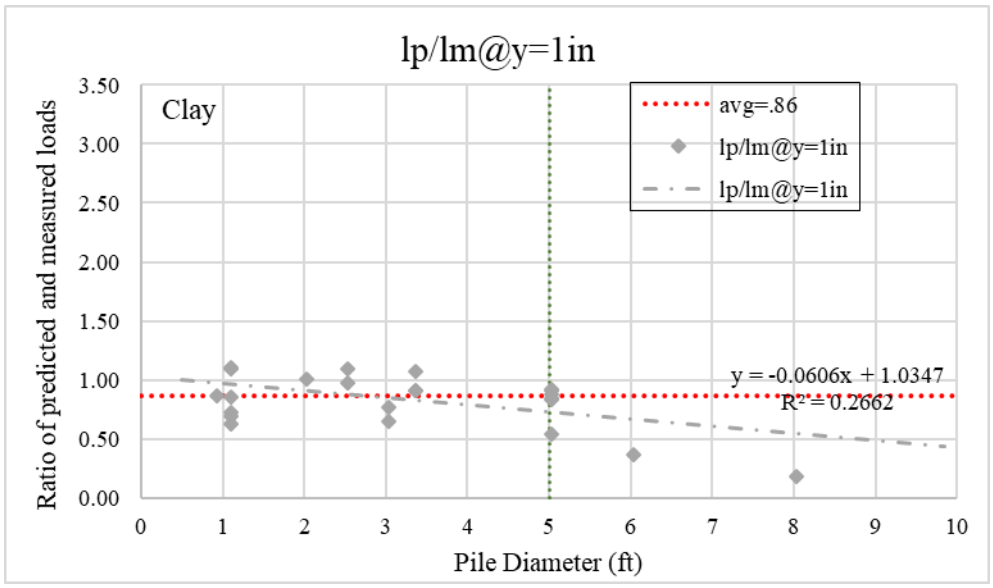

Figure 6-18. Comparison between the Ratio of Predicted and Measured Load versus Pile Diameter at Pile Top Displacement Equals to 1.0 in. in Clay.

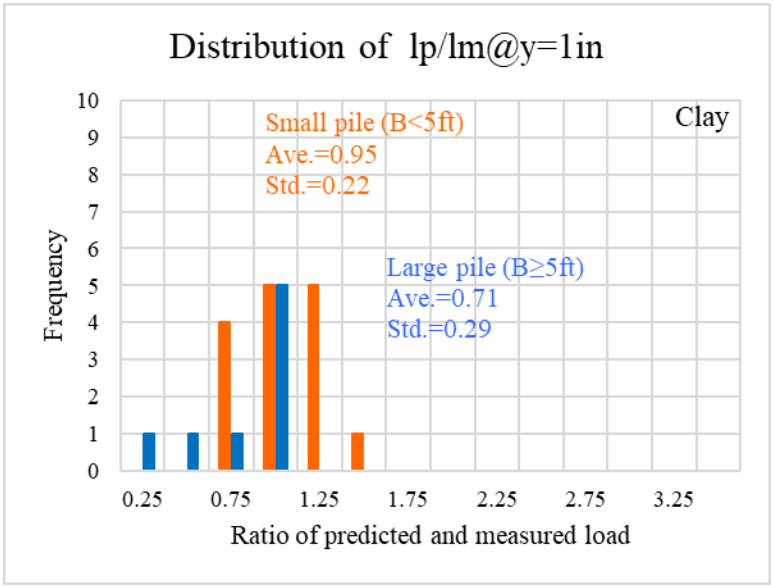

Figure 6-19. Distribution of lp/lm at y =1 in. in Clay.

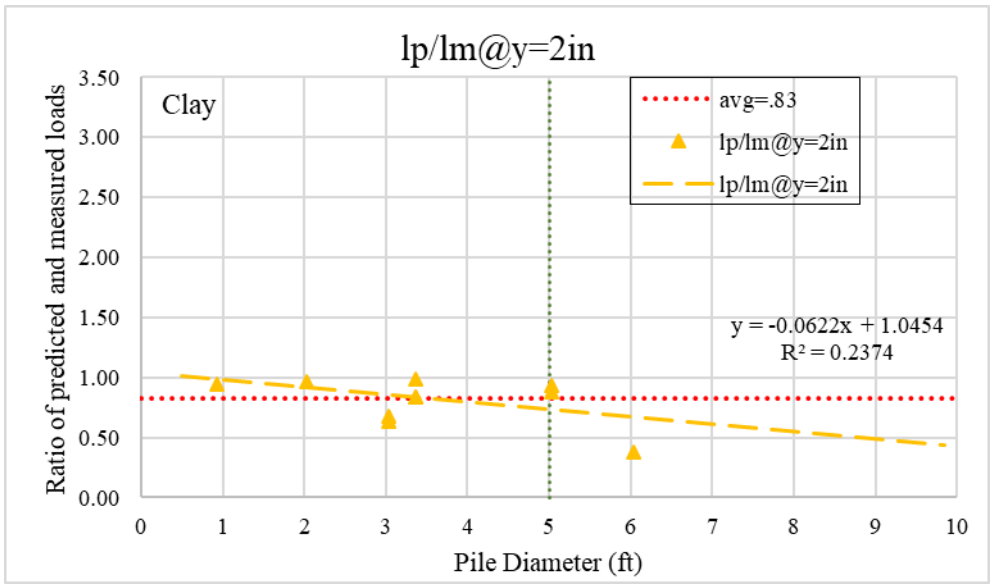

Figure 6-20. Comparison between the Ratio of Predicted and Measured Load versus Pile Diameter at Pile Top Displacement Equals to 2.0 in. in Clay.

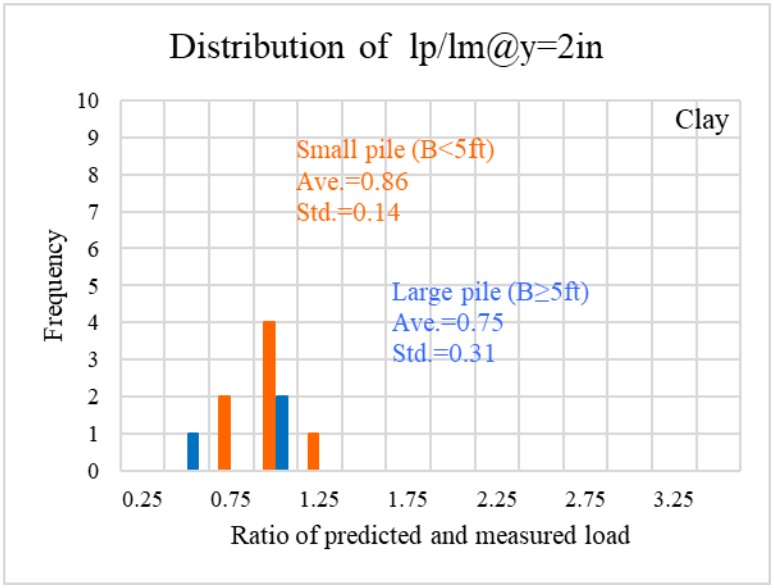

Figure 6-21. Distribution of lp/lm at y = 2 in. in Clay.

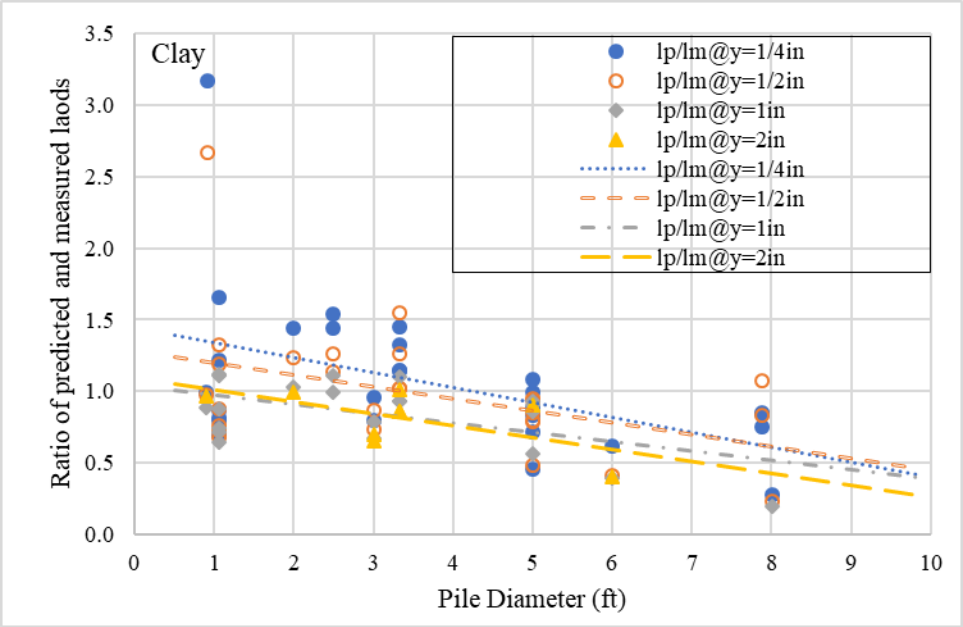

Figure 6-22. Comparison between the Ratio of Predicted and Measured Load versus Pile Diameter at Pile Top Displacement Equals to 0.25, 0.5, 1.0 in., and 2.0 in. in Clay.

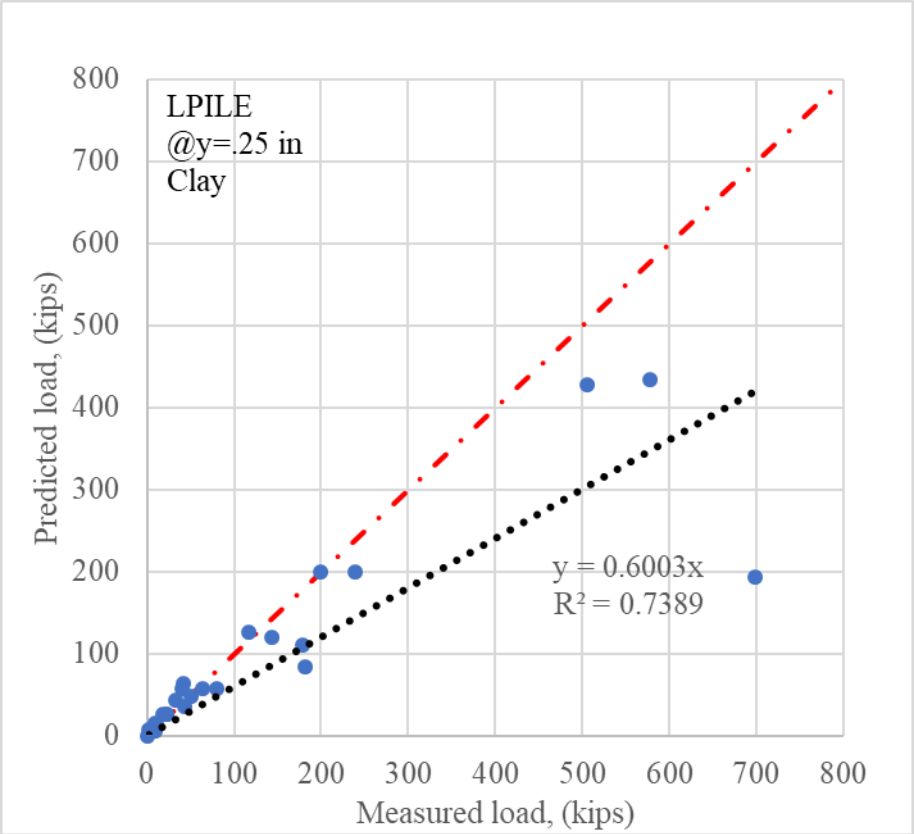

Figure 6-23. LPILE Predictions versus Measurements at Pile Top Displacement Equals to 0.25 in. in Clay.

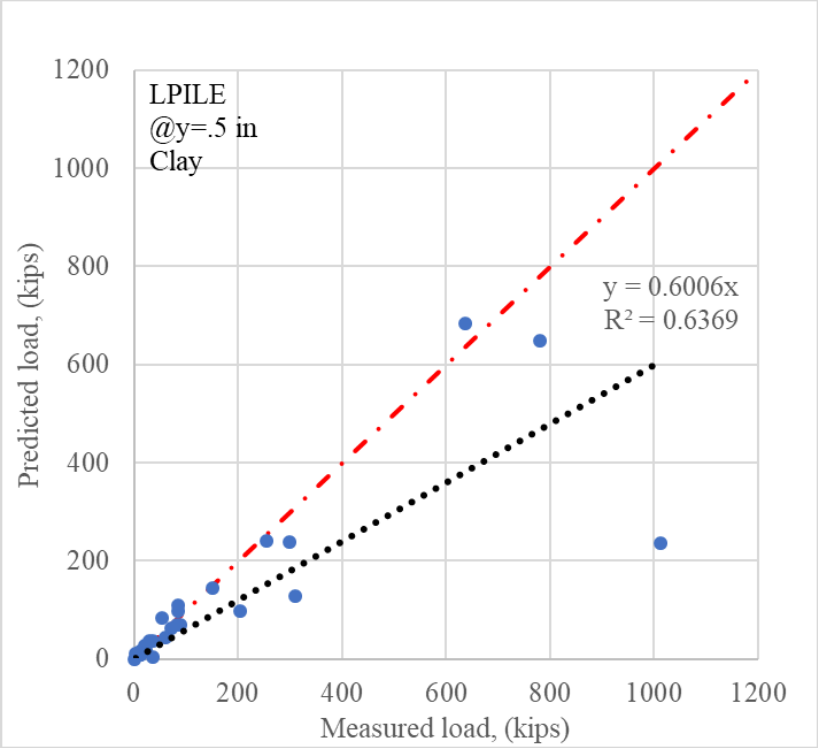

Figure 6-24. LPILE Predictions versus Measurements at Pile Top Displacement Equals to 0.5 in. in Clay.

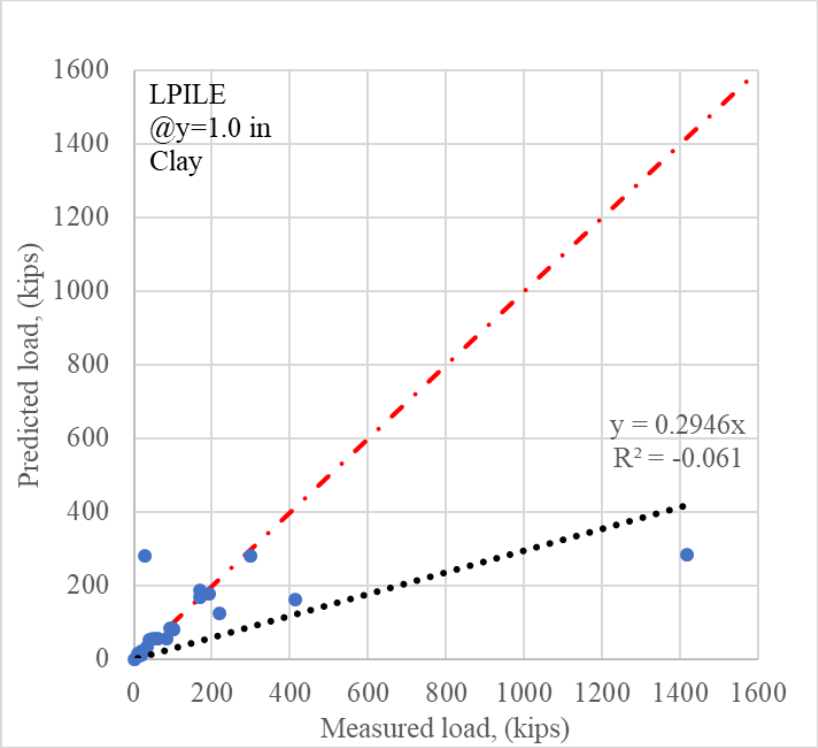

Figure 6-25. LPILE Predictions versus Measurements at Pile Top Displacement Equals to 1.0 in. in Clay.

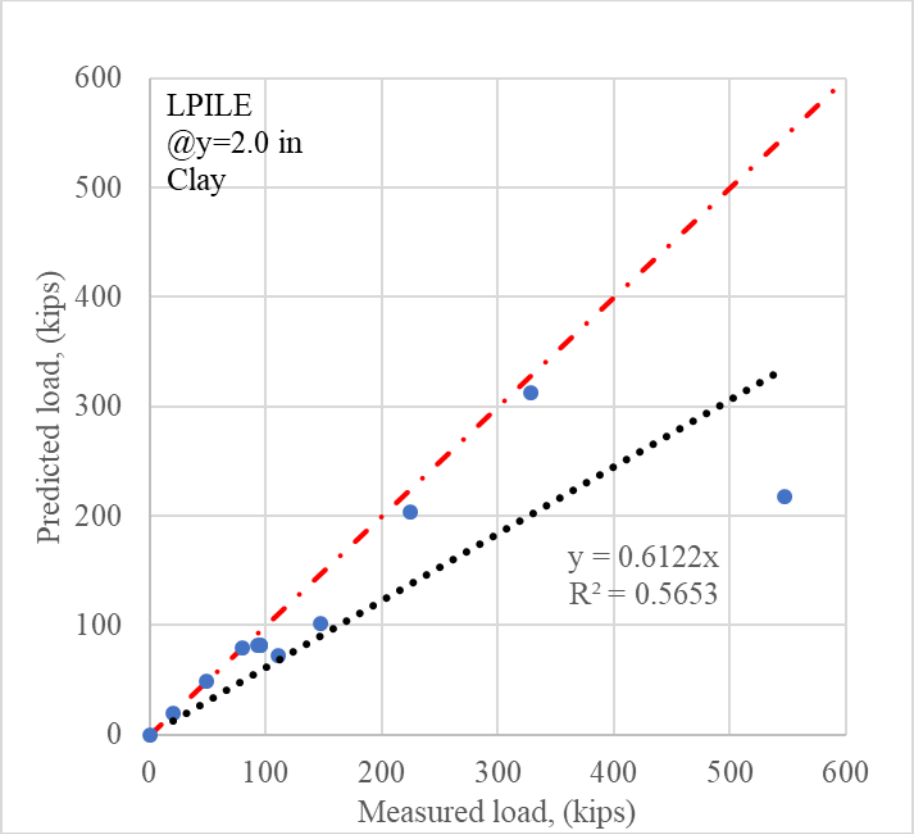

Figure 6-26. LPILE Predictions versus Measurements at Pile Top Displacement Equals to 2.0 in. in Clay.

6.3.3 Comparison of Deflections in Sand

The two previous sections presented the results of comparisons of predicted loads for given deflections varying from 0.25 to 2 in. This section presents the results of comparisons of predicted deflections for given percentages of the ultimate load H_{ou}. These percentages were set at 10 percent, 25 percent, 33 percent, and 50 percent of the ultimate lateral load H_{ou}. The ultimate load was taken as the load corresponding to a pile-head lateral displacement of 0.1B where B is the pile diameter (Briaud, 2013). Some of the load tests did not reach a deflection equal to 0.1B. In those cases, a hyperbola was fit to the load H_o versus deflection y data and used to extrapolate the deflection to 0.1B, thus obtaining the ultimate capacity H_{ou}. Sometimes the measured load-deflection curve did not require any extrapolation to obtain the ultimate load because the largest displacement was larger or equal to B/10 (e.g., Figure 6-27). Sometimes, the largest displacement was less than B/10 but not very far from it, and the extrapolation was reasonable (e.g., Figure 6-30). Sometimes the largest displacement was much smaller than B/10, and the extrapolation while needed was not reasonable (e.g., Figure 6-28). An arbitrary threshold of B/30

was set to decide whether to use an extrapolation or not. Overall, there were 39 cases out of the 89 cases that did not need any extrapolation (31 for the small diameter piles and 8 for large diameter piles). A total of 25 cases out of 89 cases (7 for small pile and 18 for large diameter pile) was not extrapolated for lack of confidence (maximum displacement less than B/30). Table 6-1 summarizes the extrapolation cases. Note that all load tests could still be used for load comparisons at given deflections as shown in the previous section.

The selected equation for the extrapolation hyperbola was:

$$H_0 = \frac{y}{a + by} \tag{40}$$

Or

$$\frac{y}{H_0} = a + by \tag{41}$$

The Inner Belt Bridge load test (RN: 1) is used as an example. Figure 4-54(b) shows the curve of the lateral load H_o versus lateral deflection y. The maximum applied load was 800 kips, and the corresponding deflection at the pile top was 4.6 in. The pile diameter was 6 ft or 72 in., which means that the ultimate load would correspond to a deflection of 7.2 in. The following process was followed to extrapolate the curve:

1. Calculate the ratio y/H_o for all the data points available where y is the pile head deflection and H_o is the applied lateral load.
2. Plot y/Ho versus y as shown in Figure 6-29.
3. Find the best fit linear regression to find the constants a and b in Equation (40) and (41).
4. Use the values of a and b in the hyperbola equation to generate the curve shown in Figure 6-30.
5. Find the ultimate capacity H_{ou} at a pile head displacement of 0.1B as shown in Figure 6-30.

Once the ultimate lateral load H_{ou} was determined either by reading the curve or using the extrapolation technique, the measured values of deflections at loads equal to 10 percent, 25 percent, 33 percent, and 50 percent of H_{ou} could be obtained.

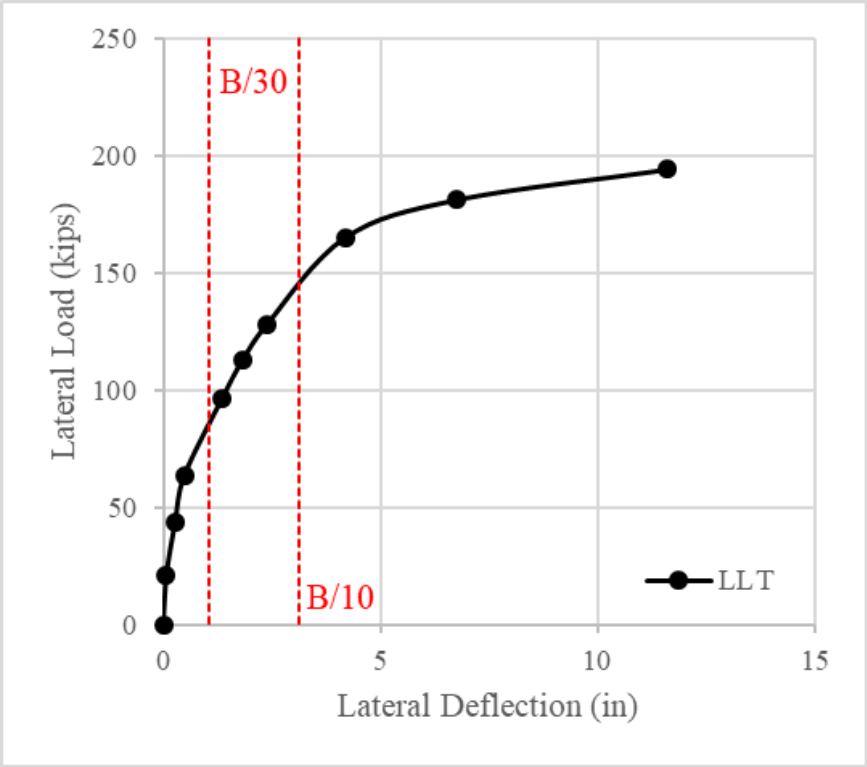

Figure 6-27. Extrapolation Not Needed (RN: 3).

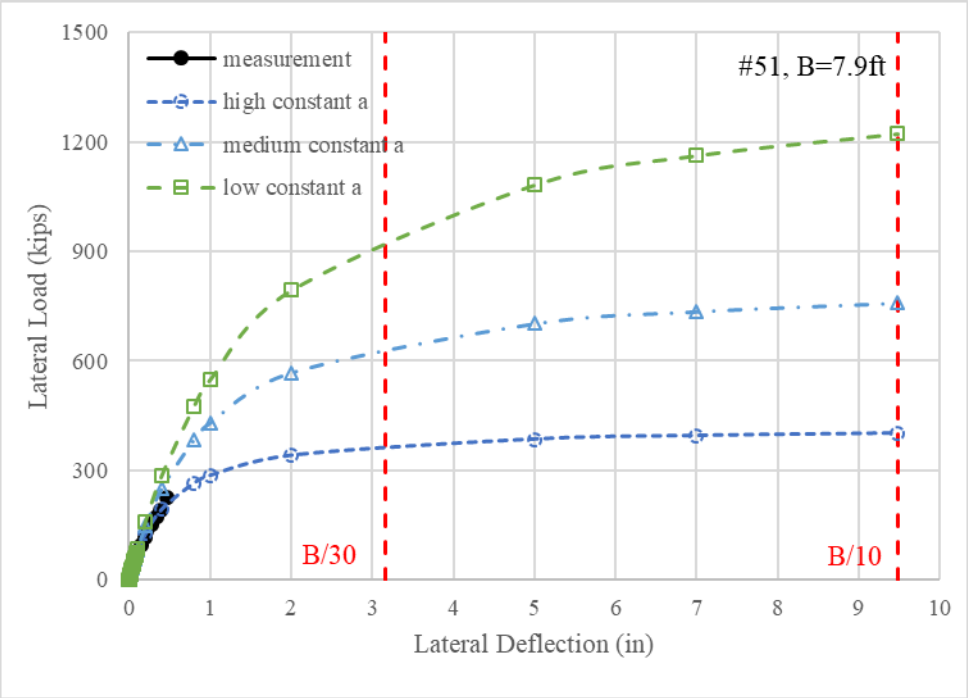

Figure 6-28. Extrapolation Needed but Not Reasonable (RN: 51).

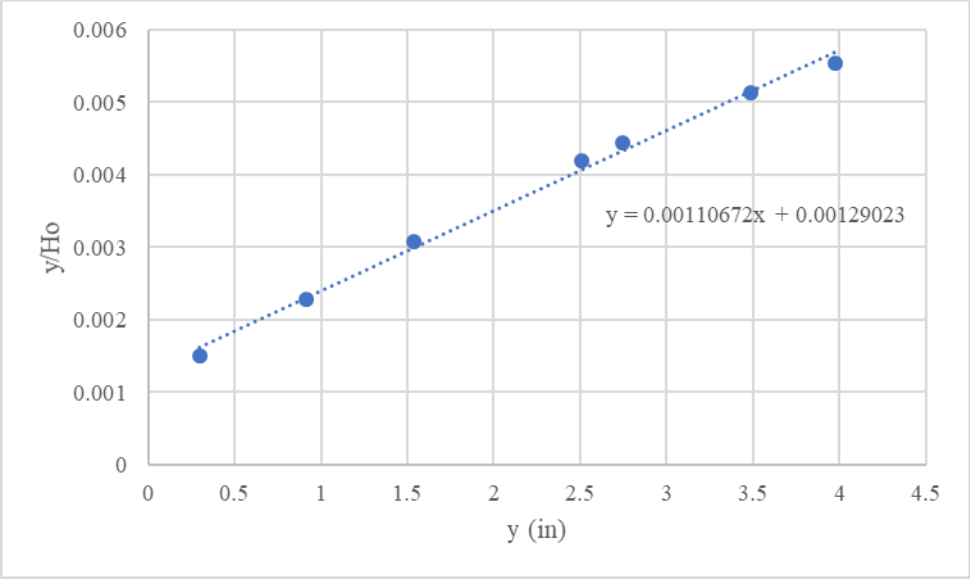

Figure 6-29. y/Ho versus y of Inner Belt Bridge Case (RN: 1).

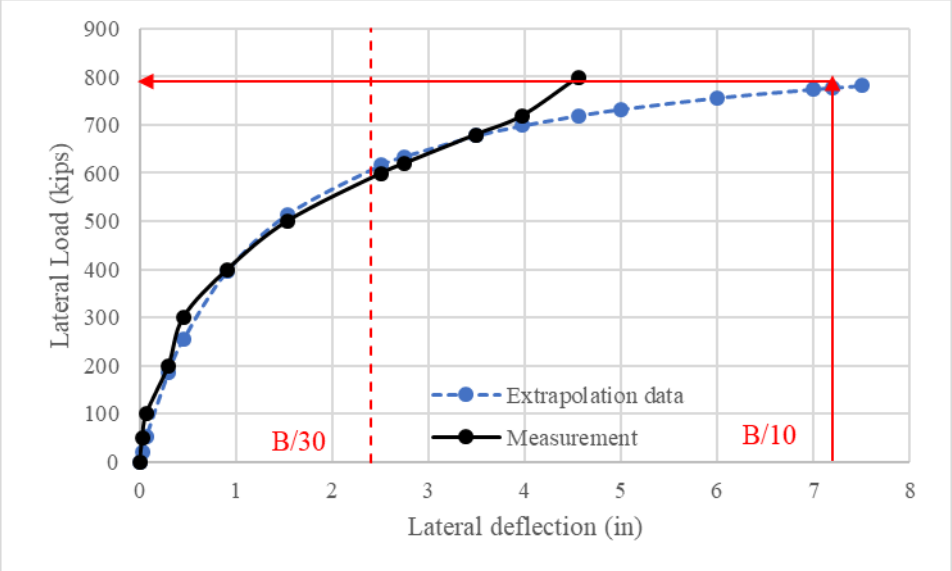

Figure 6-30. Extrapolation Curve versus Field Test Data of Inner Belt Bridge Case (RN: 1); Extrapolation Reasonable.

Table 6-1. Extrapolation Categories.

	Sand		Clay	
	B < 5 ft	B ≥ 5 ft	B < 5 ft	B ≥ 5 ft
Extrapolation not needed	17	6	14	2
Extrapolation needed and reasonable	8	3	7	7
Extrapolation needed but unreasonable	7	15	0	3
Total	31	25	21	12

The deflections were then compared to the predicted deflections using LPILE and the P-y curves. Figure 6-31, Figure 6-33, Figure 6-35, and Figure 6-37 show the ratio of the predicted deflection y_p over the measured deflection y_m as a function of the pile diameter. The average ratios are 2.11, 1.96, 1.85, and 1.71 for the 10 percent, 25 percent, 33 percent, and 50 percent of the ultimate load, respectively. The data show that the predicted deflections are typically very over predicted for small diameter piles but that the predicted deflections get much closer to the measured deflections for the larger pile diameter (~ 8 to 10 ft). Figure 6-39 shows the ratio of y_p/y_m and the pile diameter for the four different load levels. Figure 6-32, Figure 6-34, Figure 6-36, and Figure 6-38 show the frequency distribution curves of the ratio of predicted deflection y_p over measured deflection y_m in sand. The R^2 of the comparisons between predicted and measured deflections at given loads vary from 0.08 to 0.14 indicating significant scatter. These R^2 values are lower to much lower than the R^2 values for the comparisons between predicted and measured loads at given deflections. This shows that the prediction of load at given deflections is better than the prediction of deflection at given loads. Overall one can expect to have a y_p/y_m ratio between 0.2 and 5 for piles in sand with the range narrowing down for large diameter piles. Again, these results are for piles in sand.

Figure 6-40, Figure 6-41, Figure 6-42, and Figure 6-43 show the predicted versus measured deflection at loads equal to 10 percent, 25 percent, 33 percent, and 50 percent of the ultimate load, respectively, for piles in sand. They confirm the observations made on the predicted versus measured load ratio.

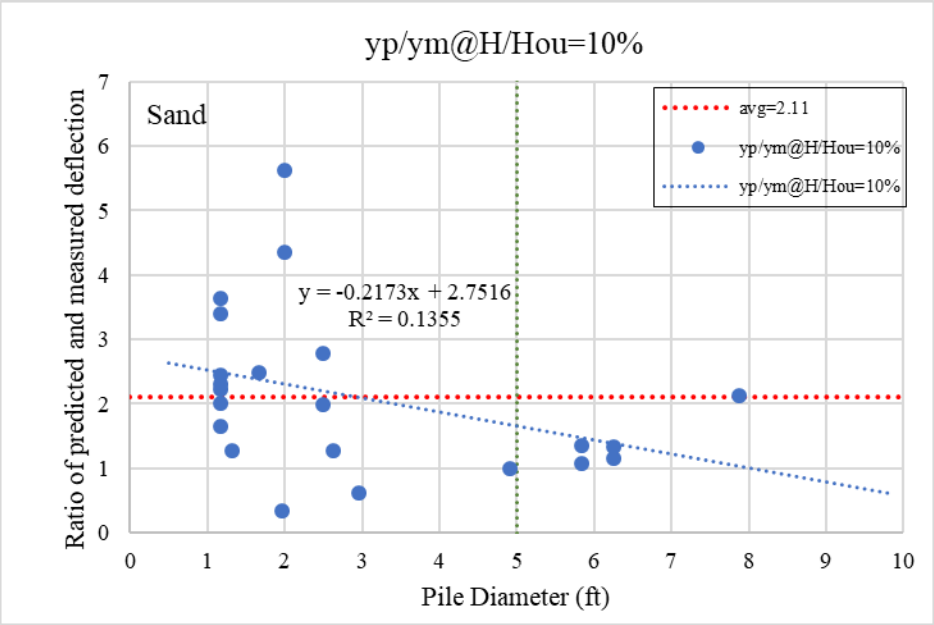

Figure 6-31. Comparison between the Ratio of Predicted and Measured Deflection versus Pile Diameter at Applied Load Equals to 10 Percent of the Ultimate Lateral Load in Sand.

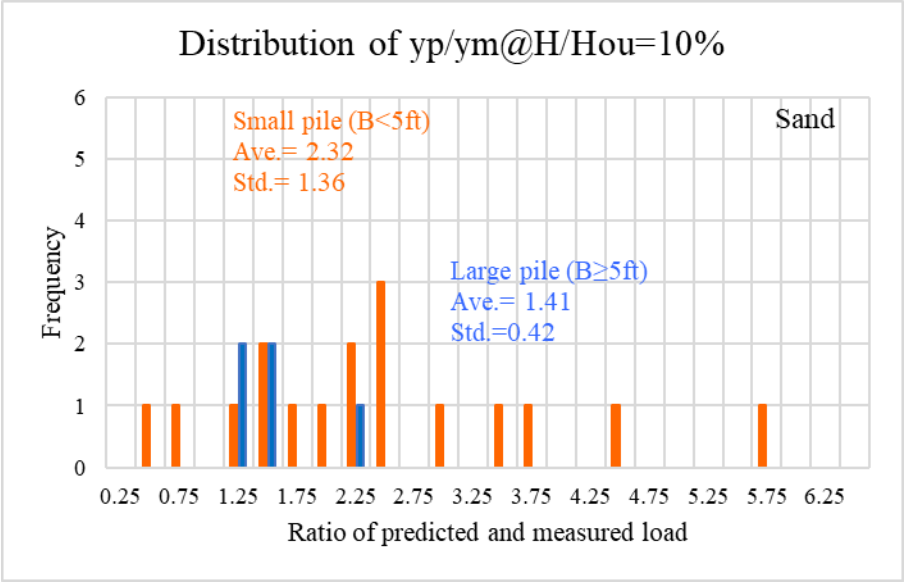

Figure 6-32. Distribution of y_p/y_m at H/H_{ou} Equals to 10 Percent in Sand.

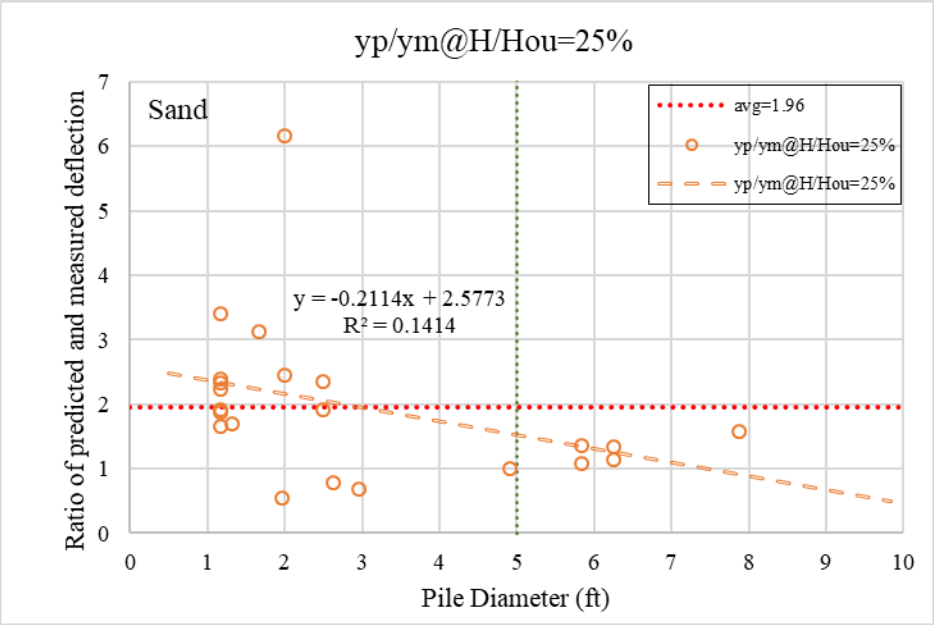

Figure 6-33. Comparison between the Ratio of Predicted and Measured Deflection versus Pile Diameter at Applied Load Equals to 25 Percent of the Ultimate Lateral Load in Sand.

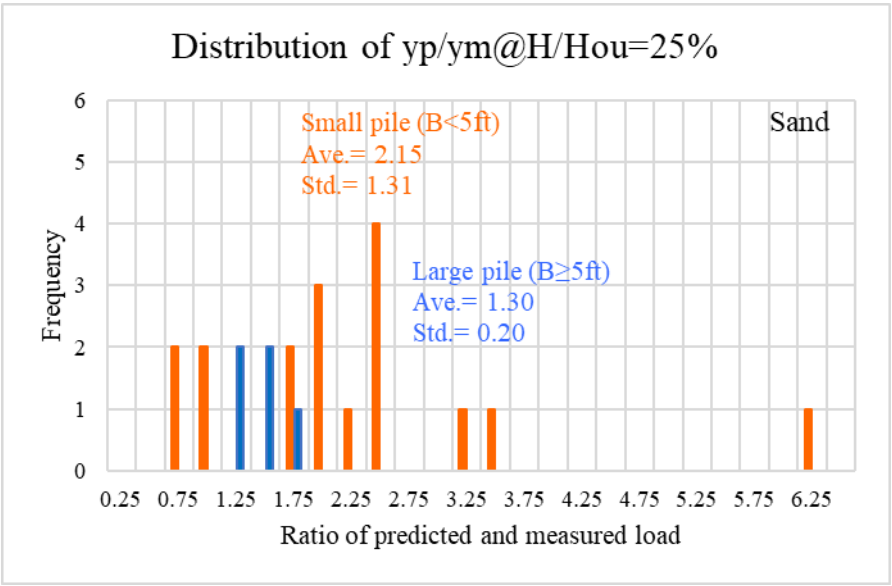

Figure 6-34. Distribution of y_p/y_m at H/H_{ou} Equals to 25 Percent in Sand.

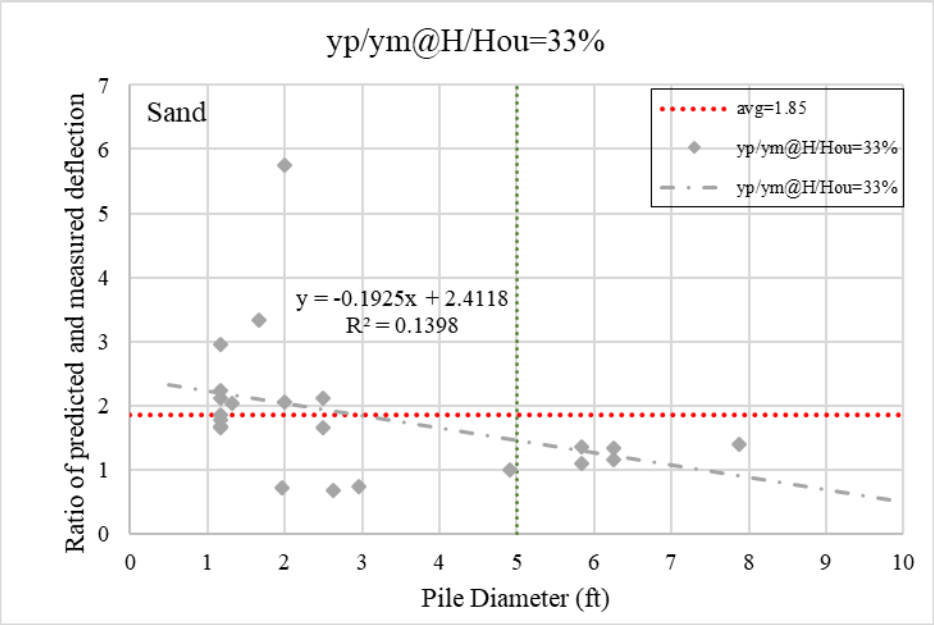

Figure 6-35. Comparison between the Ratio of Predicted and Measured Deflection versus Pile Diameter at Applied Load Equals to 33 Percent of the Ultimate Lateral Load in Sand.

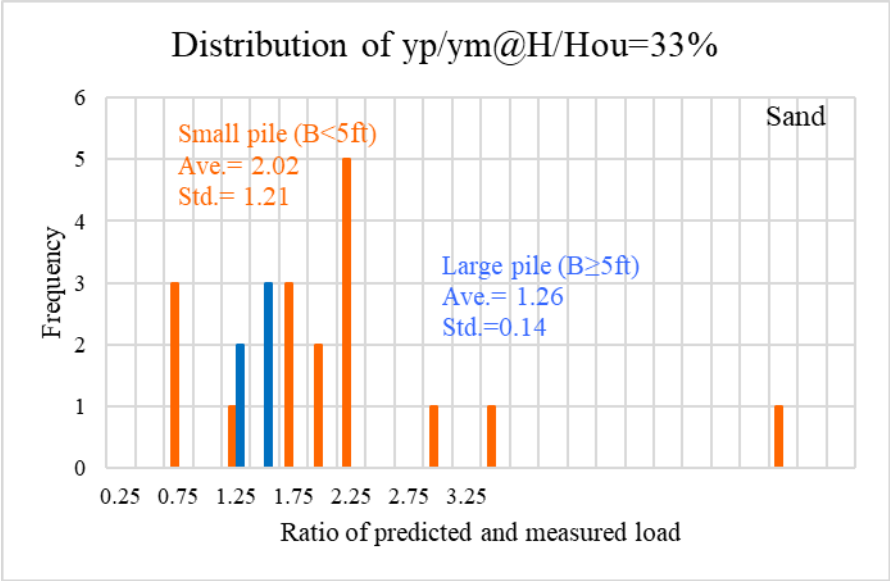

Figure 6-36. Distribution of y_p/y_m at H/H_{ou} Equals to 33 Percent in Sand.

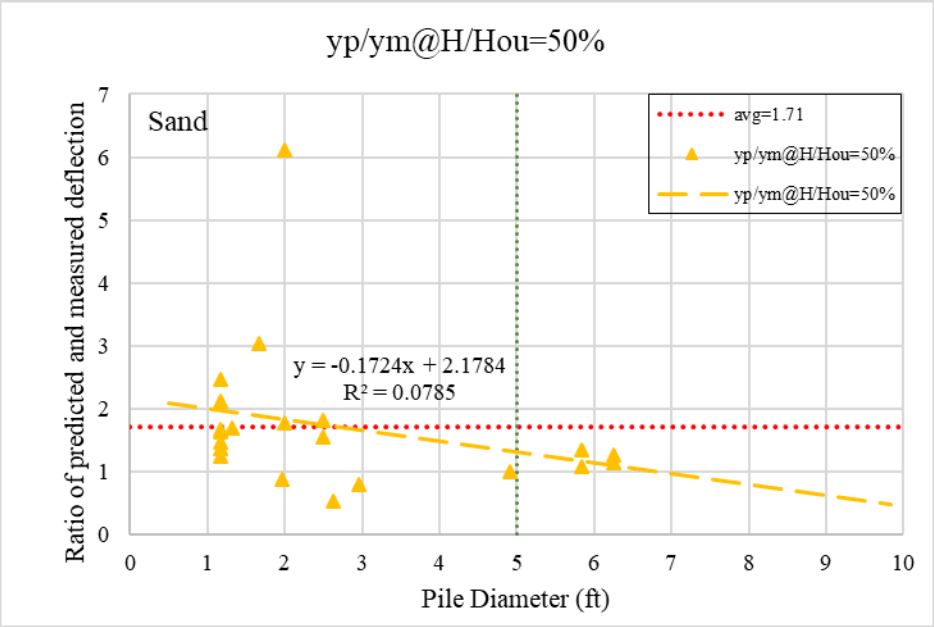

Figure 6-37. Comparison between the Ratio of Predicted and Measured Deflection versus Pile Diameter at Applied Load Equals to 50 Percent of the Ultimate Lateral Load in Sand.

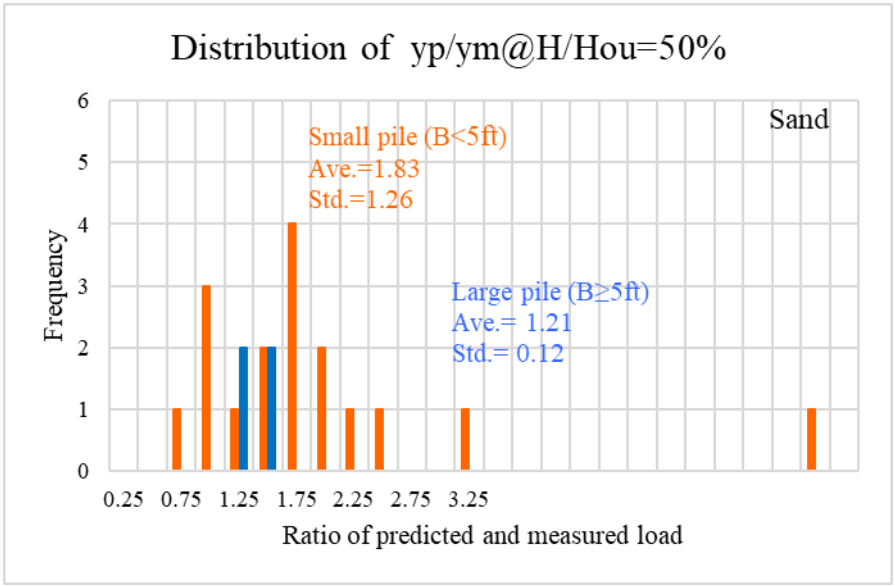

Figure 6-38. Distribution of y_p/y_m at H/H_{ou} Equals to 50 Percent in Sand.

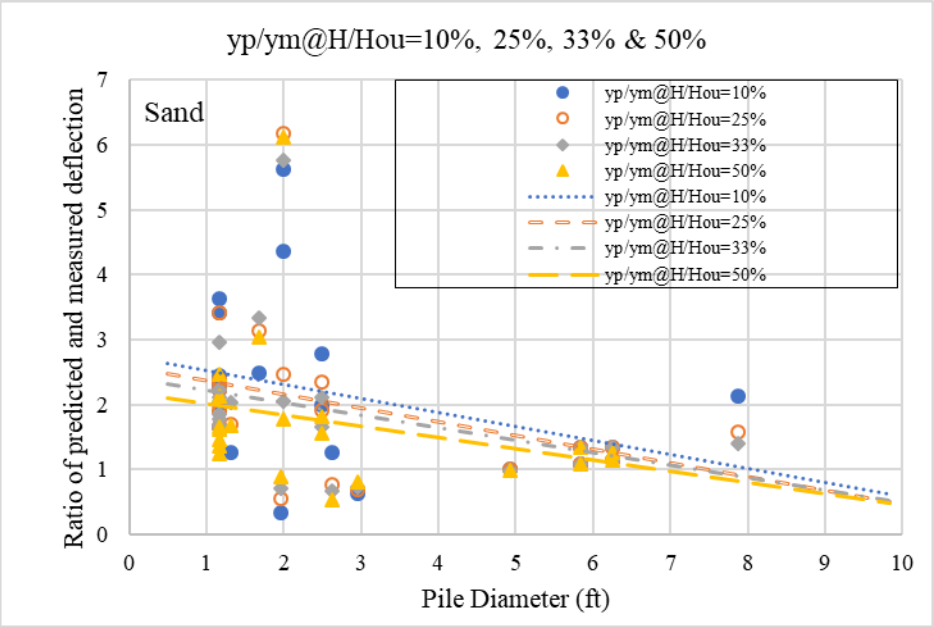

Figure 6-39. Comparison between the Ratio of Predicted and Measured Deflection versus Pile Diameter at Applied Load Equals to 10 Percent, 25 Percent, 33 Percent, and 50 Percent of the Ultimate Lateral Load in Sand.

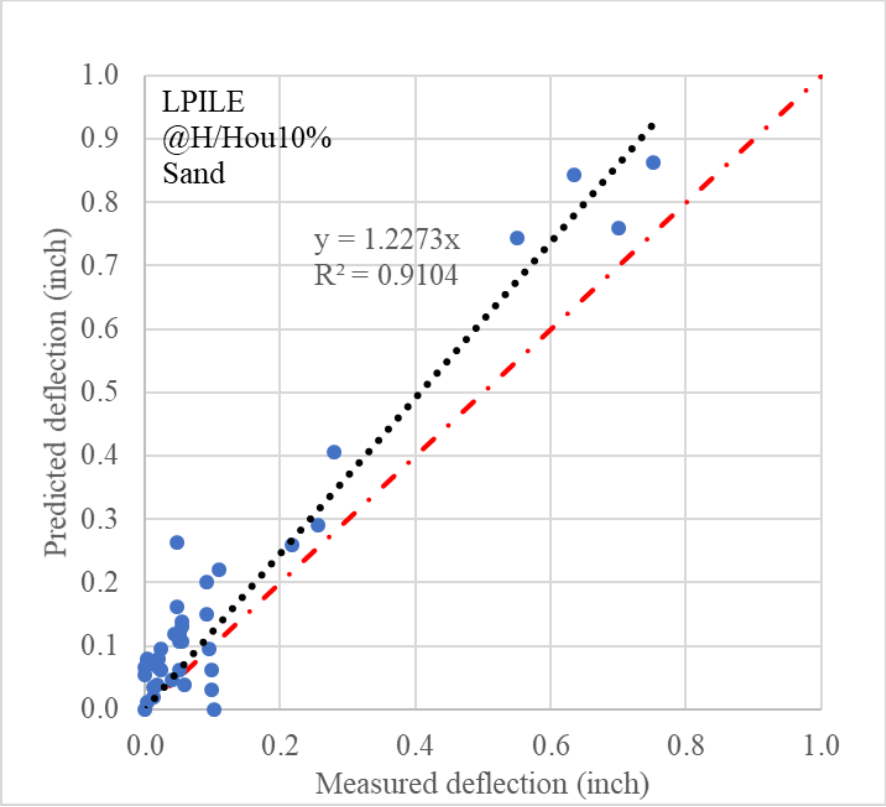

Figure 6-40. The LPILE Predicted versus Measured Deflection at Loads Equal to 10 Percent of the Ultimate Load in Sand.

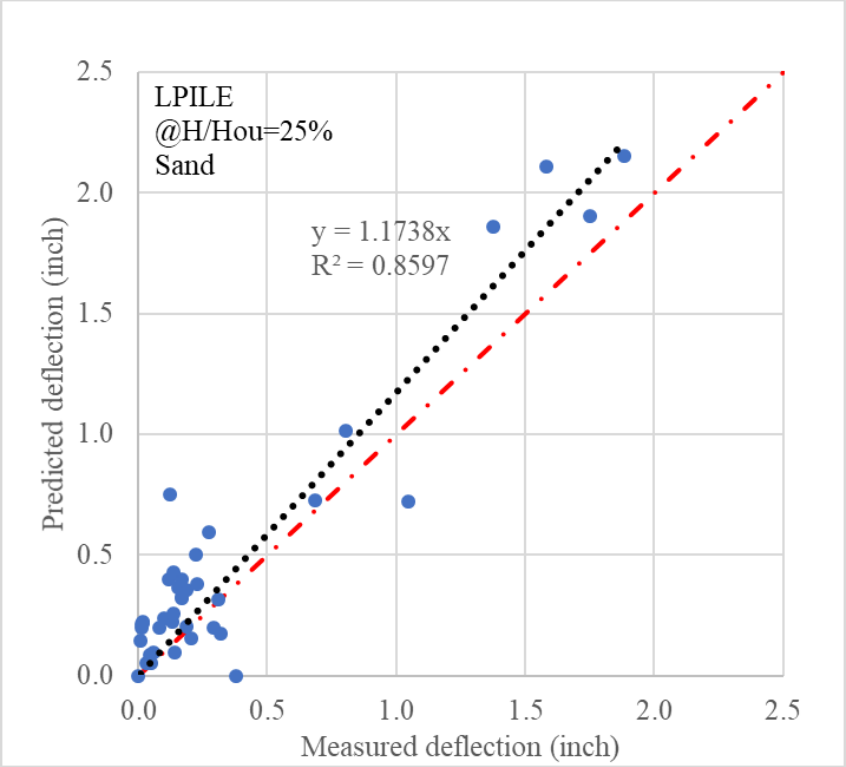

Figure 6-41. The LPILE Predicted versus Measured Deflection at Loads Equal to 25 Percent of the Ultimate Load in Sand.

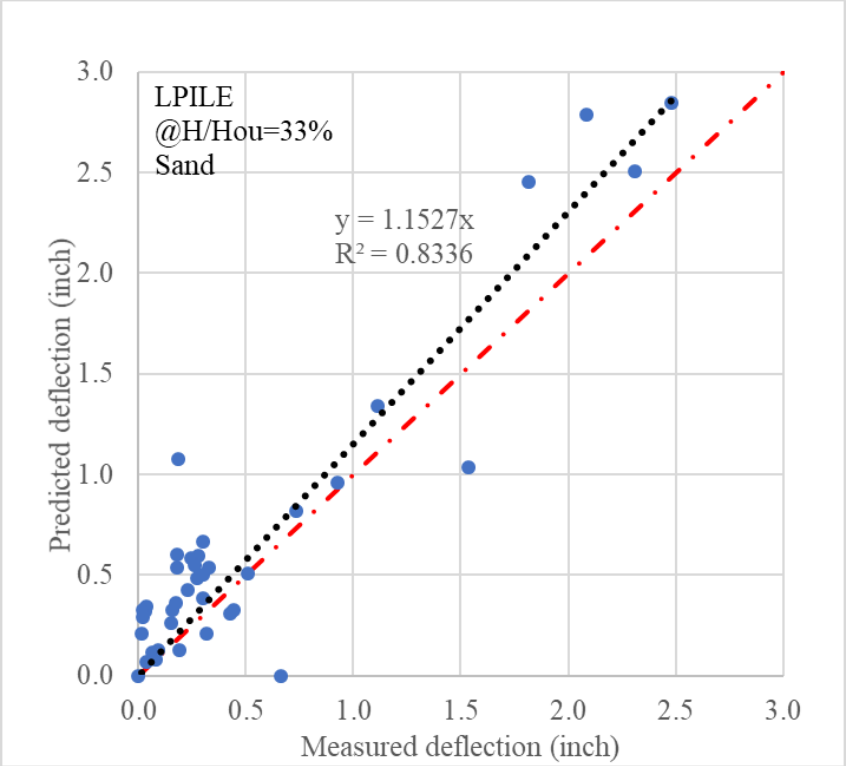

Figure 6-42. The LPILE Predicted versus Measured Deflection at Loads Equal to 33 Percent of the Ultimate Load in Sand.

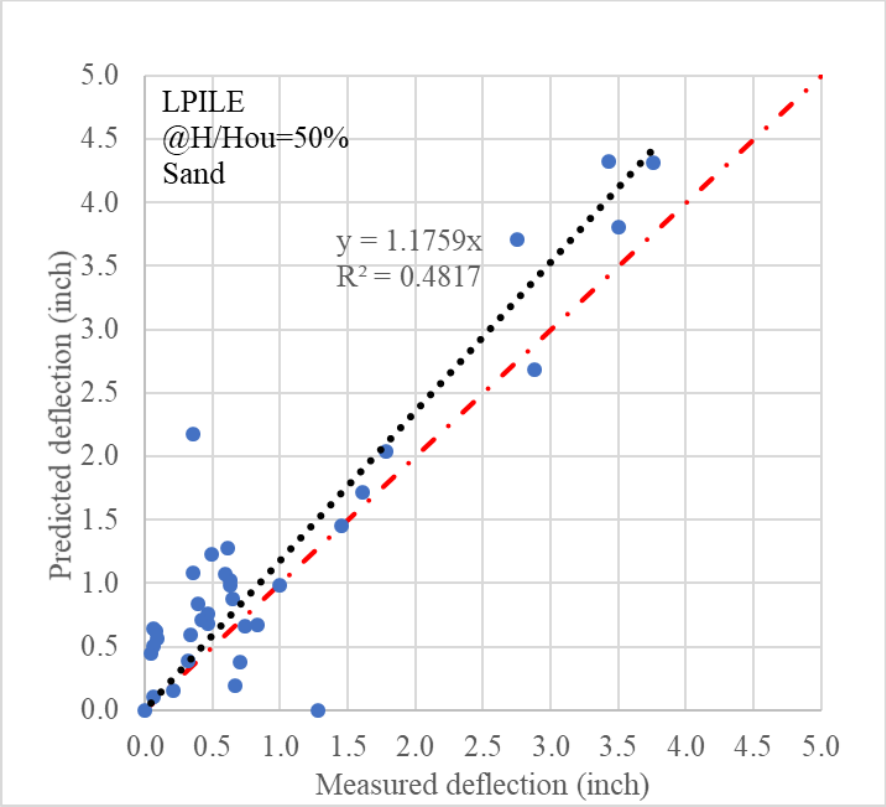

Figure 6-43. The LPILE Predicted versus Measured Deflection at Loads Equal to 50 Percent of the Ultimate Load in Sand.

6.3.4 Comparison of Deflections in Clay

This section presents the results of comparisons between predicted and measured deflections in clay at given percentages of the ultimate load H_{ou}. These percentages were set at 10 percent, 25 percent, 33 percent, and 50 percent of the ultimate lateral load H_{ou}. The ultimate load capacity was taken as the load corresponding to a pile-head lateral displacement of 0.1B where B is the pile diameter (Briaud, 2013). Some of the load tests did not reach a deflection equal to 0.1B. In those cases, a hyperbola was fit to the load H_o versus deflection y data and used to extrapolate the deflection to 0.1B as described in the previous section. Once the ultimate lateral load H_{ou} was determined either by reading the curve or using the extrapolation technique, the measured values of deflections at 10 percent, 25 percent, 33 percent, and 50 percent of H_{ou} could be obtained. In clay, the extrapolation technique had to be used a total of 14 times (7 times for small diameter piles and 7 times for large diameter piles) (Table 6-1). The measured deflections were then compared to the predicted deflections using LPILE. Figure 6-44, Figure 6-46, Figure 6-48, and Figure 6-50 show the ratio of the predicted deflection y_p over the

measured deflection y_m as a function of the pile diameter. The average ratio is 1.24, 1.31, 1.47, and 1.63 for the 10 percent, 25 percent, 33 percent, and 50 percent of the ultimate load, respectively. As can be seen, the deflection ratio in clay increases with the pile diameter contrary to the trend in sand. The deflections for smaller piles are reasonably predicted by using the soft clay P-y curve criterion (Matlock, 1970) and the stiff clay P-y curve criterion with no free water (Reese and Welch, 1975) in LPILE. However, for larger diameter piles, the deflections are significantly overpredicted. Figure 6-52 regroups the ratio of y_p/y_m and the pile diameter for the four different load levels. Figure 6-45, Figure 6-47, Figure 6-49, and Figure 6-51 show the frequency distribution curves of the ratio of predicted deflection y_p over measured deflection y_m in clay. The R^2 of the comparisons between predicted and measured deflections at given loads vary from 0.15 to 0.22 indicating significant scatter. These R^2 values are a bit higher than the R^2 values for the comparisons between predicted and measured deflections at given loads in sand. However, they are lower than the R^2 values for the comparisons between predicted and measured deflections at given loads in general. This shows that the prediction of load at given deflections is better than the prediction of deflection at given loads. Overall one can expect to have a y_p/y_m ratio between 0.2 and 3 for piles in clay. Again, these results are for piles in clay.

Figure 6-53, Figure 6-54, Figure 6-55, and Figure 6-56 show the predicted versus measured deflection at loads equal to 10 percent, 25 percent, 33 percent, and 50 percent of the ultimate load, respectively, for piles in clay. They confirm the observations made on the predicted versus measured load ratio.

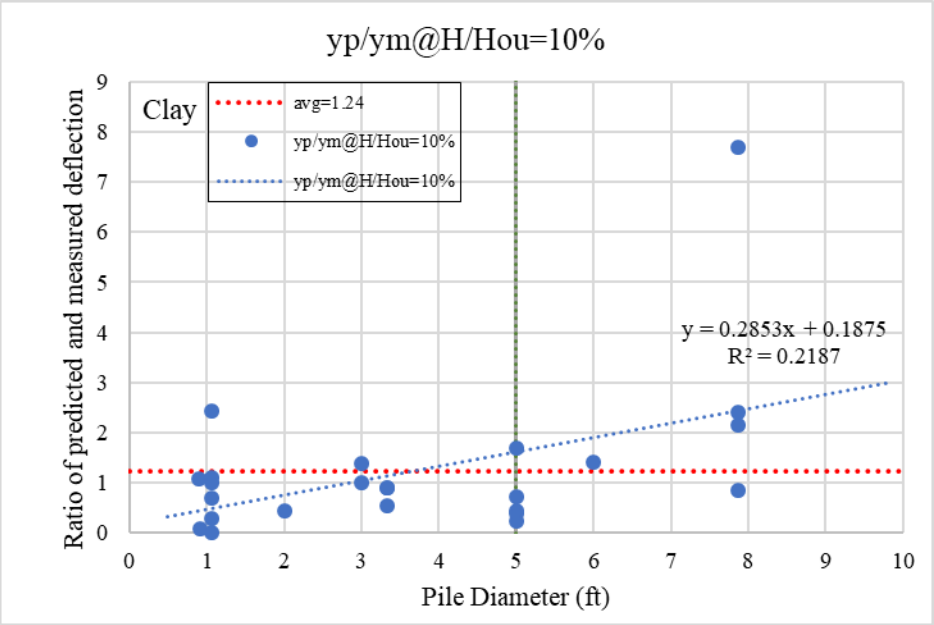

Figure 6-44. Comparison between the Ratio of Predicted and Measured Deflection versus Pile Diameter at Applied Load Equals to 10 Percent of the Ultimate Lateral Load in Clay.

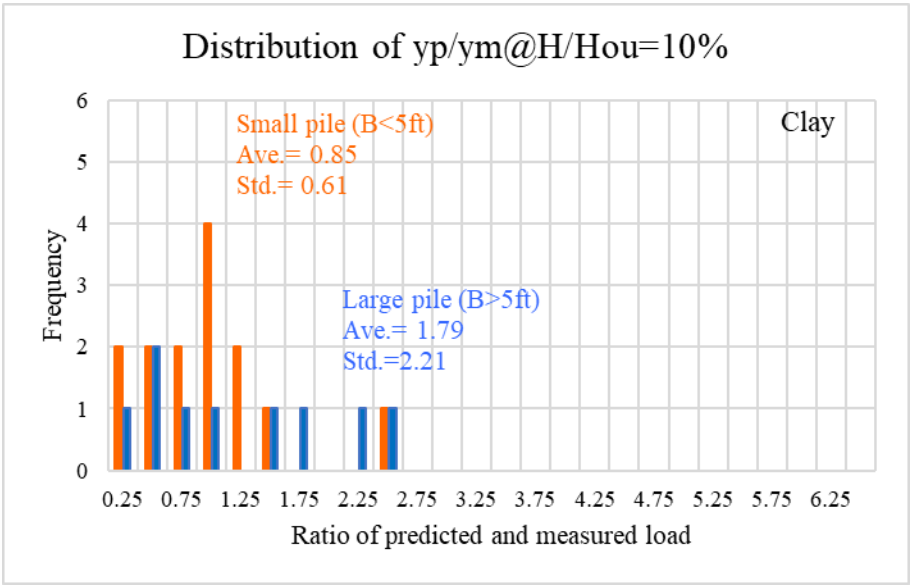

Figure 6-45. Distribution of y_p/y_m at H/H_{ou} Equals to 10 Percent in Clay.

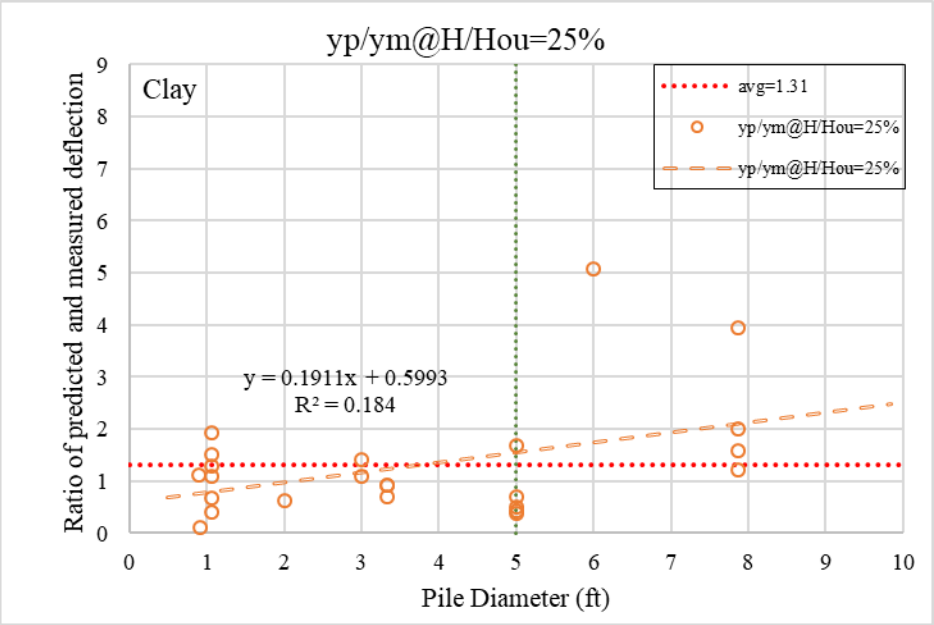

Figure 6-46. Comparison between the Ratio of Predicted and Measured Deflection versus Pile Diameter at Applied Load Equals to 25 Percent of the Ultimate Lateral Load in Clay.

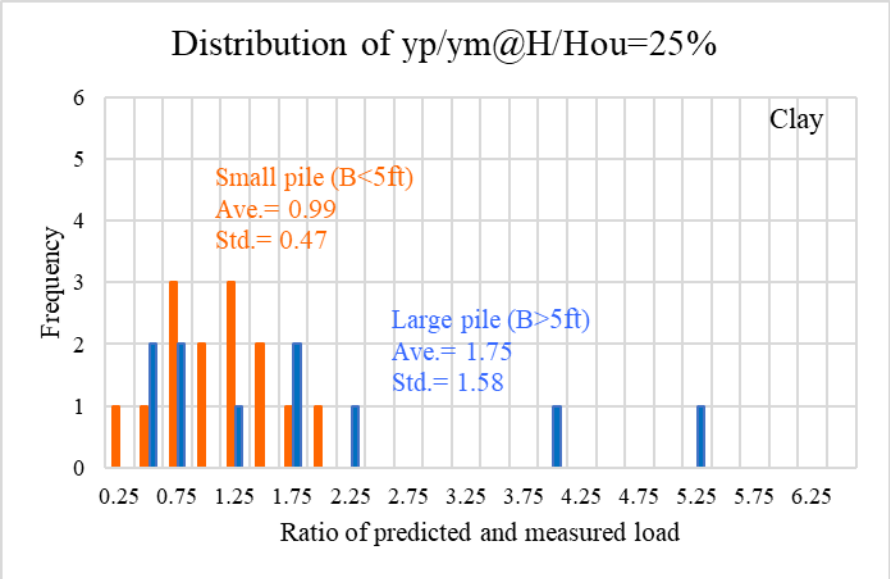

Figure 6-47. Distribution of y_p/y_m at H/H_{ou} Equals to 25 Percent in Clay.

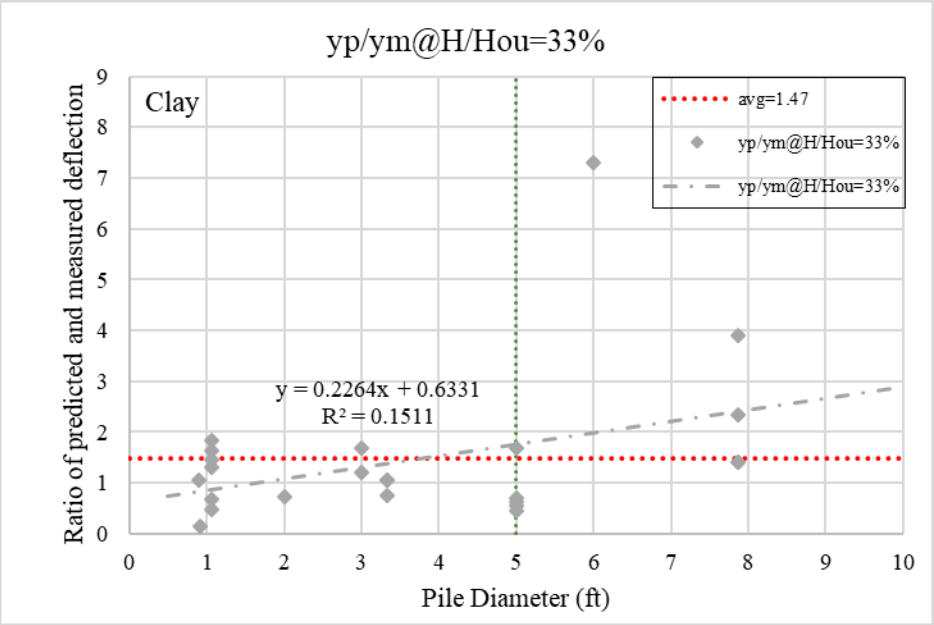

Figure 6-48. Comparison between the Ratio of Predicted and Measured Deflection versus Pile Diameter at Applied Load Equals to 33 Percent of the Ultimate Lateral Load in Clay.

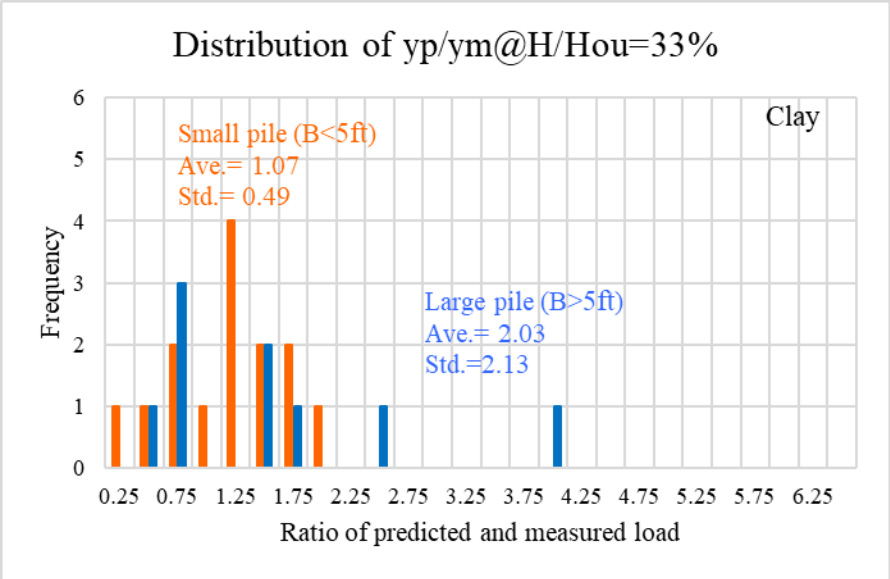

Figure 6-49. Distribution of y_p/y_m at H/H_{ou} Equals to 33 Percent in Clay.

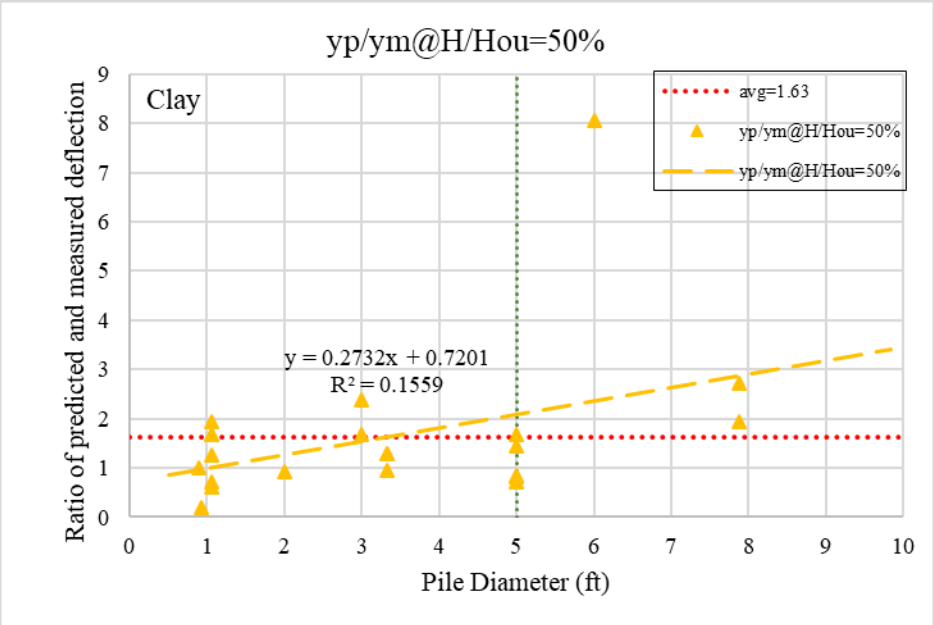

Figure 6-50. Comparison between the Ratio of Predicted and Measured Deflection versus Pile Diameter at Applied Load Equals to 33 Percent of the Ultimate Lateral Load in Clay.

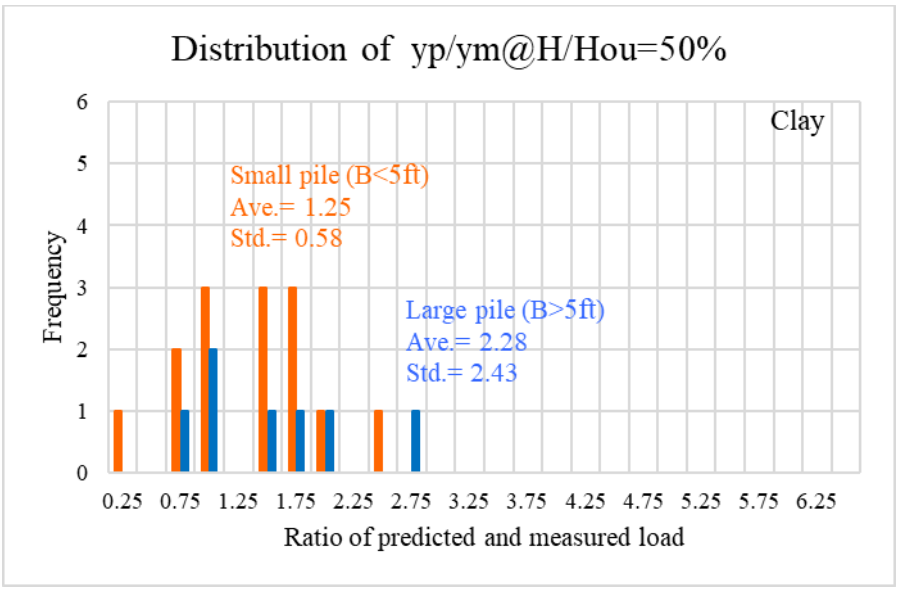

Figure 6-51. Distribution of y_p/y_m at H/H_{ou} Equals to 50 Percent in Clay.

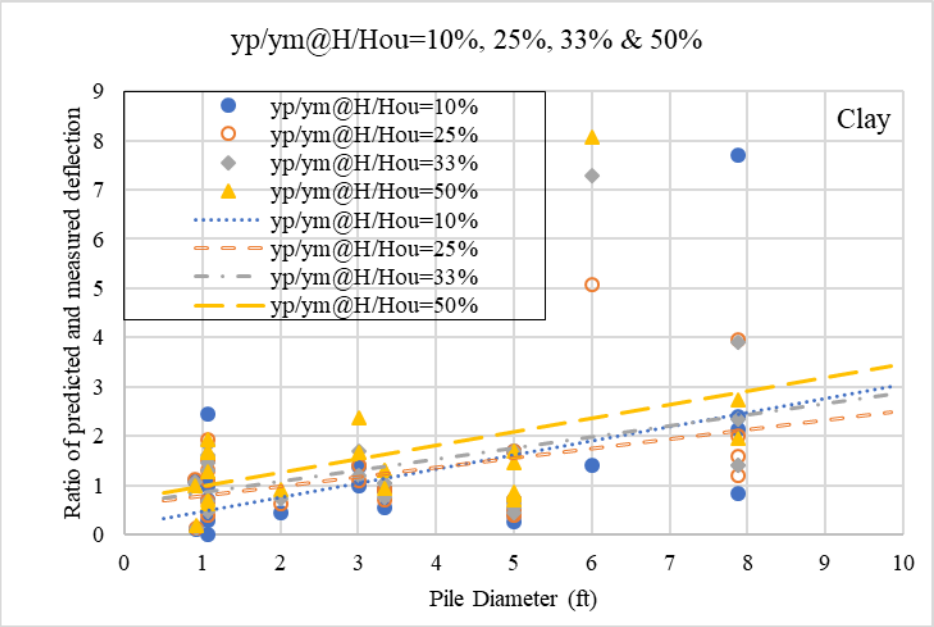

Figure 6-52. Comparison between the Ratio of Predicted and Measured Deflection versus Pile Diameter at Applied Load Equals to 10 Percent, 25 Percent, 33 Percent, and 50 Percent of the Ultimate Lateral Load in Clay.

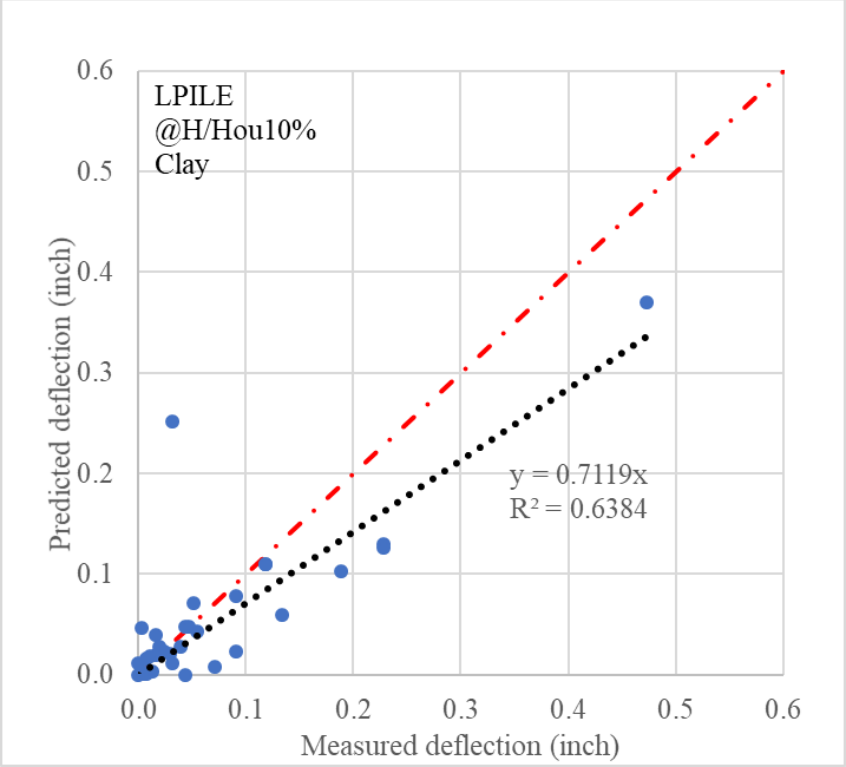

Figure 6-53. The LPILE Predicted versus Measured Deflection at Loads Equal to 10 Percent of the Ultimate Load in Clay.

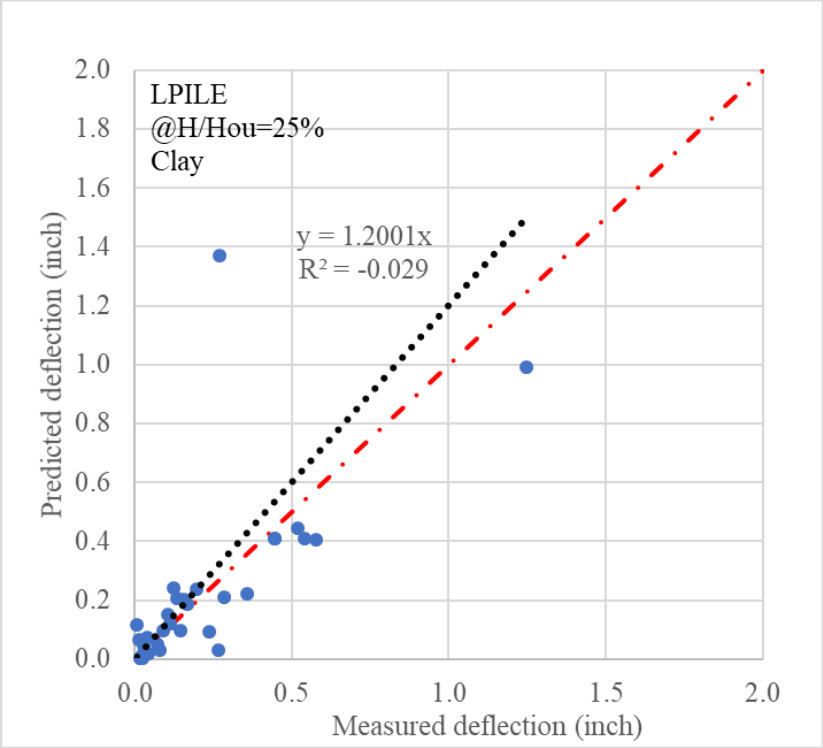

Figure 6-54. The LPILE Predicted versus Measured Deflection at Loads Equal to 25 Percent of the Ultimate Load in Clay.

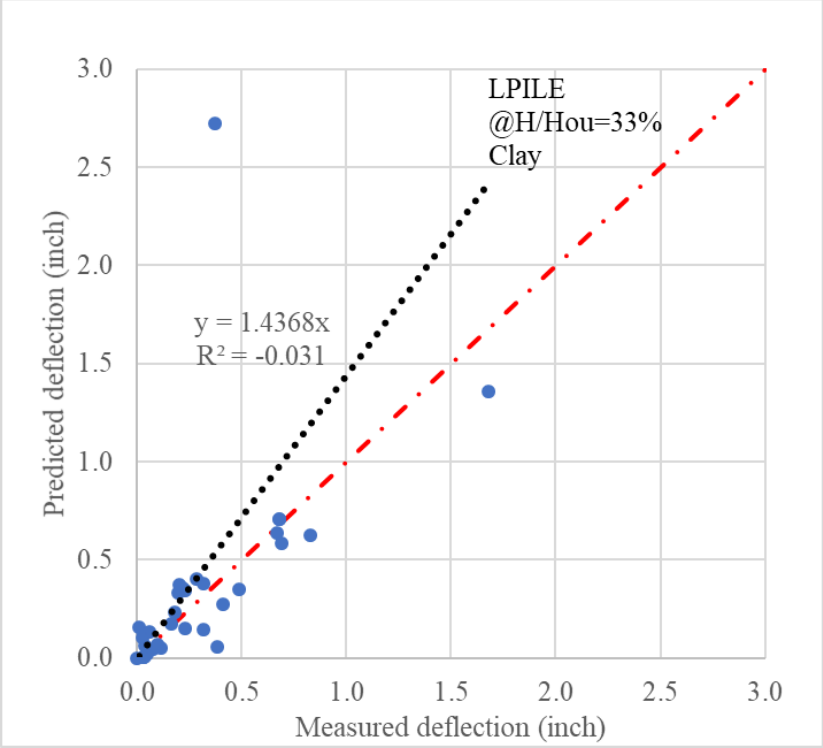

Figure 6-55. The LPILE Predicted versus Measured Deflection at Loads Equal to 33 Percent of the Ultimate Load in Clay.

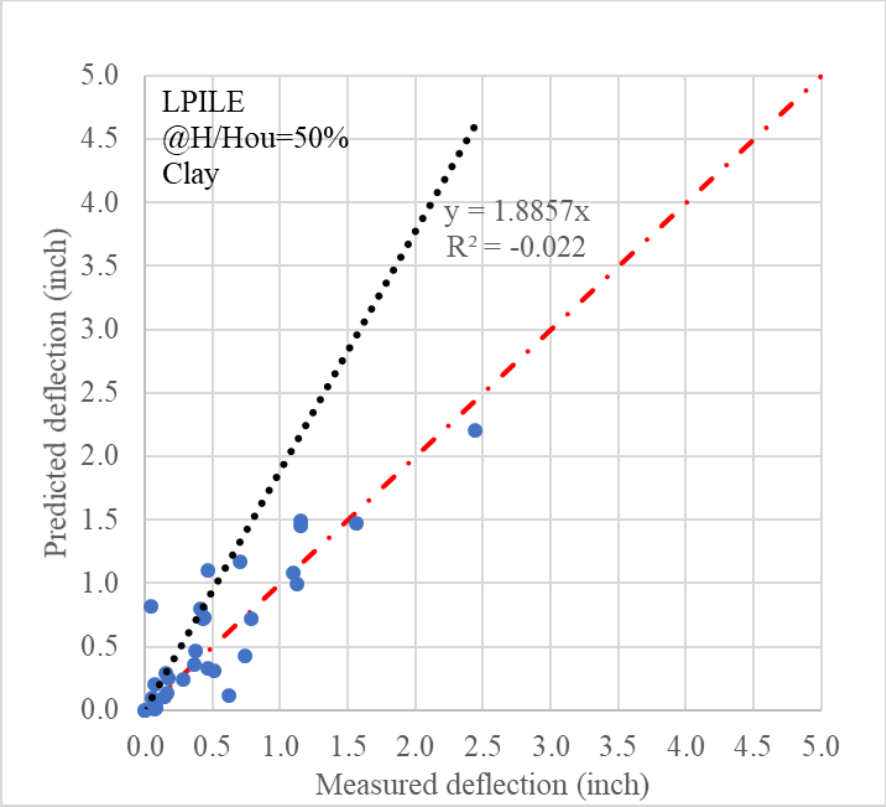

Figure 6-56. The LPILE Predicted versus Measured Deflection at Loads Equal to 50 Percent of the Ultimate Load in Clay.

6.4 THE PREDICTIONS OF SALLOP METHOD AND THE MEASUREMENTS

The measured or extrapolated ultimate lateral capacity of the pile H_{ou} was compared with the predicted value by the SALLOP method (Briaud, 1997). The SALLOP method makes use of the pressuremeter limit pressure p_L as the strength parameter in the calculation. The simple equation to predict H_{ou} is:

$$H_{ou} = \frac{3}{4} P_L B D_v \tag{42}$$

Where

$D_v = \frac{\pi}{4} l_0$, ft (m) for $L > l_0$.

$D_v = \frac{L}{3}$, ft (m) for $L < l_0$.

$l_0 = \left(\frac{4EI}{K}\right)^{0.25}$, ft (m).

p_L = limit pressure from the PMT, psi (kPa).

B = projected pile width, ft (m).

E = modulus of the pile material, psi (kN/m^2).

I = moment of inertia, in^4 (m^4)

K = 2.3 E_o = soil stiffness, psi (kN/m).

E_o = Soil modulus from PMT test, psi (kN/m).

L = length of the pile, ft (m)

H_{ou} = ultimate lateral load, kips (kN)

This semi-theoretical and semi-empirical method was used to predict the ultimate load H_{ou} for 20 full scale lateral load tests on piles. These 20 predictions were compared with the H_{ou} values measured in the 20 full-scale tests (Briaud, 1997). In this project, 7 load test results were added to the original database of 20. Further details about the SALLOP method can be found in Briaud (1997).

Figure 6-57 shows the ratio of the predicted load over the measured load L_p/L_m as a function of the pile diameter; as can be seen, the ratio is close to one for piles with diameter between 2 and 5 ft. Figure 6-58 shows the frequency distribution of that ratio with an average of 1.31 and a coefficient of variation of 0.57. Figure 6-59 shows the comparison between the predicted and measured values of the ultimate capacity H_{ou}. Figure 6-60 shows the same data for the smaller capacity piles only. In general, a very good agreement is found with this method; indeed the R^2 for the scatter plot of Figure 6-59 is 0.99. The spreadsheet used to automate the SALLOP calculations is available with this report in SI units while the results shown herein are provided in American units.

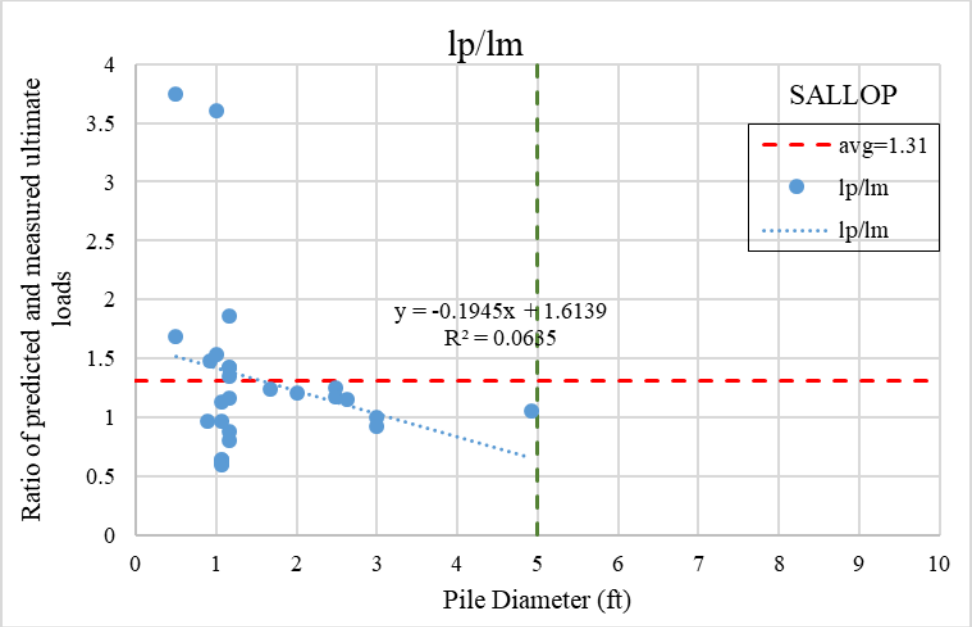

Figure 6-57. Comparison between the Ratio of Ultimate Predicted and Measured Load versus Pile Diameter at Pile Top Displacement Equals to 0.5 in. in Clay.

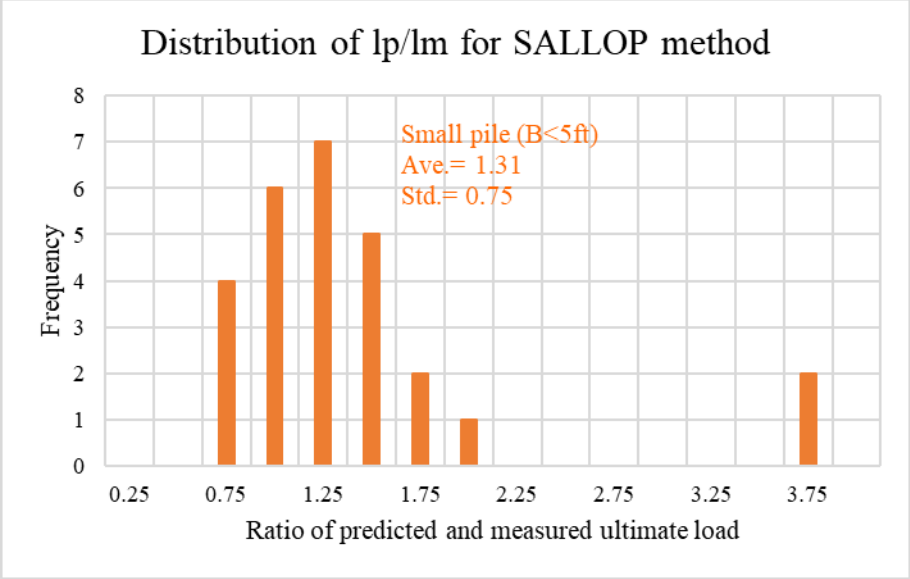

Figure 6-58. Distribution of l_p/l_m for SALLOP Method.

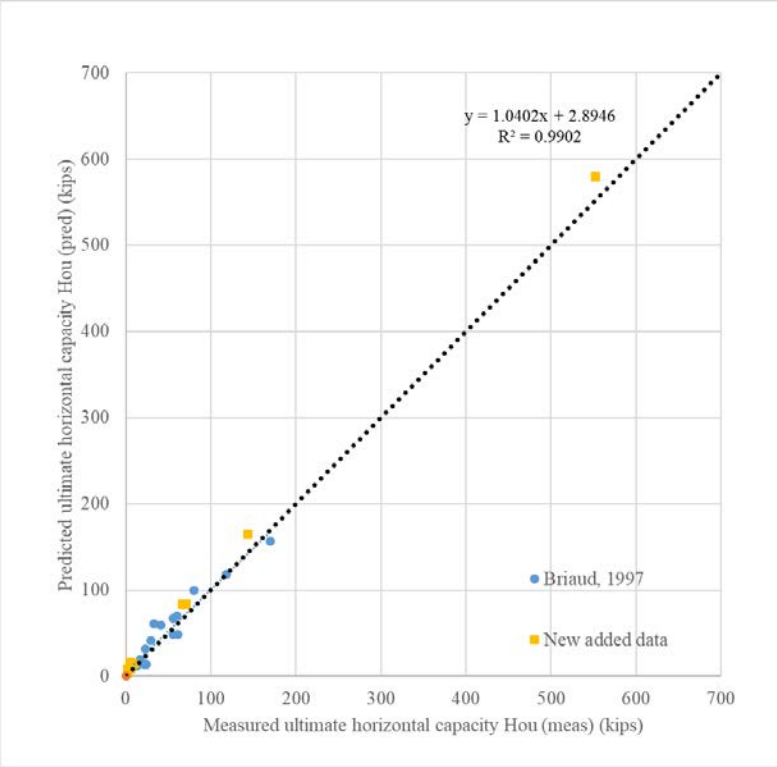

Figure 6-59. SALLOP Predictions vs. Measurements 27 of 89 Cases (Predicted with PMT Data).

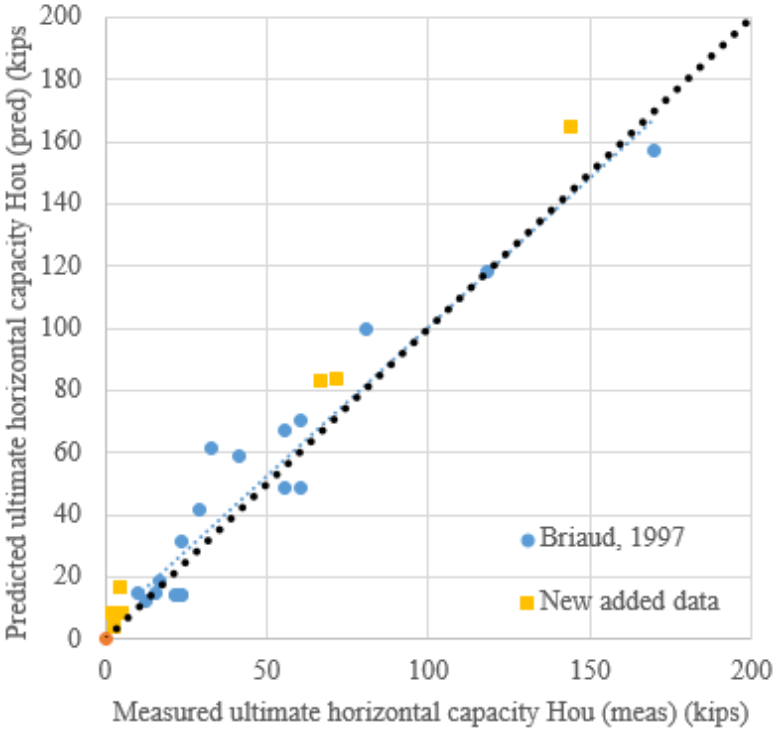

Figure 6-60. SALLOP Predictions vs. Measurements (Smaller Scale).

6.5 STATISTICAL ANALYSIS OF ULTIMATE LATERAL LOAD PREDICTIONS

As discussed in Chapter 4, 89 lateral pile load tests have been collected from eight different countries and organized in a database. In this chapter, the database is used to quantify the probability that the calculated loads will overpredict the measured loads and that the calculated displacements will underpredict the measured displacements. Recall that the LPILE predictions were based on the P-y curve criteria of Reese for sand, Matlock for soft clay, and Reese for stiff clay. Recall also that the SALLOP predictions were based on the method developed by Briaud and making use of the pressuremeter data.

The probabilistic prediction P_{prob} is based on the deterministic prediction P_{pred} obtained in the previous chapters (LPILE and SALLOP) and a modifying factor θ to account for the reliability level:

$$\mathrm{P_{prob}} = \theta \times P_{pred} \tag{43}$$

Where the factor θ is the probabilistic ratio. In the case of the prediction of lateral loads corresponding to a given displacement, the engineer is interested in ensuring that the predicted load L_{pred} will not be overestimated as this would be unsafe in design. For a given predicted load L_{pred}, the lower the value of θ is, the lower the probability that the predicted load L_{pred} will exceed the measured load L_{meas} will be. Therefore, θ is a function of the probability of overprediction in the case of loads. Conversely for the prediction of lateral displacements corresponding to a given load, the engineer is interested in ensuring that the predicted displacement D_{pred} will not be underestimated as this would be unsafe in design. For a given predicted displacement D_{pred}, the higher the value of θ is, the lower the probability that the predicted displacement D_{pred} will be lower than the measured displacement D_{meas} will be. Therefore, θ is a function of the probability of underprediction in the case of displacements. The following analysis aims at giving the relationship between the probability of overprediction (POP) as a function of the probabilistic factor θ for predicted loads and the relationship between the probability of underprediction (PUP) as a function of the probabilistic factor θ for predicted displacement.

The process to generate the POP versus θ function for loads and the PUP versus θ function for displacements is explained on the following example. The case is the load corresponding to 0.25 in. displacement for piles in sand. The process is:

1. Prepare the scatter plot of the predicted loads L_{pred} versus the measured loads L_{meas} (Figure 6-61). Count the number N_{op} of data points for which there is overprediction (predicted load > measured load). N_{op} is equal to the number of points above the 1 to 1 line on Figure 6-61. Calculate the ratio N_{op}/N_{tot} where N_{tot} is the total number of points on the scatter plot. This ratio gives an estimate of the POP for $\theta = 1$. In Figure 6-61, $N_{op} = 13$ and $N_{tot} = 52$, so POP = 0.25. The point of POP = 0.25 for $\theta = 1$ has thus been generated on then probability plot of Figure 6-65. This means that the probability of overpredicting the lateral load corresponding to a displacement of 0.25 in. for piles in sand is 25 percent.
2. Multiply all predicted load values by $\theta = 0.5$ and prepare a new scatter plot of 0.5 L_{pred} versus L_{meas}. Figure 6-62 shows such a plot. Repeat the process of step 1 above. In this case $N_{op} = 1$, N_{tot} is still 52, therefore POP has decreased to 0.02. A new point has been generated on the probability plot of Figure 6-65.
3. Repeat step 2 for different values of θ (Figure 6-63 and Figure 6-64) and complete the plot of POP versus θ (Figure 6-65).
4. Choose the probability of overprediction that you wish to accept for your design (say 10 percent) and read the corresponding θ value on the POP versus θ plot (Figure 6-65, in this case $\theta = 0.65$). According to this methodology, if the LPILE predicted load for a deflection of 0.25 in. is multiplied by 0.65, there is a 90 percent probability that the measured load will be more than the predicted load for piles in sand.

The plot of the PUP (PUP = 1 – POP) for predicted loads corresponding to 0.25 in. and for piles in sand versus the probabilistic factor θ is plotted in Figure 6-66. Figure 6-65, Figure 6-67, Figure 6-68, and Figure 6-69 present the POP versus θ plots for LPILE predicted load at displacements y = 0.25, 0.5, 1, and 2 in. in sand, respectively. Figure 6-70, Figure 6-71, Figure 6-72, and Figure 6-73 present the POP versus θ plots for LPILE predicted loads at displacements y = 0.25, 0.5, 1, and 2 in. in clay, respectively.

In the case of predicted deflections at a fraction of the ultimate load, it is the underprediction that is of concern. Therefore in this case the plots generated are the PUP versus the probabilistic factor θ. Figure 6-74, Figure 6-75, Figure 6-76, Figure 6-77, Figure 6-78, Figure 6-79, Figure 6-80, and Figure 6-81 show these plots. Figure 6-82 presents the POP versus θ plots for SALLOP predicted ultimate load.

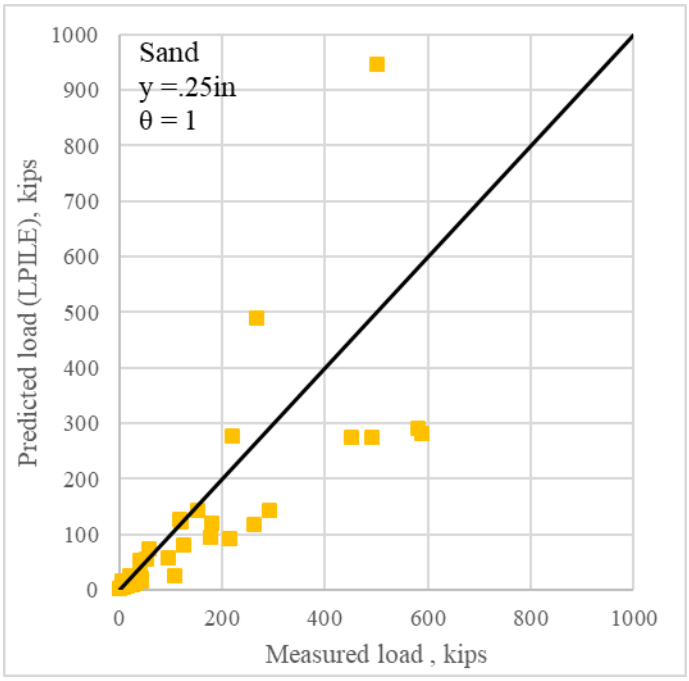

Figure 6-61. Comparison between Predicted and Measured Load for θ = 1.0 at y = .25 in. in Sand.

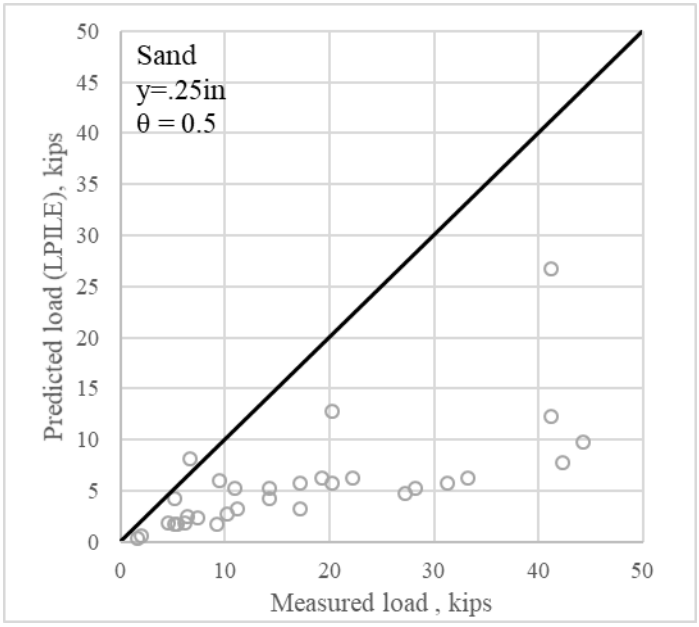

Figure 6-62. Comparison between Predicted and Measured Load for θ = 0.5 and y = .25 in. in Sand (Smaller Scale).

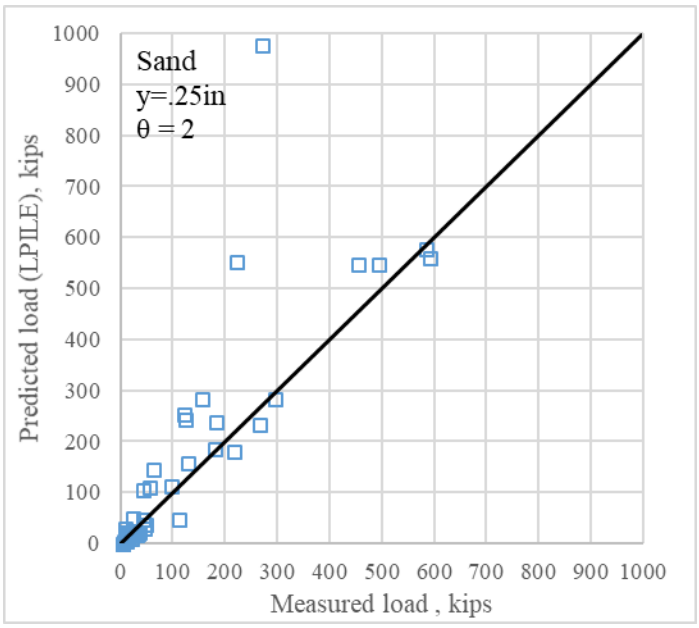

Figure 6-63. Comparison between Predicted and Measured Load for θ = 2 and y = 0.25 in. in Sand (Smaller Scale).

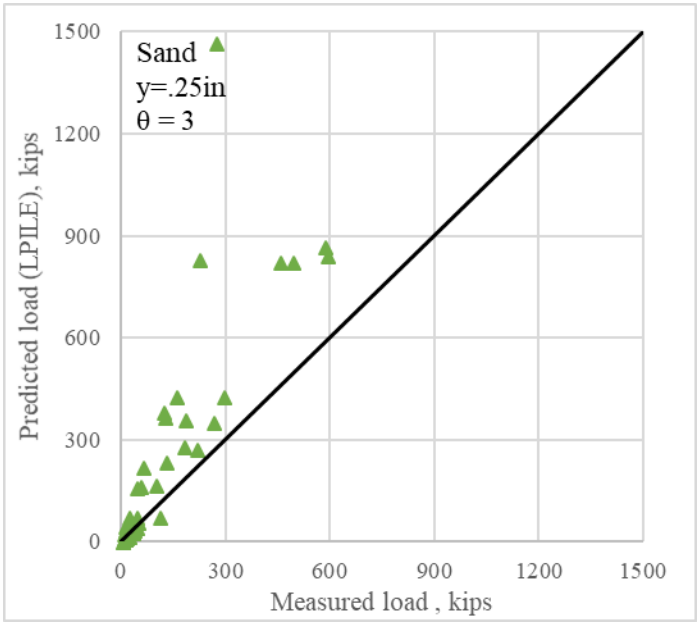

Figure 6-64. Comparison between Predicted and Measured Load for θ = 3 and y = 0.25 in. in Sand (Smaller Scale).

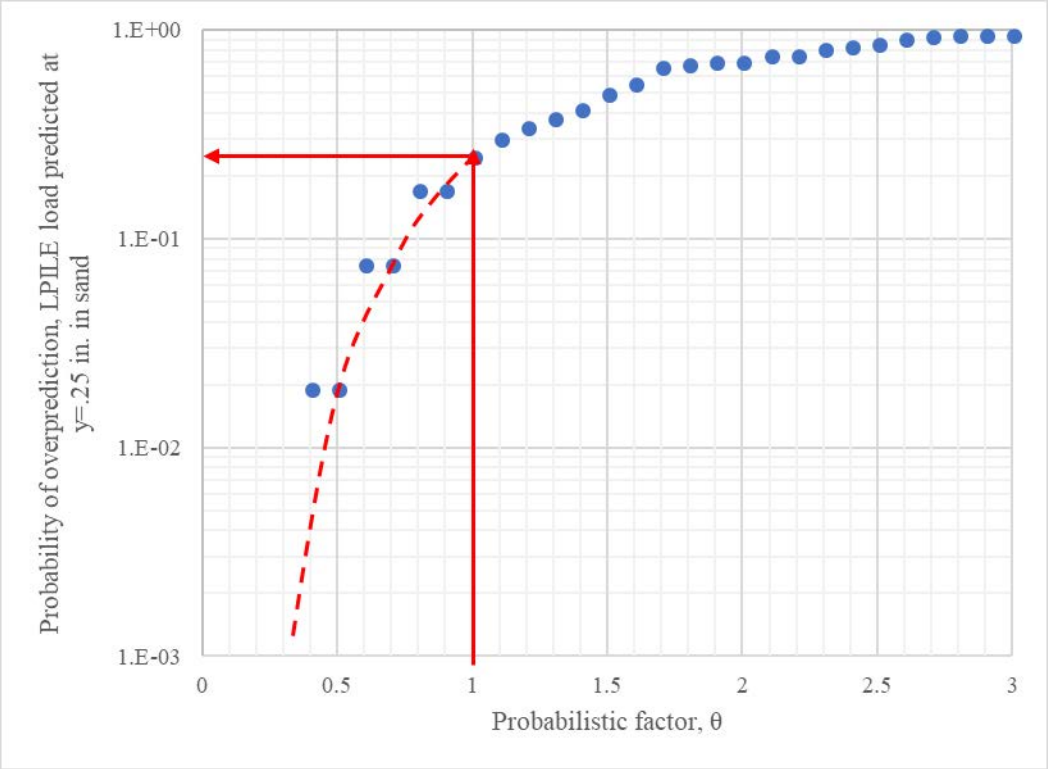

Figure 6-65. Calibration of Overpredicted Load Using LPILE at y = .25 in. in Sand.

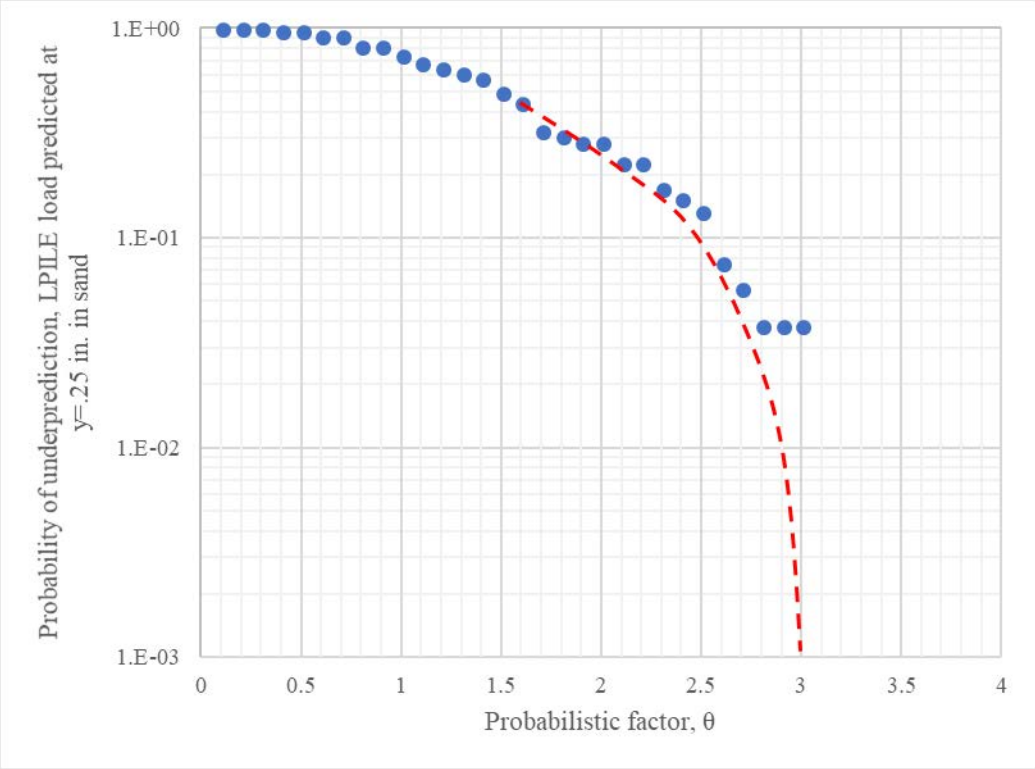

Figure 6-66. Calibration of Underpredicted Load Using LPILE at y = .25 in. in Sand.

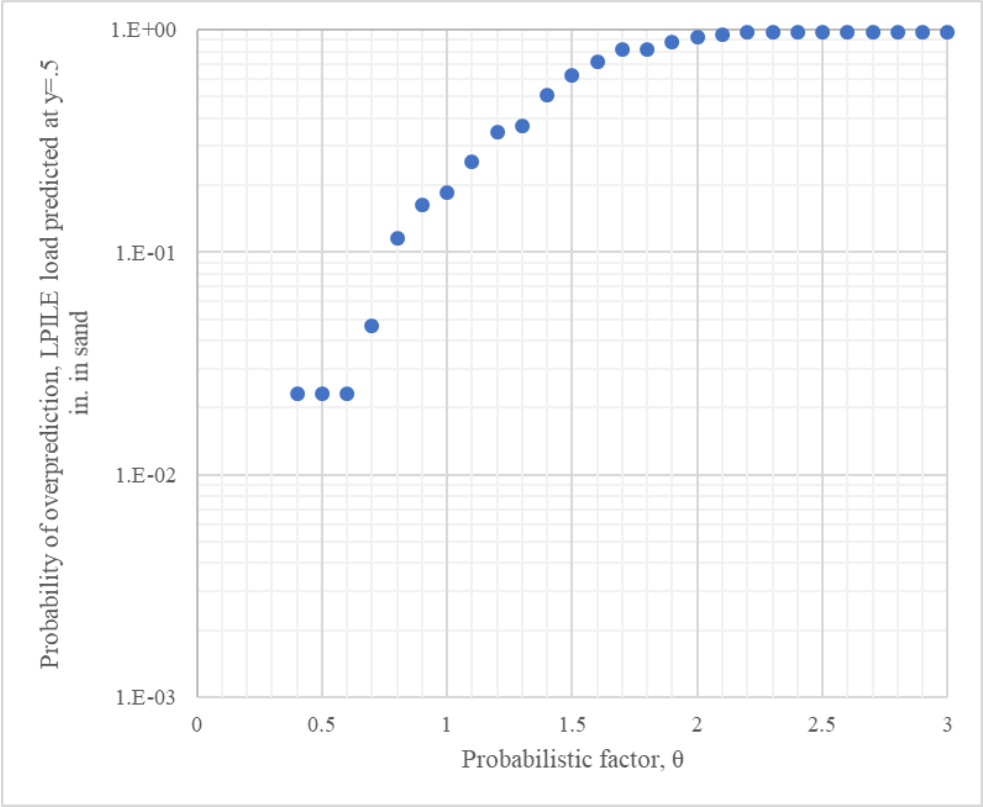

Figure 6-67. Calibration of Overpredicted Load Using LPILE at y = .5 in. in Sand.

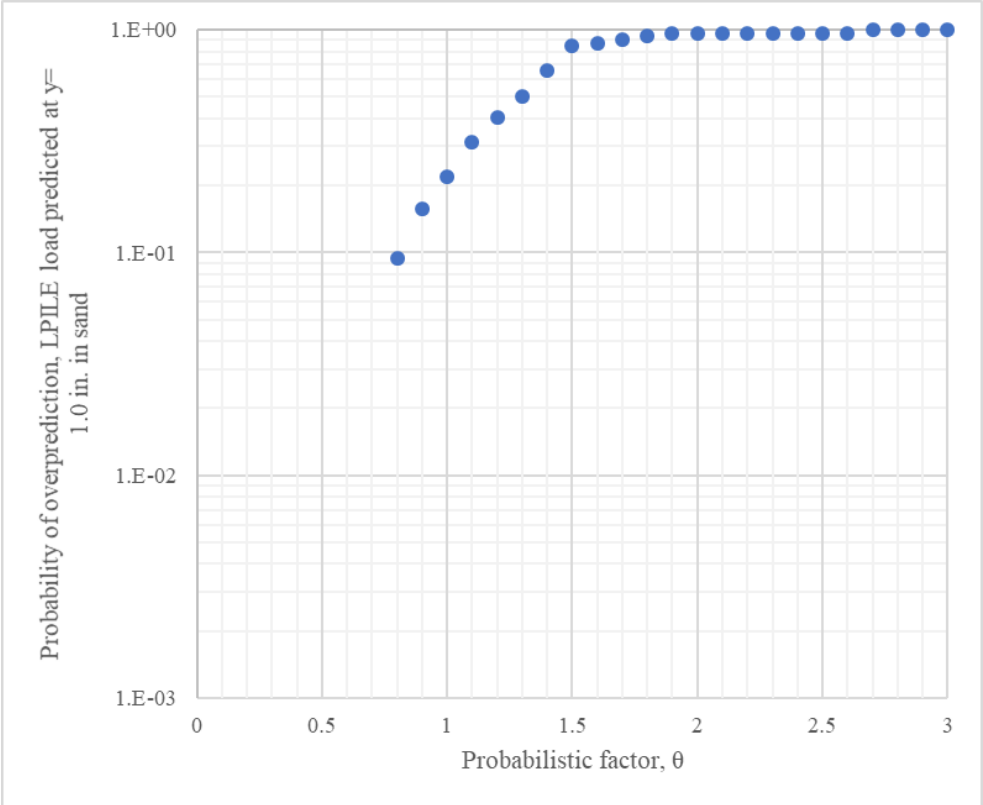

Figure 6-68. Calibration of Overpredicted Load Using LPILE at y = 1.0 in. in Sand.

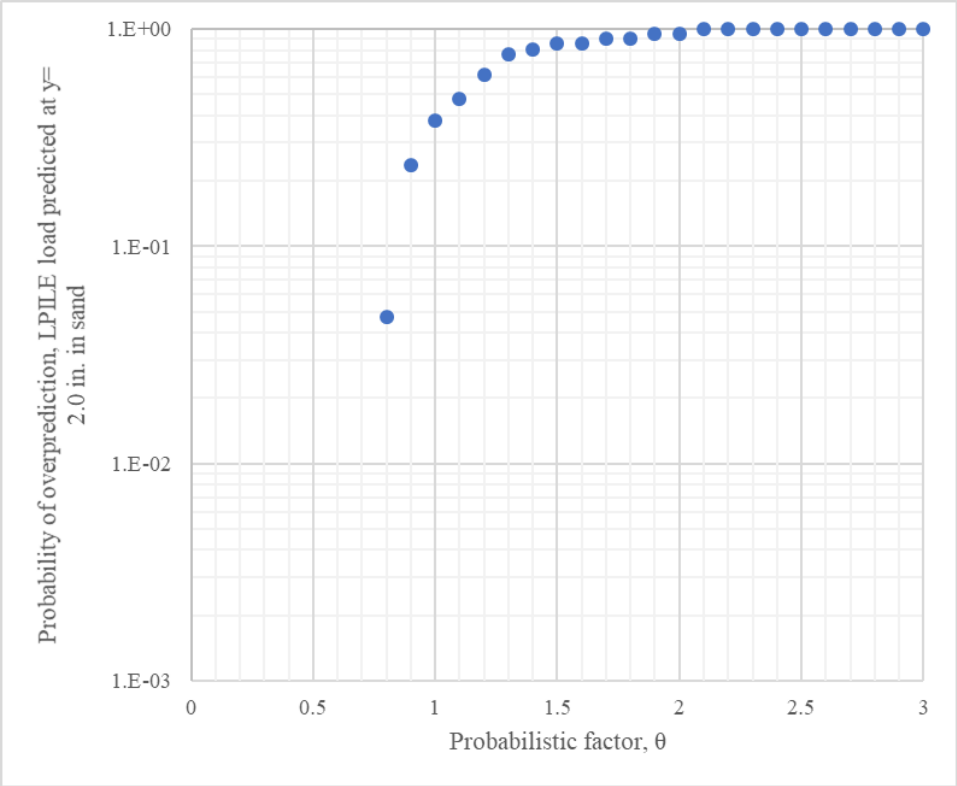

Figure 6-69. Calibration of Overpredicted Load Using LPILE at y = 2.0 in. in Sand.

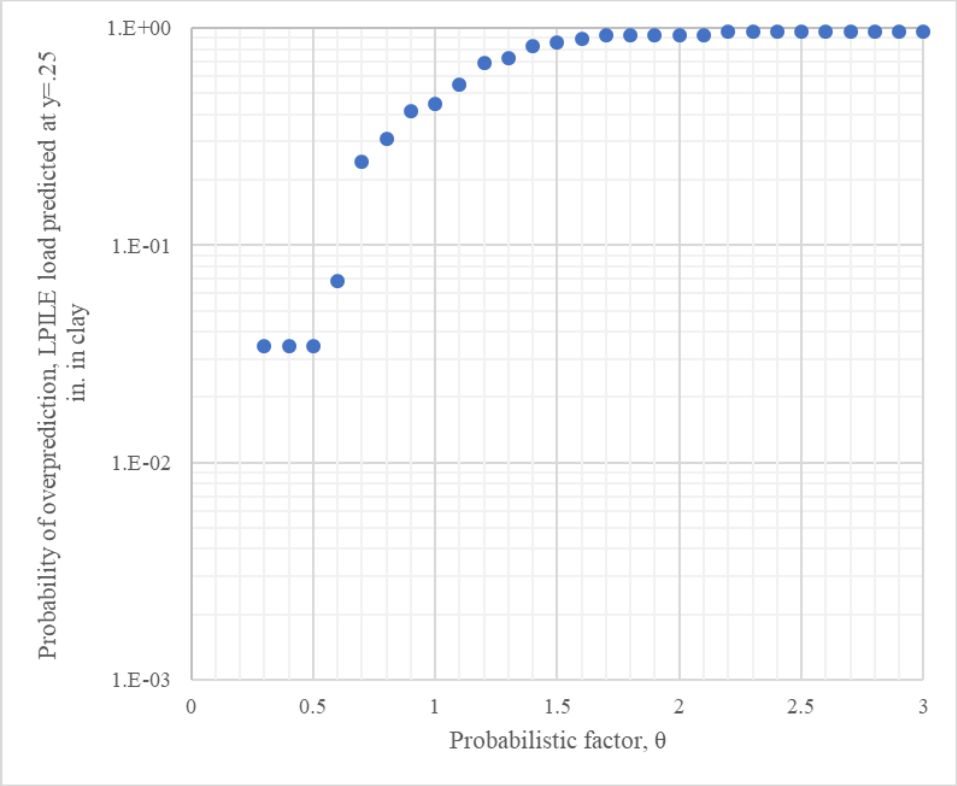

Figure 6-70. Calibration of Overpredicted Load Using LPILE at y = .25 in. in Clay.

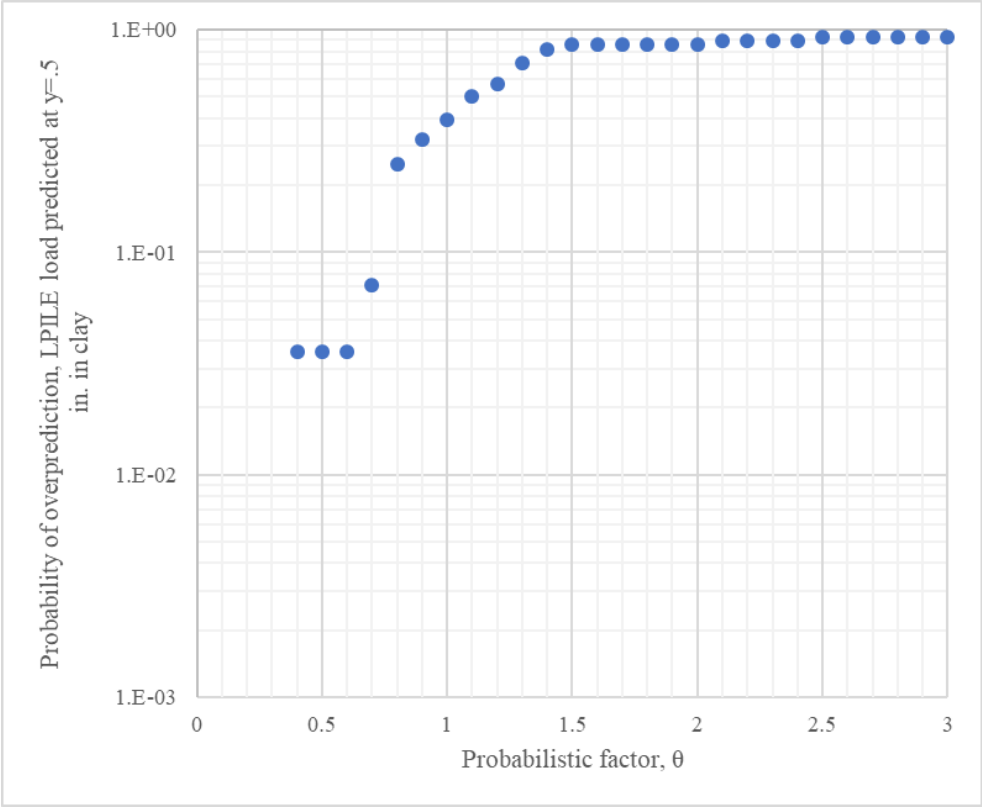

Figure 6-71. Calibration of Overpredicted Load Using LPILE at y = .5 in. in Clay.

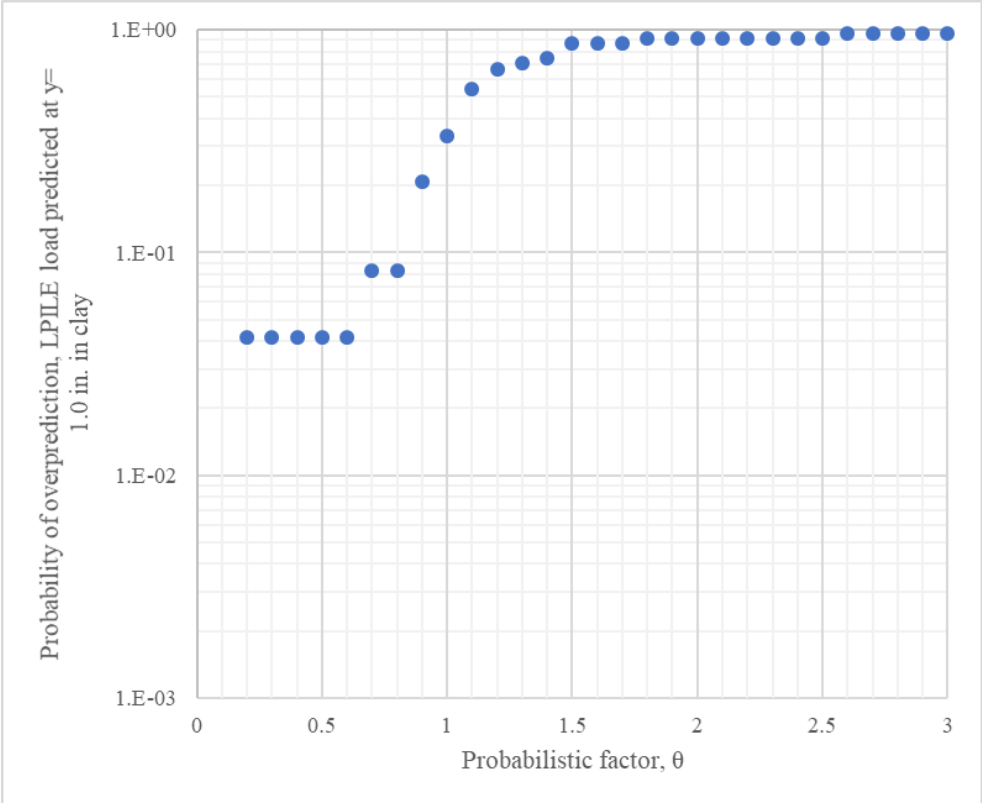

Figure 6-72. Calibration of Overpredicted Load Using LPILE at y = 1.0 in. in Clay.

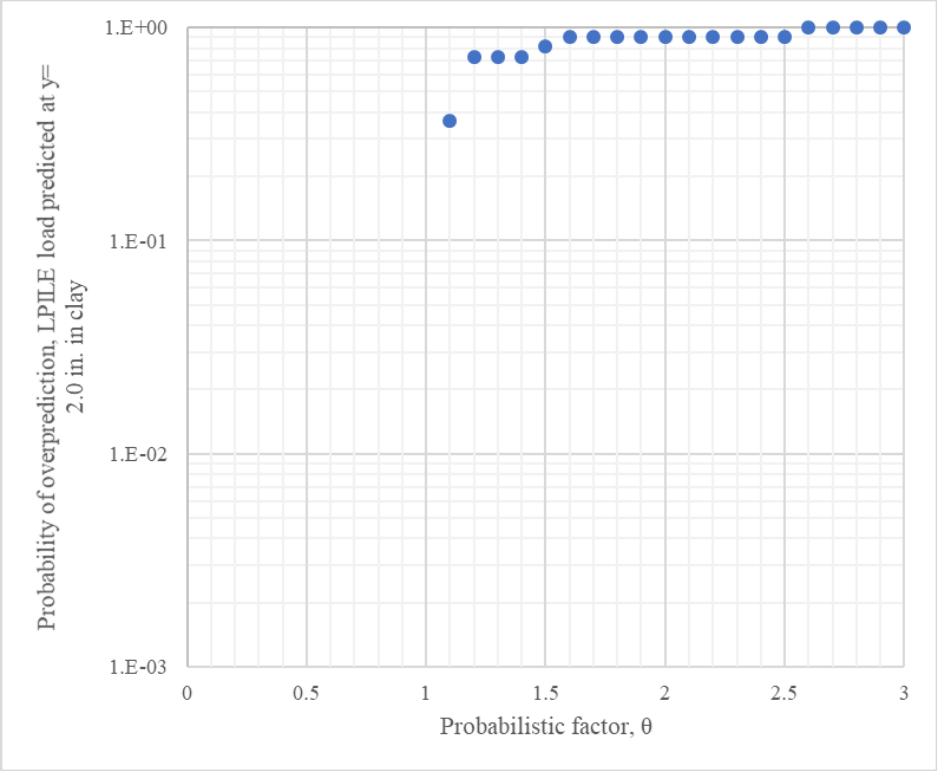

Figure 6-73. Calibration of Overpredicted Load Using LPILE at y = 2.0 in. in Clay.

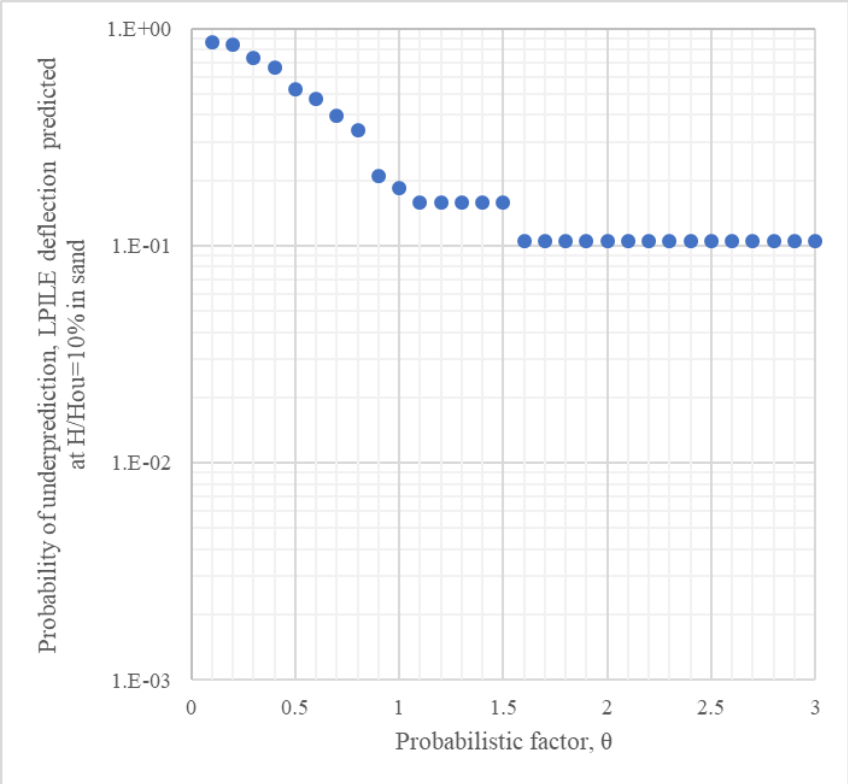

Figure 6-74. Calibration of Underpredicted Deflection Using LPILE at H/H_{ou} = 10 Percent in Sand.

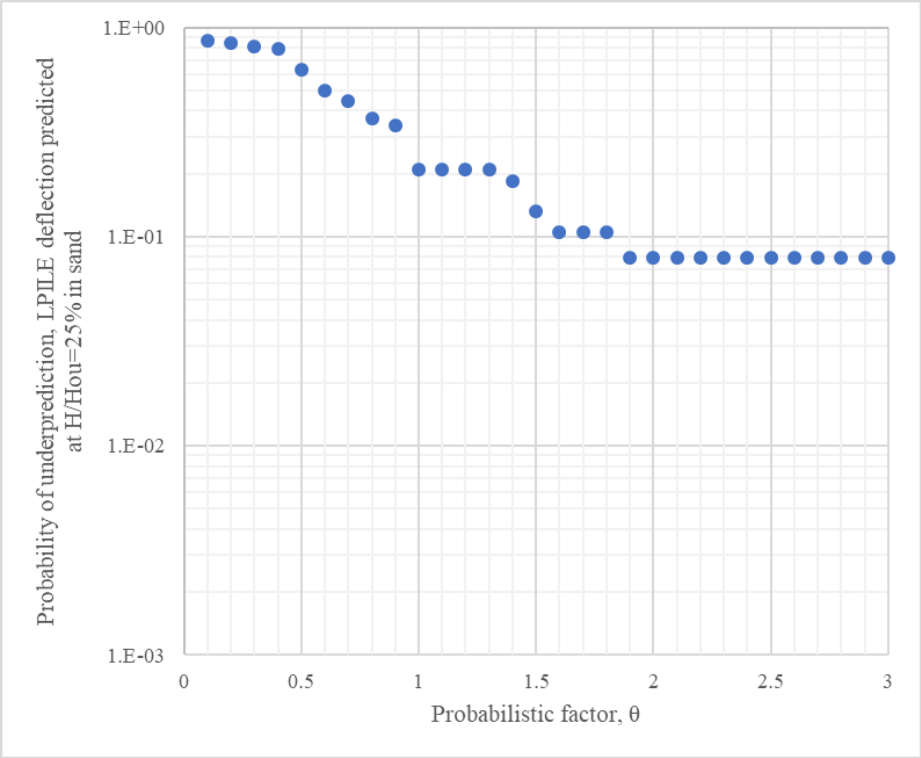

Figure 6-75. Calibration of Underpredicted Deflection Using LPILE at H/H_{ou} = 25 Percent in Sand.

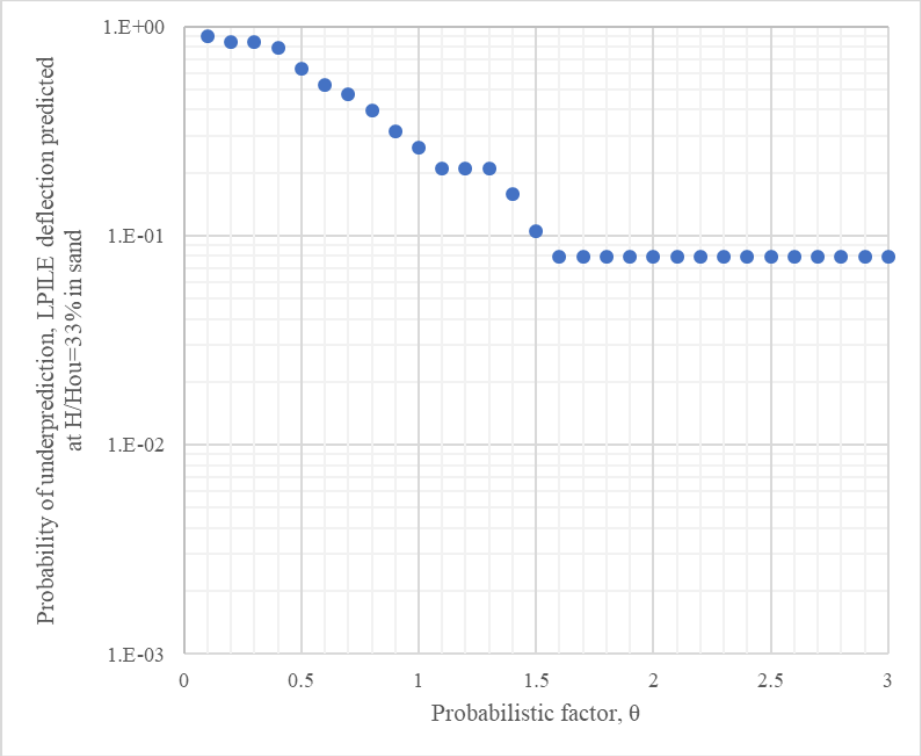

Figure 6-76. Calibration of Underpredicted Deflection Using LPILE at H/H_{ou} = 33 Percent in Sand.

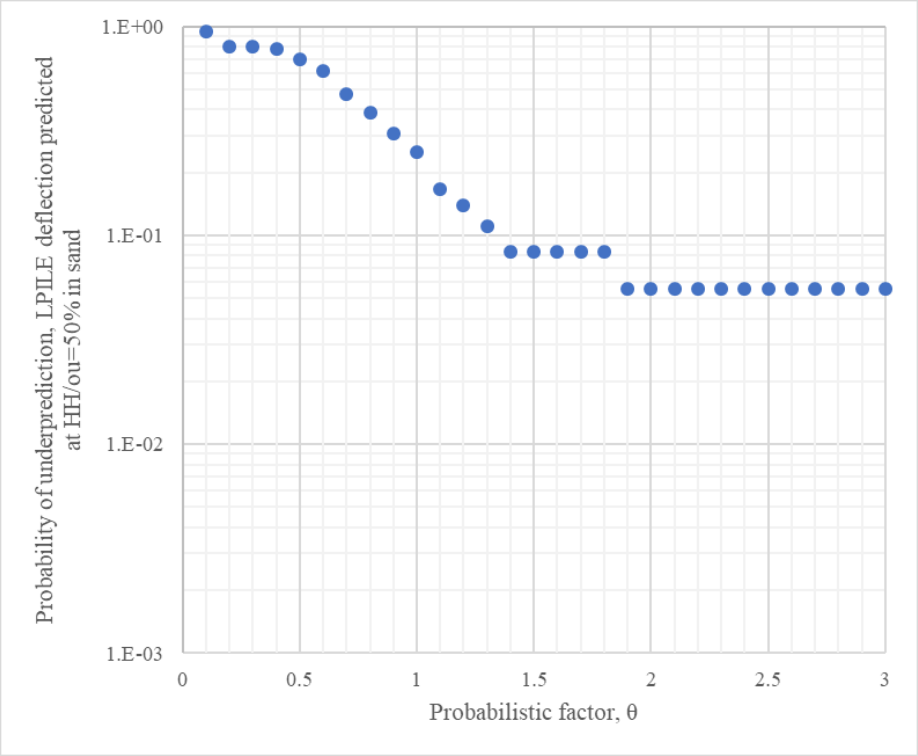

Figure 6-77. Calibration of Underpredicted Deflection Using LPILE at H/H$_{ou}$ = 50 Percent in Sand.

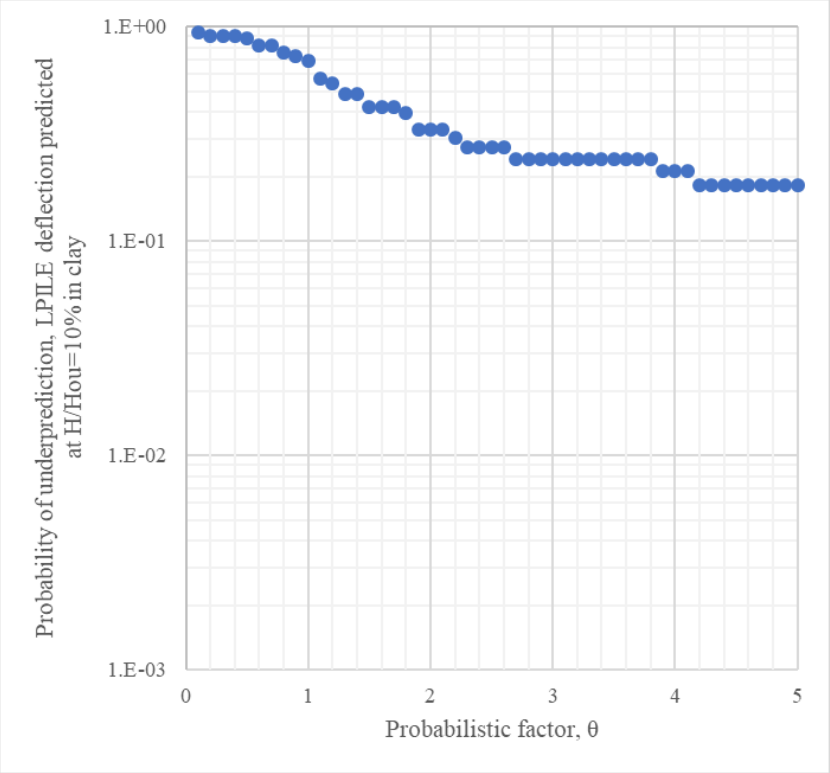

Figure 6-78. Calibration of Underpredicted Deflection Using LPILE at H/H$_{ou}$ = 10 Percent in Clay.

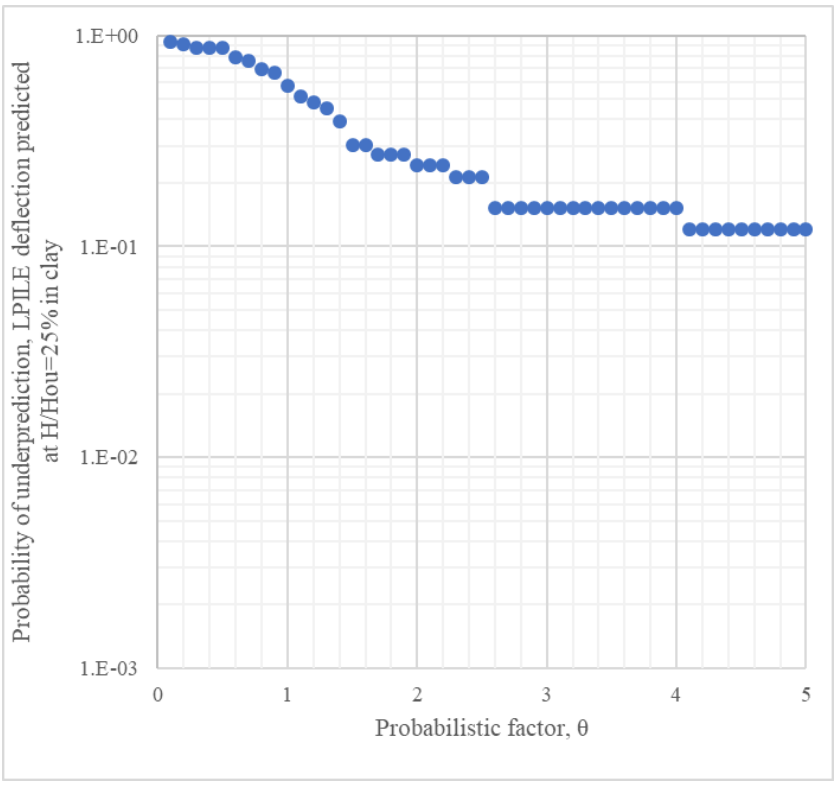

Figure 6-79. Calibration of Underpredicted Deflection Using LPILE at H/H_{ou} = 25 Percent in Clay.

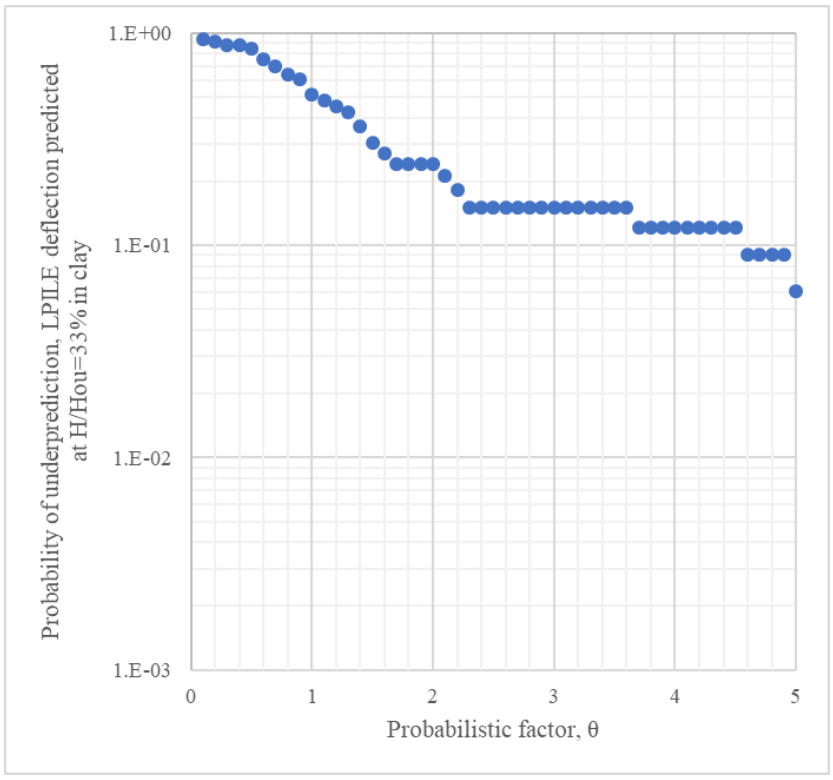

Figure 6-80. Calibration of Underpredicted Deflection Using LPILE at H/H_{ou} = 33 Percent in Clay.

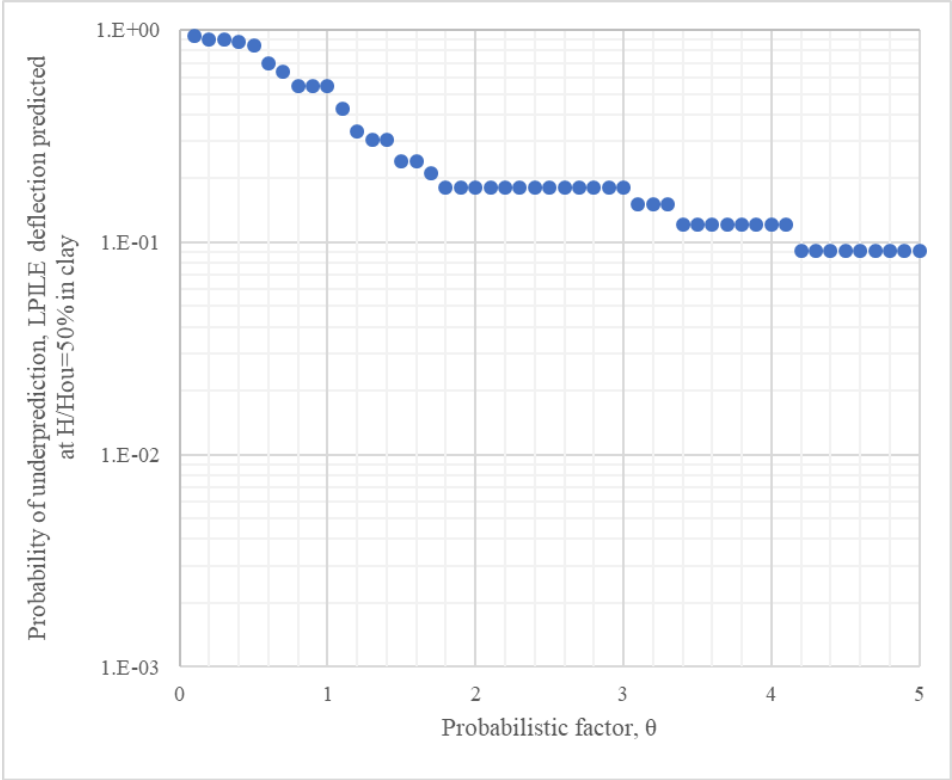

Figure 6-81. Calibration of Underpredicted Deflection Using LPILE at H/H_{ou} = 50 Percent in Clay.

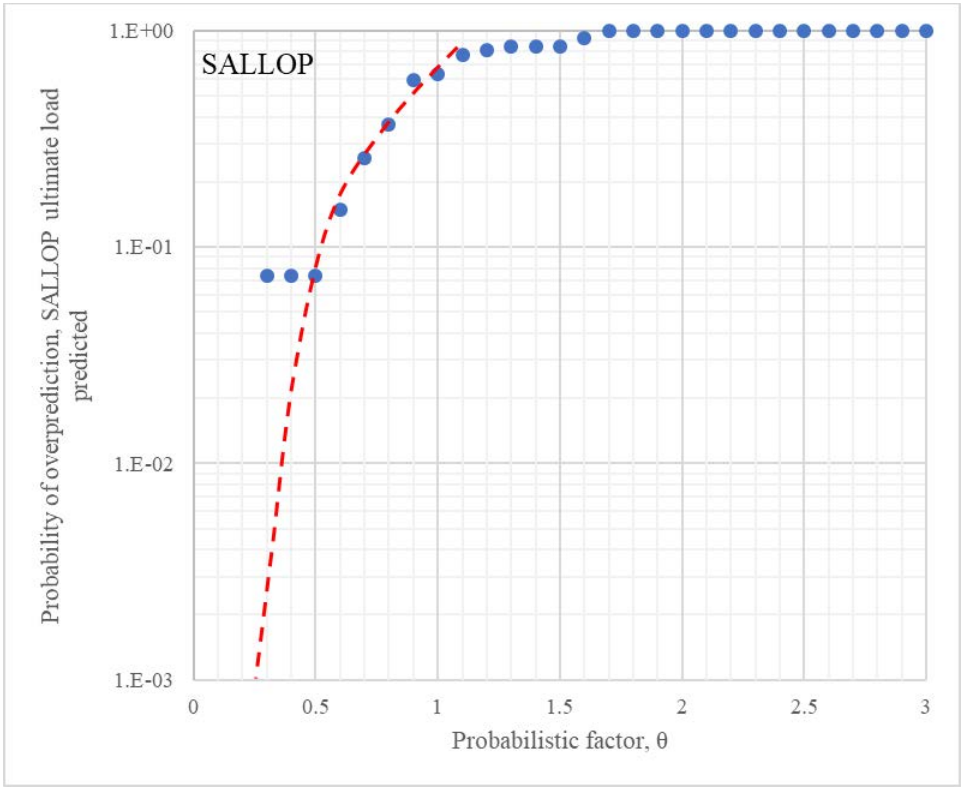

Figure 6-82. Calibration of Overpredicted Load Using SALLOP Method.

6.6 SUMMARY OF FINDINGS AND SUGGESTED IMPROVEMENTS

The main results of this study are summarized in several figures. They are:

- Figure 6-1, Figure 6-3, Figure 6-5, and Figure 6-7 show the ratios L_{pred}/L_{meas} (LPILE predicted load over measured load) at given deflections equal to 0.25, 0.5, 1, and 2 in. versus pile diameter in sand.
- Figure 6-10, Figure 6-11, Figure 6-12, and Figure 6-13 show the LPILE predicted loads versus measured loads at given deflections equal to 0.25, 0.5, 1, and 2 in. in sand.
- Figure 6-16, Figure 6-14, Figure 6-18, and Figure 6-20 show the ratios L_{pred}/L_{meas} at given deflections equal to 0.25, 0.5, 1, and 2 in. versus pile diameter using LPILE in clay.
- Figure 6-23, Figure 6-24, Figure 6-25, and Figure 6-26 show the LPILE predicted loads versus measured load at given deflections equal to 0.25, 0.5, 1, and 2 in. in clay.
- Figure 6-31, Figure 6-33, Figure 6-35, and Figure 6-37 show the ratios y_{pred}/y_{meas} (LPILE predicted pile head displacement over measured pile head displacement) at given percent of the ultimate load equal to 10, 25, 33, and 50 percent versus pile diameter in sand.
- Figure 6-10, Figure 6-11, Figure 6-12, and Figure 6-13 show the LPILE predicted deflections versus measured deflections at given percent of the ultimate load equal to 10, 25, 33, and 50 percent in sand.
- Figure 6-44, Figure 6-46, Figure 6-48, and Figure 6-50 show the ratios y_{pred}/y_{meas} at given percent of the ultimate load equal to 10, 25, 33, and 50 percent versus pile diameter in clay.
- Figure 6-23, Figure 6-24, Figure 6-25, and Figure 6-26 show the LPILE predicted deflections versus measured deflections at given percent of the ultimate load equal to 10, 25, 33, and 50 percent in clay.
- Figure 6-57 shows the ratio L_{pred}/L_{meas} versus pile diameter using the SALLOP method.
- Figure 6-59 and Figure 6-60 show the SALLOP predicted ultimate lateral capacity versus the measured ultimate lateral capacity.

- Figure 6-65, Figure 6-66, Figure 6-67, Figure 6-68, Figure 6-69, Figure 6-70, Figure 6-71, Figure 6-72, Figure 6-73,Figure 6-74, Figure 6-75, Figure 6-76, Figure 6-77, Figure 6-78, Figure 6-79, Figure 6-80, Figure 6-81, and Figure 6-82 show the probability of overprediction and underprediction for loads and displacements for piles in sand and piles in clay when using LPILE and when using SALLOP.

The results for SALLOP are satisfactory as is. The results of LPILE show more scatter and some trends with increasing diameter.

The trend for piles in sand is that the load ratio L_{pred}/L_{meas} at a given displacement increases with increasing diameter while the displacement ratio y_{pred}/y_{meas} at a given percent of ultimate load decreases with increasing diameter. The following explanation is offered.

The reason for this trend is rooted in the use of a flawed parameter: the modulus of subgrade reaction k. The modulus of subgrade reaction k is defined as the ratio of the mean lateral pressure p on a unit length of pile divided by the displacement y of that unit length of pile.

$$\mathrm{k} = \frac{\mathrm{p}}{\mathrm{y}} \tag{44}$$

The parameter k is in units of pounds per cubic feet (pcf). The elastic formula below is used to show the fundamental problem with the k parameter:

$$\mathrm{y} = \mathrm{I}(1 - \nu^2) \times \frac{pB}{E} \tag{45}$$

Where I is primarily a shape factor, ν is Poisson's ratio (dimensionless), B is the pile width (ft), and E is the soil modulus (psi). This equation shows that:

$$\mathrm{k} = \frac{\mathrm{p}}{\mathrm{y}} = E/I(1 - \nu^2)B \tag{46}$$

This indicates that the modulus of subgrade reaction k increases with the soil modulus but also decreases with the pile diameter B. The first observation is that a k value based on certain pile diameter is only valid for that diameter and not for any different diameter. Since the recommended k values in LPILE were developed by calibration against load tests on small diameter piles, they should not be used for large diameter piles. The k values associated with

small diameter pile are higher (stiffer) than the k values needed for large diameter piles since k is inversely proportional to B. The use of small diameter pile k values for large diameter piles will therefore lead to underestimated deflections for a given load or overestimated loads for a given displacement. This is what Figure 6-25 and Figure 6-9 are showing. The SALLOP method does not use the modulus of subgrade reaction k but uses the soil modulus from the pressuremeter. This is one of the reasons why it is not affected by the pile diameter.

The trend for piles in clays is that the load ratio L_{pred}/L_{meas} at a given displacement decreases with increasing diameter while the displacement ratio y_{pred}/y_{meas} at a given percent of ultimate load increases with increasing diameter. The following explanation is offered. The resistance of a pile to lateral loading is strongly influenced by the soil resistance near the surface. The ultimate pressure around the pile at shallow depth is expressed as:

$$p_{us} = N_{ps} S_u = \left(3 + J\left(\frac{z}{B}\right) + \frac{\gamma z}{S_u}\right) S_u \tag{47}$$

The ultimate pressure around the pile at large depth is expressed as:

$$p_{ud} = N_{pd} S_u = 9 S_u \tag{48}$$

The intersection of these two p_u profiles occurs at a critical depth Z_c where p_{us} is equal to p_{ud}. The value of Z_c is:

$$z_c = \frac{6 S_u B}{J S_u + \gamma B} \tag{49}$$

Where

z_c is the critical depth, J is the dimensionless fitting coefficient, s_u is the undrained shear strength, B is the pile diameter and γ is soil unit weight.

Therefore, for common values of J, s_u and γ, Z_c increases with B. Figure 6-83 shows an example relationship between Z_c and B. As can be seen for a 3-ft diameter pile Z_c is about 20 ft but for a 9 ft diameter pile Z_c is 34 ft. Therefore the zone of reduced soil resistance against the pile is deeper for the large diameter pile than for the small diameter pile (Figure 6-84). For that reason, the P-y curves for the large diameter pile are softer over a larger depth than for the small

diameter pile. As a result, the deflection predicted at a given load is larger and the load predicted at a given deflection is smaller for the larger diameter pile.

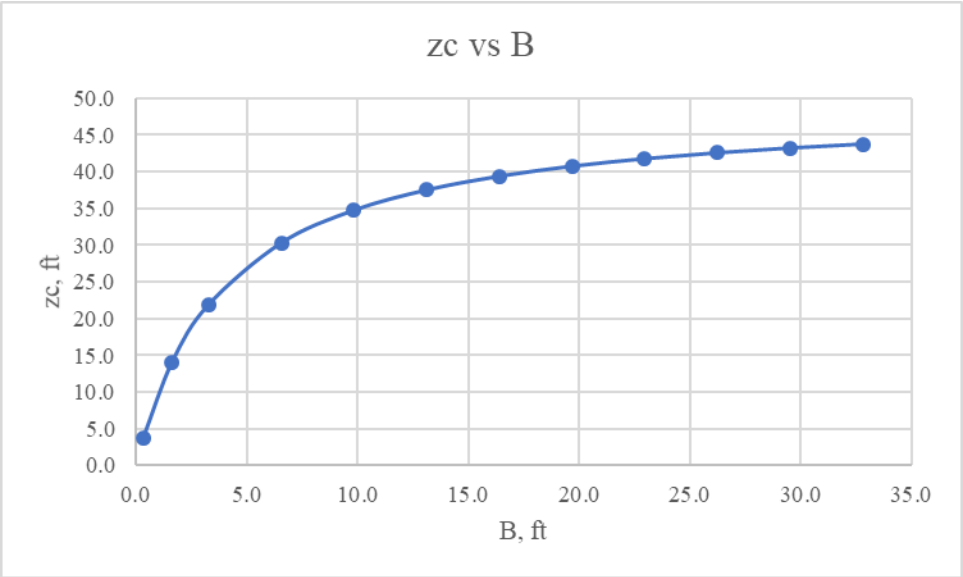

Figure 6-83. Example of Relationship between the Critical Depth and the Pile Diameter.

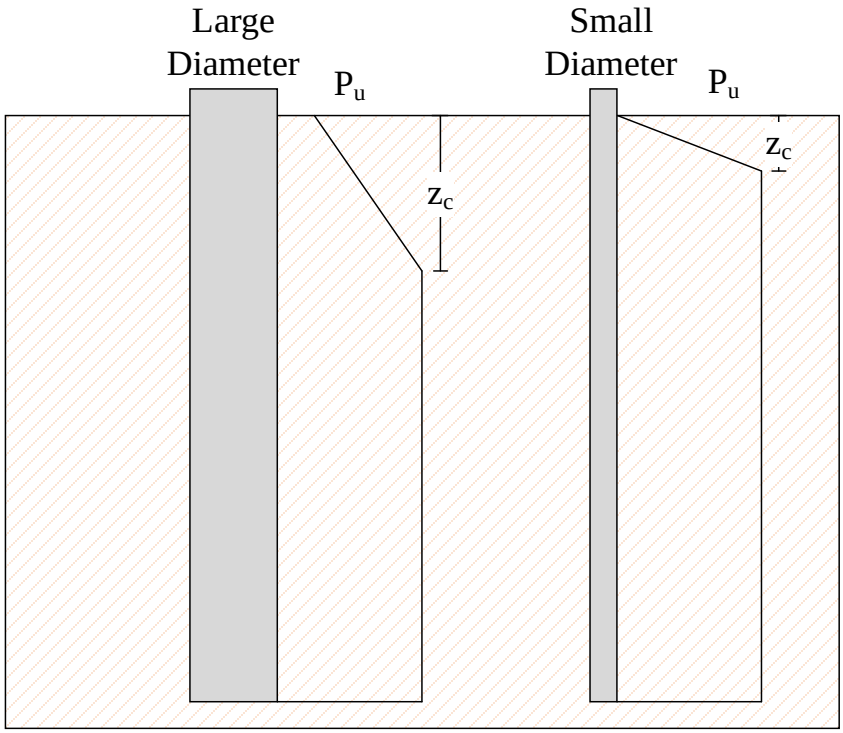

Figure 6-84. Difference in Critical Depth between a Small Diameter Piles and a Large Diameter Pile.

CHAPTER 7 CONCLUSIONS

A database of piles subjected to monotonic lateral loading was accumulated. The total number of load tests collected and organized in a spreadsheet was 89 with the distribution (Table 7-1). The data came primarily from the United States but also from 7 other countries.

Table 7-1. Pile database information

Category		Pile Diameter B<5 ft	Pile Diameter B≥5 ft
Pile diameter range (ft)		1–5	5–9.8
Pile length range (ft)		5–120	7.5–220
Number of case		54	35
Soil type	Sand	33	23
	Clay	21	12

Each load test case included the pile dimensions and material properties, the soil properties, and the lateral load versus lateral deflection curve. For each load test case, the work consisted of predicting the load-deflection curve using the program LPILE with the associated input parameters and comparing it to the measured curve.

Evaluation of the predictions took place along two main comparisons: comparison between the predicted load L_{pred} and the measured load L_{meas} at given deflections of 0.25, 0.5, 1, and 2 in. and comparison between the predicted deflection y_{pred} and measured defection y_{meas} at percentages of the ultimate lateral load equal to 10 percent, 25 percent, 33 percent, and 50 percent. The ultimate lateral load was defined as the load corresponding to a horizontal deflection equal to 10 percent of the pile diameter. This deflection was not always reached in the load tests; in those cases, a hyperbolic extrapolation was used (33 percent of all cases).

The ratio L_{pred}/L_{meas} was plotted against the pile diameter to evaluate the predictions in general and the influence of the diameter in particular. The following summarizes the findings:

- In sand, L_{pred}/L_{meas} averages about 0.9 for all piles and increases with diameter from about 0.7 for smaller diameter piles to about 1.1 for larger diameter piles. Overall, L_{pred}/L_{meas} can be expected to be between 0.4 and 1.4 most of the time.
- In clay, L_{pred}/L_{meas} averages about 0.9 for all piles and decreases with diameter from about 1.3 for smaller diameter piles to about 0.7 for larger diameter piles. Overall, L_{pred}/L_{meas} can be expected to be between 0.4 and 1.6 most of the time.

The ratio y_{pred}/y_{meas} was plotted against the pile diameter to evaluate the predictions in general and the influence of the diameter in particular. Overall more scatter was observed in the prediction of deflections at given percentages of the ultimate load than in the prediction of loads at given deflection values. The following summarizes the findings:

- In sand, y_{pred}/y_{meas} averages about 1.9 for all piles and decreases with diameter from about 2.25 for smaller diameter piles to about 1 for larger diameter piles. Overall, the ratio y_{pred}/y_{meas} can be expected to be between 0.5 and 5 most of the time.
- In clay, y_{pred}/y_{meas} averages about 1.4 for all piles and increases with diameter from about 0.9 for smaller diameter piles to about 3 for larger diameter piles. Overall, the ratio y_{pred}/y_{meas} can be expected to be between 0.2 and 5 most of the time with some values reaching 8 for larger diameter piles.

The fact that, in sand, the predicted deflection decreases as the pile diameter increases is attributed to the use of a flawed parameter: the modulus of subgrade reaction k. The reason is that, while k increases with the soil stiffness, it also decreases with the pile diameter. Therefore, recommending set values of k for all pile diameters leads to underpredicting deflections for large diameter piles. Indeed, in this case the k value will be too large. A better approach would be to use the soil modulus, which is solely dependent on the soil and independent of the pile diameter as in the SALLOP method.

The fact that, in clay, the predicted deflection increases significantly as the pile diameter increases is attributed to the fact that the depth Z_c at which the soil resistance to lateral loading switched from the shallow depth equation to the larger depth equation increases with the pile diameter. As such, the P-y curves near the surface are softer for larger diameter piles and the

predicted deflections are accordingly larger. An improved way to obtain Z_c for large diameter piles is needed.

REFERENCES

Adams, J. I. and H. S. Radhakrishna (1973). "The Lateral Capacity of Deep Augered Footings." In Proc., 8th Int. Conf. on SMFE (Vol. 2, No. 1, pp. 1-8).

Ahmed, S. S. and B. Hawlader (2016). "Numerical analysis of large-diameter monopiles in dense sand supporting offshore wind turbines." *International Journal of Geomechanics* 16(5).

API (2010). *Recommended Practice for Planning, Designing and Constructing Fixed Offshore Platforms- Working Stress Design*. API RP 2A-WSD. 21st Edition, Errata and Supplement.

Ashour, M. and A. Helal (2014). "Contribution of Vertical Skin Friction to the Lateral Resistance of Large-Diameter Shafts." *Journal of Bridge Engineering*, *19*(2), 289-302.

Ashour, M., G. Norris, and P. Pilling (2002). "Strain wedge model capability of analyzing behavior of laterally loaded isolated piles, drilled shafts, and pile groups." *Journal of Bridge Engineering*. 7(4).

Ashour, M., G. Norris, and S. Elfass (2008). *Analysis of laterally loaded long or intermediate drilled shafts of small or large diameter in layered soil*. No. CA04-0252. California. Dept. of Transportation. Division of Research and Innovation.

Baguelin, F., Jezequel, J. F., Le, M., & Lemehaute, A. (1972). Expansion of cylindrical probes in cohesive soils. *Journal of Soil Mechanics & Foundations Div*, *98*(Sm 11).

Banerjee, P. K. and T. G. Davies (1978). "The behaviour of axially and laterally loaded single piles embedded in nonhomogeneous soils." *Geotechnique*, 28(3), 309-326.

Billiet, W. and J. Sewell (2014). Dulles Corridor Metrorail Project – Phase 2 Package A. Load Test Report of Aerial Guideway Load Test Program, Loudon and Fairfax County, Virginia.

Bowman, E. R. (1958). "Investigation of the lateral resistance to movement of a plate in cohesionless soil" Doctoral dissertation, University of Texas at Austin.

Briaud, J.-L. (1997). “SALLOP-Simple Approach for Lateral Loads on Piles.” *Journal of Geotechnical and Geoenvironmental Engineering.* 123(10), 958-964.

Briaud, J.-L. (2013). Geotechnical engineering: unsaturated and saturated soils. John Wiley & Sons.

Briaud, J.-L. and C. A. Makarim (1986). *Pressuremeter Standard and Pressuremeter Parameters*. In *The Pressuremeter and its Marine Applications: Second International Symposium.* ASTM International.

Broms, B. B., 1965. “Design of Laterally Loaded Piles,” Journal of the Soil Mechanics and Foundations Engineering Division, ASCE, Vol. 91, No. SM3, pp. 79-99.

Castelli, R. J. and K. Fan (2002). *Lateral Load Test Results on Drilled Shafts in Marl at Jacksonville, Florida.* In Deep Foundations 2002: An International Perspective on Theory, Design, Construction, and Performance (pp. 824-835).

Cho, K. H., Clark, S., Keaney, B., Gabr, M., & Borden, R. (2001). “Laterally Loaded Drilled Shafts Embedded in Soft Rock.” *Transportation Research Record* 1772.

Comodromos, E. M., and K. D. Pitilakis (2005). “Response evaluation for horizontally loaded fixed-head pile groups using 3-D non-linear analysis.” *International Journal for Numerical and Analytical Methods in Geomechanics*, 29(6), 597-625.

Daugiala, A. (2015). *Geotechnical Nominal Resistance Test Results for Lateral Test on Drilled Shafts S-3 and S-4 for the Kosciuszko Bridge Project – Phase 1.* Report No. 0042-TI-002-001. New York City.

DiGiola, A. M.; Rojas-Gonzalez, L.; and Newman, F. B., (1989). “Statistical Analyses of Drilled Shaft and Embedded Pole Models,” *Proceedings*, Foundation Engineering: Current Principals and Practices, ASCE, Vol. 2, pp. 1338-1352.

Donthireddy, S. (1995). *Simple pressuremeter approach to lateral loads on piles*. Diss. Texas A&M University.

Donthireddy, S. and J.-L. Briaud (1995). *Simple Pressuremeter Approach to Lateral Loads on Piles*. Civil Engineering, Texas A&M University. Master of Science.

Hokmabadi, A. S., Fakher, A., & Fatahi, B. (2012). Full scale lateral behaviour of monopiles in granular marine soils. *Marine Structures*, 29(1), 198-210.

Holloway, G. L., Coyle, H. M., Bartoskewitz, R. E., & Sarver, W. G. (1978). Field test and preliminary design method for laterally loaded drilled shafts in clay (No. FHWATX78-211-2 Intrm Rpt.).

Huang, A. B., Lutenegger, A. J., Islam, M. Z., & Miller, G. A. (1989). Analysis of Laterally Loaded Drilled Shafts Using In Situ Test Results. *Transportation Research Record*, (1235), 60-67.

Huang, A. B., Hsueh, C. K., O'Neill, M. W., Chern, S., & Chen, C. (2001). Effects of construction on laterally loaded pile groups. *Journal of geotechnical and geoenvironmental engineering*, 127(5), 385-397.Isenhower, W. M., and S. Wang (2016). *Technical Manual for LPile 2016 (Using Data Format Version 9)*. Ensoft Inc., Austin, TX.

Ishikawa (1985). “Study on lateral resistance of large diameter pile,” 土木試驗所月報. (In Japanese)

Ismael, N. F. (1990). “*Behavior of Laterally Loaded Bored Piles in Cemented Sands.*” *Journal of Geotechnical Engineering, 116(11), 1678-1699.*

Janoyan, K. D., Wallace, J. W., & Stewart, J. P. (2006). “Full-Scale Cyclic Lateral Load Test of Reinforced Concrete Pier-Column.” *ACI Materials Journal, 103(2), 178.*

Jeanjean P. (2009). *Re-assessment of p-y curves for soft clays from centrifuge testing and finite element modelling.* OTC 20158, Proc. Offshore Tech. Conf., Houston, USA.

Jeanjean, P., Zhang, Y., Zakeri, A., Andersen, K. H., Gilbert, R., and Senanayake, A. I. M. J. (2017, January). “A Framework for Monotonic PY Curves in Clays.” In *Offshore Site*

Investigation Geotechnics 8th International Conference Proceeding (Vol. 108, No. 141, pp. 108-141). Society for Underwater Technology.

Jeong, S., et al. (2007). *Cyclic lateral load tests of offshore large diameter piles of Incheon Bridge in marine clay*. The Seventeenth International Offshore and Polar Engineering Conference. International Society of Offshore and Polar Engineers.

Juirnarongrit, T., and Ashford, S. A. (2004). "Lateral load behavior of cast-in-drilled-hole piles in weakly cemented sand." *Transportation Research Record: Journal of the Transportation Research Board*, 1868(1), 190-198.

Kahle, K. J., and D. A. Brown (2002). "*Performance of Laterally Loaded Drilled Sockets Founded in Weathered Quartzite.*" Alabama Department of Transportation.

Kasch, V. R., Coyle, H. M., Bartoskewitz, R. E., & Sarver, W. G. (1977). "*Lateral load test of a drilled shaft in clay.*" No. FHWA-TX-77-211-1 Intrm Rpt. Texas Transportation Institute.

Klar A and Randolph MF. (2008). "Upper-bound and load-displacement solutions for laterally loaded piles in clays based on energy minimisation." Géotechnique 58(10): 815-820.

Lemnitzer, A., Khalili-Tehrani, P., Ahlberg, E. R., Rha, C., Taciroglu, E., Wallace, J. W., & Stewart, J. P. (2010). "Nonlinear efficiency of bored pile group under lateral loading." *Journal of Geotechnical and Geoenvironmental Engineering.* 136(12).

Liang, R. Y., Shatnawi, E. S., & Nusairat, J. (2007). "Hyperbolic P-Y Criterion for Cohesive Soils." *Jordan Journal of Civil Engineering.* 1(1). 38-58.

Little, R. L., and Briaud, J. L. (1988). *Full scale cyclic lateral load tests on six single piles in sand* (No. TAMU-RR-5640). Texas A&M University, College Station, Dept of Civil Engineering.

Load Test Consulting, Ltd. (2018). *LTC Data Report - Lateral Load Test Results for ATS-3, Merced Avenue Overpass.* Load Test Consulting load test report.

LPILE (2018). Laterally loaded pile analysis software developed by Ensoft Inc. http://www.ensoftinc.com.

Lutenegger, A. J. and G. A. Miller (1993). *Behavior of Laterally Loaded Drilled Shafts in Stiff Soil.* International Conference on Case Histories in Geotechnical Engineering. Session 1.1 (3)

Macklin, P. R. and N. N. S. Chou (1988). "A Lateral Load Test on Seven Foot Diameter Caissons." In *Foundation Engineering: Current Principles and Practices (pp. 1122-1131). ASCE.*

Makarim, C. A. (1986). *Pressuremeter Method for Single Piles Subjected to Cyclic Lateral Loads in Overconsolidated Clay.* Civil Engineering, Texas A&M University. Doctor of Philosophy.

Matlock H. (1962). "Correlations for design of laterally loaded piles in soft clays." Report to Shell Development Company, Sept.

Matlock, H. (1970). "Correlations for design of laterally loaded piles in soft clay." *Offshore Technology in Civil Engineering Hall of Fame Papers from the Early Years*: 77-94.

Matlock, H., and Tucker, R. L. (1961). *Lateral-load tests of an instrumented pile at Sabine, Texas.* A Report to Shell Development Company, Houston.

McClelland, B., & Focht, J. A., (1958). "Soil modulus for laterally loaded piles." Transactions of the American Society of Civil Engineers, 123(1), 1049-1063.

Motta, E. (2012). "Lateral deflection of horizontally loaded rigid piles in elastoplastic medium." *Journal of Geotechnical and Geoenvironmental Engineering*, 139(3), 501-506.

Murff, J. D., and J. M. Hamilton (1993). "P-ultimate for undrained analysis of laterally loaded piles." *Journal of Geotechnical Engineering*. 119(1).

Naramore, S. A. and F. Y. Feng (1990). *Field Tests of large Diameter Drilled Shafts Part I-Lateral Loads. ReportNo. FHWA/CA/SD-88/02, California Department of Transportation, Sacramento, California.*

Janoyan, K., Stewart, J. P., & Wallace, J. W. (2001). Analysis of py curves from lateral load test of large diameter drilled shaft in stiff clay. In Proceedings of the 6th Caltrans workshop on seismic research, Sacramento, CA.

Poulos, H. G. (1971). "Behavior of laterally loaded piles I. Single Piles." *Journal of Soil Mechanics and Foundations Div.* Vol 97, No SM 5

Randolph, M. F. (1981). "The response of flexible piles to lateral loading." *Geotechnique.* 31(2).

Randolph, M. F., and G. T. Houlsby (1984). "The limiting pressure on a circular pile loaded laterally in cohesive soil." *Geotechnique*. 34(4).

Randolph M. F., (2013). "Analytical contributions to offshore geotechnical engineering." The Second ISSMGE McClelland Lecture. Proc., 18th Int. Conf. Soil Mech. and Geot. Eng., Paris.

Reece, L. C., Cox, W., and Koop, F. (1975). "Field testing and analysis of laterally loaded piles in stiff clay." In 7th offshore technology conference (Vol. 2, pp. 671-690).

Reese, L. C. (1958). Discussion of "Soil modulus for laterally loaded piles" by McClelland and Focht. *Transactions*, ASCE, Vol. 123, pp 1071-1074.

Reese, L. C., and Welch, R. C. (1975). "Lateral loading of deep foundations in stiff clay." *Journal of Geotechnical and Geoenvironmental Engineering*, 101(ASCE# 11456 Proceeding).

Reese, L. C., William R. Cox, and Francis D. Koop (1974). "Analysis of laterally loaded piles in sand." *Offshore Technology in Civil Engineering Hall of Fame Papers from the Early Years:* 95-105.

Rinne, E., Thompson, J., and Vanderpool, W. (1996). *I-15/U.S. 95 Load Test Program Las Vegas, Nevada*. Proj. No. 31-215903-07A, Kleinfelder, Inc.

Ruesta, P. F., and Townsend, F. C. (1997). "Evaluation of laterally loaded pile group at Roosevelt Bridge." *Journal of Geotechnical and Geoenvironmental Engineering*. 123(12), 1153-1161.

Senanayake A. (2016). *Design of large diameter monopiles for offshore wind turbines in clay*. Ph.D. dissertation, The University of Texas at Austin, August.

Smith, T. D. (1983). *Pressuremeter Design Method for Single Piles Subjected to Static Lateral Load.* Doctor of Philosophy thesis. Civil Engineering, Texas A&M University.

Stevens, J. B., and J. M. E. Audibert (1979). "Re-examination of py curve formulations." Offshore technology conference.

Sullivan, WR, Reese, LC, and Fenske, CW. (1980). "Unified method for analysis of laterally loaded piles in clay." In Numerical methods in offshore piling (pp. 135-146). Thomas Telford Publishing.

Terzaghi, K. (1955). "Evaluation of Coefficients of Subgrade Modulus," *Géotechnique*, Vol. 5, No. 4, pp. 297-326.

Thompson, G. R., (1977). "Application of the Finite Element Method to the Development of p-y Curves for Saturated Clays," M.S. thesis, The University of Texas at Austin.

Tucker, L. M. and J.-L. Briaud (1987). *Analysis of the Pile Load Test Program at the Lock and Dam 26 Replacement Project.* Texas A&M University.

Vesic, A. S. (1977). "Design of pile foundations." National Cooperative Highway Research Program Synthesis of Practice no. 42. *Transportation Research Board*, Washington, DC, 32-48.

Woodward-Clyde Consultants (1979). *Foundation Investigation and Test Program, Lock and Dam No. 26, Mississippi River, Alton, Illinois*. Report prepared for St. Louis District, U.S. Army Corps of Engineers.

Yu J, Huang M, and Zhang C. (2015). "Threedimensional upper-bound analysis for ultimate bearing capacity of laterally loaded pile in undrained clay." *Can. Geotech. J.* 52: 1775-1790.

Yegian, M., and Wright, S. G., (1973). "Lateral Soil Resistance-Displacement Relationships for Pile Foundations in Soft Clays," Proceedings, 5th Offshore Technology Conference, Vol. II, pp. 663-676.

Zhang, L., and S. Ahmari (2013). "Nonlinear analysis of laterally loaded rigid piles in cohesive soil." *International Journal for Numerical and Analytical Methods in Geomechanics*. 37(2).

Zhang, Y., K. H. Andersen, and G. Tedesco (2016). "Ultimate bearing capacity of laterally loaded piles in clay–Some practical considerations." *Marine Structures* 50.

BIBLIOGRAPHY

API RP 2GEO (2014). *Recommended Practice for Geotechnical and Foundation Design Considerations.* 1st Edition Addendum 1, Published by the American Petroleum Institute.

Ashford, S. and T. Juirnarongrit (2004). *Evaluation of force based and displacement based analysis for response of single piles to lateral spreading.* Proceedings of 11th International Conference on Soil Dynamics and Earthquake Engineering and 3rd International Conference Earthquake Geotechnical Engineering, University of California, Berkely.

Baguelin, F., J. F. Jezequel, and D. H. Shields (1978). *The Pressuremeter and Foundation Engineering*, Clausthal-Zellerfeld. Trans Tech Publications, W. Germany.

Briaud, J.-L. and D. S. Barrios (2010). *Foundation Engineering for Static Loads.*

Brown, D. A. (2007). "Rapid Lateral Load Testing of Deep Foundations." *DFI Journal* 1(1).

Brown, D. A., Turner, J. P., & Castelli, R. J. (2010). "Drilled Shafts: Construction Procedures and LRFD Design Methods." *Geotechnical Engineering Circular* No. 10.

Brown, D. and W. M. Camp (2002). *Lateral Load Testing Program for the Cooper River Bridge, Charleston, SC. In Deep Foundations 2002: An International Perspective on Theory, Design, Construction, and Performance.* pp. 95-109

Byrne, B. W., McAdam, R. A., Burd, H. J., Houlsby, G. T., Martin, C. M., Gavin, K., ... & Potts, D. M. (2015). "Field testing of large diameter piles under lateral loading for offshore wind applications." *Geotechnical Engineering for Infrastructure and Development.* 1255-1260.

Byrne, B. W., McAdam, R., Burd, H. J., Houlsby, G., Martin, C., Zdravković, L., ... & Schroeder, F. C.(2015). *New design methods for large diameter piles under lateral loading for offshore wind applications.* In 3rd International Symposium on Frontiers in Offshore Geotechnics (ISFOG 2015), Oslo, Norway, June (pp. 10-12).

Byrne, B. W., McAdam, R. A., Burd, H., Houlsby, G. T., Martin, C. M., Beuckelaers, W. J. A. P., ... & Ushev, E. (2017). *Pisa: New Design Methods for Offshore Wind Turbine Monopiles.* OSIG.

Dapp, S. and D. Brown (2010). *Evaluation of Base Grouted Drilled Shafts at the Audubon Bridge.* In GeoFlorida 2010: Advances in Analysis, Modeling & Design (pp. 1553-1562).

DiGioia, A. M., Davidson, H. L., & Donovan, T. D. (1981). "Laterally Loaded Drilled Piers A Deisgn Model." Drilled piers and caissons: proceedings of a session/sponsored by the Geotechnical Engineering Division at the ASCE National Convention, St. Louis.

Dunnavant, T. W. and M. W. O'Neill (1989). "Experimental p-y Model for Submerged, Stiff Clay." *Journal of Geotechnical Engineering,* 115(1), 95-114.

Guo, W. D. and B. T. Zhu (2004). "*Laterally Loaded Fixed-Head Piles in Sand.*" In *Proc., 9th Australia-New Zealand Conf. on Geomechanics* Vol. 1, pp. 88-94.

Hughes, J. M. O., Goldsmith, P. R., & Fendall, H. D. W. (1979). *Full Scale Laterally Loaded Pile test at the Westgate Freeway Sire, Melbourne, Australia: Load Deflection Predictions and Field Results.* University of Auckland, School of Engineering, Department of Civil Engineering.

Ismael, N. F. (2009). "Behavior of Step Tapered Bored Piles in Sand under Static Lateral Loading." *Journal of Geotechnical and Geoenvironmental Engineering* 136(5): 669-676.

Ismael, N. F. and T. W. Klym (1980). "Behavior of Rigid Piers in Layered Cohesive Soils." *Journal of Geotechnical Engineering* 106.

Janoyan, K. D. (2001). *Interaction between Soil and Full Scale Drilled Shaft under Cyclic Lateral Load*. Civil Engineering, University of California. Doctor of Philosophy.

Jardine, R. J. "Pile Load Testing Performed for HSE Cyclic Loading Study at Dunkirk, France."

Khalili-Tehrani, P., Ahlberg, E. R., Rha, C., Lemnitzer, A., Stewart, J. P., Taciroglu, E., & Wallace, J. W. (2014). "Nonlinear Load-Deflection Behavior of Reinforced Concrete

Drilled Piles in Stiff Clay." *Journal of Geotechnical and Geoenvironmental Engineering, 140(3), 04013022.*

Kim, K., Nam, B. H., & Youn, H. (2015). "Effect of Cyclic Loading on the Lateral Behavior of Offshore Monopiles Using the Strain Wedge Model." *Mathematical Problems in Engineering, 2015.*

Kim, Y. and S. Jeong (2011). Analysis of soil resistance on laterally loaded piles based on 3D soil–pile interaction. Computers and Geotechnics, 38(2), 248-257.

Kim, Y., Jeong, S., & Lee, S. (2010). Wedge failure analysis of soil resistance on laterally loaded piles in clay. Journal of Geotechnical and geoenvironmental engineering, 137(7), 678-694.

Li, W., Igoe, D., & Gavin, K. (2014). "Evaluation of CPT-based P-y models for laterally loaded piles in siliceous sand." *Geotechnique Letters*. 4(2), 110-117.

Matlock, H., and L. C. Reese (1961). "Foundation analysis of offshore pile supported structures." Proc. of 5th Int. Conf. on Soil Mechanics and Foundation Engineering, Paris.

O'Neill, M. W. and A.-B. Huang (2003). "Comparative Behavior of Laterally Loaded Groups of Bored and Driven Piles in Cohesionless Soils." *International Journal of Offshore and Polar Engineering.* 13(3).

Poulos, H. G. and A. J. Davids (2004). *Foundation design for the Emirates Twin Towers, Dubai.* Canadian Geotechnical Journal, 42(3), 716-730.

Robertson, D. T. and M. K. Muchard (2007). "Statnamic Load Testing of Large Diameter Piles at Rigolets Pass Bridge Replacement Project." In *Contemporary Issues In Deep Foundations* (pp. 1-11).

Sinnreich, J. and A. Ayithi (2014). "Derivation of p-y Curves from Lateral Pile Load Test Instrument Data." *Geotechnical Testing Journal*. 37(6).

Skanska-Kiewit-ECCO III (2015). *Geotechnical Nominal Resistance Test Results for Lateral Test on Drilled Shafts S-3 and S-4.* Kosciuszko Bridge Project Phase I.

Tara, D. J. (2012). "Pitt River bridge 2007 static pile loading test." In Full-Scale Testing and Foundation Design: Honoring Bengt H. Fellenius (pp. 289-306).

Zafir, Z. and W. E. Vanderpool. (1998) "*Lateral Response of Large Diameter Drilled Shafts: I-15/US 95 Load Test Program.*" In *Proceedings of the 33rd Engineering Geology and Geotechnical Engineering Symposium*, University of Nevada, Reno (pp. 161-176).

Zdravković, L., Taborda, D. M. G., Potts, D. M., Jardine, R. J., Sideri, M., Schroeder, F. C., ... & Martin, C. M. (2015). "*Numerical modelling of large diameter piles under lateral loading for offshore wind applications.*" In *Proceeding 3rd International Symposium on Frontiers in Offshore Geotechnics. Norway:[sn]*.